MoDOT

Research, Development and Technology

University of Missouri-Rolla

RDT 03-008

Application of Innovative Nondestructive Methods to Geotechnical and Environmental Investigations

RI 98-014
RI 98-015
RI 98-017
RI 98-019
RI 00-012

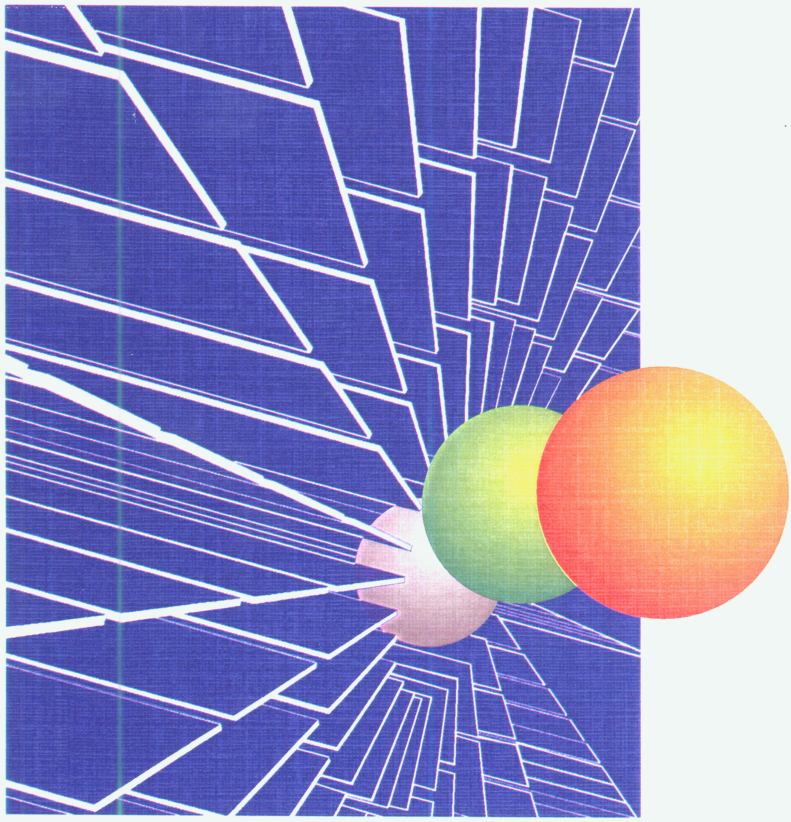

April, 2003

TECHNICAL REPORT DOCUMENTATION PAGE

1. Report No. RDT-03-008	2. Government Accession No.	3. Recipient's Catalog No.
4. Title and Subtitle Application of Innovative Nondestructive Methods to Geotechnical and Environmental Investigations		5. Report Date March 2003 6. Performing Organization Code University of Missouri-Rolla
7. Author(s) Dr. Neil Anderson, Dr. Steve Cardimona, Tim Newton		8. Performing Organization Report No. RDT03-008/RI98-014,RI98-015,RI98-017,RI98-019,RI00-012
9. Performing Organization Name and Address University of Missouri Rolla, Department of Geology and Geophysics 1870 Miner Circle Rolla, Missouri 65409-0410		10. Work Unit No. 11. Contract or Grant No.
12. Sponsoring Agency Name and Address Missouri Department of Transportation Research, Development & Technology Division P.O. Box 270, Jefferson City, MO 65102		13. Type of Report and Period Covered Final Report 14. Sponsoring Agency Code MoDOT

15. Supplementary Notes

The investigation was conducted by the University of Missouri-Rolla in cooperation with the Missouri Department of Transportation

16. Abstract

Geophysical surveys were conducted for the Missouri Department of Transportation (MoDOT) by the Department of Geology and Geophysics at the University of Missouri-Rolla. This report contains the results of several projects that utilized nondestructive, geophysical methods. The purpose of the research is to determine successful applications of geophysics to geotechnical work and gauge the effectiveness of different methods. These methods include ground penetrating radar, shallow seismic reflection, electromagnetic induction (EM), and electrical resistivity. Geophysics successfully assessed roadway and subsurface conditions with nondestructive, continuous profiles.

Case studies in this report address karst related voids and sinkholes, underground storage tanks, bridge scour, and abandoned underground mines. A protocol for evaluating the utility of ten commonly employed geophysical methods is provided in this report. This protocol serves as an aid to the highway engineer in the selection of appropriate methods for the target and site.

The GPR proved to be of useful utility in profiling the shallow subsurface soil structure and the reflection seismic survey established the bedrock structure below. Electromagnetic induction proved useful for mapping underground tanks and utilities, while resistivity was used for mapping bedrock and searching for air filled voids such as caves.

17. Key Words	18. Distribution Statement
ground penetrating radar, reflection seismic, bridge scour, electromagnetic induction, resistivity, voids, nondestructive testing, geophysics, underground storage tanks, karst	No restrictions. This document is available to the public through National Technical Information Center, Springfield, VA 22161

19. Security Classification (of this report)	20. Security Classification (of this page)	21. No. of Pages	22. Price
Unclassified	Unclassified	7 w/o appendices	

Form DOT F 1700.7 (06/98)

Application of Innovative Non-Destructive Methods to Geotechnical and Environmental Investigation

FINAL REPORT

RDT 03-008

PREPARED BY

MISSOURI DEPARTMENT OF TRANSPORTATION

PROJECT OPERATIONS DIVISION

By

Dr. Neil Anderson
Professor of Geophysics
University of Missouri - Rolla

Dr. Steven Cardimona
Assistant Professor of Geophysics
University of Missouri - Rolla

Tim Newton
Geotechnical Liaison
MoDOT

April 2003

ACKNOWLEDGMENTS

Special recognition is given to the following people for their contribution to the success of this research:

The numerous University of Missouri-Rolla, Department of Geology and Geophysics graduate students who worked on the projects.

Mr. Thomas Ryan, R.G., MoDOT District Geologist

Mr. Denny Lambert, R.G., MoDOT District Geologist

Mr. James Conley, District Soils and Geology Technologist

EXECUTIVE SUMMARY

Several geophysical surveys were conducted for the Missouri Department of Transportation (MoDOT) by the Department of Geology and Geophysics, University of Missouri-Rolla (UMR). The objectives were two-fold. First, MoDOT wanted to evaluate the utility of these non-destructive/non-invasive geophysical methods as applied to geotechnical and environmental site-investigations. Second, MoDOT engineers wanted additional independent and/or confirmational subsurface information at the geotechnical sites studied.

Four geophysical methods were employed during the course of these surveys: ground penetrating radar (GPR), high-resolution shallow reflection seismic, electromagnetic induction (EM), and electrical resistivity. Subsurface applications included identifying and locating underground storage tanks and buried utilities, quantifying fluvial scour, profiling bedrock structure, locating in-filled sinkholes and sub-pavement voids of karstic origin, the determination of the thickness and volume of surficial chat (milled waste rock), and locating abandoned mine access and ventilation shafts. The geophysical techniques employed proved capable of expediting the identification, location and mitigation of threatening geological features. A protocol for selecting appropriate non-destructive geophysical methods for specific objectives is included in this report.

The surveys explored the shallow subsurface without damaging pavement and disturbing the subgrade. Time wise, they allowed MoDOT to quickly map the subsurface. Underground objects were located and outlined on the surface to prevent damage by future drilling or excavating equipment. In contrast to geophysics, typical intrusive procedures such as drilling or backhoe excavation are time consuming and costly when used for subsurface exploration. In the case of underground tanks and buried utilities, possible damage could occur where these features are unknown. Geophysical methods were found to be capable of delineating these underground anomalies and the data was used as guidance for the drilling or excavating program. An efficient drilling plan reduces risk, liability, and cost while obtaining pertinent subsurface information. This is especially important on highways, where the goal is to minimize disruption of traffic and damage to pavement.

Table of Contents

INTRODUCTION

Several geophysical surveys were conducted for the Missouri Department of Transportation (MoDOT) by the Department of Geology and Geophysics, University of Missouri-Rolla (UMR). The objectives were two-fold. First, MoDOT wanted to evaluate the utility of these non-destructive/non-invasive geophysical methods as applied to geotechnical and environmental site-investigations. Second, MoDOT engineers wanted additional independent and/or confirmational subsurface information at the geotechnical sites studied. Currently, MoDOT contracts geophysical work as a reactionary measure when subsurface problems express themselves at the surface or where known geotechnical problems or uncertainties exist. MoDOT relies on its Geotechnical Section to discover potential subsurface problems during preliminary drilling of roadways and structures and does not contract geophysics on a routine basis.

Four geophysical methods were employed during the course of these surveys: ground penetrating radar (GPR), high-resolution shallow reflection seismic, electromagnetic induction (EM), and electrical resistivity. Subsurface applications included identifying and locating underground storage tanks and buried utilities, quantifying fluvial scour, profiling bedrock structure, locating in-filled sinkholes and sub-pavement voids of karstic origin, the determination of the thickness and volume of surficial chat (milled waste rock), and locating abandoned mine access and ventilation shafts.

In contrast to geophysics, typical intrusive procedures such as drilling or backhoe excavation are time consuming and costly when used for subsurface exploration. In the case of underground tanks and buried utilities, possible damage could occur where these features are unknown. Geophysical methods are capable of delineating these underground anomalies and the data can be used as guidance for the drilling or excavating program. An efficient drilling plan reduces risk, liability, and cost, while obtaining pertinent subsurface information. This is especially important on highways, where the goal is to minimize disruption of traffic and damage to pavement. Non-destructive testing methods such as geophysics meet these criteria.

RESULTS AND DISCUSSION

The geophysical techniques employed in this study proved capable of expediting the identification, location and mitigation of threatening manmade and geological features. A protocol for selecting appropriate non-destructive geophysical methods for specific objectives has been prepared and is included as Appendix A, "A Protocol for Selecting Appropriate Geophysical Surveying Tools Based on Engineering Objectives and Site Characteristics."

The ground penetrating radar (GPR) tool was used (in mono-static mode) to image shallow soil and/or shallow bedrock, to locate sub-pavement voids, and to determine the thickness of surficial chat. In the field, the dual GPR transmitter/receiver antenna is normally moved across the ground or water surface at a relatively constant rate (normal walking speed). The antenna (transmitter mode) emits pulsed, low frequency EM radiation at regular distance and/or time intervals (normally inches or fractions of seconds, respectively). Some of this downward propagating pulsed EM energy is reflected at subsurface interfaces (lithologic or material contacts), returned to the antenna (receiver mode) and recorded (arrival time, amplitude and antenna location). These reflected data are recorded as traces, processed and placed side-by-

side (at appropriate spatial locations), thereby provide a relatively continuous time-profile of the subsurface. Ideally, subsurface interfaces/features of interest can be identified and correlated across the GPR profiles, and time-depths can be transformed into structural depths. The effectiveness (depth penetration/resolution) of the GPR tool is dependent on the soil/rock/material properties of the features studied and the frequency of the antenna employed. Clayey soils absorb/attenuate GPR signal and often preclude the effective imaging of underlying strata. The antenna frequency also controls penetration depth and resolution, with the lower the frequency antennas (i.e., 100 Mhz) providing for greater depth penetration (tens of feet maximum) but less vertical and horizontal resolution. The maximum antenna frequency employed in this study was 1500 MHz. A detailed overview of GPR is provided in Appendix B, "Ground Penetrating Radar for Subsurface Investigation." GPR was utilized in almost every project included as part of this comprehensive report. Two of these investigations, "Ground Penetrating Radar (GPR): A Tool for Monitoring Bridge Scour" and "Evaluation of GPR as a Tool for Determination of Granular Material Deposit Volumes" are located in Appendix C and Appendix D.

The high-resolution shallow reflection seismic technique is the most time, labor and equipment intensive method employed in this study. An in-depth description of reflection seismic is in Appendix E, "Overview of the Shallow Seismic Reflection Technique." The reflection seismic tool employs a man-made acoustic energy source and arrays of motion-sensitive receivers (geophones). The tool is somewhat analogous to the GPR tool in that the arrival times and amplitudes of pulsed reflected acoustic energy is recorded and plotted to create an "essentially" continuous time profile of the subsurface. The reflection seismic tool does not provide the vertical and horizontal resolution afforded by GPR, but does allow for imaging at depths in excess of several hundreds of feet. Additionally, seismic energy is not rapidly attenuated by clays and shales. This method shows top of bedrock, faults, and sink structures quite well. The resulting images are much easier to interpret than GPR. Two separate investigations combining the reflection seismic and GPR methods are detailed in "Ground-Penetrating Radar and Reflection Seismic Study of Karstic Damage to Highway Embankments, Hannibal, Ralls County, Missouri" and "Geophysical Site Characterization: Ground-Penetrating Radar and Reflection Seismic Study of Previously Mined (Lead/Zinc) Ground, Joplin, Missouri," provided in Appendix F and Appendix G.

The electromagnetic (EM) tools employed in this survey differ from the GPR tool in that they measure the earth's inductive response to emitted, essentially continuous (over fixed time window) high-frequency, primary EM radiation. The EM induction techniques are based on the principal that the primary magnetic fields emitted from the EM tools will induce secondary electric currents within conductive subsurface materials. The relative strength and phase of these secondary electromagnetic fields is a function of the conductivity of the subsurface. The depth of investigation is similarly a function of the source frequency employed. If multiple frequency data is acquired at pre-set locations a conductivity profile of the subsurface can be created. EM proved most useful in the investigation of underground storage tanks, which is described in Appendix H, "Non-Invasive Detection and Delineation of Underground Storage Tanks."

The electrical resistivity tool employed in this study induces electrical current flow (through surface-coupled electrodes) and measure resultant potential differences at the earth's surface. The relative amplitudes of measured potential differences are direct functions of subsurface resistivities. The depth of investigation can be varied by changing the spacing of the

current electrodes. Additionally, the entire array can be shifted laterally across the surface of the area under investigation. This lateral shifting of the current and voltmeter electrodes allows the user to create a resistivity profile of the subsurface. A better explanation of electrical resistivity is found in an overview paper, "Subsurface Investigation With Electrical Resistivity," located in Appendix I. An integrated survey using electrical resistivity, GPR, and reflection seismic methods is detailed in appendix J, "Integrated Geophysical Site Characterization."

CONCLUSIONS

This study has demonstrated the effectiveness of geophysical methods to investigate subsurface threats to existing and planned roadways. Pre-construction knowledge of subsurface conditions will facilitate route planning, remediation efforts, and reduce short-term construction and long-term maintenance costs. MoDOT should integrate these geophysical tools into investigations where typical methods would be more costly and only provide limited information. It is believed the evaluations have been successful, but examination is needed of the cost to benefit ratio to establish a rationale for employing each method on a roadway project. Change of conditions claims during construction may be reduced or eliminated with the application of these tools.

The use of Ground Penetrating Radar (GPR) as an investigative tool reduced the time and cost of the projects as compared to the traditional methodology of investigation, extensive drilling and / or excavating. Without GPR, subsurface information would be obtained by drilling auger holes through the highway pavement, shoulders, and median. Relying only on point specific information to find subsurface features can be compared to finding a needle in the proverbial haystack. In the case of voids, the impact of the numerous boreholes required would have a dual effect on the stability of the roadway. The integrity of the pavement bridging the subsurface voids would be greatly reduced, and secondly, the holes would act as conduits of stormwater, flushing additional soil and accelerating the growth of the voids.

The most economical method for underground storage tanks and buried utilities is the GEM tool. It does not provide the "immediate" data that GPR is capable of, as files must be downloaded to a PC to display. There is more reliance on the grid for referencing anomalies, but the map it provides shows a 2-D view of the site with grid lines superimposed. This information would be adequate for drilling operations, showing tanks, utilities, and sometimes contamination plumes. A preliminary site visit to collect data will be required to generate maps for the drilling operations. An engineer and a technician should be able to survey a site in one 8-hour day.

It is important to realize that geophysics only shows "anomalies", those features in the subsurface that have different physical properties than the surrounding material. There must be a difference of contrast for the "target" to be detectable. Many of these anomalies from different geophysical methods directly correlate with one another, helping validate their existence. Each geophysical method provides a different view of the subsurface properties, and the combination of techniques provides the most useful interpretations. It is these validated areas of highest concern that should be further investigated by drilling. An efficient drilling program eliminates the "chance" encounter of features by drilling and confirming the anomalies.

The combination of GPR and seismic methods was very successful at complementing one another to provide a complete look into the shallow subsurface. The GPR (i.e. 500 MHz) can show soil and unconsolidated material properties to several meters depth while the reflection seismic goes deeper to illustrate bedrock lithology and structure. The penetration of GPR is dependent on the conductivity of the soil, which varies considerably with geography. Reflection seismic, which shows the underlying bedrock structure, is highly reliable but only necessary when the local geology and location of sinkholes and faults is unknown. Without GPR data, a typical mitigation of voids in the subgrade would be to tear out the overlying pavement, laying base rock, and re-paving the interstate roadway at an estimated cost of $45 per square yard, not

including excavation costs. The high cost, amount of time required, and the associated long-term traffic delays of this scenario make it the undesirable alternative.

Geophysical tools explore the shallow subsurface without damaging pavement and disturbing the subgrade. Their ability to locate subsurface features reduces the risk of penetrating unknown underground tanks and utility lines. Time wise, GPR and electromagnetic induction allowed MoDOT to quickly map underground storage tanks, find voids and unconsolidated materials, and assess the threat of future roadway subsidence. Underground objects can be located and outlined on the surface to prevent damage by drilling and/or excavating equipment. Also, once located, marking their location on the pavement, drilling, and pumping full of cement grout can easily mitigate voids.

RECOMMENDATIONS

Any threatening roadway stability situation involving a shallow subsurface that requires quick assessment is a candidate for the application of the technologies described in this report. However, ground penetrating radar (GPR) and reflection seismic are complex tools that require skilled technical persons to operate. Also, the initial cost of the equipment may be prohibitive to purchase. The results of these studies will be used to determine if the expenditure for equipment and its dedicated personnel is warranted. At this time it is recommended to establish qualified consultants that would be able to make their services available on short notice. Prior arrangements to expedite the mobilization and data collection should be made as well. This would be in the best interest of the traveling public, ensuring safety while minimizing disruption of traffic.

The following is a summary of the recommendations made as a result of the work presented in this report:

- Establish qualified consultants that can mobilize quickly to investigate distressed roadways or structures. Most of the time geophysics is used as a reaction to a problem where quick assessment and mitigation are necessary. Benefit: The safety of a structure or roadway will be evaluated in a timely manner with non-destructive techniques. This will be used to establish an efficient drilling program to define the problem areas.

- Preliminary bridge soundings in areas of known karstic voids, pinnacle rock, underground mines, or geologic faulting should employ geophysics before drilling. Pinnacle rock is where bedrock elevations vary more than about 15 feet in close proximity. Knowing exactly where rock elevation varies or the location of suspect voids will ensure that these features are defined during the drilling process. Benefit: Structures will be adequately designed and the number of "change of conditions" claims during construction is reduced. Foundations may be altered where voids are found, increasing the safety of the traveling public.

- Newly acquired right-of-way with unmapped or suspected underground storage tanks should be investigated with geophysics to confirm and locate their presence. Benefit: May prevent "change of conditions" claims during excavation. The discovery of an unknown storage tank can cause long project delays due to the environmental implications.

- Reevaluate geophysical techniques for monitoring bridge scour in the future. GPR worked well in shallow waters but the real need is for locating scour in deep, fast moving water environments such as the Missouri or Mississippi Rivers. Benefit: The advent of a deep-water scour monitoring system will reduce the number of dives in dangerous waters. This is especially applicable during floods, such as the flood of 1993, to assess the footings of a bridge for public safety.

GUIDE TO FIELD IMPLEMENTATION

The techniques described in this report apply mostly to geological work. The geotechnical section responsible for bridge soundings, foundation studies, slide repairs, and environmental investigations will benefit from these geophysical methods. The most cost effective approach is to employ geophysics during the preliminary geotechnical investigation of areas known for karst, mines, or underground storage tanks. Planning a geophysical survey should be done with due consideration to both the objectives and the site characteristics.

Successful use of GPR is based on knowing how and where the tool is useful and how to interpret the resultant data to provide the desired information. The most important factor is the competency of the persons responsible for planning and performing the geophysical survey and interpreting the data. The user must know where GPR will and will not be effective before a project is undertaken. Effectiveness is based on soil conductivity, site geology, and topography. A GPR survey crew is usually two people - one to drive or drag the antenna and one to operate the data collector. Generally, a grid system or location tick marks are set up to reference the GPR data during the survey. As GPR systems advance, the units become more specialized and easier to use. A non-geophysicist is perfectly capable of running equipment that has been set up by the manufacturer for a specific use.

The most important aspect of the resulting data is the ability to locate imaged features in the field. The data is not useful unless we can drill or dig out the anomalies to identify and confirm their existence. Therefore, investigation sites will require measuring and marking a reference grid on the ground. It is typical to label one axis with letters and the other with numbers. It is best to have at least two of the points professionally surveyed or to use a differential GPS (DGPS) receiver to collect position coordinates on as many of the points as possible. An accurate grid system tied to real world coordinates ensures that features imaged by geophysics can be scaled and precisely located in the field as well as shown on roadway plans. DGPS systems are relatively easy and cost effective to use for this purpose. DGPS is described in the chat volume study located in the appendix.

It should not be forgotten that the instruments only image "anomalies" and that the investigation sites typically require calibration and / or geological correlation drill holes to collaborate the data. The value of a correlation hole is priceless, as it aids interpretation and fine-tuning of measurements. We must know the true extent and size of the features imaged. Therefore, geophysics does not replace intrusive techniques, but greatly reduces their use. The use of geophysical methods can aid the creation of an efficient drill or dig program, eliminating unnecessary work and making sure that the targeted subsurface features are found in the area of investigation. Random or "blind" drilling does not increase the odds of success.

APPENDIX A

A PROTOCOL FOR SELECTING APPROPRIATE GEOPHYSICAL SURVEYING TOOLS BASED ON ENGINEERING OBJECTIVES AND SITE CHARACTERISTICS

*Neil Anderson, *Steve Cardimona and *Allen Hatheway

*Department of Geology and Geophysics
University of Missouri-Rolla, Rolla, Missouri 65401

ABSTRACT

Engineering geophysical techniques measure specific physical parameters and are routinely applied to highway-related problems. The engineer responsible for site investigation should ensure that geophysical technique(s) employed provide cost-effective information about physical properties of interest at the required levels of spatial resolution and target definition.

As an aid to the highway engineer, we present tabularized information about some commonly employed geophysical methods, and a generalized approach for evaluating their utility. Our discussions are intended to be informative - not exhaustive. For more rigorous treatments of the geophysical techniques the reader is referred to the selected bibliography. The engineer engaged in survey design is strongly encouraged to work with a knowledgeable geophysicist.

INTRODUCTION

Geophysical techniques measure specific physical parameters (Table 1) and are routinely applied to highway-related problems. [Commonly employed methods include seismic refraction, seismic reflection, seismic tomography, ground-penetrating radar (GPR), electromagnetics (EM), electrical resistivity, induced polarization (IP), self potential (SP), magnetics, and gravity.]

In the normal course of a engineering site investigation, one or more geophysical data sets may be acquired for the purpose of determining physical properties of interest (Table 1). Typically, non-geophysical information (borehole, geohydrologic, surficial geology, concrete thicknesses, etc.) is also acquired, all contributing to the interpretation of the geophysical data and the development of an integrated site model.

To ensure that the most appropriate geophysical techniques are employed, the highway engineer should critically evaluate the potential utility of available methods. There are several questions that should be considered including:

What are the physical properties of interest?

Which geophysical methods measure the physical properties of interest?

Which techniques will likely provide the required spatial resolution and target definition?

Which geophysical tools will perform well in the study area?

Which techniques are most cost-effective?

Which techniques will provide complementary data?

What non-geophysical data are required to constrain the interpretation of the acquired geophysical control?

Is the overall program cost-effective?

Herein we present tabularized information about some commonly employed geophysical methods, and a generalized approach for evaluating their utility. To illustrate the ideas discussed, we consider a hypothetical site characterization situation, and address the "questions" [posed above] sequentially.

In our hypothetical situation, a transportation engineer wants to detect air-filled voids (radial cavities with extended near-horizontal, linear axis) in otherwise uniform limestone at a bridge site (100m x 30m). There are no physical constraints with respect to site accessibility. The limestone is overlain by a thin (<1m thick) veneer of silly sand, and underlain by lower-velocity shale (at a depth of 50m). The geophysical technique(s) employed need to be capable of detecting small cavities (0.3m diameter) at shallow depths less than 3 m, intermediate-sized cavities (2m diameter) at depths on the order of 7.5 m, and larger cavities (7.5m diameter) at depths on the order of 20m. Cavities at depths greater than 20m do not constitute a risk.

PHYSICAL PROPERTIES OF INTEREST? WHICH GEOPHYSICAL METHODS MEASURE THESE PHYSICAL PROPERTIES?

The first step in designing a geophysical survey is to identify the *physical properties* of interest (Table 1). In our hypothetical situation, the highway engineer would recognize that shallow, air-filled cavities in limestone would be characterized by spatial variations in density, acoustic velocity, EM velocity, dielectric constant, and electrical conductivity and resistivity. The second step is to determine which geophysical method(s) measure one or more of these parameters. Based on the data provided in Table 1, several geophysical techniques would appear potentially suitable site investigation tools, including seismic refraction, seismic reflection, seismic tomography, GPR, EM, resistivity, and gravity.

SPATIAL RESOLUTION AND TARGET DEFINITION? WHICH GEOPHYSICAL TOOLS WILL PERFORM WELL IN THE STUDY AREA?

The third step is to determine which geophysical technique(s) can provide the required spatial resolution and target definition. The fourth step is to assess which tools have a reasonable probability of performing well in the study area, given the nature of the target, the target environment, and the related strengths and weaknesses of the various methods. (Information relevant to our hypothetical example is summarized in Table 2. The reader to referred to the selected bibliography for more thorough and rigorous treatments of tool resolution, definition and performance.)

Based on *spatial resolution/target definition/site utility* considerations (as provided in Table 2 only), our engineer would rank the various geophysical techniques in a manner consistent with Table 3. GPR would be rated optimal for investigating cavities at shallow to intermediate depths. Resistivity is a potentially viable tool for investigations at all requisite depths. Gravity and seismic tomography are potentially suitable for investigations at intermediate or greater depths. Seismic reflection could be a viable tool for delimiting larger cavities at depths on the order of 20m.

WHICH TECHNIQUES ARE MOST COST-EFFECTIVE? WHICH TECHNIQUES WILL PROVIDE COMPLEMENTARY DATA?

The fifth and sixth steps are to consider the cost-effectiveness and complementary nature of each geophysical tool. Cost-effectiveness is a function of both cost (planning, acquisition, processing and interpretation) and the overall usefulness of the interpreted results (target definition). In our hypothetical case study, tool options have been narrowed down to GPR, resistivity, gravity, seismic tomography, and seismic reflection. In Table 4, we summarize (given the nature of target and site accessibility) the cost-effectiveness of each tool still under consideration.

Generally, if two or more geophysical techniques provide similar target definition, and cost is the overriding concern, the less expensive method is selected. However, if accuracy of interpretation is the overriding concern, more than one technique is often employed, because complementary geophysical data sets will further constrain interpretations. Another consideration is whether a geophysical tool can

contribute information above and beyond the definition of the specific target. Seismic surveys, for example, can provide in-situ estimates of engineering rock properties.

Based on the information presented in Table 4, GPR is ranked as the most accurate (in terms of spatial resolution/target definition) and cost-effective tool for mapping voids at shallow to intermediate depths. With respect to the identification of larger cavities at greater depths, resistivity is ranked first in terms of cost and overall cost-effectiveness. (Note that seismic tomography was ranked first in terms of target definition and spatial resolution, but second in terms of overall cost-effectiveness. If the determination of elastic moduli in-situ had been a significant secondary interest, seismic tomography would have been rated as most cost-effective.)

Assume that cost-effectiveness is the primary concern (based on an evaluation of strategic needs), and that the plan is to use GPR to investigate shallow to intermediate depths, and resistivity to evaluate the subsurface at greater depths.

NON-GEOPHYSICAL DATA CONSTRAINTS? IS THE OVERALL GEOPHYSICAL PROGRAM COST-EFFECTIVE?

The seventh step is to plan for the acquisition of non-geophysical constraints. Our engineer understands that geophysical data is inherently ambiguous, and realizes that interpretations will be more rigorous if constrained and verified by ground truth. With this consideration in mind, two anchor boreholes will be drilled on-site prior to the interpretation of the geophysical data. This boring control will ensure that geophysical interpretations are calibrated and constrained. Our engineer also plans to drill two confirmation boreholes, at sites designated as anomalous (or otherwise), in order to verify geophysical interpretations.

The last is to assess the cost-effectiveness of the overall geophysical effort relative to non-geophysical alternatives such as invasive drilling (as per hypothetical example). The final decision is based on cost-effectiveness, confidence, and engineering judgement.

SUMMARY

The engineer designing or responsible for a geophysical investigation should raise several pertinent questions, and select methodologies based on the responses. Questions could include:

What are the physical properties of interest?

Which geophysical methods measure the physical properties of interest?

Which techniques will likely provide the required spatial resolution and target definition ?

Which geophysical tools will perform well in the study area?

Which techniques are most cost-effective?

Which techniques will provide complementary data?

What non-geophysical data are required to constrain the interpretation of the acquired geophysical control?

Is the overall program cost-effective?

It was not our intent to discuss these "questions" in detail in this paper. Rather, we have tried to raise and summarize pertinent related issues, in an effort to assist the engineer involved in designing geophysical surveys, and inform the engineer charged with decision responsibilities.

The reader is referred to Table 5 for a general summary of some applications of the ten geophysical methods considered in this paper. For more in-depth discussions of these geophysical methods, the

reader is referred to Table 6. This bibliographical list is not exhaustive, nor is it comprised of the most theoretically rigorous papers. Rather, it is intended to serve as a resource for the highway engineer requiring methodology information above and beyond that presented in this paper. References to well logging techniques are also included in Table 6.

REFERENCES

Blakely, R. J., 1996, Potential theory in gravity and magnetic applications, Cambridge University Press, 441 p.

Clay, C., S., 1990, Elementary exploration seismology: Prentice Hall, 346 p.

Corwin, R. F., 1990, the self-potential method for environmental and engineering applications, *in* Ward, S. H., editor, Geotechnical and environmental geophysics, volume 1: review and tutorial: Society of Exploration Geophysicists, 389 p.

Daniels, D., 1996, Surface-penetrating radar: IEEE, 320 p.

Daniels, J. J., and Keys, W. S., 1990, Geophysical well logging for hazardous waste sites, *in* Ward, S.H., editor, Geotechnical and environmental geophysics, volume 1: review and tutorial: Society of Exploration Geophysicists, 389 p.

Evans, B. J. 1997, A handbook for seismic data acquisition in exploration: Society of Exploration Geophysicists, 305 p.

Fink, J. B., Sternberg, B. K., McAlister, E. O., Wieduwilt, W. G., and Ward, S. H., editors, 1990, Induced polarization, applications and case histories: Society of Exploration Geophysicists, 414 p.

Griffiths, D.H., and King, R.F., 1981, Applied Geophysics for geologist and engineers: Pergamon Press, 230p.

Hinds, R. C., Anderson, N. L., and Kuzmiski, R., 1996, VSP interpretative processing: Theory and practice: Society of Exploration Geophysicists, 205p.

Hinze, W. J., 1990, The role of gravity and magnetic methods in engineering and environmental studies, *in* Ward, S. H., editor, Geotechnical and environmental geophysics, volume 1: review and tutorial: Society of Exploration Geophysicists, 389 p.

Howard, K. W. F., 1990, Geophysical well logging for detection and characterization of fractures in hard rocks, *in* Ward, S. H., editor, Geotechnical and environmental geophysics, volume 1: review and tutorial: Society of Exploration Geophysicists, 389 p.

Keary, P. and Brooks, M., 1991, An introduction to geophysical exploration: Blackwell scientific Publications, 254 p.

Lankston, R. W., 1990, High-resolution refraction seismic data acquisition and interpretation, *in* Ward, S. H., editor, Geotechnical and environmental geophysics, volume 1: review and tutorial: Society of Exploration Geophysicists, 389 p.

McNeill, J. D., 1990, Use of electromagnetic methods for groundwater studies, *in* Ward, S. H., editor, Geotechnical and environmental geophysics, volume 1: review and tutorial: Society of Exploration Geophysicists, 389 p.

McCann, D. M., Eddleston, M., Fenning, P. J., and Reeves, G. M., editors, 1997, Modern geophysics in engineering geology: The Geological Society of London, 441 p.

Nabighian, M. N., editor, 1988, Electromagnetic methods in applied geophysics, volume 1, theory: Society of Exploration Geophysicists, 513 p.

Sheriff, R. E., 1991, Encyclopedic dictionary of exploration geophysics, third edition: Society of Exploration Geophysicists, 376 p.

Sheriff, R. E., and Geldart, L. P., 1995, Exploration Seismology, second edition: Cambridge University Press, 592 p.

Steeples D. W., and Miller, R. D., 1990, Seismic reflection methods applied to engineering, environmental and groundwater problems, *in* Ward, S. H., editor, Geotechnical and environmental geophysics, vol. 1: review and tutorial: Society of Exploration Geophysicists, 389 p.

Telford, W. M., Geldart, L. P., and Sheriff, R. E., 1990, Applied geophysics, second edition: Cambridge University Press, 770 p.

Tychsen J., and Nielson, T., 1990, Seismic reflection used in the sea environment, *in* Ward, S. H., editor, Geotechnical and environmental geophysics, volume 1: review and tutorial: Society of Exploration Geophysicists, 389 p.

Ward, S. H., 1990, Resistivity and induced polarization methods, *in* Ward, S. H., editor, Geotechnical and environmental geophysics, volume 1: review and tutorial: Society of Exploration Geophysicists, 389 p.

Yilmaz, O., 1988, Seismic data processing: Society of Exploration Geophysicists, 526 p.

Geophysical Method	Measured Parameter	Physical Property	Physical Property Model (Highway Application)	Typical Site Model
Shallow Seismic Refraction	Travel times of refracted seismic energy (p-wave or s-wave)	Density and acoustic velocity (acoustic velocity is a function of elastic moduli and density)	Acoustic velocity/depth model	Geologic profile, with ground water surface
Shallow Seismic Reflection	Travel times/amplitudes of reflected seismic energy (p-wave/s-wave)	Density and acoustic velocity (acoustic velocity is a function of elastic moduli and density)	Acoustic velocity/depth model	Geologic profile, with ground water surface
Seismic Tomography	Travel times/amplitudes of seismic energy (p-wave or s-wave)	Density and acoustic velocity (acoustic velocity is a function of bulk elastic moduli and density)	Model depicting spatial variations in acoustic velocity	Geologic profile
GPR (ground-penetrating radar)	Travel times and amplitudes of reflected electromagnetic energy	Dielectric constant, magnetic permeability, conductivity and EM velocity	EM velocity/depth model	Geologic profile Internal material profile
Electromag-netics (EM)	Response to electromagnetic energy	Electrical conductivity and inductance	Conductivity/depth model	Geologic/hydrologic profile
Electrical Resistivity	Earth resistance	Electrical resistivity	Resistivity/depth model	Geologic/hydrologic profile
Induced Polarization (IP)	Polarization voltages or frequency dependent ground resistance	Electrical capacitance	Capacitance/depth model	Model depicting spatial variations in clay content or mineralization
Self Potential (SP)	Electrical potentials	Electrical conductivity	Model depicting spatial variations in natural electric potential of the subsurface	Hydrologic model (seepage beneath dam, through fractured bedrock, etc.)
Magnetics	Spatial variation in the strength of the geomagnetic field	Magnetic susceptibility and remanent magnetization	Model depicting spatial variations in magnetic susceptibility of subsurface	Geologic profile (location of faults, variable depth to bedrock, etc.)
Gravity	Spatial variations in the strength of gravitational field of the earth	Bulk density	Model depicting spatial variations in the density of the subsurface	Geologic profile (location of voids, variable depth to bedrock, etc.)

***Table 1**: Ten geophysical surveying methods commonly employed for highway site investigations. Each of these techniques measures different physical properties of the site being investigated. The typical physical property model is developed from single method data alone. The site model is generated using multiple geophysical data sets and available non-geophysical control.*

Method	Spatial Resolution and Target Definition	Site Conditions (Strengths)	Site Conditions (Weaknesses)
Shallow Seismic Refraction	*Spatial resolution*: intermediate (function of frequency, velocity, receiver spacing). *Target definition*: intermediate (depth/velocity estimates generally accurate to within ±10%).	Can provide reliable shallow velocity/ depth control. Often ideal for mapping top saturated zone (p-wave only) and top bedrock, and determining rippability. Relatively inexpensive compared to seismic reflection and resistivity.	Velocity/depth models usually restricted to five layers or less. Low velocity and thin, high velocity layers cannot be imaged. Resolution diminished in structurally complex and highly fractured areas. Voids cannot be directly imaged - may be characterized by anomalous travel times. Water not detected by S-waves
Shallow Seismic Reflection	*Spatial resolution*: intermediate (function of frequency, velocity and receiver spacing). *Target definition*: intermediate (depth/velocity estimates generally accurate to within ±10%).	Often ideal for imaging bedrock and sub-bedrock layers. Can provide relatively detailed velocity/depth control in structurally complex areas. Larger voids can be characterized by prominent diffractions, and effectively imaged.	Relatively expensive compared to seismic refraction, resistivity and EM. Doesn't work well if site is covered by loose, dry soils/sediment (results in poor receiver coupling).
Seismic Tomography	Intermediate to high (function of frequency, velocity, borehole spacing, and source/ receiver intervals).	Often ideal for imaging lateral/vertical heterogeneities, including cavities. Useful for determining elastic moduli in-situ.	Expensive, due to the cost of drilling boreholes. Technique doesn't work well if subsurface is comprised of thin (relative to borehole spacing) layers with significant velocity variations.
GPR (ground-penetrating radar)	Very high. Resolution/ target definition is function of frequency and velocity. Lower frequency sources provide for greater depth penetration but lower resolution.	Rapid and relatively inexpensive. Can provide detailed structural control in complex areas. Suitable for analyzing concrete, pavement, quarry rock, locating voids, etc.	Doesn't work well in conductive (clayey) environment. Limited depth penetration, compared to reflection seismic and resistivity techniques.
Electromag-netics (EM)	Low to intermediate. Lower frequencies provide for greater depth penetration but poorer resolution and definition.	Works well in conductive environment. Rapid and relatively inexpensive. Equipment doesn't need to be coupled to surface. Provides moderately detailed conductivity/depth model. Lithologies, salinities can be inferred.	Doesn't work well in highly resistive environment. Resolution/definition is usually less than that provided by seismic methods. Output models usually restricted to five layers or less.
Resistivity	Low to intermediate. Lower frequencies and increased electrode spacing provide for greater depth penetration but poorer resolution and target definition.	Works well in resistive environment. Can provide moderately detailed resistivity/ depth model in areas where seismic and EM techniques are not effective. Lithologies, salinities can be inferred. Suitable for mapping larger voids.	Doesn't work well in highly conductive environment. Resolution/definition is usually less than that provided by seismic methods. More expensive than EM. Electrodes need to be coupled to surface. Output models usually restricted to five layers or less.
Induced Potential (IP)	Low. Lower frequencies and increased electrode spacing provide for greater depth penetration, but poorer resolution and target definition.	Good indicator of clay content (or metallic mineralization). Complements resistivity data.	Low spatial resolution and target definition. Not suitable for detecting air-filled voids.
Self Potential (SP)	Low spatial resolution and target definition.	Good indicator of fluid flow in subsurface (or mineralization). Rapid and relatively inexpensive.	Low spatial resolution and target definition.
Magnetics	Low spatial resolution and target definition.	Good indicator of ferromagnetic materials in the subsurface. Rapid and inexpensive.	Interpretation is qualitative rather than quantitative. Generally low resolution/target definition.
Gravity	Low to intermediate spatial resolution and target definition.	Good indicator of substantive voids in subsurface. Equipment doesn't need to be coupled to surface.	Relatively expensive. Generally low resolution/definition. Background noise may mask data.

***Table 2**: Each geophysical tool provides for different spatial resolution and target definition. The overall utility of a particular technique is a function of site conditions.*

Ranking: Small voids (scale 1-3)	A. Rational (focus on delineating small voids at shallow depths; < 3m)	Ranking: Interm. voids (scale 1-3)	B. Rational (focus on delineating intermediate sized voids at depths on the order of 7.5m)	Ranking: Large voids (scale 1-3)	C. Rational (focus on delineating large voids at depths on the order of 20m)
1 GPR	High spatial resolution, high target definition in resistive material.	1 GPR	High resolution, reasonable definition at depth in resistive material.	1 Seismic tomography	Target should be imaged.
2 Resistivity	Target is probably too small and too shallow.	1 Resistivity	Reasonable definition at depth in resistive material.	1 Resistivity	Reasonable definition at depth in resistive material.
3 EM	Highly resistive terrain. Target is too small.	1 Seismic tomography	Target should be imaged.	1 Seismic reflection	Prominent diffractions could be imaged.
3 Gravity	Target is too small.	2 Gravity	Target may be too small to resolve.	1 Gravity	Anomalies may be large enough to delineate.
3 Seismic tomography	Target is probably too small and too shallow.	3 EM	Highly resistive terrain.	2 GPR	Problems with limited depth penetration.
3 Seismic reflection	Target is too small and too shallow.	3 Seismic reflection	Target is probably too small and too shallow.	3 EM	Highly resistive terrain.
3 Seismic refraction	Lack of prominent sub-bedrock refractors.	3 Seismic refraction	Lack of prominent sub-bedrock refractors.	3 Seismic refraction	Lack of prominent sub-bedrock refractors.

***Table 3**: Ranking of seven techniques considered for hypothetical void detection case study. Situations considered include: A) small voids at shallow depths; < 3m; B) intermediate sized voids at depths on the order of 7.5m; and C) large voids at depths on the order of 20m. Cavities are assumed to have lengths that greatly exceed their diameters.*

Ranking: Cost-Effectiveness	Cost	Effectiveness	Complementary nature of data
1 GPR	About 20 parallel GPR profiles (100m length; spaced at 2m intervals) would be required to fully investigate the shallow subsurface. Investigation of intermediate depths would require a second grid of profiles (10 lines; 100m length; 3m intervals; lower frequency antenna). Data acquisition is relatively rapid.	GPR is probably the best tool for investigating shallow to intermediate depths. Will provide required spatial resolution and target definition.	GPR profiles will provide detailed information about depth to bedrock and internal character (fracturing, bedding, lithology variations, etc.).
2 Resistivity	Resistivity profiles are expensive to acquire. The tool is probably not cost-effective with respect to the investigation at shallow depths. The deeper subsurface would probably be adequately imaged by a grid of profiles (perhaps 6 lines; 100m length (subsurface coverage); spaced at 5m intervals).	Resistivity is probably the best tool available as far as the investigation of large cavities at intermediate to greater depths is concerned.	Resistivity and simultaneously acquired IP data provide info about the subsurface (e.g., depth to ground water surface, conductivity of clay/soil, metallic mineralization, etc.).
3 Seismic reflection	Reflection seismic profiles are expensive to acquire and process, and the tool is probably not cost-effective as far as the investigation of shallow to intermediate depths are concerned. The deeper subsurface would probably be adequately imaged by a grid of profiles (perhaps 6 full fold lines; 100m in length; spaced at 5m intervals).	Large cavities can be characterized by prominent diffractions on quality reflection seismic data. Data quality might be compromised by cavities at shallow depths.	Reflection seismic data can provide info about subsurface structure below zone of primary interest (ground water surface, and depths to layers at depths in excess of a couple hundred meters or more).
4 Seismic tomography	Seismic tomography data are expensive to acquire and process. The tool functions much better below the water table than above. The technique is probably not cost-effective as far as the mapping of smaller voids is concerned. Larger voids could be effectively imaged by a grid of boreholes (perhaps 8; depths on the order of 40m). Costs would be very high compared to resistivity and reflection seismic profiling.	If a grid of closely spaced boreholes was employed, excellent results could be expected. However, this approach could be prohibitively expensive, unless the boreholes were used for injecting grout.	Seismic tomography data (p-wave and s-wave) will provide information about the elastic moduli of bedrock at various depths. This information could be useful if excavations are planned, or if the site is in a seismically-active area.
5 Gravity	The shallow and intermediate targets are probably too small to resolve/define. The larger cavities may be too small as well. Gravity data are expensive to acquire and process, and the tool is probably not cost-effective as far as the investigation site of is concerned.	Gravity data are the most ambiguous of the five techniques (re: spatial resolution and target definition).	The gravity tool probably would provide relatively little additional information about the character of the study site.

***Table 4**: Ranking of five techniques considered for hypothetical void detection case study. Cost and overall effectiveness are considered.*

Application	Seismic refract.	Seismic reflect.	Seismic tomo.	GPR	EM	Resist.	IP	SP	Mag.	Grav.
Mapping lithology (<10m depth)	M	x		M	x	x				
Mapping lithology (>10m depth)	x	M	X		x	x				
Estimating clay/mineral content					M	x	x			
Locating shallow sand and gravel deposits				M	M					
Locating sand and gravel deposits (that contain heavy minerals)									M	
Determining volume of organic material in filled-in lakes or karsted features	M	M			M					M
Mapping top of ground water surface	M P-wave	M P-wave		M	M	M				
Determining water depths (including bridge scour)				M						
Mapping groundwater cones of depression	x	x		M	x	x				
Subsurface fluid flow								M		
Mapping contaminant plumes				M	M	x		x		
Mapping crop land salination and desalination over time					M	M				
Locating underwater ferromagnetic objects				M					M	
Mapping bedrock topography (<10m depth)	M			M	x	x				x
Mapping bedrock topography (>10m depth)	x	M			x	x				x
Mapping sub-bedrock structure	x	M		x	x	x				
Delineating steeply dipping geologic contacts (<10m depth)	M			M	M	M				
Delineating steeply dipping geologic contacts (>10m depth)	x	M	x		x	x			x	
Mapping fracture orientation (near-surface bedrock)	M			M						
Mapping fracture orientation	M		M							
Identifying regions of potential weakness (e.g., shear zones and faults; <10m depth)	M		x	M	x	x			x	
Identifying regions of potential weakness (e.g., shear zones and faults; >10m depth)	x	x	M		x	x			x	
Identifying near-surface karstic sinkholes and the lateral extent of their chaotic, brecciated, and otherwise disrupted ground	M	M		M	x	x				x
Mapping air-filled cavities, tunnels (<10m depth)	x	x	x	M	x	M				x
Mapping air-filled cavities, tunnels (>10m depth)	x	M	M		x	x				x
Mapping water-filled cavities, tunnels	x P-wave	M P-wave	M	x						
Mapping clay-filled cavities, tunnels	x	M	M		x	x				

Table 5: *Potential applications of various geophysical methods in engineering and environmental studies (M-major; x-minor)*

Application	Seismic refract.	Seismic reflect.	Seismic tomo.	GPR	EM	Resist.	IP	SP	Mag.	Grav.
Estimating rippability	M		x							
Foundation integrity studies	M		x	M						
Dam-site integrity studies	M	M	M	M	x	x		M		
Landslide site evaluation	M		M	x	M	M				
Locating buried well casings (metal)				M	M				M	
Locating buried drums, pipelines and other ferromagnetic objects				M	M				M	
Locating buried non-magnetic utilities				M						
Mapping archeological sites (buried ferro-magnetic objects, fire beds, burials, etc)				M	M				M	
Mapping archeological sites (non magnetic - excavations, burials, etc)				M						
Concrete integrity studies and inspection				M						
Detection of incipient concrete spallage on bridge decks				M						
Locating rebar in concrete				M	M				M	
Detection of corrosion of rebar embedded in concrete				M						
Evaluation of presence, pattern and density of rebar embedded in concrete destined for demolition				M	x				x	
Pavement integrity studies				M						
Detection of voids beneath pavement				M						
Detection and delimitation of zones of relatively thin sub-grade or base course material				M						
Detection and monitoring of areas of insufficiently dense sub-base				M						
Large-area differentiation and monitoring of insufficient thickness of pavement as a quality assurance measure during construction				M						
Large-area differentiation and monitoring of insufficient pavement thickness as post-construction monitoring technique				M						
Detection of bodies of sub-grade in which moisture content is anomalously high, as a precursor to development of pitting and potholes				M						

***Table 5** (continued): Potential applications of various geophysical methods in engineering and environmental studies (M-major; x-minor)*

Application	Seismic refract.	Seismic reflect.	Seismic tomo.	GPR	EM	Reslst.	IP	SP	Mag.	Grav.
Mapping/locating landfills	x			x	M	x			M	
Determining in-situ rock properties (bulk, shear and Young's moduli)	M		M							
Estimating in situ rock properties (saturation, porosity, permeability)					M	M				
Determining in situ rock densities										M
Determining in situ rock properties (dielectric constant)				x						
Mapping abandoned, infilled open-pit mines and quarries	M	M		x	x	x			x	x
Mapping abandoned underground mines		M	x			x				
Detecting abandoned Mine shafts		x	x	M	M	x			x	

***Table 5** (continued): Potential applications of various geophysical methods in engineering and environmental studies (M-major; x-minor)*

Geophysical Technique	Suggested References
Seismic refraction	Clay (1990), Evans (1997), Griffiths and King (1981), Keary and Brooks (1991), Lankston (1990), McCann et al. (1997), Sheriff (1991), Sheriff and Geldart (1995), Telford et al. (1990), Griffiths, D.H., and King, R.F., 1981,
Seismic reflection	Clay (1990), Evans (1997), Hinds et al. (1996), Keary and Brooks (1991), McCann et al. (1997), Sheriff (1991 Griffiths and King (1981), Sheriff and Geldart (1995), Telford et al. (1990), Tychsen and Nielson (1990), Yilmaz (1988)
Seismic tomography	Clay (1990), Hinds et al. (1996), Keary and Brooks (1991), McCann et al. (1997), Sheriff (1991), Sheriff and Geldart (1995), Telford et al. (1990)
GPR	Daniels (1996), McCann et al. (1997), Sheriff (1991)
EM	Griffiths and King (1981), Keary and Brooks (1991), McNeill (1990), McCann et al. (1997), Nabighian (1988), Sheriff (1991), Telford et al. (1990)
Resistivity	Griffiths and King (1981), Keary and Brooks (1991), McCann et al. (1997), Sheriff (1991), Telford et al. (1990) Ward (1990)
IP	Griffiths and King (1981), Fink et al. (1990), Keary and Brooks (1991), McCann et al. (1997), Sheriff (1991), Telford et al. (1990), Ward (1990)
SP	Corwin (1990), Keary and Brooks (1991), Griffiths and King (1981), McCann et al. (1997), Sheriff (1991), Telford et al. (1990)
Magnetics	Blakely (1996), Hinze (1990), Griffiths and King (1981), Keary and Brooks (1991), McCann et al. (1997), Sheriff (1991), Telford et al. (1990)
Gravity	Blakely (1996), Hinze (1990), Griffiths and King (1981), Keary and Brooks (1991), McCann et al. (1997), Sheriff (1991), Telford et al. (1990)
Well logging	Daniels and Keys (1990), Howard (1990), Keary and Brooks (1991), McCann et al. (1997), Sheriff (1991), Telford et al. (1990)

***Table 6**: Selected bibliography*

APPENDIX B

GROUND PENETRATING RADAR FOR SUBSURFACE INVESTIGATION

Steve Cardimona*

*Department of Geology and Geophysics, University of Missouri-Rolla, Rolla, MO

ABSTRACT

The ground penetrating radar geophysical method is a rapid, high-resolution tool for non-invasive investigation. Ground penetrating radar records microwave radiation that passes through the ground and is returned to the surface. The radar waves propagate at velocities that are dependent upon the dielectric constant of the subsurface, and reflections are caused by changes in the dielectric constant that are due to changes in the subsurface medium. A transmitter sends a microwave signal into the subsurface, and the time it takes energy to return to the surface relates to the depth at which the energy was reflected. Thus, interpretation of this reflected energy yields information on structural variation of the near subsurface. Ground penetrating radar transmitters operate in the megahertz range, and the choice of source signal peak frequency correlates to expected depth of penetration and resolution. Higher frequency sources will offer greater vertical resolution of structure but will not penetrate as deep as lower frequency sources. The choice of appropriate source will be target and project-goal dependent. Data are most often collected along a survey profile, so that plots of the recorded signals with respect to survey position and travel-time can be associated with images of geologic structure as a function of horizontal position and depth. Ground penetrating radar can be collected fairly rapidly, and initial interpretations can be made with minimal data processing, making the use of ground penetrating radar for shallow geophysical investigation quite cost-effective.

INTRODUCTION

Detailed structural interpretation can be important for hydrological and geotechnical applications such as determining soil and bedrock characteristics in the shallow subsurface. In addition, high-resolution imaging is important for monitoring structural integrity of buildings, mine walls, roadways and bridges. Ground penetrating radar (GPR) is the only geophysical technique that can offer the horizontal and vertical resolution necessary for many of these applications.

The GPR method records microwave radiation that passes through the ground and is returned to the surface. A transmitter sends a microwave signal into the subsurface, and the radar waves propagate at velocities that are dependent upon the dielectric constant (also known as relative permittivity) of the subsurface medium. Changes in the dielectric constant that are due to changes in the subsurface materials cause the radar waves to reflect, and the time it takes energy to return to the surface relates to the depth at which the energy was reflected. Thus, interpretation of this reflected energy yields information on structural variation of the near subsurface.

Because GPR transmitting antennae operate in the megahertz range, the waves that propagate tend to have wavelengths on the order of 1m or less. Horizontal and vertical resolution are dependent upon the wavelength, such that the smaller the wavelength, the better the resolution. Although higher frequency sources will yield smaller wavelengths (better resolution), the higher frequency signals will not penetrate as deep as lower frequencies. Thus a careful choice must be made regarding the GPR antennae to use in a survey based on expected target and the project goals. Once a source antenna is chosen for a particular survey, GPR data can be collected fairly rapidly. The GPR method can be used for reconnaissance (anomaly location) as well as for more detailed study (structural interpretation).

This paper is meant to be an overview of pertinent ideas that relate to the GPR method. We suggest the reader refer to the overviews in Hempen and Hatheway (1992) and Daniels (1989), and the comprehensive introductory text by Daniels (1996) for more discussion of the related topics.

BACKGROUND

The fact that radar waves are basically the same as light waves may leave the casual reader feeling a little confused; however, the ability to use radar waves to image the near subsurface of the earth defines the first principal under which the GPR method operates:

Principal #1--> Radar (electromagnetic) waves *do* pass through earth materials.

The visual region is only a portion of the wide spectrum (different frequency components) of electromagnetic radiation. Microwave radiation (radar) with frequencies on the order 10MHz to 1000MHz is not in the visual spectrum, but will propagate at the speed of light in a vacuum just as all other electromagnetic radiation. The subsurface of the earth is, of course, not a vacuum, which introduces the second important principal for understanding GPR:

Principal #2--> Each material is described by specific electrical properties.

These properties are magnetic permeability, electrical conductivity, and electric permittivity. Most earth materials (soils and rocks) are non-magnetic, so that the permeability of free space is a good representation for the magnetic permeability of the subsurface. The conductivity is important because it controls the amount of energy lost in the propagating signal (due to conductive attenuation). When the permittivity of the medium (ε) is compared to the permittivity of free space (ε_o), we get a value for the relative permittivity(ε_r), or dielectric constant (k), of the material

$$\varepsilon_r = k = \frac{\varepsilon}{\varepsilon_0}.$$

The dielectric constant defines the index of refraction of the medium and is a material constant which controls the speed of electromagnetic waves in the material.

$$v = \frac{c}{\sqrt{k}},$$

where c is the speed of light in air and v is the velocity of the electromagnetic energy in the subsurface medium. Thus, changes in the subsurface material will effect the index of refraction, and reflected energy will be produced related to the contrast in the dielectric constant across a boundary between two materials. Table 1 lists typical dielectric constants for some common materials. Note that the dielectric constant is controlled mainly by water content.

Table 1

Material	Typical Dielectric Constant	Radar propagation velocity (m/ns)
Air	1	0.30
Water	81	0.033
Granite	9	0.10
Limestone	6	0.12
Sandstone	4	0.15
Rocks	4-12	0.15-0.087
Dry sand	4-6	0.15-0.12
Wet sand	30	0.055
Dry clay	8	0.11
Wet clay	33	0.052
Dry soils	3-8	0.17-0.11
Wet soils	4-40	0.15-0.047
Asphalt	3-6	0.17-0.12
Concrete	9-12	0.10-0.087

Most GPR transmitters are pulse-radar, operating in the time-domain to send a time-pulse of energy (source wavelet) propagating into the subsurface. When a GPR transmitter sends a signal into the subsurface, an expanding spherical wavefront describes the propagating electromagnetic energy as it travels away from the source (Figure 1). This can be listed as our third principal:

Principal #3--> Pulse-radar propagates time-pulse energy away from source along an expanding wavefront.

Although principal #3 describes the true physics of the propagating electromagnetic wavefield, we make an approximation to this by introducing the concept of the ray (Figure 1):

Approximation #1--> A single ray path represents the wavefield traveling in a specific (ray) direction.

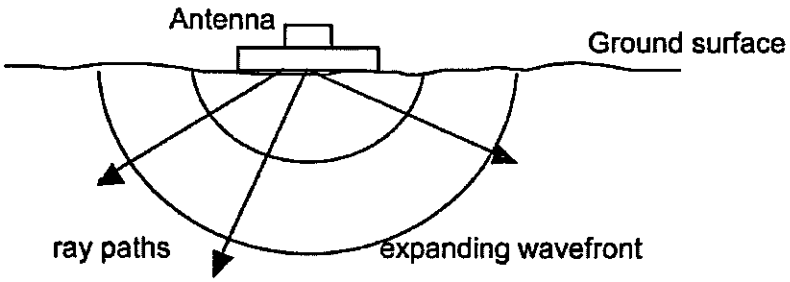

Figure1. Electromagnetic energy propagating away from the source can be described by an expanding wavefront. Ray paths help to describe energy traveling in any one particular direction.

We can then describe the entire wavefield by an infinite number of rays traveling in all directions away from the source. This reasonable approximation (ray theory) allows us to more easily describe the traveling wave in the subsurface. The radiation pattern for a GPR antenna is actually more complex than shown in Figure 1. Although most GPR antennae are shielded, some electromagnetic energy does travel upward into the air. Also, radar antennae do not have simple hemispherical radiation patterns (Figure 2).

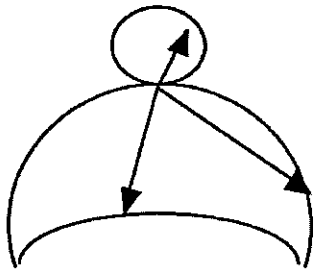

Figure 2. Radiation pattern for electromagnetic energy propagating away from GPR antenna on surface of the Earth. Energy propagating into the air is non-zero, and wavefronts in subsurface are not simple.

When ray paths intersect boundaries between materials, the energy in the traveling wave is partitioned between reflected and transmitted waves. Thus we have our fourth operating principal:

Principal #4--> Inhomogeneity (variations in electrical properties) cause reflections.

Snell' Law of ray theory describes how the reflected and transmitted (refracted) waves propagate away from the boundary. Of course, it is the reflections that propagate back to the surface that are recorded on the GPR receiver. After a GPR survey is conducted, data are normally presented as plots of the returned signal as a function of time (associated with depth) and survey position (horizontal coordinate). This 2-D profile is then interpreted as an image of structural variation below the survey line, leading us to our second approximation:

Approximation #2: All inhomogeneity is directly below the GPR survey line.

We make this assumption because our normal form of data presentation displays an image of structure which has placed all returned energy below the survey line in the 2-D profile. However, this approximation

is invalid. The electromagnetic radiation travels in all directions away from the source, not just in the plain described by the horizontal survey coordinate and the depth of investigation. This energy will be scattered off of discontinuities that are not directly below the survey line, but the energy will still be recorded by the survey receiver. Plotting the data in 2-D cross-sections is truly a matter only of convenience. Care must be taken during interpretation as some of the features in the 2-D profile of subsurface structure will be artifacts due to the energy scattered from outside the imaging plain.

DATA COLLECTION

Survey design for GPR work requires the determination of what type of survey one wishes to undertake and what operating frequency one will use for the source, although this may be a function of equipment availability. The most common survey technique used with the GPR method is common offset profiling. Certain GPR instruments are designed to be able to collect common midpoint survey data also. Higher frequency sources will offer greater resolution of structure but will not penetrate as deep as lower frequency sources.

Common offset profiling

The most common survey technique used with the GPR method is common offset profiling. In this technique, the transmitting and receiving antennae are kept a fixed distance apart, and progressively moved along a survey line to record returned signals from the subsurface. The result is a data set presented in a 2-D profile with intent to create an image of subsurface structure. There are two types of GPR systems available to be used to collect common offset data: monostatic and bistatic units.

A true monostatic radar system uses the same antenna as the source and the receiving antenna; however, radar instruments that have both transmitting and receiving antennae housed within the same instrument are normally considered to be coincident and monostatic because they cannot be separated. Monostatic GPR units allow for rapid data collection. Instruments are normally pulled along a profile, yielding continuous data collection (Figure 3). The result is very small horizontal sampling (good horizontal resolution), but very large data files. High frequency units are quite light and portable, but lower frequency units are large and heavy, creating logistic difficulties.

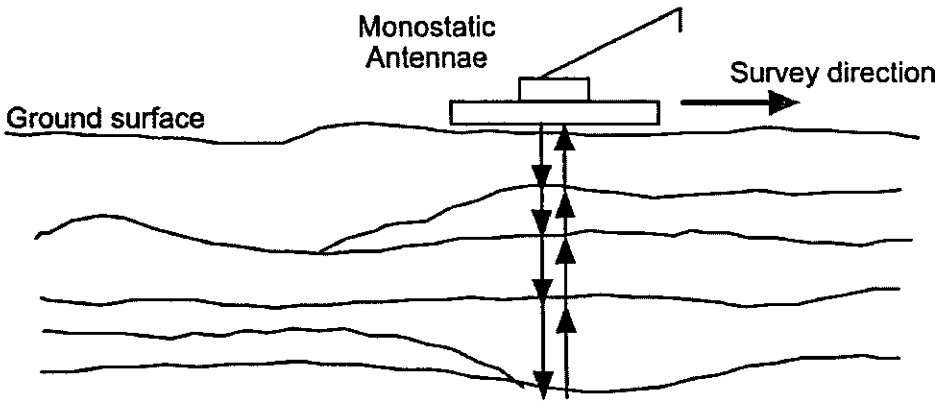

Figure 3. A monostatic GPR unit houses both transmitting and receiving antennae in the same instrument. The antennae are pulled along the profile, and data are interpreted to be normal incidence reflection signals.

Bistatic GPR antennae are separate instruments (Figure 4). With bistatic antennae, the source-receiver offset (antenna separation) is held constant for common offset profiling, and this offset can be optimized for best results. Data files are small and easily manageable, but this is because the horizontal sample

interval is normally chosen to be large (at discrete offset positions) which can reduce lateral resolution. Increasing the horizontal sample rate (decreasing the survey step interval) increases the time necessary to complete the survey, as every new survey location represents a discrete reading that must be made.

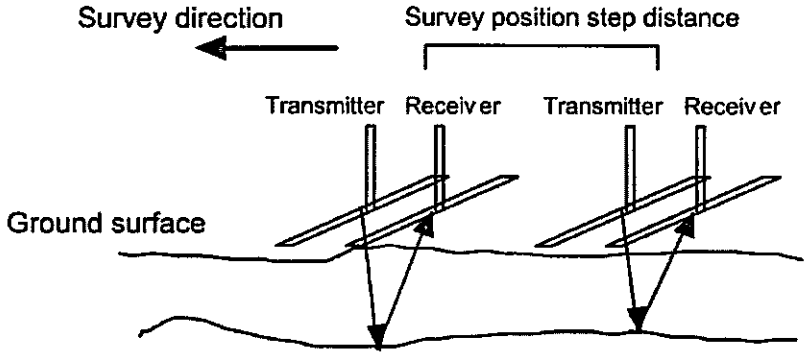

Figure 4. Bistatic GPR instrumentation includes two separate transmitting and receiving antennae units. The antennae are placed at discrete locations along the profile, and data are interpreted to be near-normal incidence reflection signals.

Common midpoint survey

A common midpoint (CMP) survey is one in which bistatic antennae are progressively moved away from each other, collecting data at each new, more distant position, but keeping the center between the two antennae fixed. This type of data can aid in interpretation by helping to determine the electromagnetic wave velocity. The change in travel time (the moveout) as a function of increasing offset between the two antennae is directly related to the electromagnetic wave velocity of the subsurface.

Obviously, this exact type of survey cannot be done with a monostatic GPR unit. Surveys with monostatic units must use another technique to estimate subsurface velocities. Pulling a monostatic unit over a known subsurface feature can give an estimate of velocity either by simple calculation (known depth divided by measured travel-time), or by measuring the moveout of a diffracted arrival from the target (Figure 5). The latter yields a monostatic version of a CMP. Again, this moveout is directly related to the subsurface electromagnetic velocity.

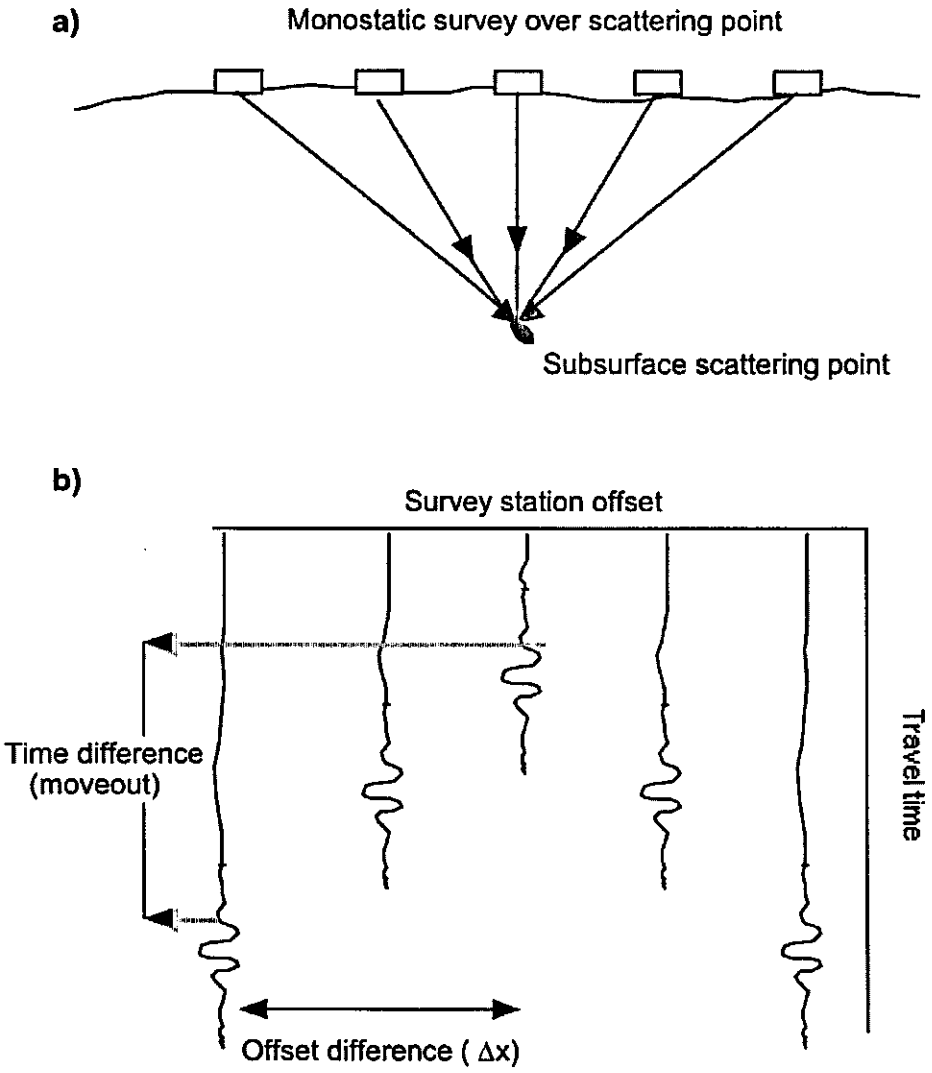

Figure 5. (a) Monostatic GPR survey over a point inhomogeneity in subsurface; (b) associated radar recordings. The time difference for the arrival of the diffracted signal as a function of survey offset (horizontal position) is determined by the electromagnetic velocity of the subsurface.

Choice of antenna frequency

Because GPR transmitting antennae operate in the megahertz range, the waves that propagate tend to have wavelengths on the order of 1m or less. Horizontal and vertical resolution are dependent upon the wavelength, such that the smaller the wavelength, the better the resolution. Although higher frequency sources will yield smaller wavelengths (better resolution), the higher frequency signals will not penetrate as deep as lower frequencies. Thus a careful choice must be made regarding the GPR antennae to use in a survey based on expected target and the project goals.

Antenna frequency will effect the intrinsic resolution in both the vertical and horizontal directions. Resolution is a measure of the smallest separation that can be distinguished between discrete targets. Thus, a small resolution is in fact better than a large resolution. Vertical resolution is based primarily on

the wavelength (velocity of propagation divided by the dominant radar frequency) of the electromagnetic energy, given simply as 1/4 the wavelength.

Horizontal resolution is affected by survey design (mentioned earlier) as well as the more intrinsic resolution related to the frequency content of the probing electromagnetic wave. The survey method (monostatic versus bistatic) will determine the lateral variations that are able to be imaged (i.e., those larger than the horizontal sample rate), whereas the lateral averaging introduced due to the propagating wavefield will be dependent on the dominant wavelength and the depth of investigation. The farther the target is from the source, the larger the wavefield "footprint", the worse the resolution (Figure 6).

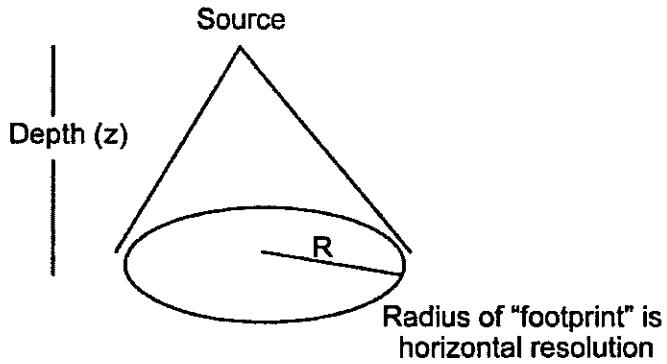

Figure 6. An electromagnetic wave with dominant frequency given by f and traveling at velocity v will have a finite "footprint" at a distance z from the source

$$R \cong \sqrt{z\frac{v}{f}}$$

In-field signal enhancement

During data acquisition, multiple radar scans are normally taken at each survey location. These scans are then summed (stacked) together to reduce incoherent noise in favor of coherent reflection or diffraction signals. This averaging is normally done explicitly with bistatic antennae, so that at each survey location the recorded radar data trace is commonly a stack of as many as 128 scans.

With monostatic GPR, a scan rate (scans/s) is normally chosen by the operator, and in field stacking can also be implemented by most instruments so that each recorded trace will be a stack of more than one radar scan. However, because the monostatic unit is in motion (pulled along the survey line), the stacked data will actually incorporate some lateral averaging, as each scan in the stack will be over a slightly different survey position (related to the speed of acquisition). When the rate of acquisition is known (m/s), this lateral averaging can be estimated by dividing the scan rate by the acquisition rate to yield the number of scans per meter. As an example, if a monostatic unit is collecting data at 36 scans/s with an acquisition speed of 1 m/s, then the number of scans per meter is 36. With a stacking rate of 18 scans/record, the lateral averaging would be across half of a meter.

Monostatic versus bistatic

The different methods for common offset data collection and signal enhancement described above (continuous versus discrete) are not fundamental differences between monostatic and bistatic radar systems. They are practical differences. The monostatic unit can be used in a discrete acquisition mode, but its strength is in the ability to perform rapid surveying in a continuous mode. A pair of bistatic antennae can be set in a frame that allows the operator to pull the unit in a continuous acquisition mode, but its strength is in data enhancement at the discrete locations. The discussion to follow associates monostatic radar with continuous acquisition and bistatic radar with discrete acquisition.

NORMAL PROCESSING

Some survey questions (e.g., anomaly detection) can be answered in the field by looking at the raw GPR data. However, most often data undergoes a series of simple processing steps (filtering operations). The basic processing is slightly different depending upon the type of GPR system. Monostatic systems require a little more massaging of the raw field records.

Monostatic processing

1) zero-time adjust (static shift) – need to associate zero-time with zero-depth, so any time offset due to instrument recording must be removed before interpretation of the radar image.
2) subtract average trace to remove banding -- need to remove the ringing that is inherent in monostatic units due to the close proximity of the source and receiving antennae
3) horizontal (distance) stretch to get constant trace separation (horizontal normalization) -- need to remove the effects of non-constant motion along the profile. Data are collected continuously, and will not be represented correctly in the image if steps are not taken to correct for the variable horizontal data coverage.
4) gain -- need to compensate for amplitude variations in the GPR image; early signal arrival times have greater amplitude than later times because these early signals have not traveled as far. The loss of signal amplitude is related to geometric spreading as well as intrinsic attenuation. Various time-variable gain functions may be applied in an effort to equalize amplitudes of the recorded signals.

Bistatic processing

1) zero-time adjust (same as for monostatic)
2) gain (same as for monostatic)

ADVANCED PROCESSING

Other filtering operations can be applied to GPR data. Many of these advanced techniques are used routinely in processing seismic data (Yilmaz, 1987). The most common processing steps that might be applied to GPR data would be lateral averaging, frequency filtering, deconvolution, and migration.

Lateral averaging

At each station in a bistatic GPR survey, the data record consists of one trace, with the signal recorded for a certain length of time, where the greater the time window, the greater the potential depth of imaging. Lateral averaging can be used across each trace to improve signal (reflection) coherency. This lateral averaging is most effective, however, for a monostatic survey where the horizontal sample rate is large (small horizontal sample interval). Lateral averaging (stacking, or summing data traces directly) can improve the ratio of signal to noise. For example, with a monostatic survey collecting data at 40 traces/m (which is a lot of data!), the extra data can be used more effectively in a lateral averaging step than leaving the interpreter to study the complex variation on the order of 1/40th of a meter.

Frequency filtering

Although GPR data are collected with source and receiver antennae of specified dominant frequency, the recorded signals include a band of frequencies around the dominant frequency component. Frequency filtering is a way of removing unwanted high and/or low frequencies in order to produce a more interpretable GPR image. High-pass filtering maintains the high frequencies in the signal but removes the low frequency components. Low-pass filtering does just the opposite, removing high frequencies and retaining the low frequency components. A combination of these two effects can be achieved with a band-pass filter, where the filter retains all frequencies in the pass band, but removes the high and low frequencies outside of the pass band.

Deconvolution

When the time-domain GPR pulse propagates in the subsurface, convolution is the physical process that describes how the propagating wavelet interacts with the earth filter (the reflection and transmission response of the subsurface). Deconvolution is an inverse filtering operation that attempts to remove the effects of the source wavelet in order to better interpret GPR profiles as images of the earth structure. Deconvolution operators can degrade GPR images when the source signature is not known.

Deconvolution operators are designed under the assumption that the propagating source wavelet is minimum phase (i.e., most of its energy is associated with early times in the wavelet). This assumption is not necessarily valid for GPR signals. With GPR, the ground becomes part of the antennae, and the source pulse can vary from trace-to-trace and is not necessarily minimum phase. All filtering operations borrowed from seismic data processing must be applied with care as some of the underlying assumptions for elastic waves generated at the surface of the earth are not valid or are different for electromagnetic waves.

Migration

Migration is a processing technique which attempts to correct for the fact that energy in the GPR profile image is not necessarily correctly associated with depths below the 2-D survey line (approximation #2 above). As with deconvolution, migration can be seen as an inverse processing step which attempts to correct the geometry of the subsurface in the GPR image with respect to the survey geometry. For example, a subsurface scattering point would show up in a GPR image as a hyperbolic-shaped feature (similar to Figure 5). Migration would associate all the energy in the wavelets making up the hyperbolic feature with the point of diffraction, and imaging of the actual earth structure (the heterogeneity represented by the point diffractor) would be imaged more clearly. Migration operators require a good estimate of subsurface velocity structure in order to apply the correct adjustments to the GPR image.

INTERPRETATION

If the subsurface was perfectly homogeneous, the GPR unit would not record any reflections. Thus, the fact that the earth is heterogeneous gives us radar reflection data to interpret. We associate radar reflections with changes in dielectric constant, which in turn are related to changes in soil or rock bedding, buried man-made objects, geologic intrusives, void space, fractures, clay type, and moisture content. Because an increase in moisture content dramatically reduces radar propagation velocity (increases dielectric constant), the average dielectric constant is often proportional to the water saturation of the soils/rock in the subsurface.

When the propagating source pulse passes through the heterogeneous earth, reflections are sent back to the surface where the receiving antenna records a scaled version of the source wavelet. This scaling is related to the reflection coefficient, which is a function of the dielectric contrast that describes the inhomogeneity encountered by the traveling wave. The deeper the inhomogeneity, the longer it takes for the scattered energy to travel back to the surface. Thus, when the antenna measurements are plotted with respect to time, information in the signal at later times is associated with greater depths. As the survey progresses, data are collected with respect to profile distance and measurements in each recording (trace) are associated with depth below the surface. In this way the GPR data represent an image of the subsurface structure. The radar propagation velocity is proportional to the square root of the dielectric constant. With a good estimate of the propagation velocity, images with respect to travel time (two-way travel time down and back to the surface) can be transformed directly to images with respect to depth.

Figure 7 displays GPR data over a heterogeneous sand and gravel aquifer from both a monostatic survey and a bistatic survey. The coherent reflection in both images at 200-300ns is the basal clay aquitard. Structure within the overlying aquifer appears slightly different in the two GPR profiles. There is a little more vertical resolution achieved with the monostatic radar, even though the nominal dominant frequency is less than that of the bistatic unit for this particular example. Otherwise, data look very similar. One thing to note is that the bistatic data were collected with a station interval of 1 meter. The monostatic

data in Figure 7 were plotted at 1 trace/m, but were actually recorded at about 40 traces/m. The fine horizontal sampling of the monostatic unit can be used to interpret smaller lateral changes. Where the gross structure is important, the extra data can be averaged to improve the signal coherency (reflections).

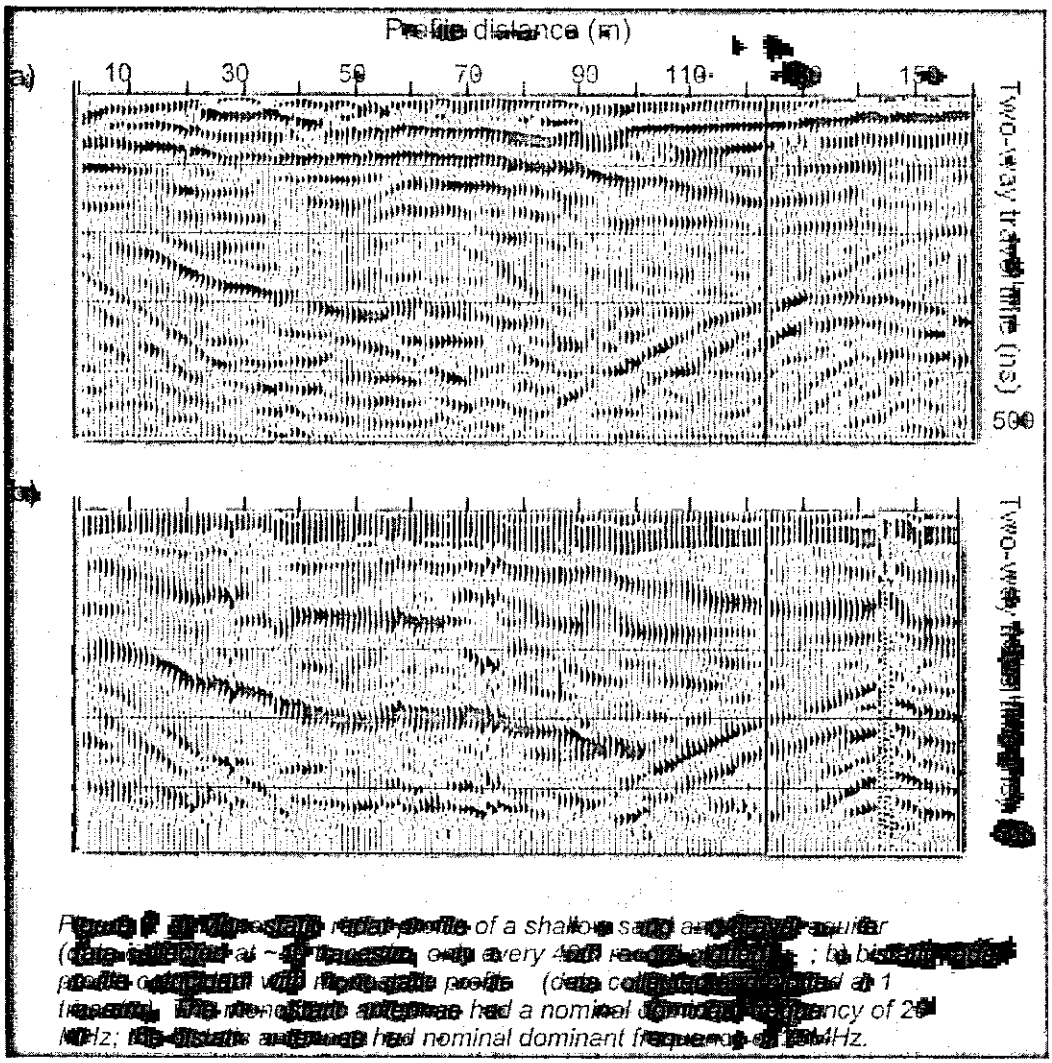

Figure 8. Monostatic radar profile of a shallow sand aquifer (data collected at ~40 traces/m, only every 4th trace plotted) ; b) bistatic radar profile corresponding with figure 7 profile (data collected at 1 trace/m). The monostatic antenna had a nominal dominant frequency of 25 MHz; the bistatic antenna had nominal dominant frequency of 100 MHz.

Electromagnetic wave velocity decreases with depth (in general), so that the theoretical resolution increases with depth as described earlier. However, this improvement is offset by the loss of high frequencies in the signal as it propagates which effectively reduces resolution. Attenuation is dependent upon conductivity, and increases with increasing frequency. Good radar media implies low conductive attenuation. On the other hand, a poor radar media implies higher conductivity which attenuates signal and reduces penetration. Table 2 shows some common examples of good and poor radar media.

Table 2

Good radar media	Poor radar media
dry salt	salt water
snow	metals
ice and fresh water	clay
peat	clay-rich soils
wet or dry sand	conductive minerals
dry rocks	

To summarize, the deepest penetration will occur in dry, nonclayey soils, and in dry rocks with no clay cementation. Snow and ice cover (and permafrost) will not adversely affect GPR data. When the soils or rocks are saturated, the conductive nature of the filling liquid becomes important. Fresh water is the most favorable for radar penetration.

Figure 8 displays examples of bistatic radar profiles collected with three different transmitter source frequencies, 200, 100 and 50MHz. All three profiles in Figure 8 were collected along the same survey line over a heterogeneous sand and gravel aquifer. The increased shallow resolution for the higher frequencies, offset by the shallower depth of penetration is evident.

The recording time windows for the three different surveys in Figure 8 were different, based on the expected increase in depth of penetration with decreasing dominant frequency. Although measurements were recorded for longer than 100ns with the 200MHz source, clearly there is no coherent signal in the deeper portion of the image. Similarly, for the 100MHz source. Although data were collected beyond 150ns, there is no coherent signal from depths associated with those times. In contrast, there appears to be signal well into the deepest portions of the 50MHz GPR image.

The soil stratigraphy displayed in the radar images of Figure 8 correlate across each profile. However, the higher frequencies in the 200MHz image offer the best vertical resolution. The 100MHz image has intermediate resolution, and the 50MHz image shows the grossest structural variation.

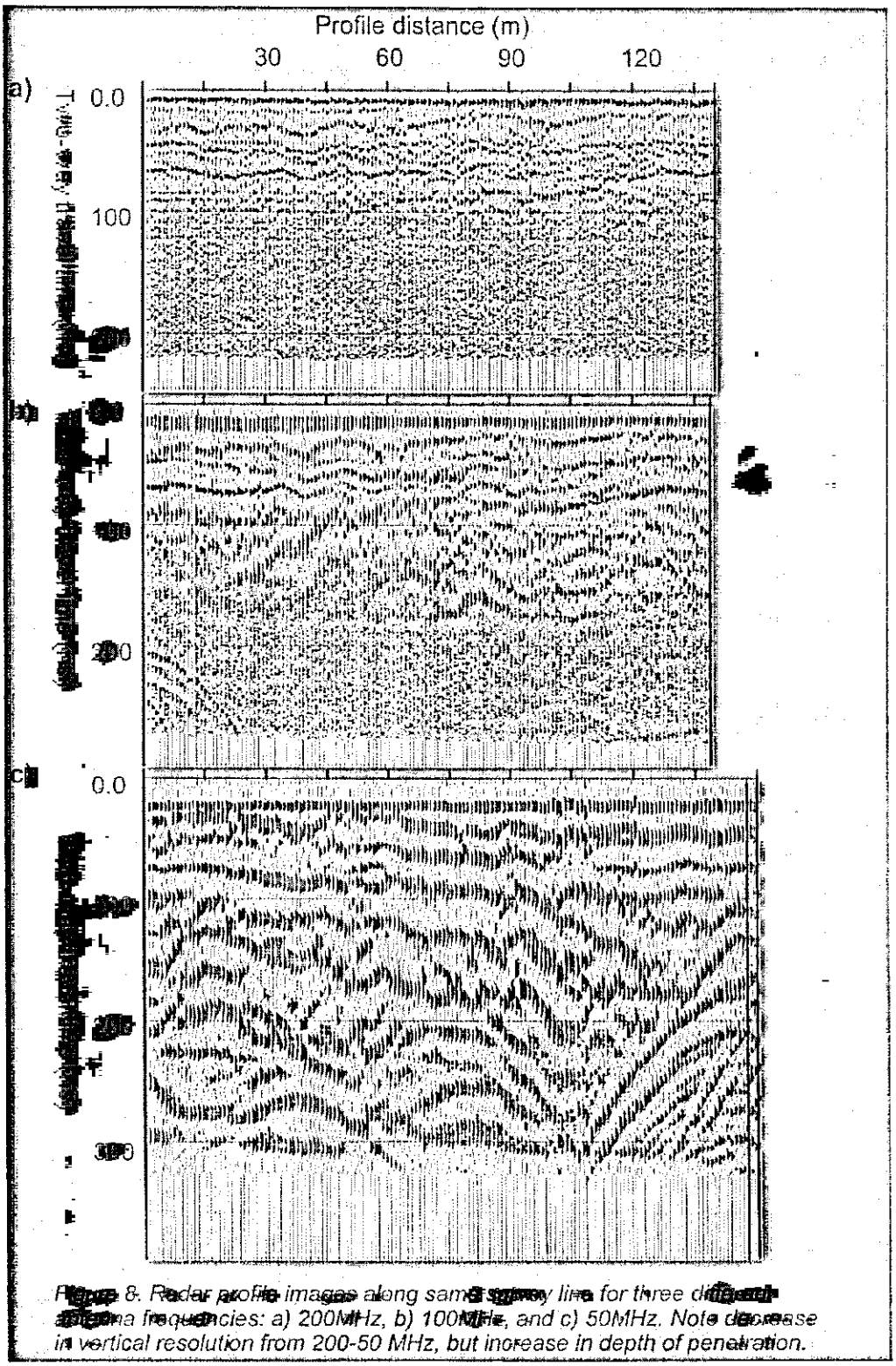

Figure 8. Radar profile images along same survey line for three different antenna frequencies: a) 200MHz, b) 100MHz, and c) 50MHz. Note decrease in vertical resolution from 200-50 MHz, but increase in depth of penetration.

Qualitative interpretation of GPR profiles is fairly straightforward, because the data are displayed in an (x-z) image plane. Soil and/or rock structural variation as a function of survey position and depth is readily seen. In addition, certain GPR signatures can relate to specific underground targets:

- attenuation losses related to conductive regions (clays, increased saturation)
- distinct natural layering versus chaotic in-filled trenches or excavation areas
- reflection strength variation may relate to changes in conductivity
- diffractions from point scatterers

There are two major things that will cause problems when interpreting GPR data: the presence of clay minerals and very inhomogeneous materials.

Clay minerals

When clay minerals are present in the rocks and soils, dissolution will create ionic solutes. These ions become mobilized in saturated pore space, and conductivity increases. The presence of clay minerals will tend to increase conductivity and thus increase the amount of conductive attenuation. It is hard for radar to "see through" clayey soils.

Very inhomogeneous materials

When materials are extremely inhomogeneous, coherent reflections will be hard to find in the GPR images. Instead, the recorded signals will be made up primarily of diffraction (scattered) energy. The scattering can often be related to point inhomogeneities (diffractors, or scatterers) in subsurface and/or above ground, and the diffraction apex can give information about the point diffractors; although true analysis of this sort requires 3-D visualization/interpretation. Diffractions are only clearly represented in 2-D if the survey is perpendicular to a 2-D object (e.g., a buried pipe). Otherwise, the electromagnetic radiation travels in all directions away from the source, not just in the plain described by the horizontal survey coordinate and the depth of investigation. This energy will be scattered off of discontinuities that are not directly below the survey line, but the energy will still be recorded by the survey receiver. Plotting the data in 2-D cross-sections is truly a matter only of convenience. Care must be taken during interpretation as some of the features in the 2-D profile of subsurface structure will be artifacts due to the energy scattered from outside the imaging plain. If the inhomogeneity is too strong, there may not even be any coherent diffractions to interpret.

Forward modeling of electromagnetic waves in lossy (attenuative) dielectric media can be helpful for qualitative and quantitative interpretation. Quantitative information can also be obtained with limited ground truth or along with interpretation of other geophysical data sets.

CONCLUSION

The GPR method records microwave radiation that passes through the ground and is returned to the surface. A transmitter sends a microwave signal into the subsurface, and the radar waves propagate at velocities that are dependent upon the dielectric constant of the subsurface medium. Changes in the dielectric constant that are due to changes in the subsurface materials cause the radar waves to reflect, and the time it takes energy to return to the surface relates to the depth at which the energy was reflected. Thus, interpretation of this reflected energy yields information on structural variation of the near subsurface. Data are most often collected along a survey profile, so that plots of the recorded signals with respect to survey position and travel-time can be associated with images of geologic structure as a function of horizontal position and depth. Ground penetrating radar can be collected fairly rapidly, and initial interpretations can be made with minimal data processing, making the use of ground penetrating radar for shallow geophysical investigation quite cost-effective.

Detailed structural interpretation can be important for hydrological and geotechnical applications such as determining soil and bedrock characteristics in the shallow subsurface. In addition, high-resolution imaging is important for monitoring structural integrity of buildings, mine walls and roadways and bridges. Ground penetrating radar (GPR) is the only geophysical technique that can offer the horizontal and

vertical resolution necessary for many of these applications. The GPR method can be used for reconnaissance (anomaly location) as well as for the more detailed studies.

REFERENCES

Daniels, D., 1996, Surface-penetrating radar: Inst. Electr. Eng.

Daniels, J., 1989, Ground penetrating radar: *in* Symposium on the application of geophysics to engineering and environmental problems, March 13-16, 1989, Colorado School of Mines, Golden, Colorado, Fitterman, D., Anderson, A., Bell, R., Corbett, J., Davenport, C., Bierley, C., Hulse, S., Lepper, M., Nicholl, J., Paillet, F., and Romig, P., eds: The Environmental & Engineering Geophysical Society.

Hempen, G. L., and A. W. Hatheway, 1992, Geophysical methods for hazardous waste site characterization, Special Pub. No. 3: Assn. Eng. Geol.

Yilmaz, O., 1987, Seismic data processing, Investigations in Geophysics No. 2: Soc. Expl. Geophys.

APPENDIX C

GROUND PENETRATING RADAR (GPR): A TOOL FOR MONITORING BRIDGE SCOUR

Doyle J. Webb*, Neil L. Anderson*, Tim Newton+ and Steve Cardimona*

*Department of Geology and Geophysics, University of Missouri-Rolla, Rolla, MO 65401
+Missouri Department of Transportation, Jefferson City, MO

ABSTRACT

The University of Missouri-Rolla (UMR) and the Missouri Department of Transportation (MoDOT) acquired ground-penetrating radar (GPR) profiles across streams at ten different bridge sites in southeast and central Missouri. The intent was to determine whether GPR is an effective tool for monitoring bridge scour (i.e., estimating water depths and identifying in-filled fluvial scour features).

The interpretation of the acquired profiles indicates that the GPR tool can be used to accurately estimate water depths in shallow fluvial environments (<20 feet). In some instances, in-filled (paleo) scour features can also be imaged and mapped.

GPR has certain advantages over alternate methods for estimating water depths. GPR can provide an essentially continuous profile-type image of the stream channel and the sub-water bottom sediment along the route selected. The GPR antennae are non-invasive and can be moved rapidly across (or above) the surface of a stream at the discretion of the operator. The GPR tool does not need to be physically coupled to the water surface and can be operated remotely, ensuring that neither the operator nor equipment need be endangered by floodwaters.

INTRODUCTION

The determination of seasonal variations in water depth (monitoring of bridge scour), and the assessment of erosional and depositional patterns in the vicinity of existing or planned bridge piers is essential to understanding the fluvial scour process on a site-specific scale. The design of preventative (during bridge construction) or remediation measures is most efficient and cost-effective if the local scour process is understood.

Unfortunately, riverbed scour occurs mostly during high flow stages. Scour depth/breadth information can be very difficult (and dangerous) to acquire at such times. Additionally, scour features are often in-filled as peak flow subsides making the direct measurements of maximum scour depth/breadth impossible after the fact.

In an effort to assess the utility of GPR when employed as a bridge scour monitoring/investigation tool, UMR and MoDOT acquired GPR profiles across streams at ten different bridge sites in southeastern and central Missouri. The GPR profiles were acquired using GSSI SIR-10B radar unit equipped with a 200 MHz monostatic antenna. (At some sites, duplicate profiles were acquired using an additional higher frequency antenna.) A scaled meter was used to manually measure stream depths at specific control locations.

The report submitted to MoDOT included a brief synopsis of the bridge scour process, overviews of both the GPR method and alternate methods for studying bridge scour, and example interpreted GPR profiles.

TYPES OF SCOUR: CLASSIFICATIONS

The erosion of riverbed material at bridge sites is a result of natural stream processes, particularly seasonal variations in water depth and velocity. Indeed, maximum scour depths are often estimated by assuming that depth is proportional to the rise of the water surface elevation (Xanthakos, 1995). Bridge scour is also influenced by bridge components such as piers, abutments, roadway embankments, and the superstructure itself, and is classified as general, contraction, and local (Figure 1).

General Scour is illustrated in Figure 1a. In this process, progressive erosion at the outer

bends along a meandering river cause the progressive lateral shifting of the stream channel and attendant variations in water depths. General scour can result in the undermining of abutments, if certain precautionary measures such as the placement of concrete or asphalt mats over the riverbank, and installation of abutment foundations below the lower depth of possible scour, are not taken.

Contraction Scour is illustrated in Figure 1b. In this process, the narrowing of the waterway at a bridge site increases water velocity and accentuates erosion. A remedy is to enlarge the channel, or ensure the channel under the bridge is the same size as the channel adjacent to the bridge.

Local Scour is illustrated in Figure 1c. In this process, river obstructions such as bridge piers cause contraction of channel cross section resulting in higher flow velocities and accentuated erosion. The magnitude of scour is dependent upon pier configuration and inclination with respect to flow, contraction of waterways, and volume of debris accumulated at bridge.

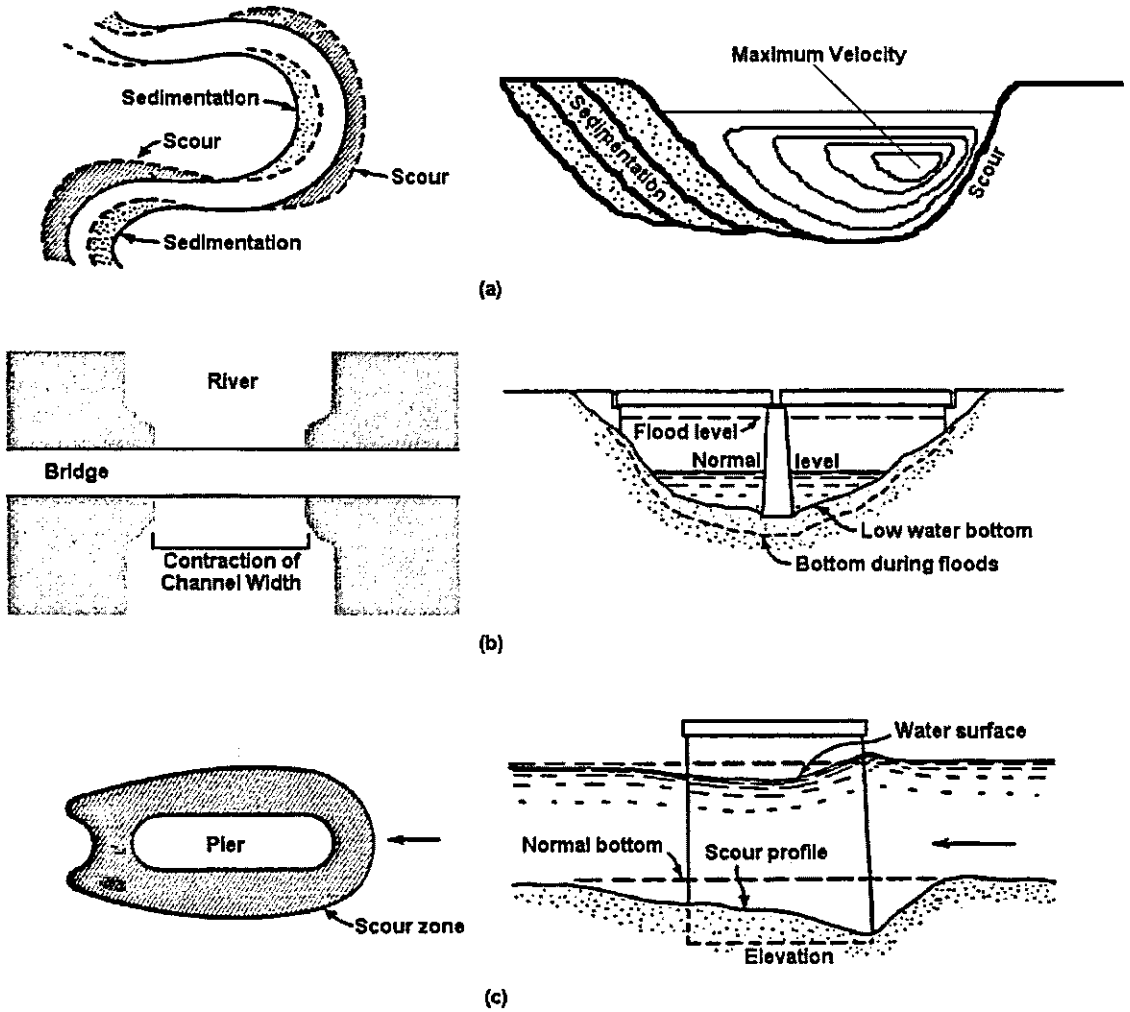

Figure 1. *Forms of scour in waterways: (a) general scour, (b) contraction scour, and (c) local scour (after Xanthakos, 1995). Left side plan view and right side cross-section.*

GEOPHYSICAL METHODS FOR EVALUATING SCOUR

Several geophysical techniques are commonly used to measure water depths and/or depth/breadth of in-filled scour features. Techniques include reflection seismic profiling, echo sounding (in continuous or spot survey mode), electrical conductivity probing, and ground penetrating radar (GPR). Each tool has characteristic strengths and weaknesses.

REFLECTION SEISMIC PROFILERS

The reflection seismic profiling technique typically employs a coupled acoustic source transducer/receiver transducer placed immediately beneath the surface of the water. The acoustic source transducer produces a short period (frequencies in kilohertz range) pulsed acoustic signal at regular time or distance intervals as it towed across the surface of the water. The high-frequency pulsed seismic signal propagates through the water column and into the sub-water bottom sediment. Some of the acoustic energy is reflected at the water bottom and at other prominent acoustic impedance interfaces (e.g., lithological and/or facies interfaces; Figure 2) and returned to the receiver. The receiver measures and digitally records the magnitude of the reflected energy as a function of two-way travel time. Magnitude of reflected signal vs. arrival time for each source/receiver location is visually displayed as a time-trace. Traces from adjacent source locations are plotted side-by-side forming an essentially continuous time-depth profile of the stream bottom and shallow sub-strata (including in-filled scour features). Estimated seismic interval velocities can be used to transform the time-depth profile into a depth profile. Water velocities are a function of suspended sediment load, and can vary appreciably.

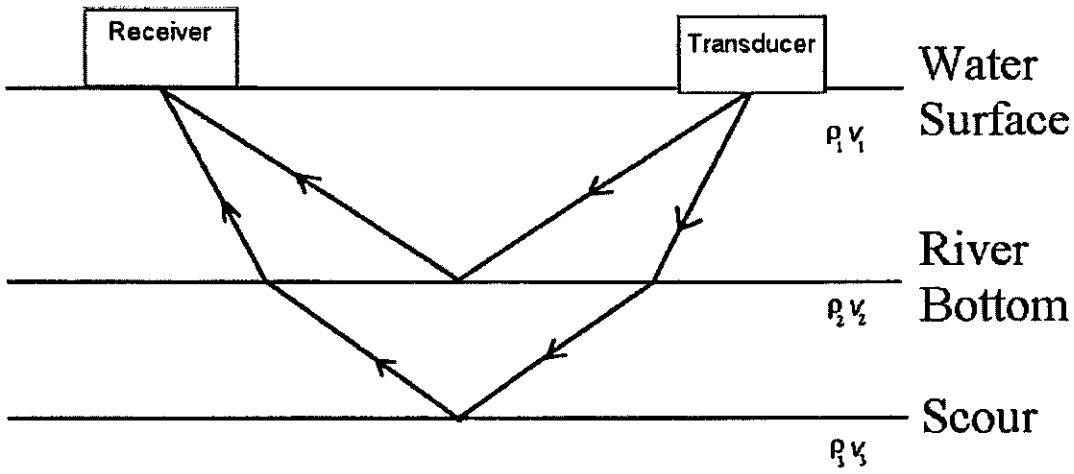

Figure 2. *Reflection seismic profiling. Some of the pulsed acoustic energy emitted from the transducer is reflected from the water bottom, the base of in-filled scour features and other prominent acoustic interfaces, and returned to the receiver.*

The main advantages of reflection seismic profiling are as follows:

1. The tool can provide an accurate depth-structure model of the water bottom (to depths on the order of tens of meters), and an image of the sub-water bottom sediment to depths on the order of meters (dependent upon the frequency of the acoustic source).

2. Post acquisition processing (including 2-D migration) can be applied.

3. The tool can provide an accurate image of the sub-water bottom sediment to depths on

the order of meters. Lithological/facies units with thickness on the order of 0.1 m can be imaged with higher-frequency antenna (14 kHz units).

The main disadvantages of the reflection seismic profiling tool are as follows:

1. The source and receiver need to be submerged. Profiles cannot be extended across emerged bars or onto the shore.

2. The equipment is relatively expensive (hardware and software).

3. Data may be contaminated by noise (multiple reflections, and echoes from the shoreline, water bottom, and/or piers).

4. Post acquisition processing (including migration) may be required in areas where significant structural relief is present.

ECHO SOUNDERS (FATHOMETERS)

Echo sounders (fathometers) are similar to the reflection seismic profilers in that they also employ a coupled acoustic source transducer/receiver transducer placed immediately beneath the surface of the water. Echo sounders differ from reflection seismic profilers in that they emit higher frequency acoustic source pulses (frequencies in 100 kHz range), some of which is reflected at the water bottom, returned to the receiver, and stored digitally. (Because of the rapid attenuation of the high frequency pulsed acoustic energy, relatively little signal is transmitted into or reflected from within sub-water bottom sediment.) Traces from adjacent source/receiver locations are plotted side-by-side to form an essentially continuous time-depth profile of the stream bottom. Estimated seismic interval velocities can be used to transform the time-depth profile into a depth profile. Water velocities are a function of suspended sediment load, and can vary appreciably.

The main advantages of the echo sounding tool (in continuous mode) are as follows:

1. The tool can provide an accurate depth-structure model of the water bottom (if acoustic velocities are known).

2. Post acquisition processing (migration) can be applied.

The main disadvantages of the echo sounding tool (in continuous mode) are as follows:

1. The source and receiver need to be submerged. Profiles cannot be extended across emerged sand bars or onto the shore.

2. The equipment is relatively expensive (hardware and software).

3. Data may be contaminated by noise (multiple reflections, and echoes from the shoreline, water bottom, and/or piers).

4. Post acquisition processing (migration) may be required in areas where significant structural relief is present.

5. The tool cannot be used to image in-filled scour features within sub-water bottom sediments.

Echo sounders are also employed in a spot survey mode. In this type of survey, sounding data (single reflection traces) are acquired at irregularly (or uniformly) spaced intervals (typically on the order of meters) at the water surface. The first high-amplitude reflected event is usually

interpreted to be the water bottom reflection. Note, that spot data usually cannot be accurately migrated because of aliasing problems.

The main advantages of the echo sounders (in spot mode) are as follows:

1. The tool can provide an accurate depth-structure model of the water bottom if acoustic velocities are known.

2. The equipment is relatively inexpensive.

The main disadvantages of the echo sounders (in spot mode) are as follows:

1. The source and receiver need to be submerged. Data cannot be acquired across emerged sand bars or onto the shore.

2. Data may be contaminated by noise (i.e., the first high amplitude event may not be from the water bottom).

3. Water depths may be significantly underestimated in areas of extreme water bottom relief (curved surfaces with radii less than water depth).

ELECTRICAL CONDUCTIVITY PROBES

The electrical conductivity probe method works on the principle that the conductivity of the riverbed and the river water are different. The nature of suspended sediment, dissolved ions and chemical characteristics of water determine its conductivity. Parent materials and the composition of the water in the sediments determine the electrical conductivity of the riverbed. In this technique, multiple conductivity sensors are placed on a probe, which is driven vertically into the riverbed at the desired location and left for periodic monitoring. At least one of the probe's sensors extends above the riverbed, while multiple sensors are placed within the sub-water bottom sediments (Hayes 1995). If scour occurs at the location of the probe to the extent that one or more previously buried sensors are exposed to water, then those newly exposed sensors will measure the conductivity of the flowing water instead of the sediments in the riverbed. Hayes (1995) states the method works well only if the conductivity of the riverbed and water differ significantly. Hayes (1995) also states that the tool cannot be used for direct measurement of in-filled scour features.

The main advantages of the electrical conductivity probe method are as follows:

1. The tool allows for long term monitoring.

2. The method is relatively inexpensive.

The main disadvantages of the electrical conductivity probe method are as follows:

1. The tool only monitors scour at the location of the probe.

2. The tool can be used effectively only where water and sediment conductivities differ appreciably.

3. The tool may pose a hazard to navigation.

4. Scour features can be grossly underestimated.

5. The tool cannot be used to image scour features within the sub-water bottom sediments.

GROUND PENETRATING RADAR (GPR)

The ground-penetrating radar (GPR) tool typically employs a coupled source antenna/receiver antenna placed on or immediately above the surface of the water. The source transducer produces a short period (frequencies in megahertz range) pulsed electromagnetic signal at regular time or distance intervals as it towed across or above the surface of the water. Some of this pulsed electromagnetic (EM) energy is reflected from the water bottom and other prominent dielectric interfaces (facies contacts), and returned to the receiver. The arrival time and magnitude of the reflected energy is recorded at the surface by the receiver antenna. Traces from adjacent source locations are generally plotted side-by-side to form an essentially continuous time-depth profile of the stream bottom and shallow sub-strata (including in-filled scour features). Estimated EM velocities can be used to transform the time-depth profile into a depth profile. Velocities are a function of suspended sediment load, and can vary appreciably.

The main advantages of the GPR profiling tool are as follows:

1. The source and receiver do not need to be submerged. Profiles can be extended across emerged sand bars or onto the shore.

2. The tool can provide an accurate depth-structure model of the water bottom and sub-bottom sediments (to depths on the order of 9 m).

3. Post acquisition processing (migration) can be applied.

4. Lithological/facies units with thickness on the order of 0.1 m can be imaged with intermediate-frequency units (200 MHz).

The main disadvantages of the GPR profiling tool are as follows:

1. The equipment is relatively expensive (hardware and software).

2. Data may be contaminated by noise (multiple reflections and echoes from pier footings).

3. Post acquisition processing (migration) may be required in areas where significant structural relief is present.

4. The tool is not normally effective when water depths exceed 9 m.

5. The tool cannot be used in saline waters.

ACQUISITION OF GROUND PENETRATING RADAR AT TEN BRIDGE SITES

In an effort to assess the utility of GPR when employed as a bridge scour investigation tool, GPR profiles were acquired at ten different bridge sites in southeastern and central Missouri. A Geophysical Survey Systems (GSSI) SIR-10B unit equipped with a 200 MHz antenna was employed. A sampling rate of 50 scans/second and a range (trace length) between 125 and 350 nanoseconds was employed. At some sites, duplicate profiles were acquired using a 400 MHz antenna.

At each bridge site, GPR profiles were collected both parallel and perpendicular to current flow (Figure 3). At some bridge sites, GPR data could not be collected immediately adjacent to piers, due to obstructions (usually snagged debris). Data were acquired by maneuvering the antenna across the surface of the water in one of three ways: from the bridge deck, manually, or by boat. The acquisition method used at each of the ten bridges investigated is displayed in Table 1.

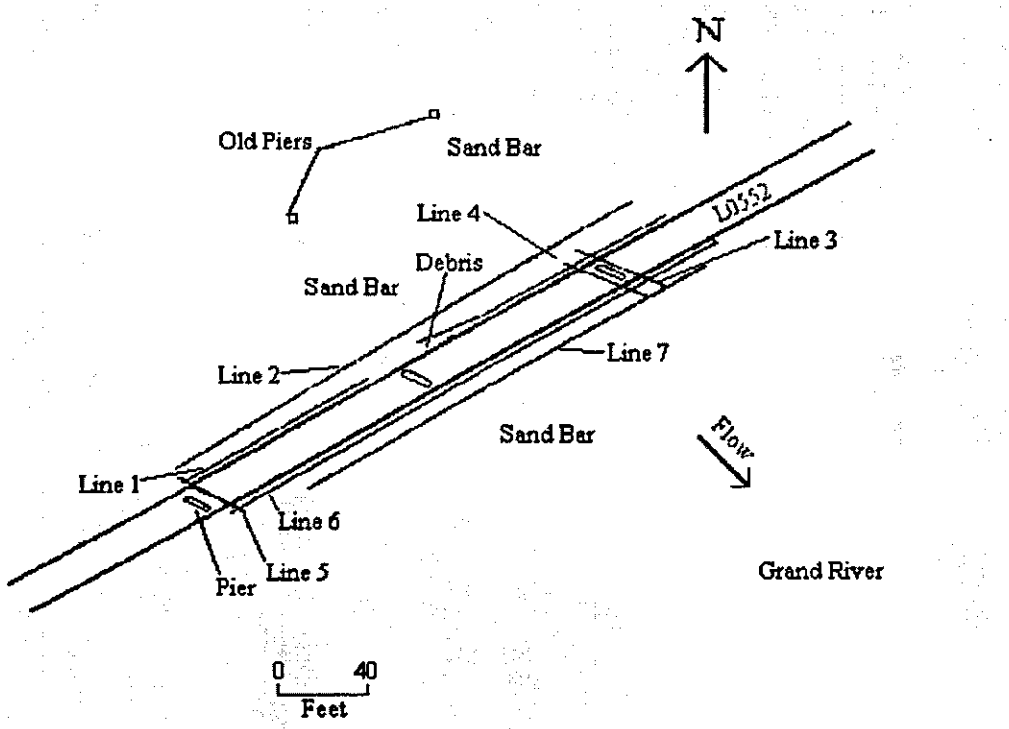

Figure 3. *Survey site 3, Grand River, Livingston, Missouri. Profiles were acquired either parallel (e.g., lines 3, 4 and 5) or perpendicular (e.g., lines 1, 2, 6 and 7) to current flow.*

PROCESSING OF GPR DATA

The acquired GPR data were processed on a Pentium PC using the commercial processing package RADAN. The following run stream was employed.

1. Distance normalization
2. Horizontal scaling (stacking)
3. Vertical frequency filtering
4. Horizontal filtering
5. Velocity corrections
6. Migration
7. Gain

The applied processing steps increased the interpretability of the GPR profiles by removing unwanted random noise and enhancing the amplitude of events of interest (reflections from water bottom and base of in-filled scour features). Unfortunately some of the GPR data were contaminated by high-amplitude water-bottom multiple reflections which could not be removed effectively using the RADAN software. These multiple events arrived after the primary water bottom reflection and in places mask reflections from the base of in-filled scour features.

Site	Bridge number	Location (County)	Waterway	Height of bridge above water (ft)	Maximum water depth (ft)	Data collection method
1	A-3708 A-3709	Butler	St. Francis River	31	16.6	Bridge deck
2	L927 A5648	Stoddard	Wahite Ditch # 1	Not measured	5.9	Bridge deck
3	L05552	Livingston	Grand River	40	5.5	Wading
4	A-2867	Chariton	Grand River	Not measured	7.6	Boat
5	L-302	Dunklin	Elk Chute ditch	20	3.2	Wading
6	A-2336	Dunklin	Drainage Ditch # 259	21	3.8	Wading
7	A-2333	Dunklin	Drainage Ditch # 1	22	4.9	Wading
8	A-2332	Dunklin	Drainage Ditch # 81	19.8	7.7	Bridge deck
9	A-2334	Dunklin	Drainage Ditch # 66	24.3	3.5	Wading
10	A-2334	Dunklin	Drainage Ditch # 251	22	7	Wading

Table 1. *Site logistics and characteristics. Example GPR profiles from Sites 1, 6, 7 and 10 are incorporated into this paper.*

INTERPRETATION OF EXAMPLE GPR PROFILES

GPR PROFILES ACQUIRED PARALLEL TO FLOW

Selected, representative GPR profiles (parallel to flow) from sites with different channel characteristics are presented in this section. Study sites 6 and 7 are shown as Figures 4 and 6, respectively. Representative versions of example GPR profiles are shown in Figures 5 and 7.

In Figures 5 and 7, non-interpreted stacked, migrated, and velocity-corrected GPR sections are presented as captions a, b, and c, respectively. Interpreted stacked, migrated, and velocity-corrected GPR sections are shown as captions d, e, and f, respectively. The depth scales on the stacked and migrated sections were calculated using EM (electromagnetic) water velocities only. As a result, the estimated water bottom depths on the stacked and migrated sections are relatively accurate, however depths to sub-water bottom structures (including in-filled scour features) are inaccurate. In contrast, scaled depths on the velocity-corrected profiles were calculated using different EM velocities for the water and sub-water bottom sediment. Estimated depths on the velocity-corrected profiles are therefor more accurate, particularly within the sub-water bottom section. (Note: Water velocities were estimated on the basis of known water depths and recorded GPR transit times. Sub-water bottom velocities were estimated on the basis of on-site field tests during which metal plates were buried beneath fluvial sediment.)

The arrows on Figures 5 and 7 represent flow directions. The superposed gray line on the interpreted GPR profiles represents the interpreted water bottom. The superposed white line on the interpreted GPR profiles represents reflections from the base of interpreted in-filled scour features. The thickness of in-filled scour features (represented by "S") can be estimated by measuring the distance from the white line to the top of the gray line on velocity-corrected profiles (only). The maximum amount of scour and in-filled scour at each site is listed in Table 1. Piers along the profile are displayed as rectangular columns on the sections. Reflections from the flanks or footings of some of piers are characterized as prominent diffractions on the GPR profiles.

Example Profile 4, Site 6 (Figure 4): The Site 6 bridge, located on Highway 164, crosses

a drainage ditch near the town of Kennet, Missouri. GPR profile 4 (Figure 5) was acquired parallel to current flow, and immediately adjacent to two piers. The reflection from the water bottom is clearly evident on all of the processed profiles. Diffractions originating from one of the pier footings are also evident on all profiles, including the migrated sections. (Note, the GPR data were migrated using the water velocity only (limitation of RADAN software), and as a result the diffractions originating from the sub-water bottom footing were not effectively collapsed.) Water bottom depths (gray reflector) can be estimated most accurately from the analysis of the migrated GPR profiles. The depth and thickness of sub-water bottom layers (in-filled scour features) is accurately depicted only on Figures 5c and 5f. The first-order water bottom multiple is labeled on the GPR profiles.

Example Profile 3, Site 7 (Figure 6): The Site 7 bridge, located on Highway 164, crosses a drainage ditch near the town of Kennet, Missouri. GPR profile 3 (Figure 7) was acquired parallel to current flow, and immediately adjacent to a pier. (The diffractions originating from the pier footings are evident on the stacked, migrated and velocity-corrected profiles.) The reflection from the water bottom is clearly evident on all of the processed profiles. The data were migrated using the water velocity only, and as a result the diffractions originating from the sub-water bottom footing were not effectively collapsed. Water bottom depths (gray reflector) can be estimated most accurately from the analysis of the migrated GPR profile. The depth and thickness of sub-water bottom layers (in-filled scour features) is accurately depicted only on Figures 7c and 7f. The first-order water bottom multiple is labeled on the GPR profiles, as is the multiple originating from the footing of the pier.

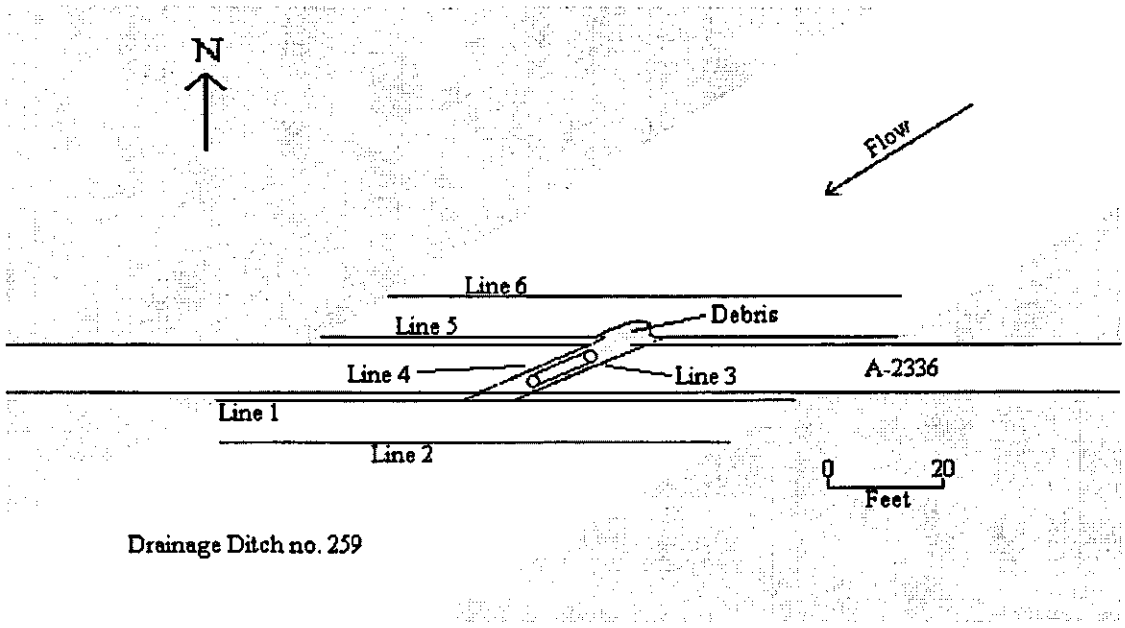

Figure 4. *Survey site 6 (Table 1), drainage ditch # 259, Dunklin County, Missouri.*

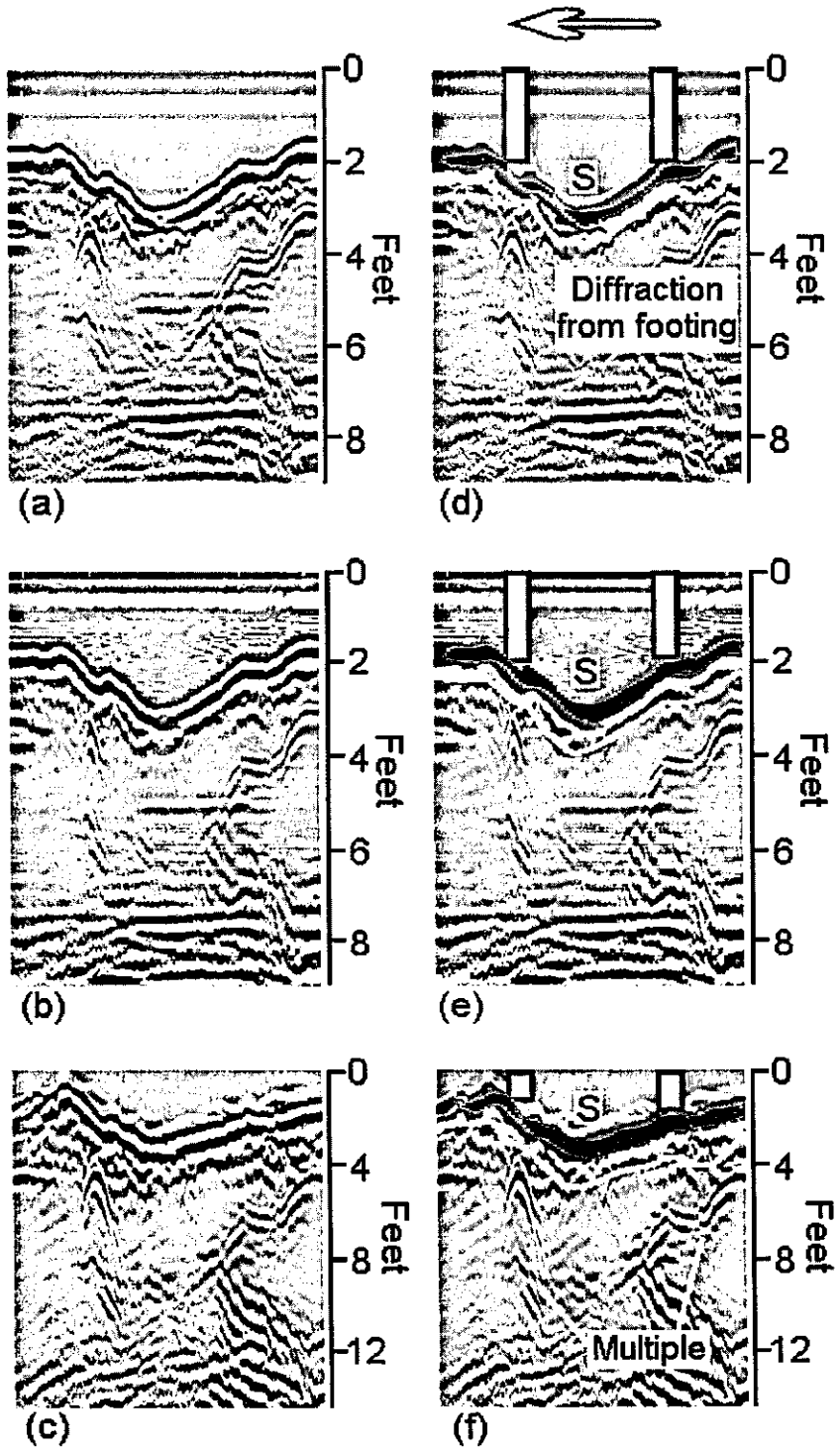

Figure 5. *Profile 4, site 6 (Figure 4): (a) stacked, (b) migrated, (c) velocity corrected, and interpreted (d) stacked, (e) migrated, and (f) velocity corrected versions. Gray and white lines identify water bottom and extent of in-filled scour, respectively.*

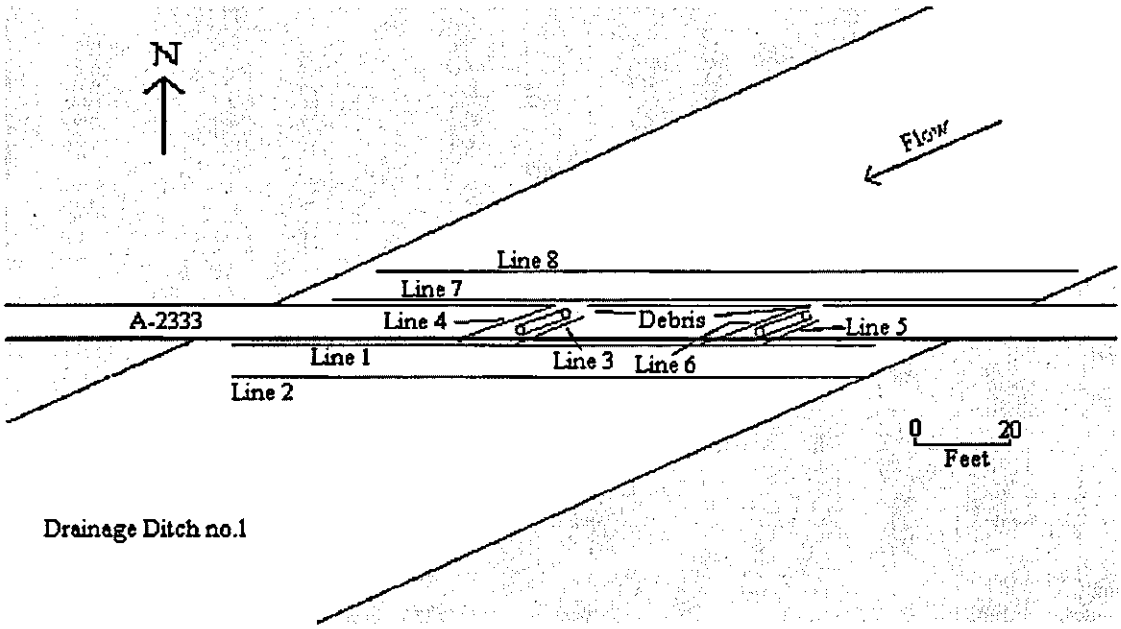

Figure 6. *Survey site 7 (Table 1), drainage ditch #1, Dunklin County, Missouri.*

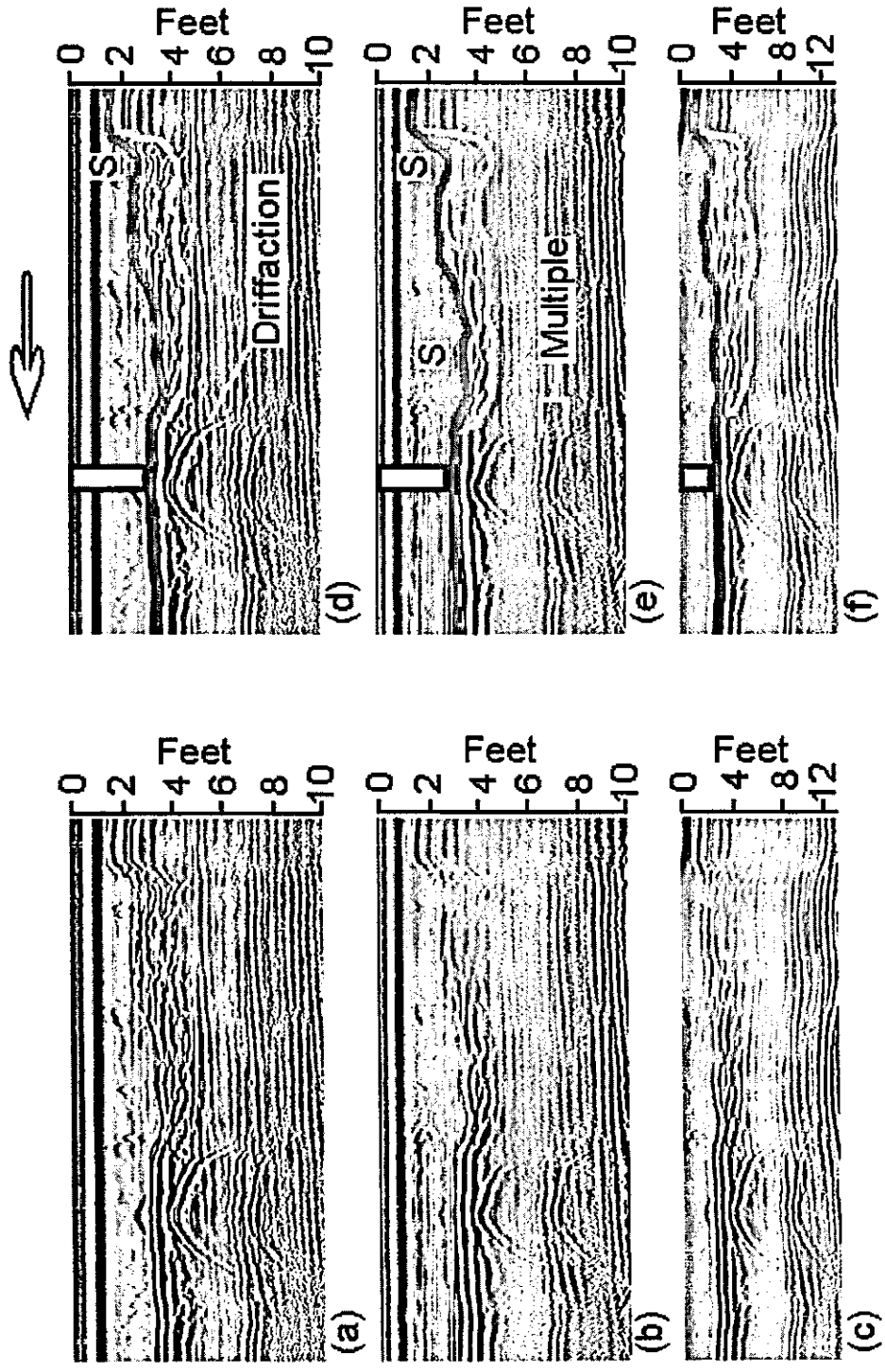

Figure 7. *Profile 3, site 7 (Figure 6): (a) stacked, (b) migrated, (c) velocity corrected, and interpreted (d) stacked, (e) migrated, and (f) velocity corrected versions. Gray and white lines identify water bottom and extent of in-filled scour, respectively.*

PROFILES ACQUIRED PERPENDICULAR TO CURRENT FLOW

Selected, representative GPR profiles from three sites with different channel characteristics are presented in this section. Study sites 1 and 9/10 are shown as Figures 8 and 9 respectively. Representative profiles are shown as Figures 10-11, 12-15/16-17, respectively.

Stacked and migrated profiles (both non-interpreted and interpreted), are presented for Profile 1, Site 1 (Figures 10 and 11). Stacked, migrated, and velocity-corrected profiles (non-interpreted and interpreted) are presented for the Profile 1, Site 9 example (Figures 12-15). Stacked and migrated profiles (non-interpreted and interpreted) are presented for Profile 7, Site 10 (Figures 16-17). Depth scales on the stacked and migrated profiles were calculated using EM water velocities only. The water depths on the migrated profiles are accurate, however depths to any sub-water bottom structures are inaccurate. The estimated depths on the velocity-corrected profiles were calculated using different EM velocities for water and sediment, and present a more accurate depth image of the water bottom and sub-water bottom sediment structure.

The gray lines on the interpreted GPR profiles represent the interpreted water bottom. The white lines across the GPR profiles represents reflections from the base of interpreted in-filled scour features. The thickness of in-filled scour features (represented by "S") can be estimated by measuring the distance from the white line to the top of the gray line on velocity-corrected profiles. The maximum amount of scour and in-filled scour at each site is listed in Table 1. Piers along the profile are displayed as rectangular columns on the sections. Reflections from the flanks or footings of some of the piers are characterized as prominent diffractions on the GPR profiles.

Example Profile 2, Site 1: Site 1 bridge, located on Highway 60, crosses the St. Francis River near the town of Poplar Bluff, Missouri. The reflection from the water bottom (gray event) is clearly evident on the processed profiles (Figures 10 and 11). The data were migrated using the water velocity only. Water bottom depths (gray reflector) are most accurately depicted on the migrated GPR profile. Note that significant in-filled scour features were not identified on the GPR profile; hence velocity corrections were not applied. Note also that the GPR profile 2 crosses deeply incised scour features (about 8 feet deep).

Example Profile 1, Site 9: The Site 10 bridge, located on Highway 164, crosses a drainage ditch near the town of Kennet, Missouri (Table 1; Figure 9). The reflection from the water bottom is clearly evident on all of the presented GPR profiles (Figures 12-16). However, water bottom depths (gray reflector on interpreted GPR sections) are most accurately depicted on the migrated GPR profile (Figures 12b and 13b). Non-interpreted and interpreted stacked and velocity-corrected sections are displayed in Figures 14 and 15.

Example Profile 7, Site 10: The Site 10 bridge, located on Highway 164, crosses a drainage ditch near the town of Kennet, Missouri (Table 1, Figure 11). GPR profile 7 (Figures 17-18) was acquired perpendicular to current flow, and adjacent to a pier, however prominent diffractions from the pier footings are not evident on the stacked, migrated or velocity-corrected profiles. The reflection from the water bottom is clearly evident on all of the processed profiles. Water bottom depths (gray reflector) can be estimated most accurately from the analysis of the migrated GPR profile (Figure 17b). The depth and thickness of sub-water bottom layers (in-filled scour features) is accurately depicted only on Figure 18b. Evidence of two previous scour events is observed on the GPR profiles.

CONCLUSION

During high-flow stages streambed materials around bridge piers are frequently removed by floodwaters. This process can compromise the structural integrity of the bridge and in extreme cases, lead to failure or collapse. An understanding of local scour processes at specific bridge sites is therefore essential.

During the summer and fall of 1999, ground-penetrating radar data were collected, processed and interpreted in an effort to test this tool's ability to image water bottom and in-filled scour features in shallow Missouri waterways. Multiple GPR profiles were acquired at ten bridge sites, each of which was characterized by different channel characteristics.

Based on the analysis of the acquired data, we have concluded that GPR can be a useful, cost-effective tool for estimating water depths and identifying and mapping in-filled scour features.

The main advantages of the GPR profiling tool are as follows:

1. GPR can provide an essentially continuous image of the stream channel and the sub-water bottom sediment along the route selected.

2. The GPR tool can provide an accurate depth-structure model of the water bottom and sub-water bottom sediments (to depths on the order of 30 feet). Lithological/facies units with thickness on the order of 0.3 feet can be imaged with intermediate-frequency antenna (200 MHz).

3. The GPR antennae are non-invasive and can be moved rapidly across (or above) the surface of a stream at the discretion of the operator. The GPR tool does not need to be physically coupled to the water surface and can be operated remotely, ensuring that neither the operator nor equipment need be endangered by floodwaters.

4. Profiles can be extended across emerged sand bars or onto the shore.

5. The digital GPR data can be stored, and post acquisition processing (including migration) can be applied.

The main disadvantages of the GPR profiling tool are as follows:

1. The equipment is relatively expensive (re: hardware and software).

2. Data may be contaminated by noise (multiple reflections and echoes from pier footings).

3. Post acquisition processing (migration) may be required in areas where significant structural relief is present.

4. The tool is not normally effective when water depths exceed 30 feet.

5. The tool cannot be used in saline waters.

REFERENCES

Xanthakos, Petros P., 1995, Bridge Substructure and Foundation Design. Upper Saddle River, NJ: Prentice Hall, 1995

Hayes, D.C. and Drummond, F.E., 1995, Use of Fathometers and Electrical-Conductivity Probes to Monitor Riverbed Scour at Bridge Piers. U.S.G.S. Water-Resource Investigations Report 94-4164. Richmond, VA, 1995

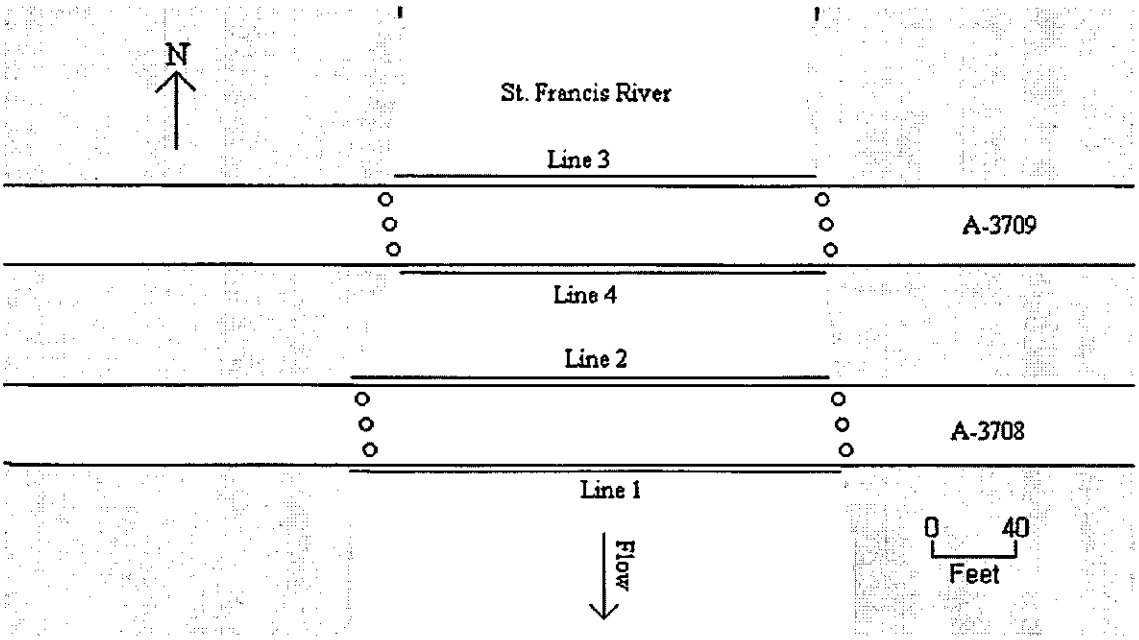

Figure 8. *Survey site 1 (Table 1), St. Francis River, Butler County, Missouri.*

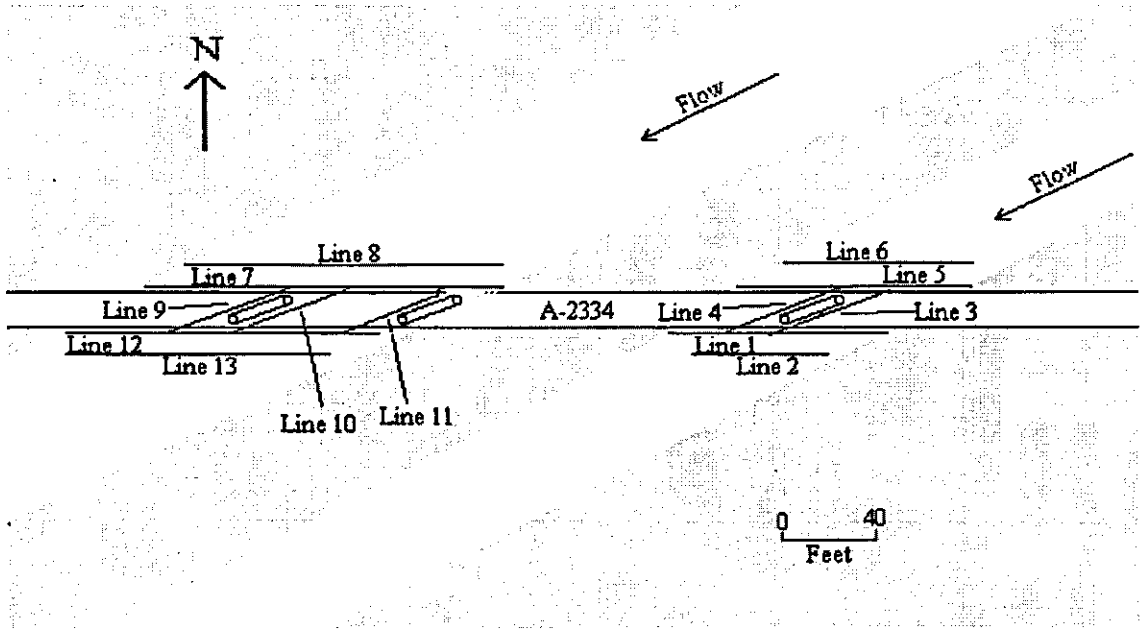

Figure 9. *Survey sites 9 and 10 (Table 1), drainage ditch #66, Dunklin County, Missouri*

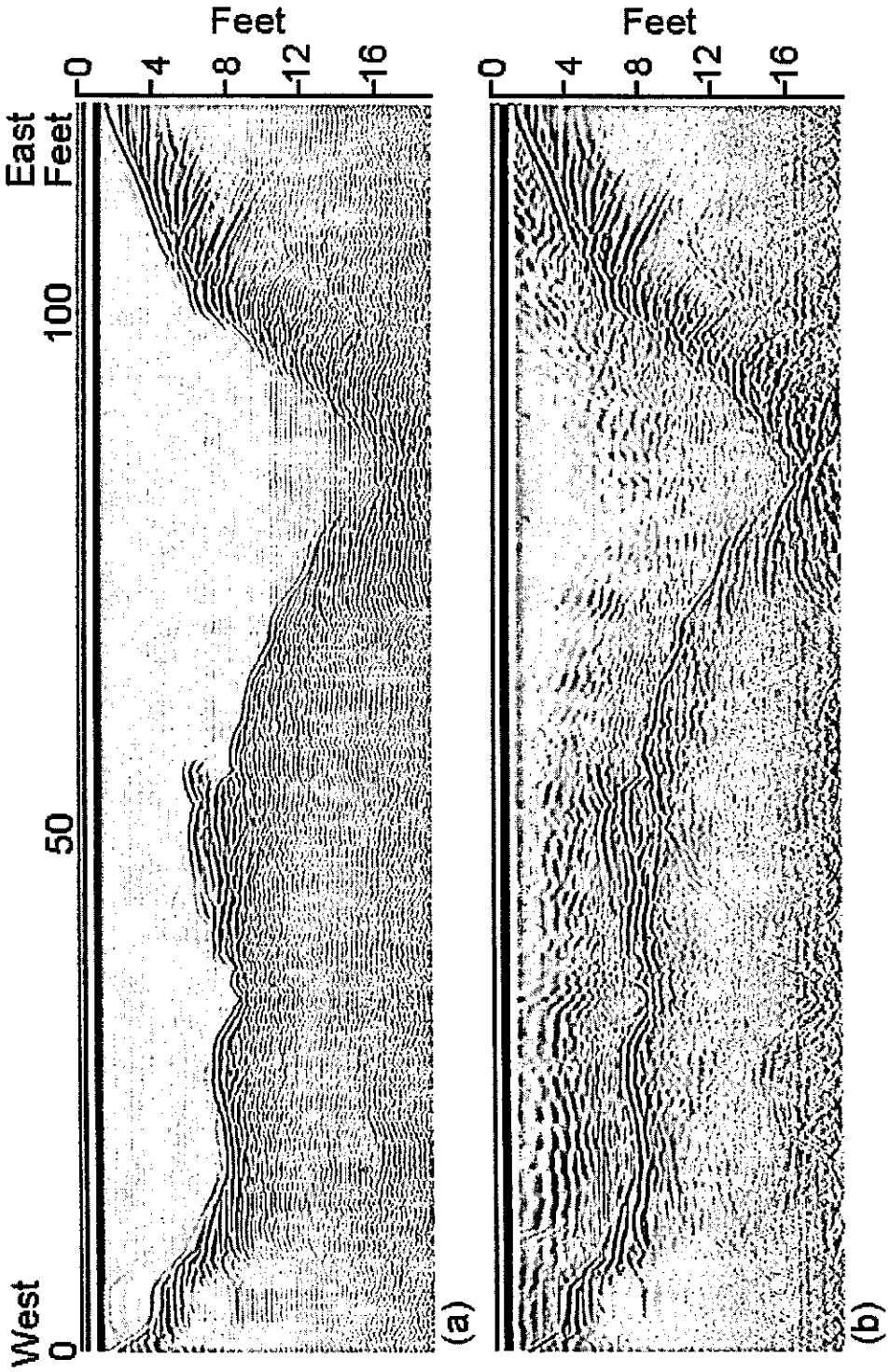

Figure 10. *Profile 2, site 1 (Figure 8): (a) stacked and (b) migrated versions.*

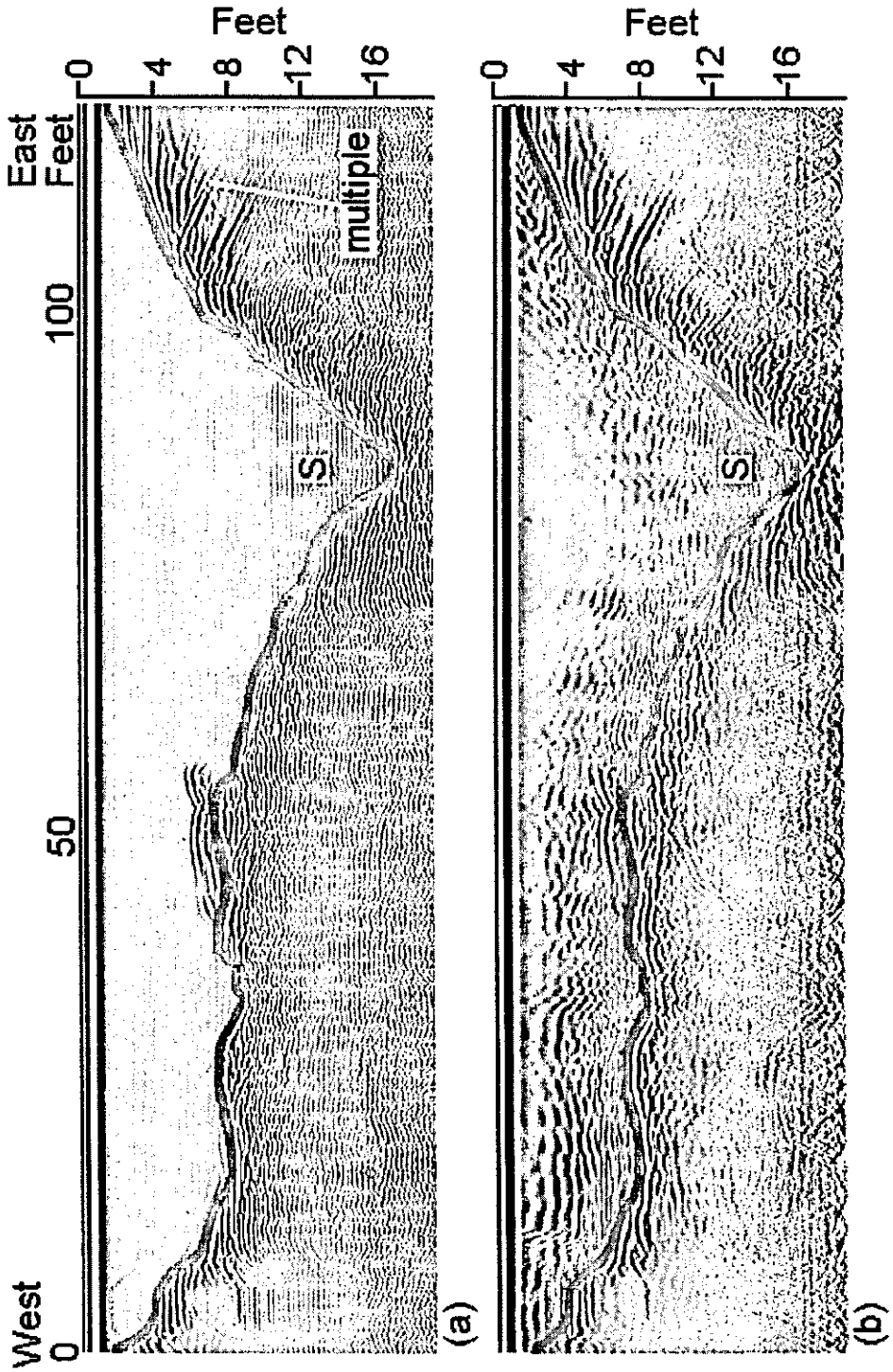

Figure 11. *Profile 2, site 1 (Figure 8): (c) interpreted stacked and (b) interpreted migrated versions. Gray line identifies water bottom. Existing scour feature is marked with an "S".*

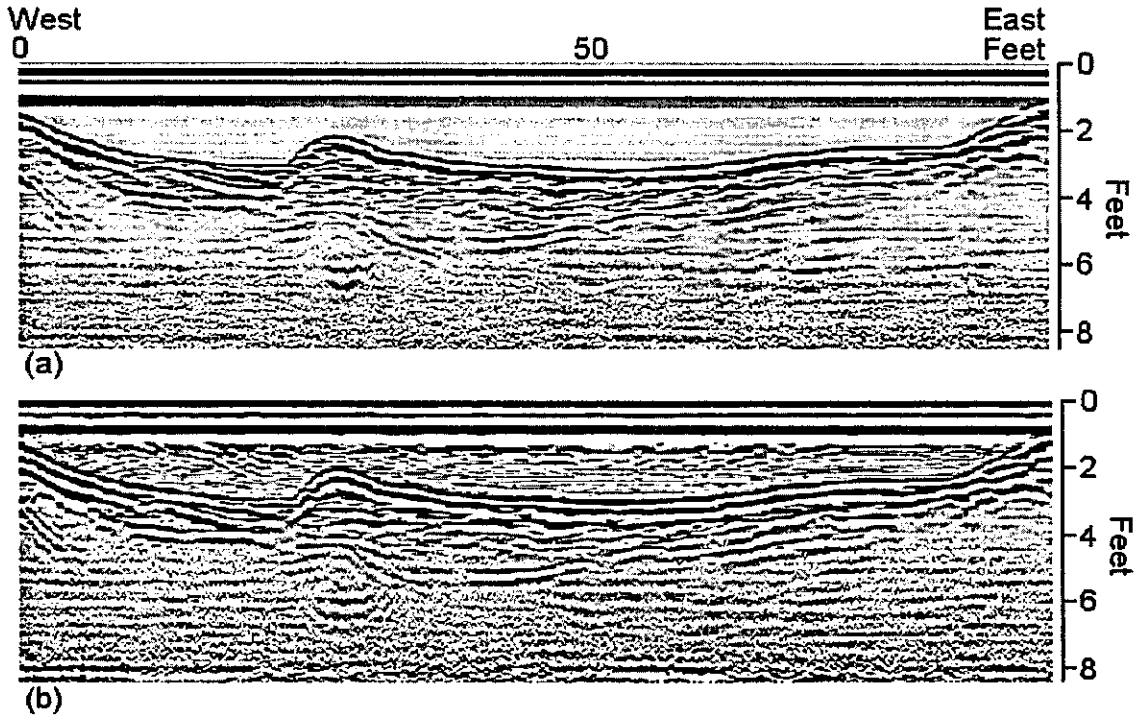

Figure 12. *Profile 1, site 9 (Figure 9): (a) stacked and (b) migrated versions.*

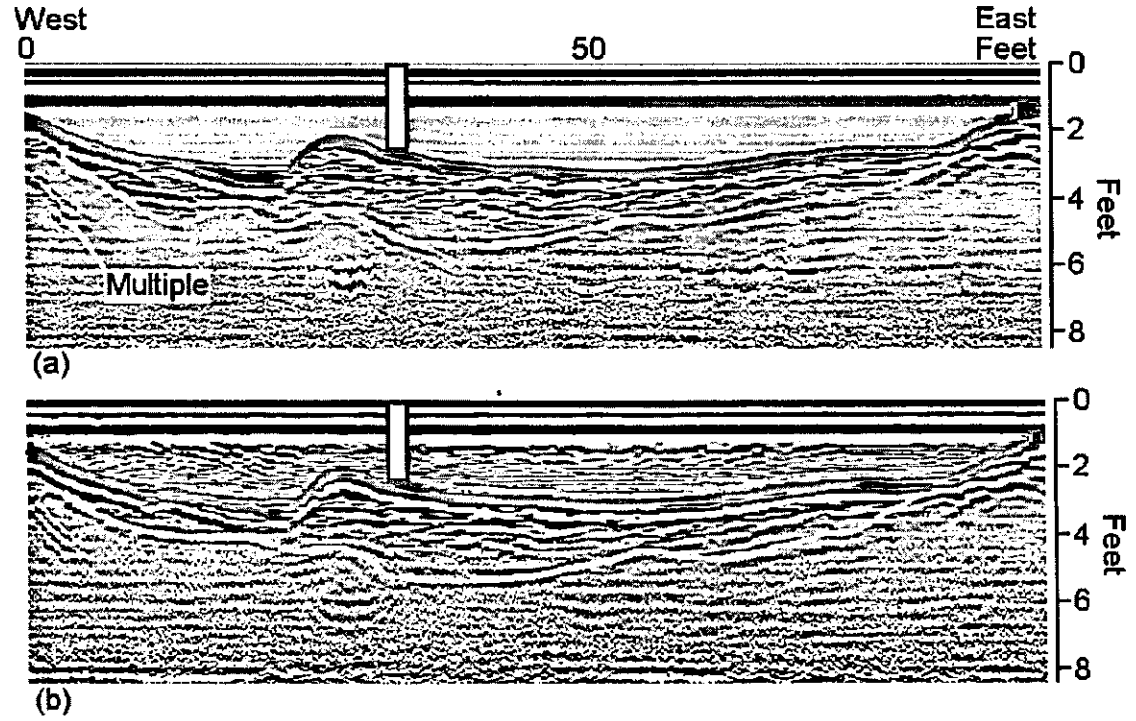

Figure 13. *Profile 1, site 9 (Figure 9): interpreted (a) stacked and (b) migrated versions. Gray and white lines identify water bottom and extent of in-filled scour, respectively.*

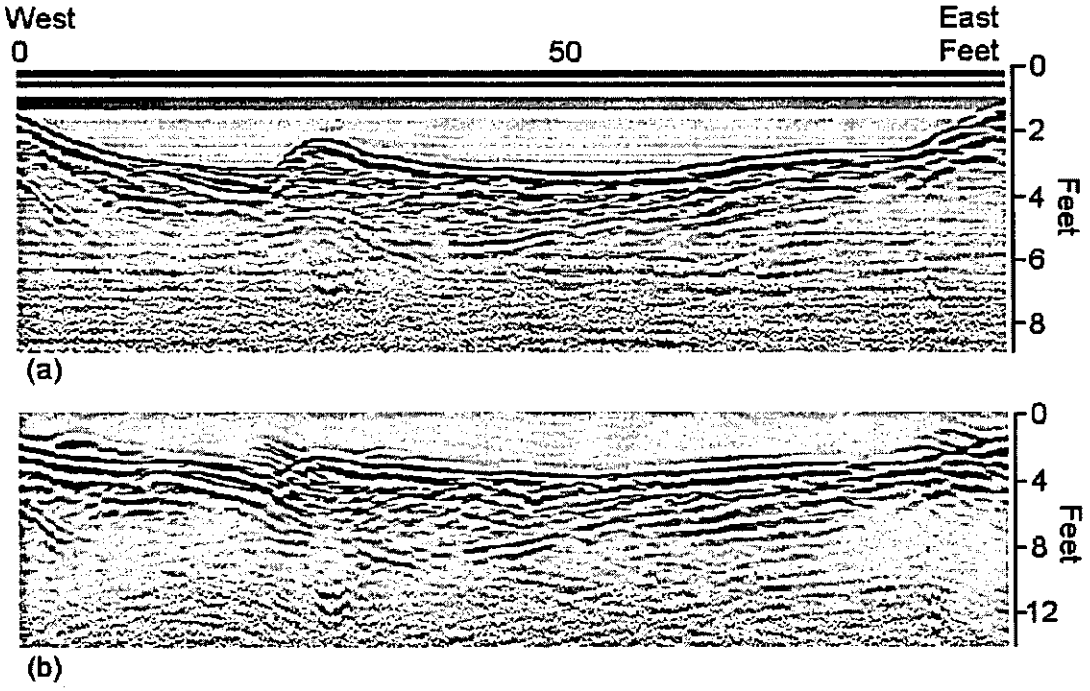

Figure 14. *Profile1, site 9 (Figure 9): (a) stacked and (b) velocity corrected versions.*

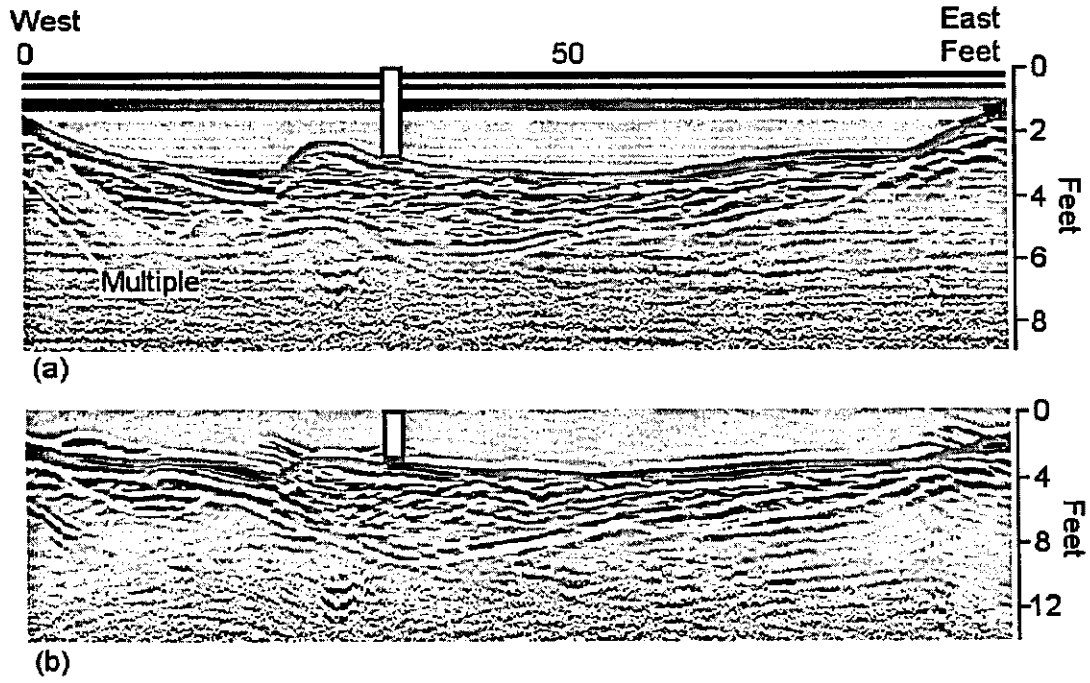

Figure 15. *Profile 1, site 9 (Figure 9): interpreted (a) stacked and (b) velocity corrected versions. Gray and white lines identify water bottom and extent of in-filled scour, respectively.*

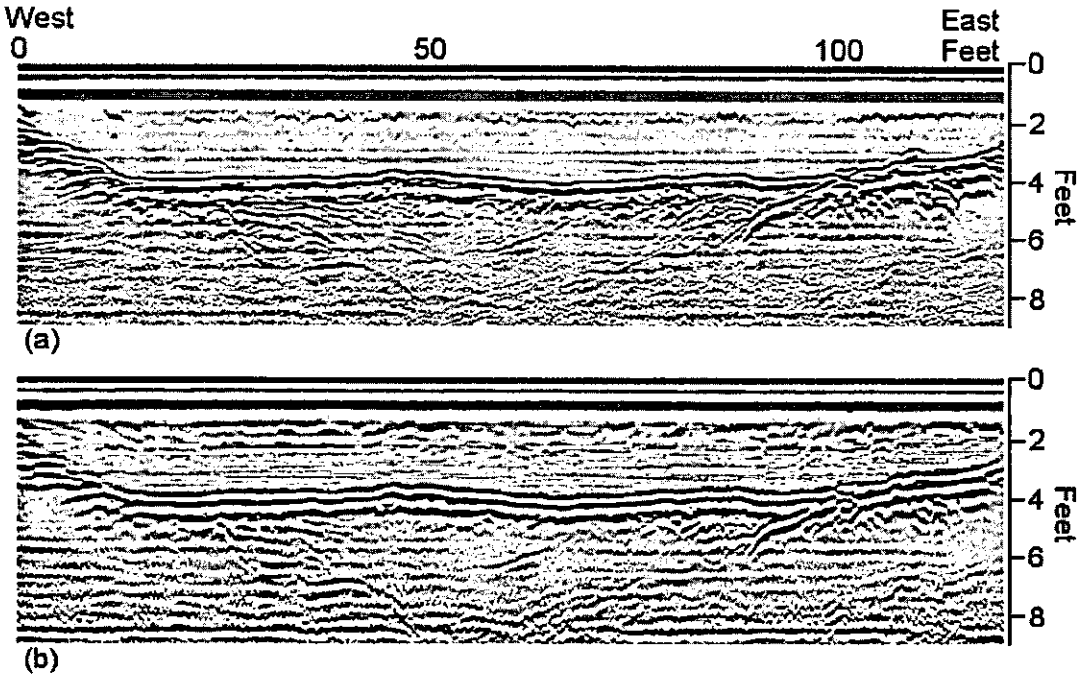

Figure 16. *Profile 7, site 10 (Figure 9): (a) stacked and (b) migrated versions.*

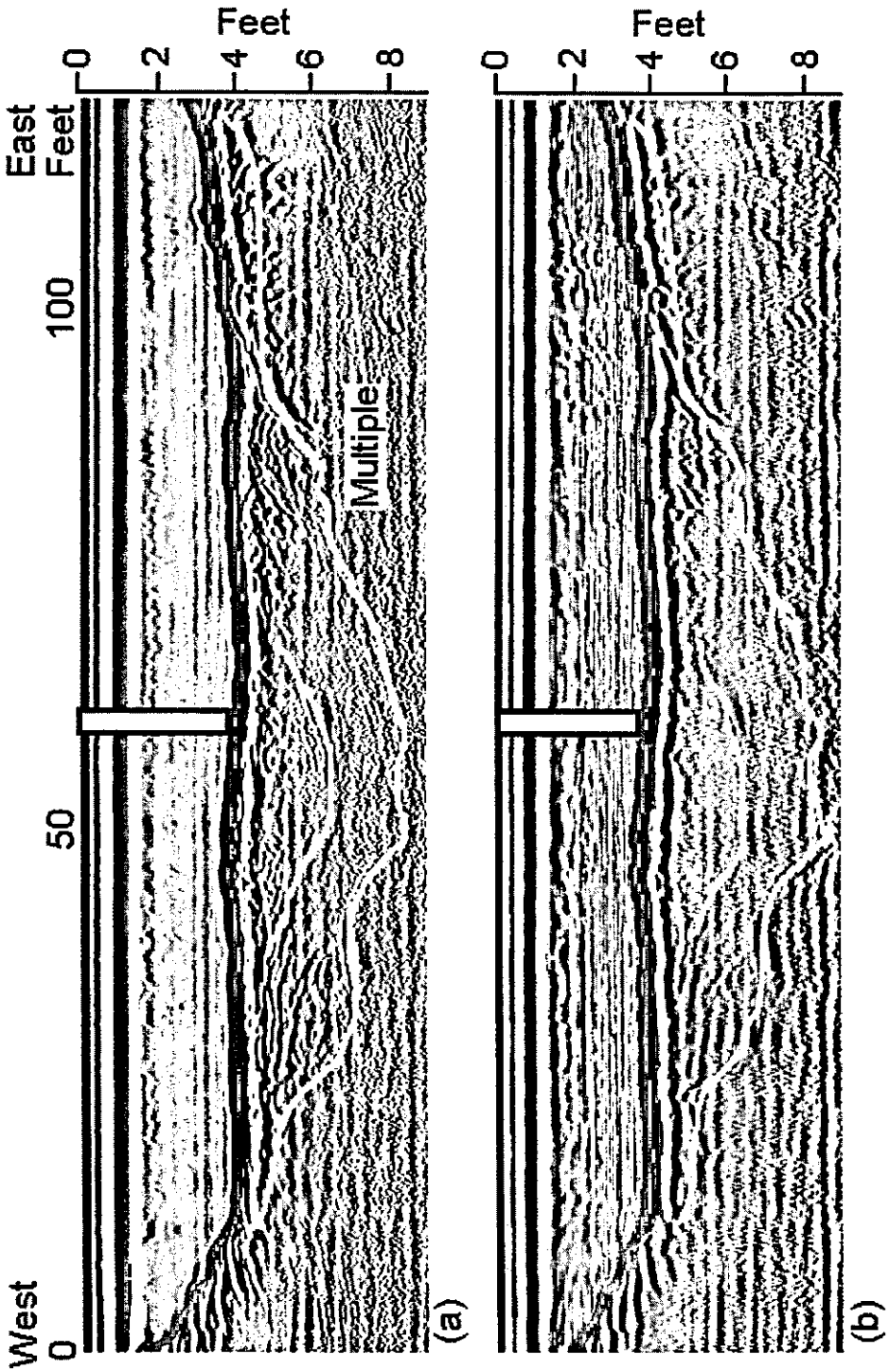

Figure 17. *Profile 7, site 10 (Figure 9): interpreted (a) stacked and (b) migrated versions.*

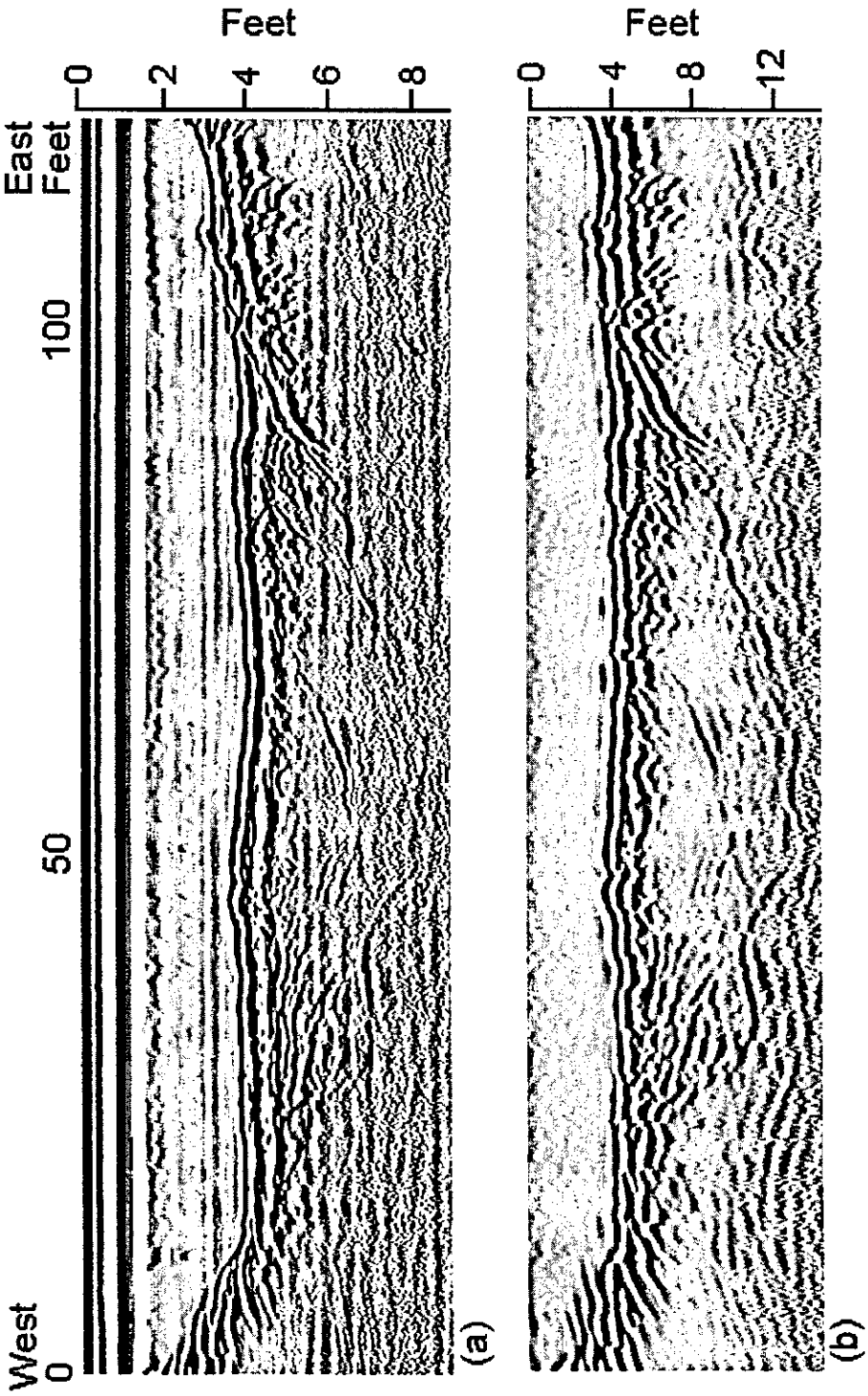

Figure 18. *Profile 7, site 10 (Figure 9): (a) stacked and (b) velocity-corrected versions.*

APPENDIX D

EVALUATION OF GPR AS A TOOL FOR DETERMINATION OF GRANULAR MATERIAL DEPOSIT VOLUMES

Steve Cardimona* and Tim Newton^

***Department of Geology and Geophysics,**
University of Missouri–Rolla,
Rolla, MO, 65401

^ The Missouri Department of Transportation,
1617 Missouri Blvd., P.O. Box 270, Jefferson City, MO 65102

ABSTRACT

University of Missouri Rolla, Department of Geology and Geophysics utilized the ground penetrating radar and Differential Global Positioning System (DGPS) tools to investigate thickness of fine gravel sized milled rock over natural ground throughout a large area of previous mine workings near Joplin, Missouri. Using a 400MHz frequency radar antenna, UMR achieved signal penetration sufficient for this study and data quality was high. Clearly evident in the data is the interface between the milled rock and clay soil. An average radar velocity for all sites was obtained by calibrating the radar signals with one point of available ground truth and the time-to-depth conversion was determined from this. The average depth to the soil layer across all the sites varied from 27cm to 96cm. DGPS was used to map both the areas and GPR survey lines. The GPS data provided the elevation profiles and areas necessary to calculate three-dimensional volumes of the material. The techniques described in this report can be employed for estimating the volume of the granular deposits that is essential for determining available fill material for roadway construction projects.

OBJECTIVES

The objective of this study is to evaluate the utility and cost effectiveness of ground penetrating radar as a tool for determining volumes of aggregate material overlying clay soil or natural ground. A secondary objective is to integrate real time differential GPS (DGPS) to accurately map the materials and provide data essential to calculate volumes.

BACKGROUND

In the Tri-State Mining District of southwestern Missouri, much of the ground is covered by gravel and tailings left behind from the numerous lead and zinc mine mills, where ore laden rock was crushed to extract metals. These materials range in size from fine gravel chat to fine sand sized tailings. Other parts of Missouri have similar but natural granular deposits of gravel and sand. As part of the highway construction process, MoDOT plans to incorporate granular materials that are currently located within highway right-of-way into the roadway fills. MoDOT will be involved with the excavation, transport, and placement of these materials as part of construction. An estimate of the volume of chat material available is necessary for highway designers to determine quantities of fill available. The current method is to backhoe a small portion of each area to determine the chat / soil interface. This interface greatly fluctuates and relying on one dig site may produce an inaccurate approximation of chat volume. Ground penetrating radar has the potential to display this gravel to natural ground transition and provide accurate volumetric estimates. A few GPR profiles would be both more expedient and accurate than digging test pits. A complete GPR profile across a site may show all the depth fluctuations rather than the depth at one location. In the interest of saving time and providing accurate estimates, ground penetrating radar was attempted.

GEOPHYSICAL SURVEY DESIGN

With the ground penetrating radar (GPR) method, a transmitter sends a microwave signal into the subsurface, and the radar waves propagate at velocities that are dependent upon the dielectric constant of the subsurface medium (Cardimona, et al., 1998). Changes in the dielectric constant will be due to changes in the subsurface materials, and these will cause the radar waves to be reflected back to the surface. The time it takes energy to return to the surface relates to the depth at which the energy was reflected. Thus, interpretation of the GPR signal with respect to the travel time of reflected energy yields information on structural variation of the near subsurface.

The GPR survey was successfully completed using 400MHz antennae and electronics designed by Geophysical Survey Systems Inc. UMR deployed the GPR equipment to investigate the thickness of milled rock (chat) over a large area near Joplin, Missouri, where old mine workings and debris cover large portions of the land. The interface between the native soil and the overlying granular material is a high-contrast point where electromagnetic energy will reflect back to the surface to be recorded by the GPR instrumentation. The focus of the survey was to map the depth of the chat-soil interface along survey lines at all 30 field sites. In order to cover the large number of sites, UMR collected data along 1 to 3 survey lines per site. Lines were pre-marked in an "X" pattern on most area sites. The radar survey lines were then DGPS-located by personnel of the Missouri Department of Transportation.

GPS MAPPING AND VOLUME CALCULATIONS

A Trimble Pro XRS unit was used for the GPS part of the study. This unit has an integrated Coast Guard Beacon receiver that acquires differential corrections (DGPS) from the Coast Guard broadcast. Beacons are located along the Missouri and Mississippi Rivers for navigational purposes. MoDOT's testing of this instrument has found it to be submeter accurate in the horizontal plane and 2 meters accurate in the vertical plane.

Areas were mapped quickly by walking their perimeters with the DGPS unit while acquiring position data every 5 seconds, resulting in a point every 3 meters. This allowed the designated areas to be overlain on highway plans and provided area calculations. When choosing a data-logging interval, area size and mapping speed must be taken into consideration. A 5 second interval at walking pace provides a position about every 3 meters, which is adequate for the large areas which ranged from 5,000 to 120,000 square meters. Too much data and detail would be burdensome. The chat piles were much smaller and thus a 1 or 2 second interval was used to provide adequate detail. A position was also acquired at the top of the pile to estimate height for volume calculations. Piles were calculated as 1/3 x area x height while areas were simply calculated as area x average depth.

Without DGPS, areas would be either be scaled from aerial photos at a much lower accuracy or surveyed by traditional methods. Survey crews would be kept busy for weeks mapping the large areas at an accuracy not required for volume estimates. DGPS provided elevation profiles and positions of the radar lines as well. The integration of GPR and GPS proved beneficial, as the resulting time and cost savings were substantial as compared to traditional surveying.

WHAT IS GPS?

The NAVSTAR Global Position System consists of 24 satellites in very high, stable orbits at 20,000 km (12,600 miles) elevation that are controlled by ground-based monitoring stations. The satellite orbits are in 6 planes with a 55-degree rotation, with each plane having 4 or 5 satellites. The system was developed and is currently maintained by US Department of Defense. A satellite revolution is completed in about 12 hours. NAVSTAR GPS provides all weather, "worldwide", accurate three-dimensional positioning 24 hours a day. Like AM-FM radio, the satellite signals support an unlimited number of users. The advantage of using satellites over ground based methods is that they eliminate the traditional "line of sight" survey requirement. Instead of "leap frogging" around ground clutter, receivers are placed where

there is a clear view of the sky, allowing longer baselines. Another advantage is that GPS is a "dynamic" positioning system, allowing a person to map while moving. It is reliable due to its resistance to intentional jamming or interference and is capable of highly accurate geodetic surveying.

Differential GPS (DGPS) is a technique that significantly improves both the accuracy and the integrity of the Global Positioning System. DGPS involves the use of two receivers - one at a fixed location, the "base station", and one that the user maps with, called the "roving" or "rover" receiver. DGPS requires high quality GPS base station receivers at accurately surveyed locations. GPS data is collected and each position and its corresponding "errors" are tagged with GPS time at both the base and roving unit. The base station compares the satellite measurements with the known x,y,z position and then estimates the error components. The difference between the GPS calculated position and the known position is the error. These errors are occurring everywhere within same vicinity, at the same time. The base station quickly forms a correction for each satellite in view. An x, y, z correction is generated and will adjust the rover position accordingly to bring it from the false position to "truth". This correction either is archived into a computer for later use, called "post processing" or broadcast immediately by radio for "real time corrections".

The Coast Guard has implemented a series of local area differential stations to cover harbors, inland waterways, and coastal waterways of the United States. This correction service is free and requires a special radio to receive the signals. Some private services use a frequency modulation (FM) subcarrier to transmit corrections to small areas. The disadvantage of ground based broadcasts is that radio is "line of sight" and the receiver may lose signal in ground clutter such as trees, structures, and valleys. Electromagnetic interference can be another problem, usually caused by car engines or thunderstorms. Another private industry segment uses geostationary satellites as the communications link to broadcast corrections. These systems consist of several reference stations located around the country, networked through a centralized satellite uplink facility. The satellite broadcast eliminates much of the loss of radio signal caused by topography. Both FM and Satellite correction services require a subscription and the users must purchase a radio receiver and pay an annual fee, around $800 per year per unit as of January 2000.

GPR DATA

Radar equipment was carried in a pickup truck, and the antennae were pulled along the pre-marked survey lines. Acquisition was difficult in the rough terrain, but data quality was quite high (Figures 1-4). The average depth to the soil layer across all the sites varied from 27cm to 96cm, using an average electromagnetic dielectric constant of 27.9.

Ground truth on one survey line allowed us to determine the general stratigraphy that consisted of dry chat, wet chat, soil mixed with chat, and soil. The strongest reflection in the GPR data came from areas where water was perched above the clay-rich soil (Figures 1 and 2). The target zone, the chat-to-soil interface, was clearly distinguishable in the data (Figures 3 and 4), especially when viewed on the computer screen with judicious application of amplitude enhancement color transforms that clearly highlight the change in soil stratigraphy.

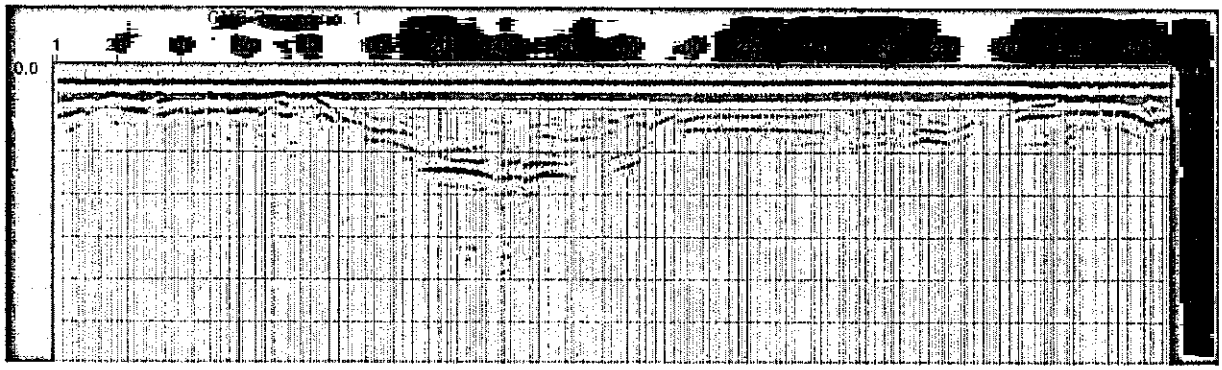

Figure 1. First 70 ns of recorded GPR data along test line up and over a small chat mound. Band-pass filter applied, but no amplitude gain applied. Distinct interface is due to water within the granular material above the clay-rich soil.

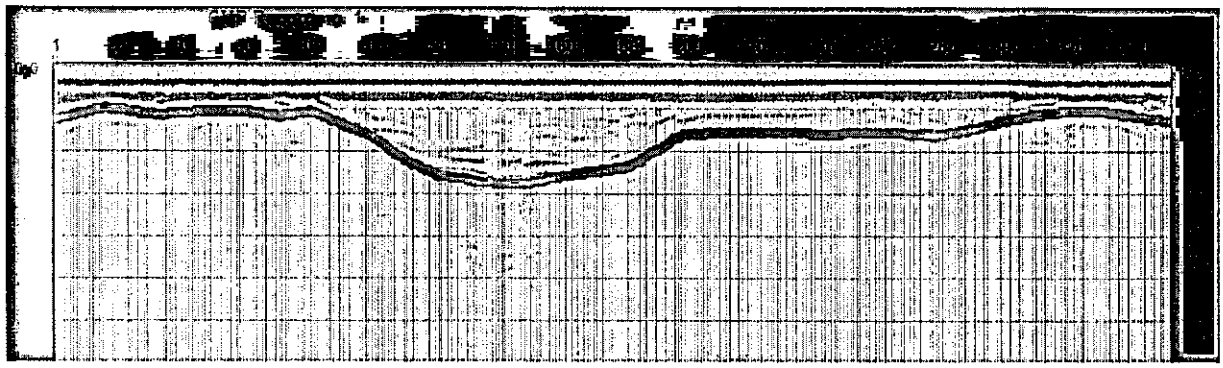

Figure 2. Interpreted first 70 ns of recorded GPR data along test line up and over a small chat mound (same as in Figure 1). Band-pass filter applied, but no amplitude gain applied. Distinct interface is due to water within the granular material above the clay-rich soil.

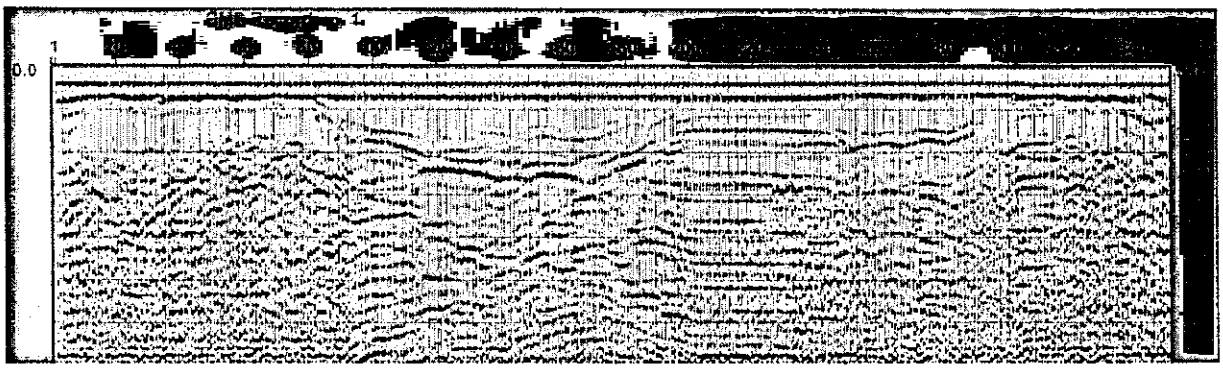

Figure 3. First 70 ns of recorded GPR data along test line up and over a small chat mound (same as in Figures 1-2). Amplitude gain function and band-pass filter applied. Chat-to-soil interface as well as water table evident.

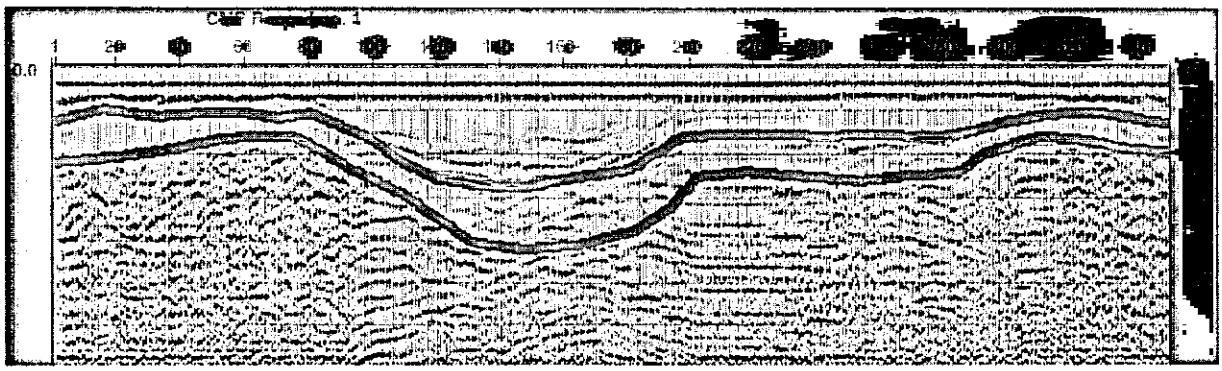

Figure 4. Interpreted first 70 ns of recorded GPR data along test line up and over a small chat mound (same as in Figures 1-3). Amplitude gain function and band-pass filter applied. Chat-to-soil interface as well as water table evident.

SUMMARY

Ground penetrating radar proved to be very effective in imaging the interface between soil and granular overburden at the sites in this study. Estimates of overburden thickness based on the high quality GPR data can be used for estimating granular material volume at all sites investigated. An average radar velocity was applied to all data. Additional ground truth would allow for the calculation of variable radar velocity parameters across the site, for even more accurate thickness estimations.

Quick and accurate volume estimates of available gravel and other granular material will reduce the possibility of cost overruns and prevent shortages and acquisitions of additional fill. Highway designers can anticipate the calculated volume to exist in the field and design their subbase or fill heights accordingly. Soil surveys would also benefit by the ability to delineate and quantify natural gravel or sand deposits.

The integration of GPS and GPR to provide accurate positions proved to be both reliable and beneficial. The time and cost savings using the GPS unit are tremendous, as a survey crew would be required to bring in survey control well beyond the established right of way. The work GPS was able to do simultaneously with GPR data acquisition would have taken a 6 person survey crew 2 weeks to perform. It is recommended that this marriage of technologies continue with future projects.

IMPLEMENTATION

The integration of GPS and GPR is easily applied where granular material covers clay soil. GPR profiles can be collected in areas covered with silt, sand or gravel to allow highway designers to estimate the volume of granular material available as fill. Natural gravel deposits could be addressed with GPR during the roadway soil survey, mapping their extent and quantifying their volume. Highway designers need to know how much "borrow" is available before construction and survey control in brought into the new area. The use of differential GPS expedites the mapping of the materials and provides the elevations and profile line lengths necessary to calculate volumes. This method could also be used at existing rock mills and quarries where the depth of milled rock is unknown, however, the GPR technique is not recommend for tall piles that exceed the limit of radar depth penetration. Pile volumes above ground can be estimated with DGPS alone as long as elevations are acquired at the top and bottom.

RESULTS

Analysis of the GPR records allowed us to create spreadsheet data for all the chat sites surveyed. Chat thickness was estimated along GPR survey lines every 2 meters or less, and at many sites every meter. Chat thickness estimates are based on:

1) picking the radar reflection time at the base of chat (below the chat-with-soil-matrix layer), and

2) using one dielectric constant (27.9) from a test line where we dug down through all layers for ground truth (dry chat, wet chat, chat-with-soil-matrix, down to "no-chat").

Below is the average thickness for each of the areas in this study:

Area	Average Thickness along GPR survey line (cm)		
A	48 (line1)	63 (line2)	
AA	60		
B	60		
BB	96		
C	46		
CC	53		
E	83		
EE	55		
F	52		
FF	33 (line 1)	34 (line 2)	
G	65		
HH	27		
I	78 (line1)	56 (line2)	
II	64 (line 1)	95 (line 2)	
JJ	61		
K	62 (line1)	52 (line2)	
L	75 (line1)	54 (line2)	70 (line3)
M	57 (line1)	47 (line2)	
MM	58 (line1)	44 (line2)	
besideMM	30		
NN	53 (line1)	86 (line2)	
O	55		
P	87		
R	94		
S	59		
T	68		
V	75 (line1)	50 (line2)	
W	38		
Y	50		
Z	69 (line1)	68 (line2)	

Figure 5. Map showing planned Route 249 and the corresponding chat areas.

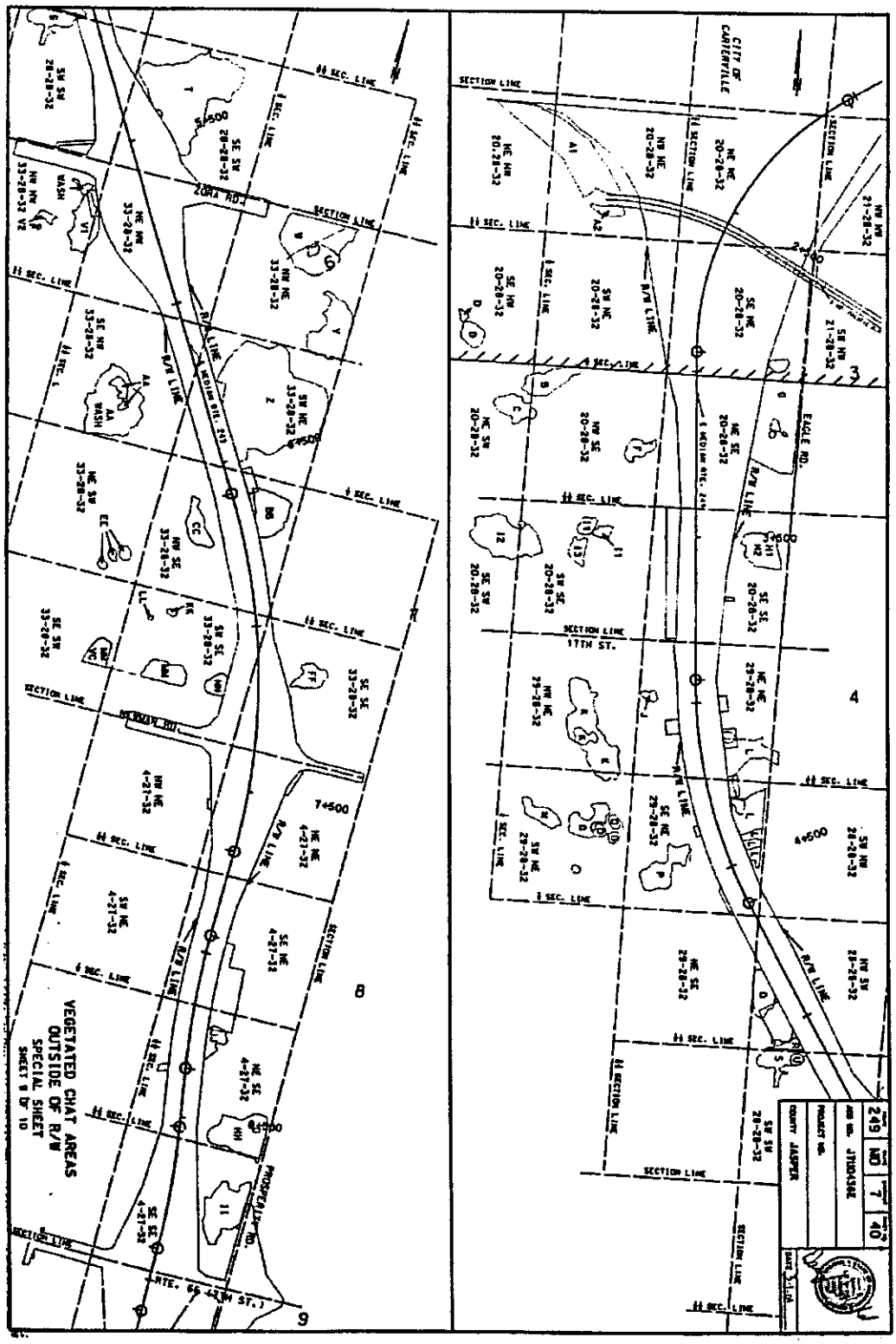

REFERENCES

Cardimona, S., M. Roark, D. J. Webb and T. Lippincott, 1998. Ground penetrating radar, *Highway Applications of Engineering Geophysics with an Emphasis on Previously Mined Ground,* pp. 41-56.

APPENDIX A -- Photos

Aerial Photo of Portion of Study Area

APPENDIX A – Photos

Representative Photos of Chat Piles and Chat Covered Ground

APPENDIX A – Photos

Representative Photos of Chat Piles and Chat Covered Ground

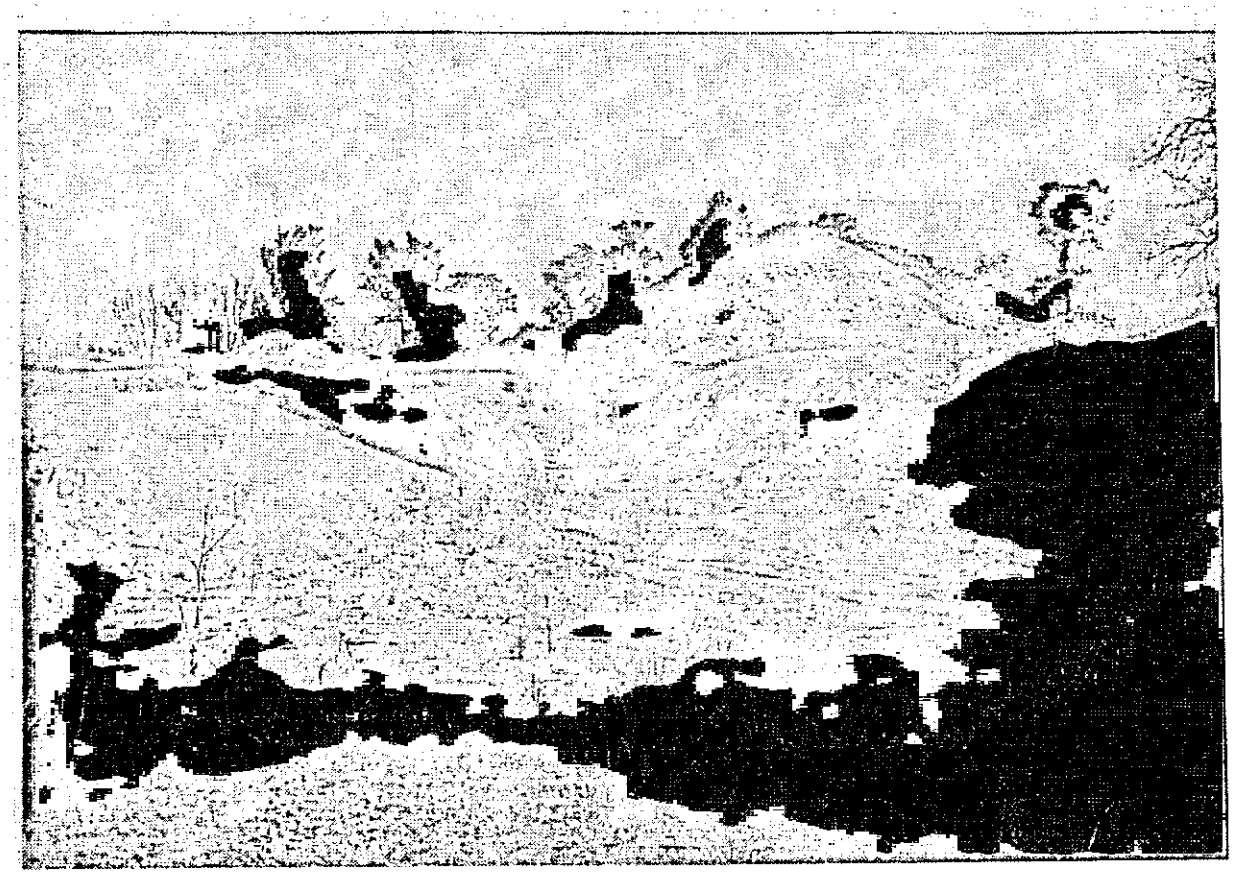

APPENDIX A – Photos

Ground Penetrating Radar Equipment

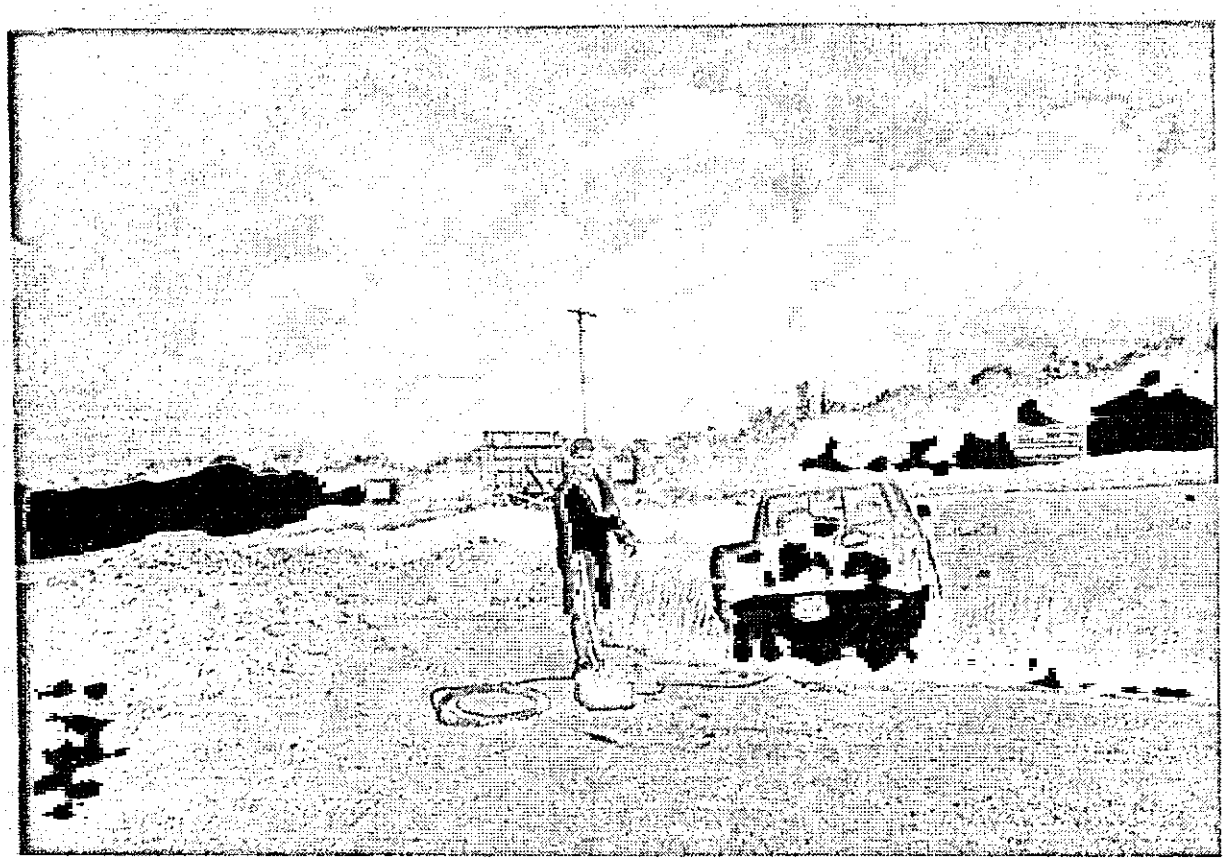

APPENDIX E

OVERVIEW OF THE SHALLOW SEISMIC REFLECTION TECHNIQUE

Neil Anderson

Department of Geology and Geophysics
University of Missouri-Rolla, Rolla, Missouri 65401

ABSTRACT

The shallow seismic reflection technique is relatively straightforward from a conceptual perspective. Essentially, we generate a high-frequency, short-duration pulse of acoustic energy at the earth's surface, and measure the arrival times and magnitudes of "echo pulses" that are reflected from subsurface horizons (i.e., water table, bedrock, lithologic and facies contacts, etc.) and returned to the earth's surface. Ideally, the travel times and magnitudes of these recorded "echoes" can be used to create a 2-D or 3-D velocity/depth model of the subsurface. If borehole lithologic control is available, a geologic image of the subsurface can be generated.

In practice however, the reflection seismic technique is complex - mostly because the echoes (reflected energy or seismic events) of interest are contaminated by both coherent and random noise. To compensate, sophisticated acquisition and processing methodologies have been developed to enhance the relative amplitude of the reflected events of interest. Many of these methodologies are site and target dependent. The interpretation of reflection seismic data is also a complex process, and as much an art as a science. Interpreted velocity/depth models can be unreliable because of either inaccurate velocity control or incorrect seismic event identification. Similarly, seismic amplitudes can be misinterpreted because of gain distortions. Forward seismic modelling and the inclusion of external geological and geophysical constraints are often the key to successful interpretations, and the development of a reasonable subsurface geologic image.

The potential user should bear in mind that the quality of reflection seismic data is technique, site, and target dependent. Interpretable data will not be generated if improper acquisition and/or processing techniques are employed. In certain instances, interpretable data cannot be recorded (using cost-effective conventional methodologies) because of adverse site conditions, or because the target characteristics (i.e., small size, lack of anomalous attributes, etc.) preclude its delineation.

INTRODUCTION

The fundamental concepts of shallow reflection seismic surveying are relatively simple. The actual acquisition, processing and interpretation methodologies however, are relatively complex - mostly because sophisticated processes are employed to enhance the quality of the reflection data at the expense of noise.

To facilitate the reader's understanding of the shallow reflection seismic tool, we present a summary of the fundamentals of the shallow reflection seismic technique, and brief overviews of data acquisition, processing and interpretation methodologies. There are a number of excellent papers and books on these topics; most however, are focused on conventional exploration seismology and were written for the geophysicist - not the engineer. For more detailed information about the reflection seismic technique the reader is referred to the shallow seismic overview paper by Steeples and Miller (1990), the introductory textbook by Keori and Brooks (1991), or the more comprehensive textbook by Sheriff and Geldart (1995). Evans (1997) is an excellent reference for seismic acquisition; Yilmaz (1987) is the definitive text on data processing; excellent interpretation atlases/textbooks include those by Anderson and Hedke (1995), Brown (1996), and Weimer and Davis (1996). For terminology, the reader is referred to the encyclopedic dictionary by Sheriff (1991).

FUNDAMENTAL CONCEPTS

The shallow seismic reflection method is predicated on several fundamental assumptions/principles, which from a practical perspective generally prove to be relatively robust.

Assumption/principle 1: The shallow subsurface can be subdivided into a finite number of layers (laterally continuous or discontinuous) of effectively uniform density and seismic velocity. (Seismic velocity is a function of density and elastic moduli. The product of velocity and density is referred to as acoustic impedance.) The water table, the bedrock surface, lithologic contacts, or unconformable surfaces generally separate these layers of essentially uniform acoustic impedance (Figure 1).

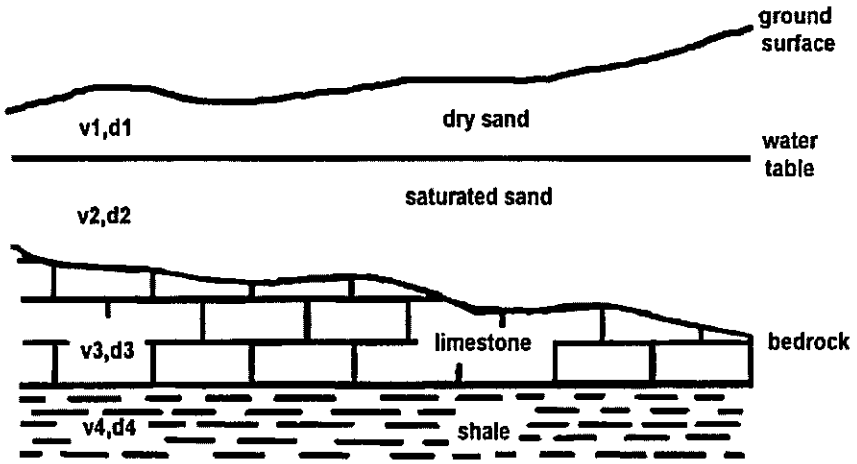

Figure 1: The earth can be subdivided into a finite number of layers of effectively uniform acoustic impedance. The water table, lithologic contacts and unconformable surfaces generally separate these layers.

Assumption/principle 2: A seismic source (generally an explosion, weight drop, or projectile impact) emits body wave energy into the subsurface. There are two fundamental types of body waves: compressional (p-waves) and shear (s-waves). Compressional waves are characterized by particle motion parallel to the direction of wave propagation; shear waves are characterized by particle motion perpendicular to the direction of propagation (Figure 2).

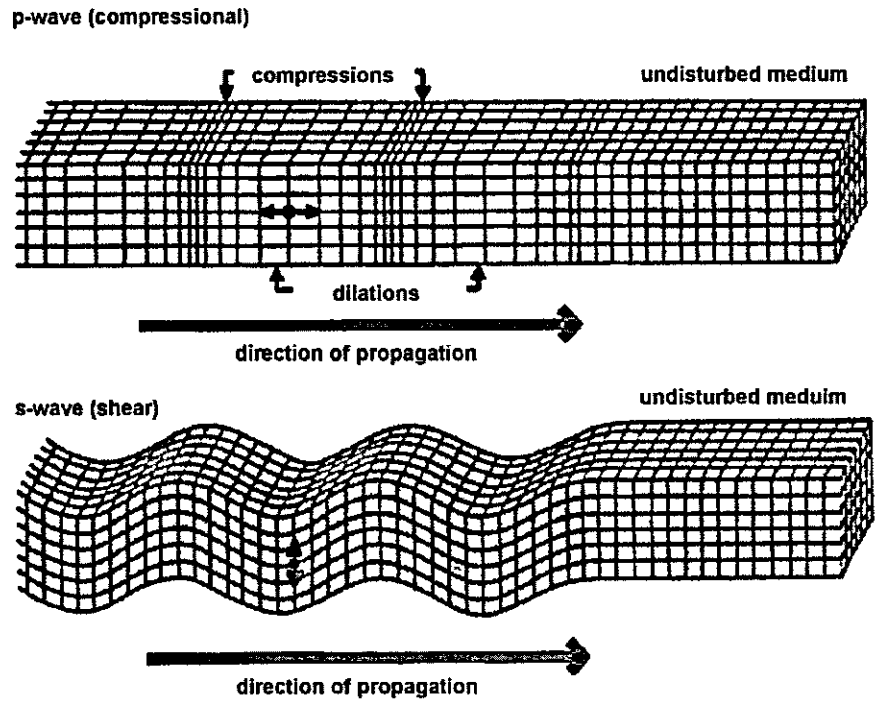

Figure 2: Compressional (p-waves) waves are characterized by particle motion parallel to the direction of wave propagation; shear waves (s-waves) are characterized by particle motion perpendicular to the direction of propagation. (After Keary and Brooks, 1991).

Assumption/principle 3: In homogeneous media, body wave energy propagates away from a surface source as hemispherical wave fronts (Figure 3). The velocity of a wave front (V_p or V_s) is a function of the engineering properties of the medium through which it is passing (Figure 4 and Table 1).

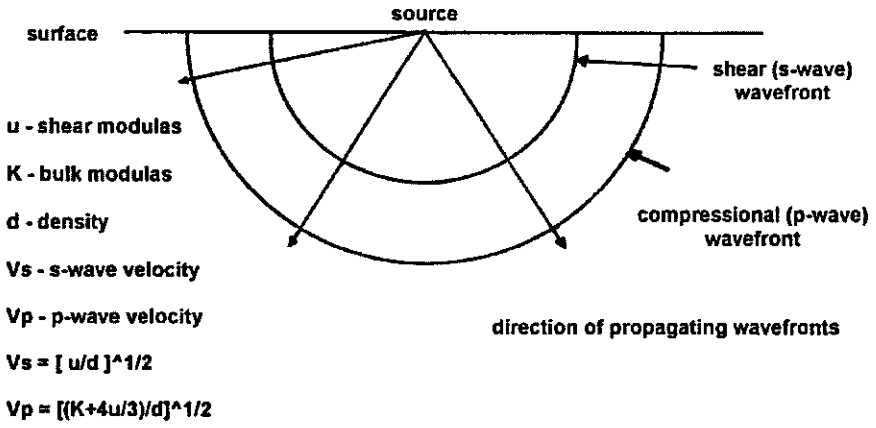

Figure3: *In homogenous media, surface-generated body wave energy propagates away from the source as hemispherical wave fronts. The velocity of a wave front is a function of the engineering properties of the medium through which it propagates*

Material	P-wave velocity (km/s)
Dry Sand	0.2 -.0.1
Wet Sand	1.5 - 2.0
Clay	1.0 - 2.5
Permafrost	3.5 - 4.0
Tertiary Sandstone	2.0 - 2.5
Pennant Sandstone	4.0 - 4.5
Cambrian Quartzite	5.5 - 6.0
Cretaceous Limestone	2.0 - 2.5
Carboniferous Limestone	5.0 - 5.5
Dolomites	2.5 - 6.5

Material	P-wave velocity (km/s)
Rock Salt	4.5 - 5.0
Anhydrite	4.5 - 6.5
Gypsum	2.0 - 3.5
Granite	5.5 - 6.0
Gabbro	6.5 - 7.0
Ultramafic Rocks	7.5 - 8.5
Air	0.3
Water	1.4 - 1.5
Ice	3.4
Petroleum	1.3 -1.4

Table 1: *Typical compressional wave velocities of various consolidated and unconsolidated materials. (After Keary and Brooks, 1991.)*

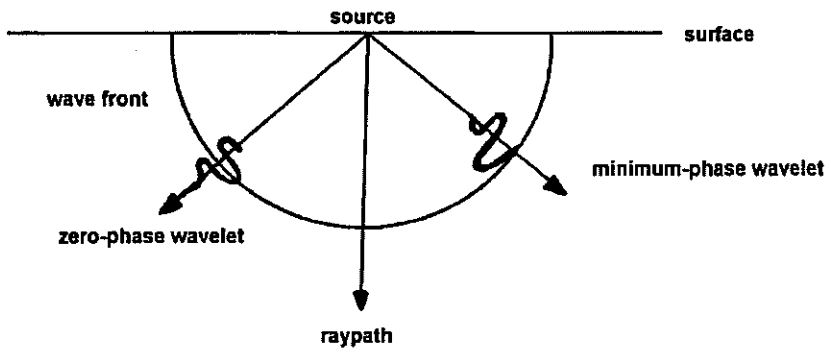

Figure 4: *A wave front can be modelled as "wavelets" travelling along a finite number of ray paths. The amplitudes of seismic wavelets variously represent particle velocity (land surveys) or changes in hydrostatic pressure (marine surveys).*

Assumption/principle 4: For computation, modelling and interpretation purposes, a wave front can be often be represented by a finite number of ray paths. The amplitudes of the associated wavelets variously represent particle velocity (land surveys) or changes in hydrostatic pressure (marine surveying; Figure 4).

Assumption/principle 5: A seismic wavelet can be characterized by its maximum amplitude, dominant frequency and wavelength (Figure 5). Impulsive sources usually generate minimum-phase type wavelets. During processing, data are often converted to zero-phase to facilitate computer-aided interpretation (Figure 4).

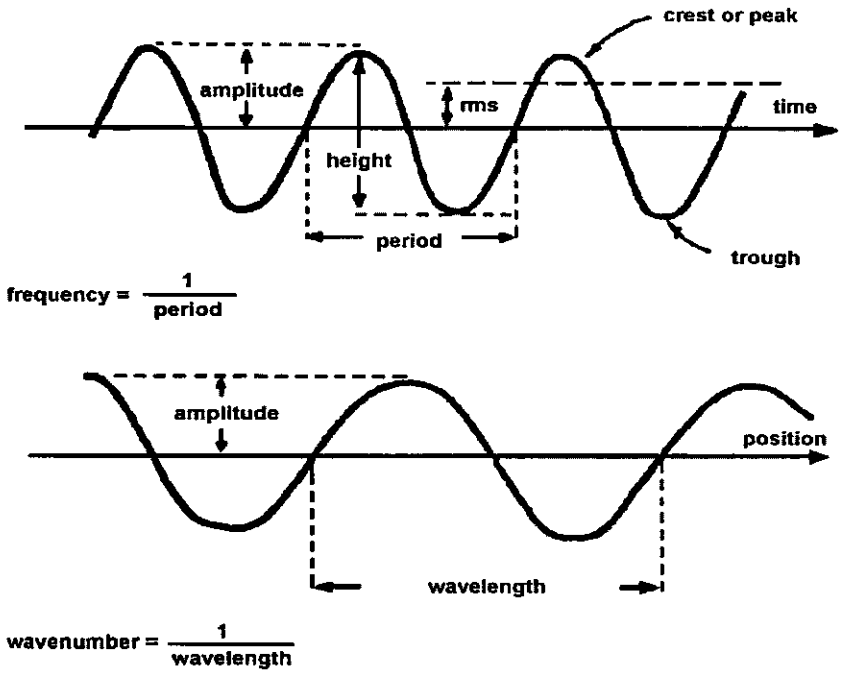

Figure 5: A seismic wavelet can be characterised by its maximum amplitude, dominant frequency, and wavelength. (After Sheriff and Geldart, 1995.)

Assumption/principle 6: When a ray path is incident on a layer boundary (acoustic impedance surface), energy will be reflected and refracted in accordance with Snell's law (Figure 6). Mode conversion (p-wave to s-wave or vice-versa will also occur).

Figure 6: When a ray path is incident on a layer boundary (acoustic impedance surface), energy will be reflected and refracted (in accordance with Snell's law). Mode conversion (p-wave to s-wave or vice-versa) will also occur. (After Keary and Brooks, 1991.)

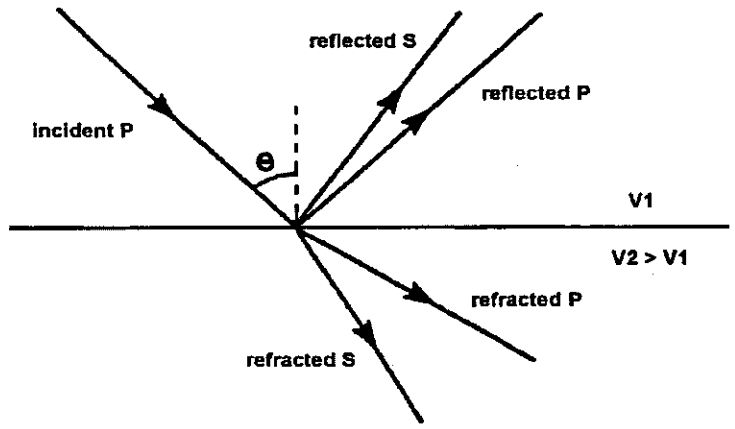

Assumption/principle 7: The relative amplitudes of the reflected and transmitted wavelets can be calculated from the Zoeppritz equations (derived assuming conservation of particle displacement and stress; Figure 7). Generally, for modelling and interpretation, vertical incidence is assumed, and the relative amplitudes of the reflected wavelets are calculated as shown in Figure 8.

$$\begin{bmatrix} \sin\theta_1 & \cos\phi_1 & -\sin\theta_2 & \sin\phi 2 \\ -\cos\theta_1 & \sin\phi_1 & -\cos\theta_2 & -\sin\phi_2 \\ \sin 2\theta_1 & K_1\cos 2\phi_1 & K_2\sin 2\theta_2 & K_3\cos 2\phi_2 \\ \cos 2\phi_1 & K_4\sin 2\phi_2 & K_5\cos 2\phi_2 & K_6\sin 2\phi_2 \end{bmatrix} \begin{bmatrix} A_{RP} \\ A_{RS} \\ A_{TP} \\ A_{TS} \end{bmatrix} = \begin{bmatrix} -\sin\theta_1 \\ -\cos\theta_1 \\ \sin 2\theta_1 \\ -\cos 2\phi 1 \end{bmatrix}$$

***Figure7:** Zeoppritz equations. (R – reflected; T – transmitted; P – compressional; S – shear).*

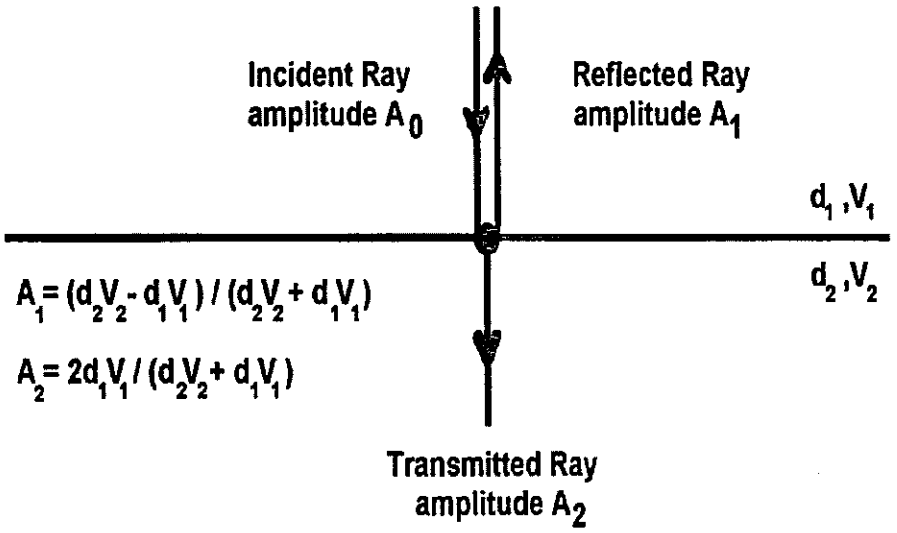

***Figure 8:** Generally vertical incidence is assumed, and the relative amplitudes of the reflected and transmitted wavelets are then a function of the acoustic impedance contrast across the layer boundary. (Amplitude A_0 is normalised to 1).*

Assumption/principle 8: A stacked, ***migrated*** seismic profile is comprised of a suite of individual traces. The spacing between adjacent traces (CMP locations) represents the lateral subsurface control interval (Figure 9). Ray paths are assumed to be vertical, to have coincident sources/receivers located at the CMP, and to have been vertically incident on underlying reflecting horizons. On a migrated seismic profile, acoustic impedance interfaces are essentially "replaced" in time by wavelets (Figure 9). The two-way travel time to a seismic event is a direct function of vertical depth and average velocity to that interface. The relative magnitude of a seismic event is a direct function of the magnitude of the corresponding vertical incidence reflection coefficient.

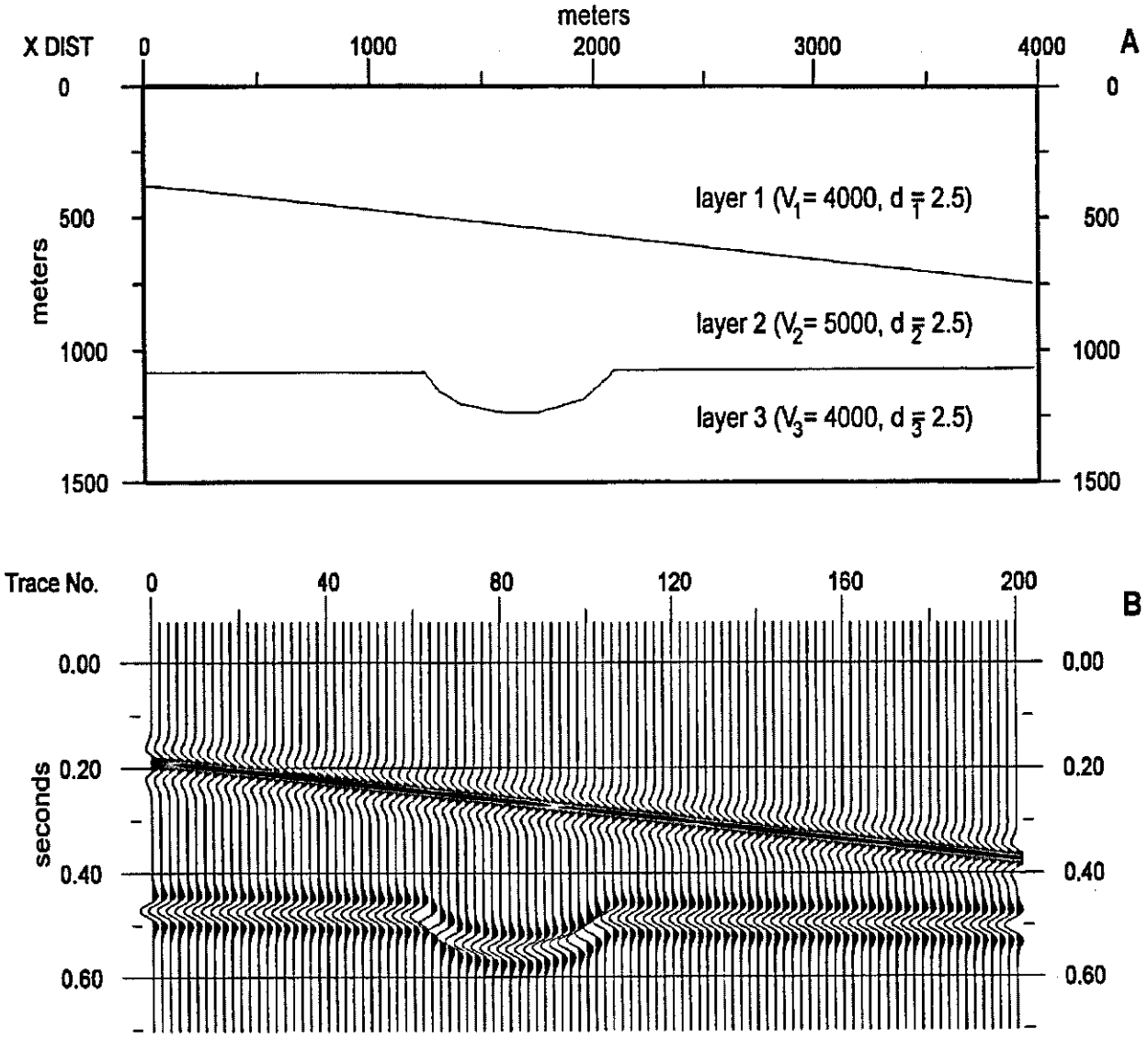

Figure 9: *Velocity/density geologic model (9A; $d_1 = d_2 = d_3$; $v_2 > v_1 = v_3$) and corresponding vertical-incidence synthetic seismic profile (9B). The profile was generated using a 30 Hz, zero-phase Ricker wavelet, and simulates gained, migrated seismic data. The trace spacing on the synthetic is analogous to common midpoint (CMP) spacing, and represents the lateral subsurface control interval. (Generated using GMA software).*

Assumption/principle 9: On ***non-migrated*** stacked seismic data, ray paths are assumed to be normally incident on layer boundaries (Figure 10). Reflected events originating from dipping surfaces are not displayed in their correct spatial locations on non-migrated seismic profiles and diffracted energy is not placed at its correct spatial point of origin. {Diffracted energy differs from reflected energy in that it originates from "point source discontinuities", rather than reflective interfaces} *Migration* is the process through which non-migrated data is converted into migrated data. Often this process is either not required or suitably applied to shallow reflection data.

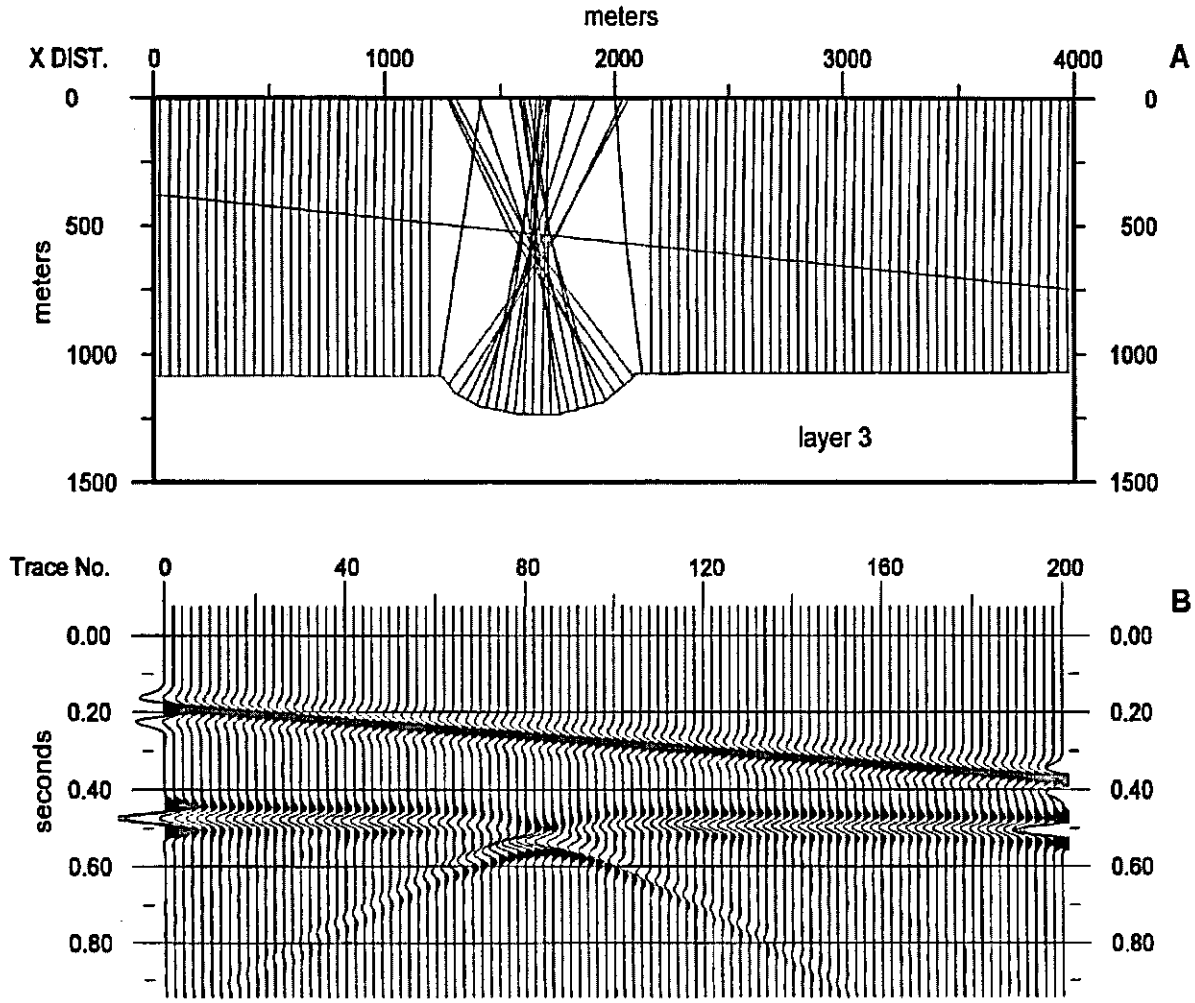

Figure 10: *Velocity/density geologic model ($d_1 = d_2 = d_3$; $v_2 > v_1 = v_3$), corresponding ray path model (10A) and normal-incidence synthetic seismic profile (10B). The profile was generated using a 30 Hz, zero-phase Ricker wavelet, and simulates gained, non-migrated seismic data. The synthetic seismic profile was generated using Geophysical Micro-Computer Applications {GMA} software.*

SEISMIC DATA ACQUISITION

Reflection seismic data are acquired using multiple sources and receivers. The sources generate the seismic wavelets (or a variable frequency "sweep" in the case of Vibroseis); the receivers record the travel times and amplitudes of the reflected seismic energy (Figure 11). Numerous sources have been developed/used for shallow reflection seismic surveying including silenced 30-06 and 50-calibur rifles, 10 KJSpark Pak, sledge hammers, 8-, 10- and 12-gauge shotguns, mini-primacord, EWG weight drop, dynasource, mini-sosie, vibroseis, and dynamite. Care must be taken in the selection of a source. Consideration must be given to depth penetration, wavelet frequency and character, source signal reproducibility, noise generation, and cost-effectiveness. Generally the user balances cost-effectiveness and data quality - often times compromising one for the other. The user has fewer options as far as the receivers are concerned. Generally, single, high-frequency geophones (>28 Hz) are utilized for land-based shallow reflection seismic studies. Geophones record the particle velocity associated with the reflected seismic energy (Figure 12). At some stage in processing a gain function is applied to the recorded data to compensate for amplitude attenuation over time. The relative magnitude of a wavelet on a gained seismic section is presumed to be a direct function of the magnitude of the corresponding reflection coefficient.

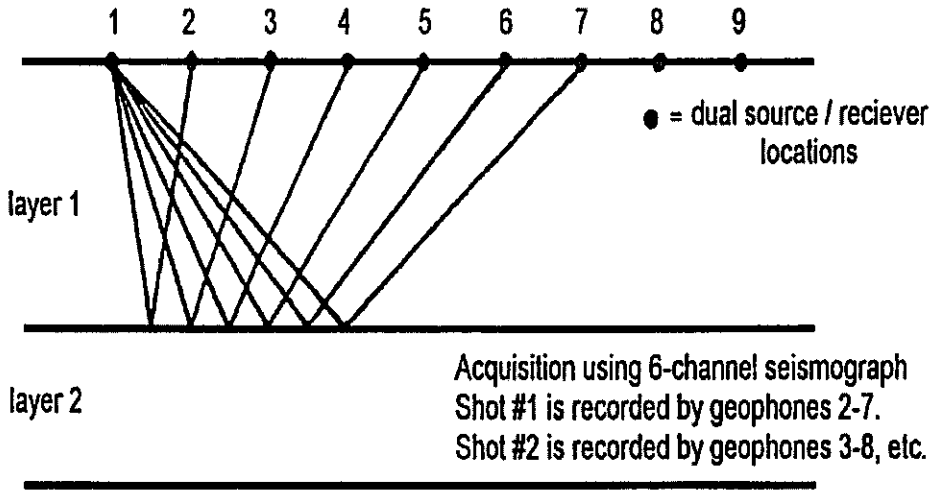

Figure 11: *Reflection seismic data are acquired using multiple sources and receivers. The sources generate the seismic wavelets; the receivers record the travel times and amplitudes of the reflected seismic energy.*

When we analyse reflection seismic profiles, we interpret the data as though zero-offset (coincident) sources/receivers were employed (Figures 9 and 10). In practice however, reflection seismic data are acquired using mostly non-zero offset sources and receivers. Two typical field shot/receiver arrays are depicted in Figure 13. In both situations, multiple, non-zero offset geophones record reflected energy for each shot. During the course of a typical reflection seismic survey, multiple shots are acquired, and multiple traces are recorded for each shot (Figure 14). The objective is to end up with a number of non-zero offset traces for each common midpoint (CMP) location along the length of the seismic profile (Figures 9 and 15). Multiple offset data enable us to estimate subsurface velocities. Ultimately, all of the traces for each common midpoint location will be appropriately processed (to facilitate noise reduction), summed, and output as the single trace corresponding to that midpoint location.

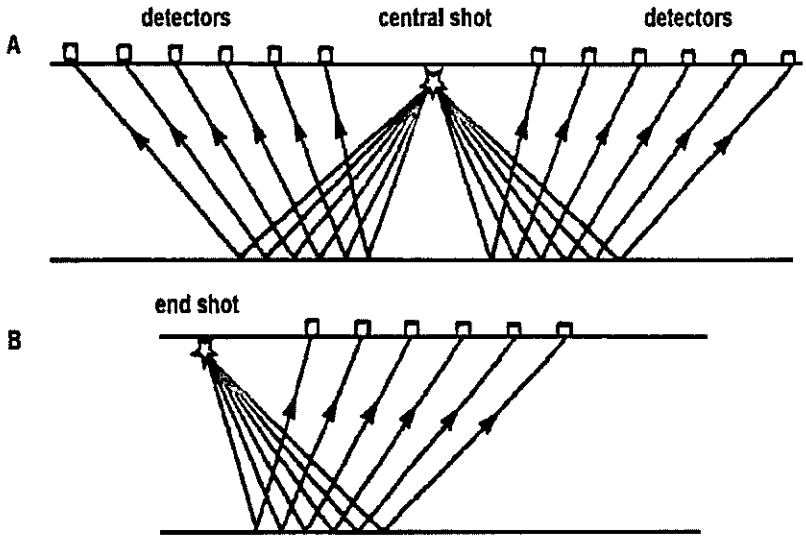

Figure 13: Split-spread shot array (13A) and end-on shot array (13B). (After Keary and Brooks, 1991.)

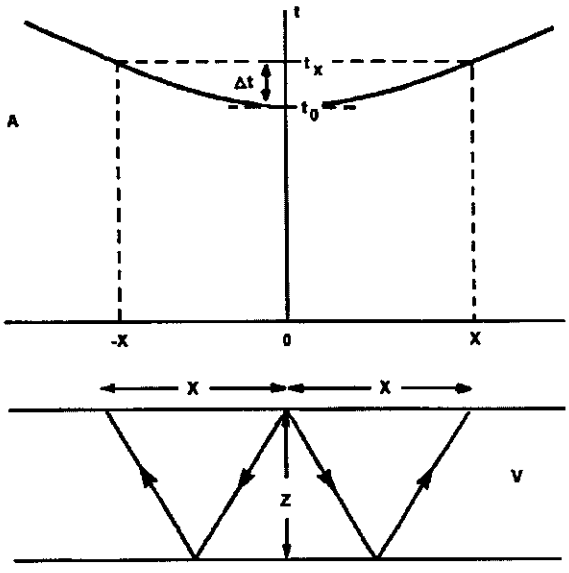

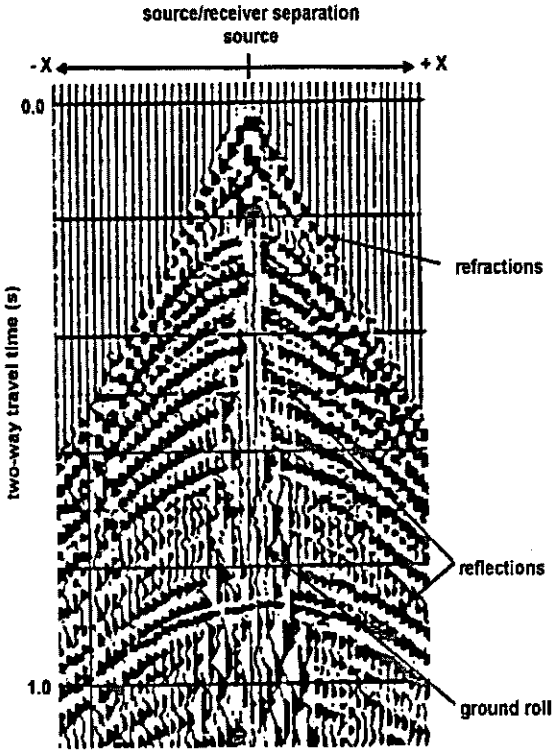

Figure 14: Common shot gather for split-spread array (14A). Reflected energy is aligned along hyperbolic travel time curves (14B). Noise is superposed on the reflected energy. (After Keary and Brooks, 1991.)

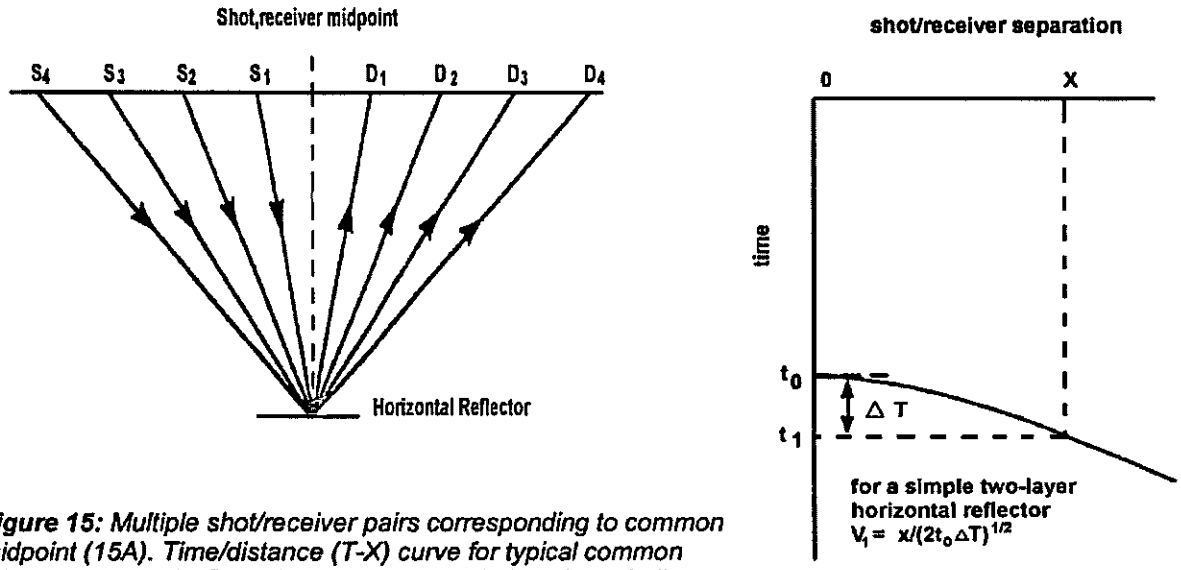

Figure 15: *Multiple shot/receiver pairs corresponding to common midpoint (15A). Time/distance (T-X) curve for typical common midpoint gather. Reflected energy is aligned along hyperbolic travel time curves (15B; after Keary and Brooks, 1991.)*

The quality, utility, and cost of the output stacked migrated (or non-migrated) seismic profile are functions of the array parameters. Careful consideration must be given to line spacing, the fold of the data, and to array design, particularly: line length, line orientation, near offset, far offset, receiver spacing, number of receivers, array type, receiver (group) configuration, and shot spacing (Figure 16). These parameters are usually best determined in the field. Generally, an attempt is made to minimise costs, without overly sacrificing data quality.

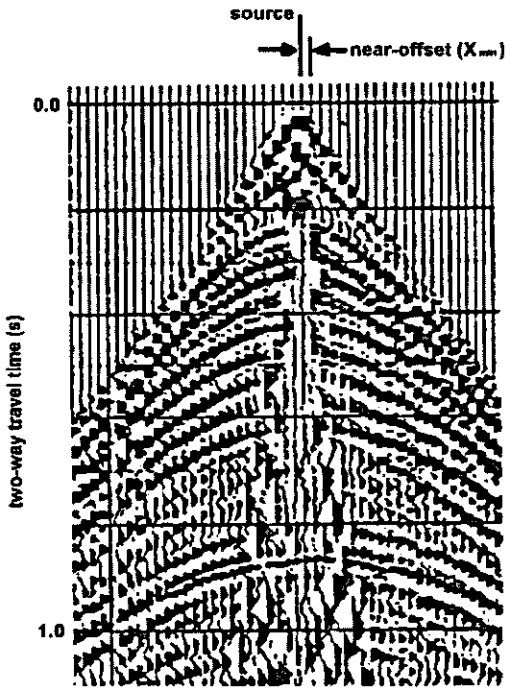

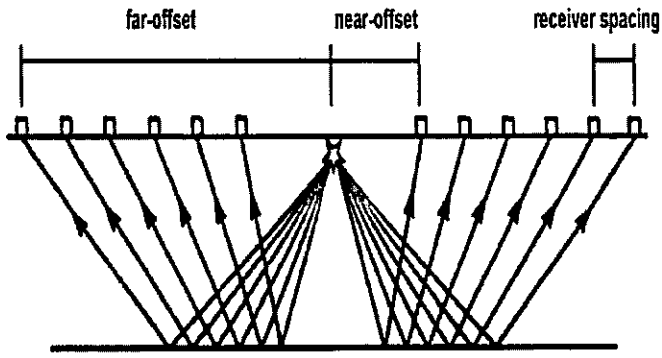

Figure 16: *Typical split spread field array (16A) and corresponding shot gather (16B). Careful consideration must be given to line spacing, the fold of the data, and array design, particularly: line length, line orientation, near offset (X_{min}), far offset (X_{max}), receiver spacing, number of receivers, array type, group (receiver) interval, and shot spacing. (After Keary and Brooks, 1991.)*

Line spacing: The spacing of seismic lines should be a function of our target size and overall objective. For example, if our target has a basal diameter of 30 m, and it is imperative that we locate and map each such target in a specified area, our lines should be spaced at 15-m intervals or less (Figure 17). In contrast, if we are only interested in determining regional dip in an area of essentially planar stratigraphy, our line spacing could be on the order of several hundreds of meters or more. If we need closely spaced structural control in an area, a 3-D survey may be more cost-effective than a suite of 2-D lines (Figure 18). A 3-D survey will also provide for better lateral and vertical resolution (target definition). Usually, shallow 3-D surveys are not cost-effective.

Figure 17: *The spacing of seismic lines should be a function of target size and overall objective. For example, if our target has a basal diameter of 30 m, and it is imperative that we locate and map each such target in a specified area, our lines should be spaced at 15m intervals or less. In contrast, if we are only interested in determining regional dip in an area of essentially planar stratigraphy, our line spacing could be on the order of several hundreds of meters or more.*

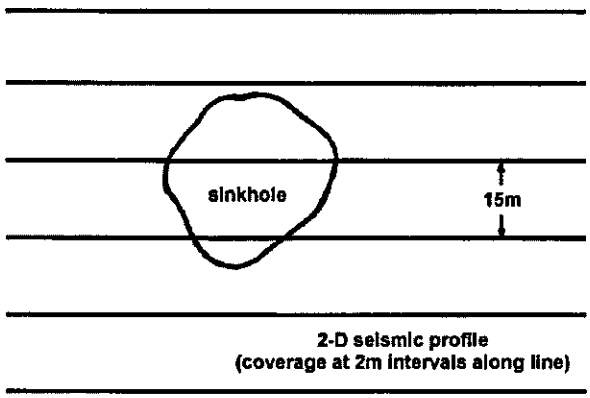

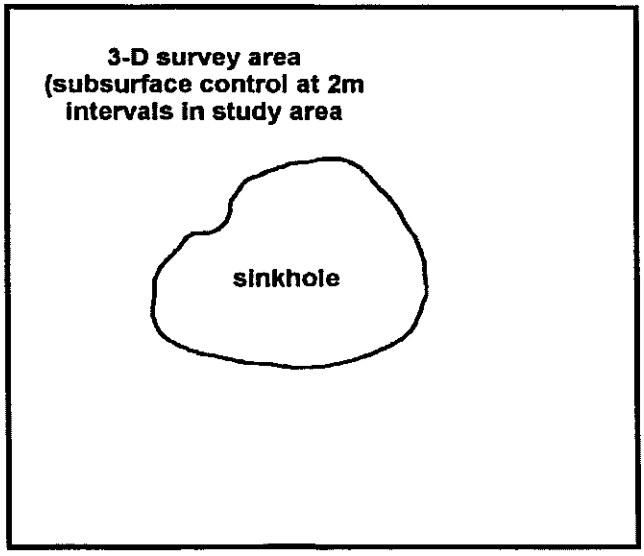

Figure 18: *If we require closely spaced subsurface structural and/or stratigraphic control in an area, a 3-D survey may be more cost-effective than a suite of 2-D lines. A 3-D survey will also provide better lateral and vertical resolution.*

Fold: The term "fold" (**F**) refers to the multiplicity (number) of traces incorporated into each common midpoint gather (Figure 15). Fold is a function of the receiver spacing (**ΔR**), the number of receivers (**R**), and the shot spacing (**ΔG**).

$$F = R/(2\,[R/\Delta G]) \qquad \text{Equation 1}$$

Statistically, the signal-to-noise ratio (**S/N**) increases as a function of $(F)^{1/2}$. Generally, an attempt is made to minimize the fold (and costs), without overly sacrificing data quality.

Line length: To facilitate the migration and interpretation of the seismic data, the minimum line length (**L**) is often set on the basis of the width of the zone of interest (**W**) and the depth to the target zone (**Z**). As a rule of thumb (Figure 19) **L** is set that:

$$L \geq W + 2Z \qquad \text{Equation 2}$$

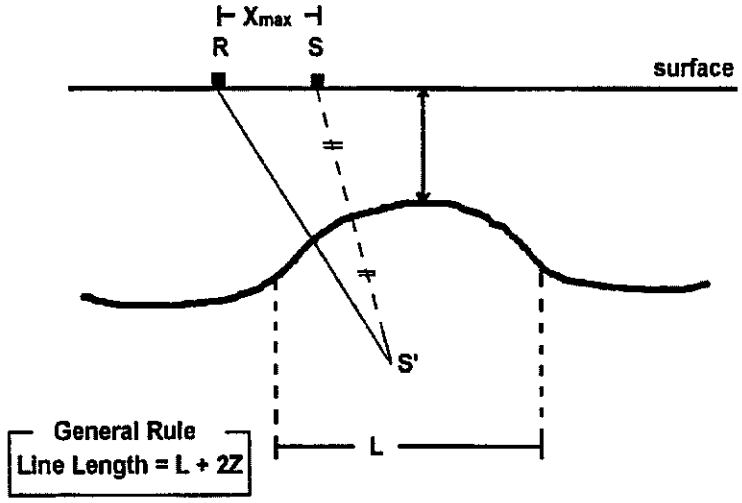

Figure 19: As a rule of thumb, the minimum line length (L) is often set on the basis of the width of the zone of interest (W) and the depth to the target zone (Z). 3-D considerations are slightly different.

Line orientation: Often, 2-D shallow seismic data are not migrated. Profiles are often acquired parallel to one another, and oriented such that acquisition time is minimized and surficial obstacles avoided. Frequently, a crossing tie-line is acquired to ensure interpretation consistency (Figure 20). However, if the 2-D data are to be migrated, they should be oriented parallel to regional dip. This later consideration does not apply to 3-D data.

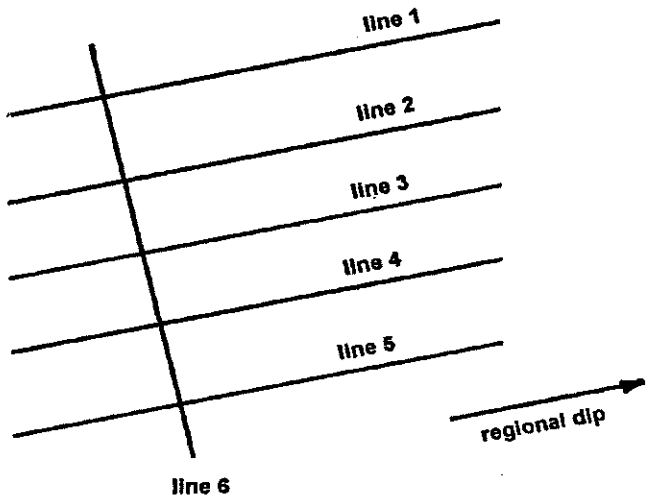

Figure 20: 2-D shallow seismic profiles are often acquired parallel to one another, and oriented such that acquisition time is minimized and surficial obstacles avoided. Frequently, a crossing tie-line is acquired to ensure interpretation consistency. If the 2-D data are to be migrated, they should be oriented parallel to regional dip to facilitate the correct migration of the reflection seismic data.

Near offset: The term "near-offset" (X_{min}) refers to the spacing between the shot and the nearest activated ("live") receiver (Figure 16). This distance should be set such that interpretable reflected energy is recorded for the shallowest horizon of interest. This energy may be masked by groundroll at lesser shot-receiver spacings, and by refractions at greater shot-to-receiver spacings (Figure 14). In practice, (X_{min}) is best determined on the basis of the examination of field test data, and in conjunction with other array parameters {(X_{max}), (R), (ΔR), and (ΔG)}.

Far offset: The term "far-offset" (X_{max}) refers to the spacing between the shot and the farthest "live" receiver (Figure 16). This distance should be set such that interpretable reflected energy is recorded for the deepest horizon of interest. Move-out should also sufficient to accurately determine subsurface velocities and attenuate multiples (Figure 14). However, (X_{max}) should not be so great that unacceptable NMO-stretch is introduced (at the level of the deepest reflector of interest) during stacking, or such that the deeper reflections are masked by refractions (Figure 14). In practice, (X_{max}) is best determined on the basis of the examination of field test data (Figure 14), and in conjunction with other array parameters {(X_{min}), (R), (ΔR), and (ΔG)}.

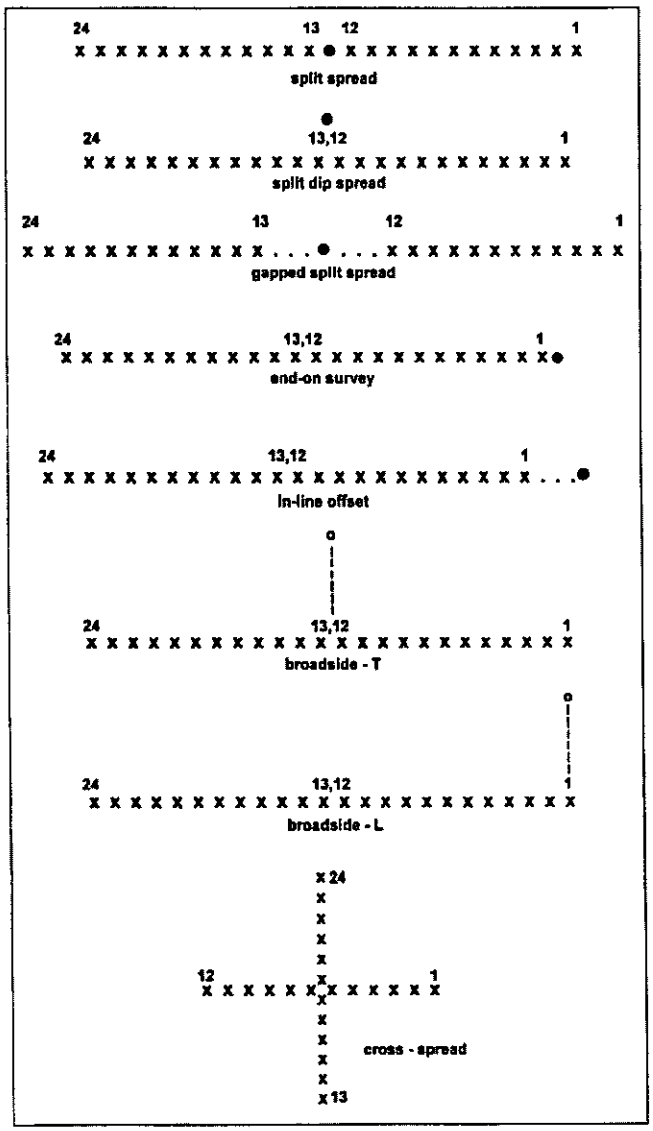

Receiver spacing (ΔR): Refers to the distance between adjacent geophones (or groups of geophones; Figure 16). Generally, subsurface coverage (trace spacing on seismic profile; Figure 9) is ½ ΔR, and should be sufficiently small to avoid aliasing. If (R) is fixed by the equipment available, (ΔR) is a direct function of (X_{min}) and (X_{max}).

Number of receivers: The number of "live" receivers (R; Figure 11) is usually a fixed function of the equipment used (i.e., 12-channel seismograph, 24-channel seismograph, 48-channel seismograph, etc.). However, if options are available, R should be determined on the basis of (ΔR), (X_{min}) and (X_{max}).

Figure 21: A number of different arrays are commonly used for shallow reflection seismic surveys. Usually an end-on or split-spread array is employed. Often times, when split-spread arrays are used, the source is offset from the linear receiver array, to minimize ground-roll effects on the near-offset traces. (After Sheriff and Geldart, 1995.)

Array type: A number of different arrays are commonly used for shallow reflection seismic surveys (Figure 21). Usually an end-on or split-spread array is employed. Often times, when split-spread arrays are used, the source is offset from the linear receiver array, to minimize ground-roll effects on the near-offset traces. The type of array employed is usually a function of (X_{min}), (X_{max}), (R), (R), and the desired fold.

Receiver (group) configuration: Usually, single high-frequency geophones (or hydrophones) are used for shallow reflection seismic surveying. In contrast, groups of spaced, coupled geophones are typically employed during deeper reflection seismic exploration, as a means of attenuating low apparent wavelength noise (mostly groundroll). This methodology does not work as well for shallow reflection studies, because energy reflected from shallow horizons is typically characterized has low apparent wavelengths (Figure 22).

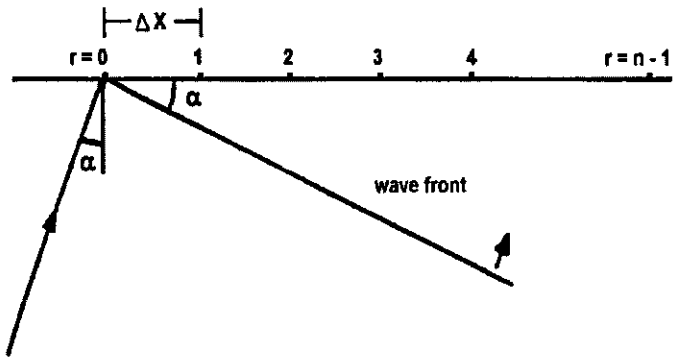

Figure 22: *Reflections originating at depth are characterized by high apparent wavelengths; groundroll (horizontally travelling coherent noise) is characterized by lower apparent wavelengths. (After Sheriff and Geldart, 1995.)*

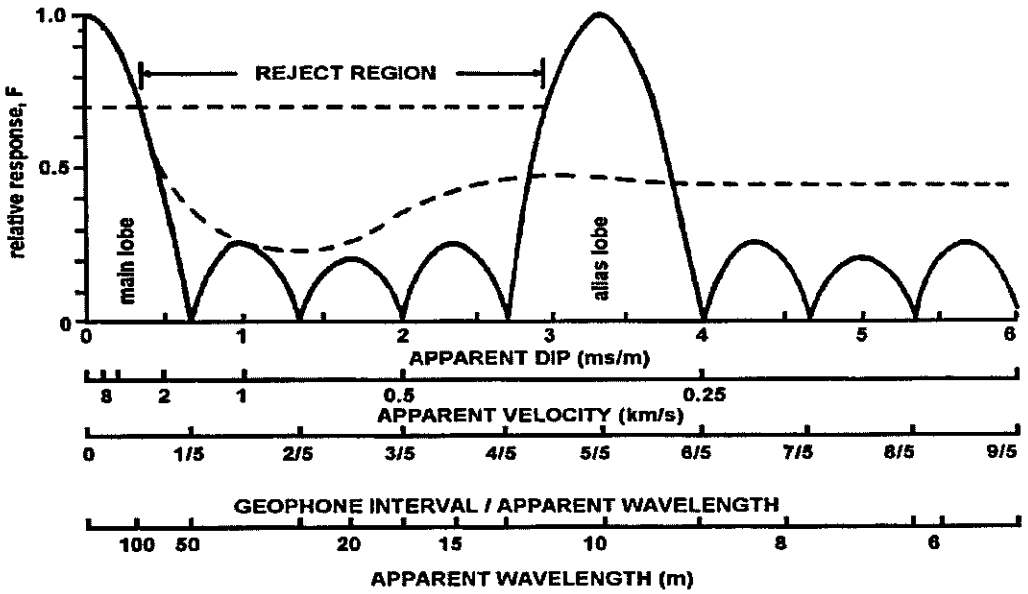

PROCESSING

Reflection seismic data are acquired in the field as common shot gathers (Figure 14). The data are modified through post-acquisition processing and ultimately displayed as the stacked seismic profile upon which most interpretations are based. The processing of shallow reflection seismic data is similar to the processing of petroleum data, generally less complex. The processing of petroleum seismic data is discussed in detail in a number of excellent texts (see references).

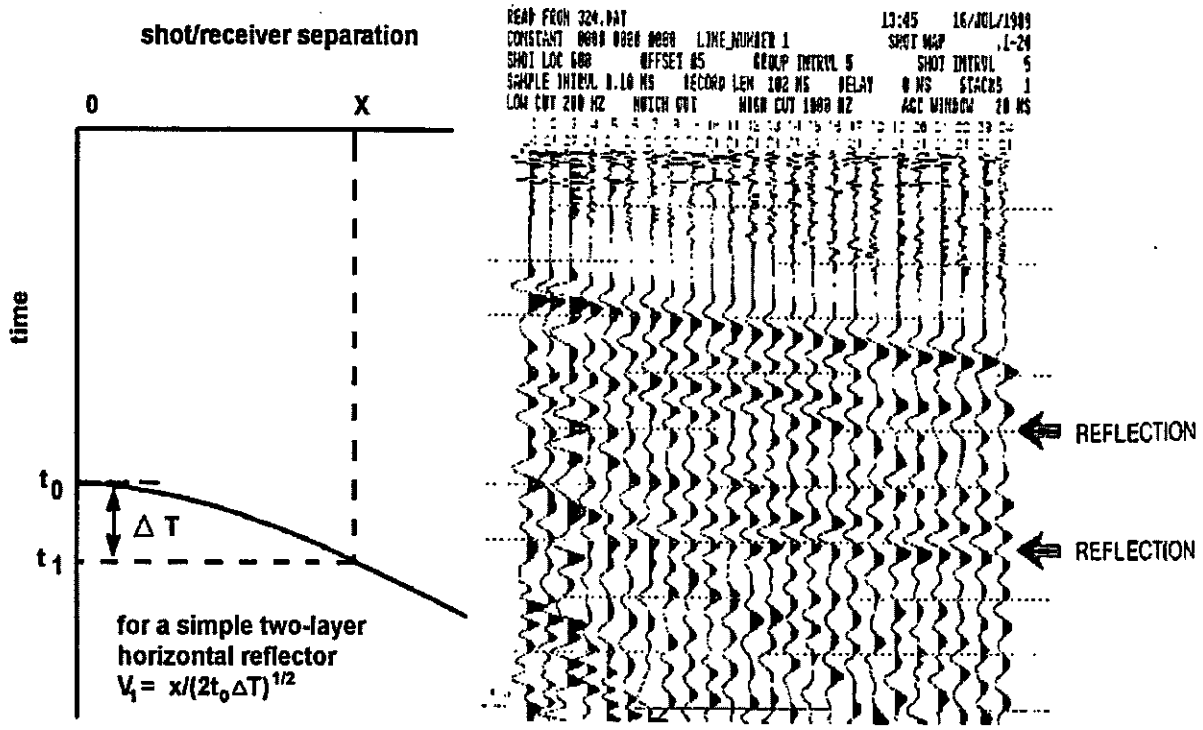

Figure 23: Example field record (common shot gather) before and after the muting of bad traces. A typical shallow seismic processing flow can include: muting of bad traces, elevation corrections, muting of first breaks, muting or filtering of air blast and ground roll, resorting into common midpoint gathers, filtering, deconvolution, velocity analysis, normal moveout corrections, residual statics, stacking, filtering, and migration.

Muting of bad traces: Examination of common shot gathers (field records; Figure 23) may reveal traces with very low signal-to-noise ratios. These traces can result from hardware problems within the recording unit, damaged cables or receivers, anomalous localized noise, uncoupled receivers, etc. Generally, it is better to mute these traces, rather than include them in the stacking process.

Elevation corrections: Generally surficial topography is irregular, and shots and receivers are located at different elevations. To compensate, elevation corrections are applied. Ideally, elevation corrected traces appear as though their shots and receivers were located along a common datum. In shallow seismic work the datum is usually at or above the highest structural location on the seismic profile. In conventional (deeper exploration) the selected datum is generally in consolidated rock beneath the water table.

Muting of first breaks: Refractions are generally considered to be noise, and are generally muted (Figure 14). Refracted acoustic energy has been critically refracted along acoustic impedance interfaces, and constitutes noise on reflection seismic data.

Muting or filtering of air blast and ground roll: Air blast is acoustic energy that has travelled from the source to the receivers through air. Ground roll consists is low-velocity, surface guided-guided acoustic energy. Both airblast and groundroll are considered to be noise, and are generally muted (Figure 14). Alternatively, F/K filters can be used to remove this coherent noise on the basis of its low apparent short apparent wavelength or long high apparent wavenumber (Sheriff and Geldart, 1995.).

Filtering: Data can be filtered at any step in the processing sequence (Figure 26). Data may be filtered to remove undesired frequency components (time or frequency domain filters), or to remove a range of undesired apparent wavenumbers (F/K filtering; Sheriff and Geldart, 1995).

Deconvolution: Deconvolution is applied to shallow seismic data generally as a means of enhancing the higher frequency components of the recorded signal, or transforming a non-zero phase data into zero-phase data. Effective deconvolution operators can be difficult to design (because of variable source signatures, short trace lengths, and high attenuation in the shallow subsurface). Deconvolution can be more destructive than constructive in many circumstances (re: quality of the output signal). Data can be deconvolved both before and/or after stacking.

Velocity analysis: Velocity analysis can be done on either common shot gathered data or common midpoint data. Subsurface interval and root mean square (RMS) velocities can be determined sequentially for the shallowest through deepest reflectors on the basis of the analysis of their respective hyperbolic traveltime curves.

Resorting into common midpoint gathers: Prior to stacking, the reflection seismic traces are resorted into common midpoint gathers (Figures 15 and 24). All of the traces in a common midpoint gather are assumed to have common subsurface reflection points.

Normal moveout corrections: Normal moveout (NMO) corrections are applied to common midpoint data. Primary reflected energy is horizontally aligned on NMO corrected gathers (Figure 24). In areas of complex subsurface structure DMO corrections may be applied.

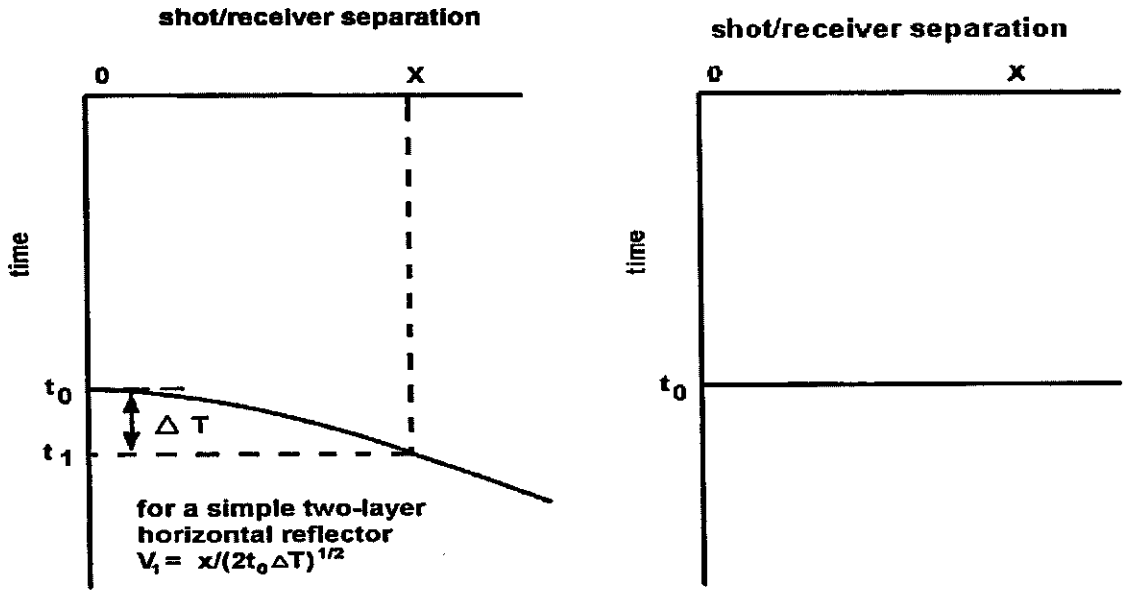

Figure 24: Example common midpoint gather (left), and NMO-corrected common midpoint gather (right). Ideally, on a common midpoint gather, the reflection events are aligned along smooth hyperbolic travel time curves. On an NMO-corrected common midpoint gather, the events should be horizontally aligned.

Residual statics: Automatic statics are generally applied to the NMO-corrected common midpoint gathers. The intent is to statistically align the reflected energy and improve the quality of the output stacked data.

Stacking: All of the traces in each NMO corrected common midpoint (CMP) gather are summed together, and output as a single trace. All of these traces are plotted at their corresponding CMP locations on the output stacked seismic profile (Figure 25).

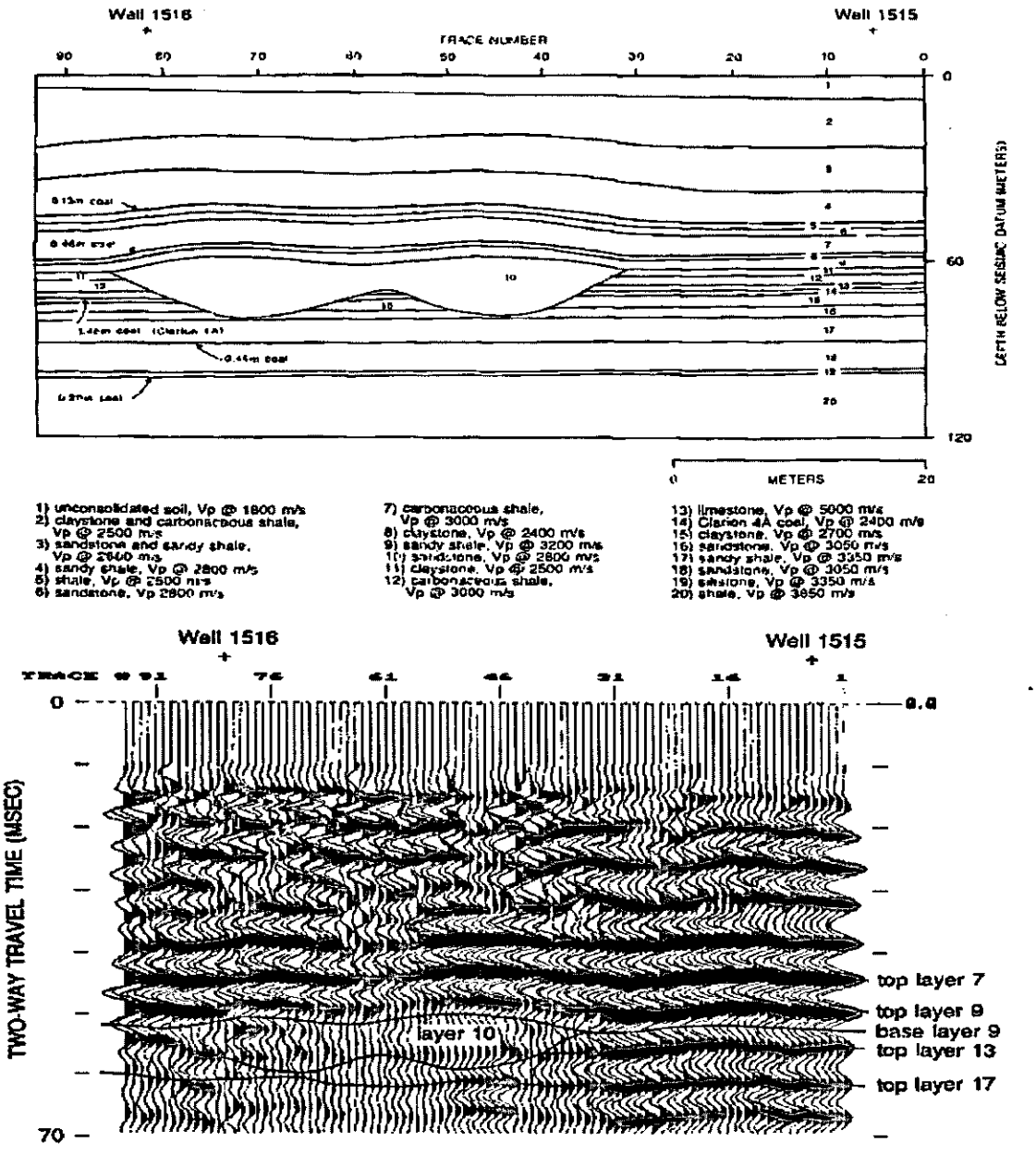

Figure 25: Segment of output stacked seismic profile. All of the NMO-corrected CMP traces are plotted at their corresponding locations on the output stacked seismic profile.

Migration: Dipping reflections are not properly located (spatially) on the output stacked seismic section unless migration has been applied. Migration effectively shifts seismic reflection energy (including diffractions) to its spatial point of origin (Figure 26). In practice however, it is usually not cost-effective to acquire shallow reflection data that is suitable (re: array considerations) for migration, and generally, acceptable interpretations can be done on non-migrated data. Problems also arise because migration of 2-D profile data will not properly shift dipping events unless the profile is oriented parallel to dip; neither will it properly migrate energy that originates out of the plane of the seismic profile. These problems can be overcome by acquiring 3-D data. However, shallow 3-D surveying is usually not cost-effective.

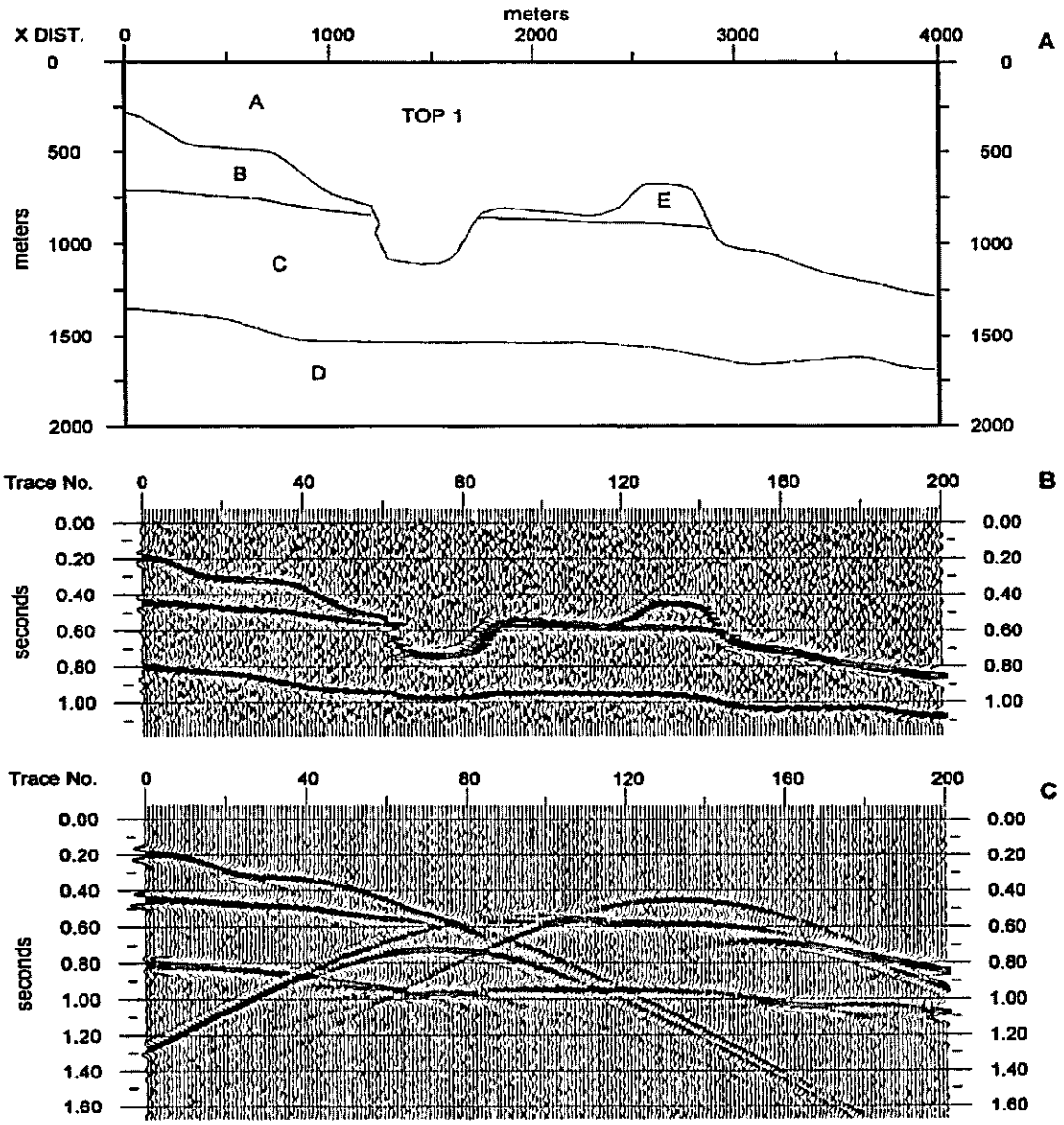

Figure 26: *Geologic model (A; $\rho_1 = \rho_2 = \rho_3$; $v_3 > v_2 = v_1$), and simulated migrated (B) and non-migrated (C) reflection seismic data.*

INTERPRETATION

The objective of seismic interpretation is to transform a stacked reflection seismic profile into a laterally continuous structural/geologic model of the subsurface (Figure 27). The interpretation of seismic data is non-unique; there are an infinite number of theoretically correct models. However, the only reasonable models are those that are consistent with available ground truth, geologic principles and processes, and generally accepted seismic interpretation methodologies. Seismic interpretation is essentially the inverse of forward modeling (Figure 9), and involves the recognition and "inversion" of the seismic signature of the subsurface (Anderson et al., this volume). Seismic interpretation is predicated on the assumption that the seismic data have been correctly processed, and that the signature of the seismic profile reflects the subsurface geology.

Structural interpretations are best done on migrated seismic data if available (using non-migrated data as an interpretational constraint). On migrated seismic data, reflections are in their proper spatial location, and time-to-depth conversions are relatively straightforward if subsurface velocities are known. In contrast, dipping reflectors are not in their proper spatial location on non-migrated seismic data, and direct time-to-depth conversions are not possible. However, an experienced interpreter can work with non-migrated reflection seismic data and develop an accurate model of the subsurface; indeed diffraction patterns on non-migrated seismic profiles often provide important clues as to the nature of the shallow subsurface.

Seismic interpretation is generally an iterative process. The first step is usually the identification and correlation of the more prominent seismic marker horizons (Figure 27). Synthetic seismograms (Anderson et al., this volume) or checkshot survey data greatly facilitate this process. Geologic borehole control and stacking velocities can also be used to estimate the two-way travel time to prominent subsurface markers. If subsurface control is not available, initial correlation must be made based on expected depths and velocities, and seismic character.

With respect to the simulated seismic profile of Figure 27, an experienced interpreter would probably first identify and correlate the high-amplitude reflections from the tops of the Wabamun, Ireton and Beaverhill Lake. (These reflections would also be correlated across any other seismic profiles in the study area.) The interpreter would note that: 1) the amplitudes of these events are essentially uniform across the seismic section; 2) the top Wabamun and top Ireton events are locally time-structurally high above the Leduc reef; 3) the Beaverhill Lake event is locally time-structurally high beneath the reef.

Step two is the correlation and tentative identification of other significant reflections on the seismic profile (Figure 27). Significant reflectors are those that characterize geologic features of interest to the interpreter. These can be prominent high-amplitude events which can be correlated across the length of the seismic profile, or subtle low-amplitude events with little lateral extent. Interpretation is both qualitative and quantitative. A good interpreter is one who can identify those reflections that are significant with respect to the geologic feature of interests.

An experienced interpreter would probably also identify and correlate the Cooking Lake and more prominent inter-shale events, and the reflection from the top of the reef. (These reflections would also be correlated across any other seismic profiles in the study area.) The interpreter would note that: 1) the platform event (Cooking Lake) is anomalously low-amplitude and time-structurally high beneath the Leduc reef; 2) the reef top event is present only between traces 46 and 70; 3) the inter-shale events terminate abruptly against the flanks of the seismic image of the reef.

In step three, the interpreter would develop preliminary structural/geologic models based on the seismic signature of the subsurface, bearing in mind that the models must be consistent with available ground truth, geologic principles and processes, and generally accepted seismic interpretation methodologies. With respect to Figure 27, the interpreter familiar with the geology of the study area would probably conclude that the anomaly was indicative of the presence of an isolated reef. The time-structure at the top Wabamun and Ireton events would be attributed to differential compaction of the reef and off-reef shale. The structure along the Cooking Lake and Beaverhill Lake events would be attributed to velocity pull-up (Anderson et al., this volume). The amplitude change along the platform event would be attributed to a change in the acoustic impedance contrast across this horizon. The inter-shale events would be interpreted as terminating against the flanks of the seismic image of the reef. If additional seismic control (a grid of seismic profiles) was available, an attempt would be made to map the areal extent of the reef.

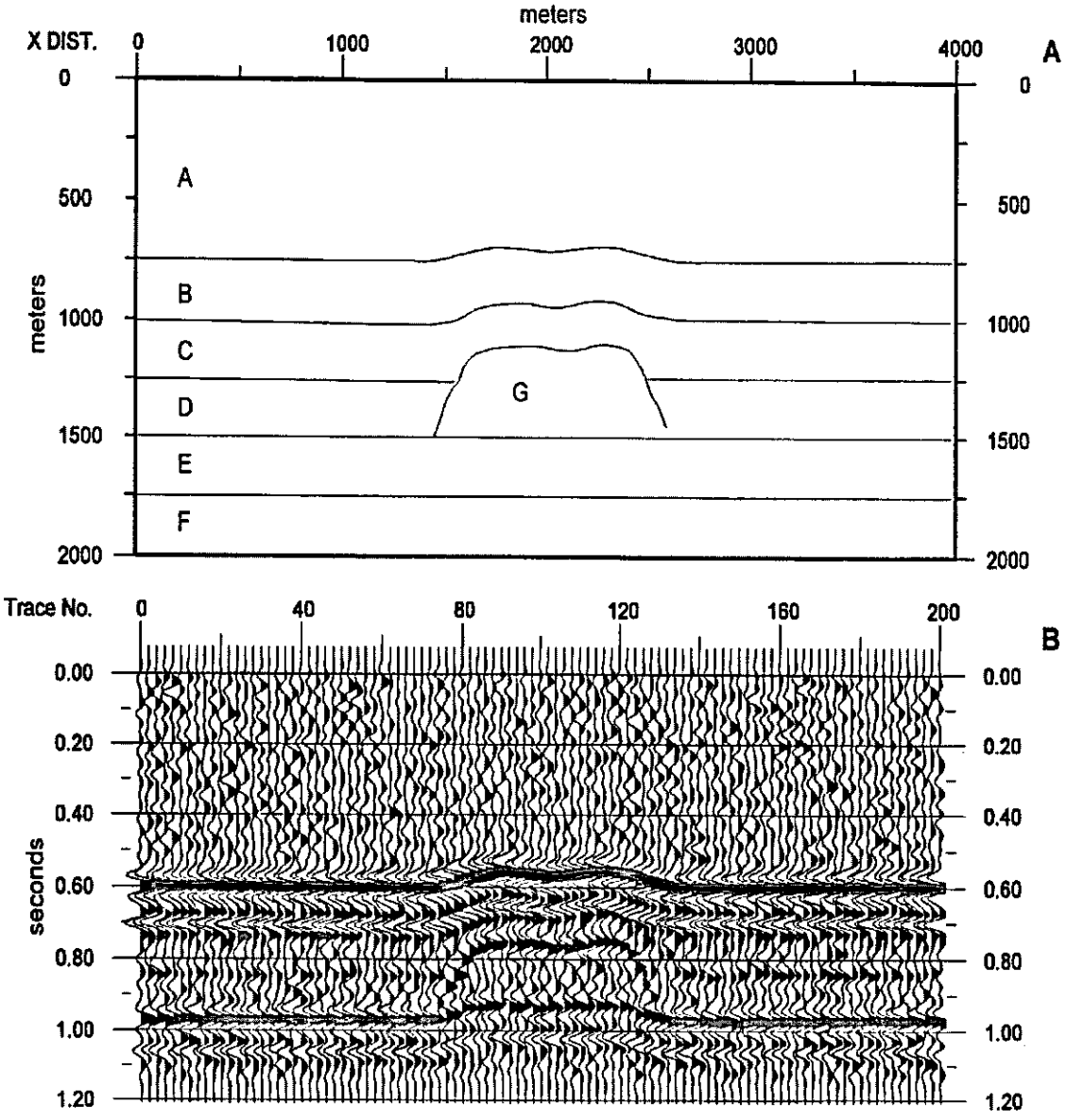

Figure 27: *Geologic model and corresponding 2-D synthetic seismic profile. This vertical incidence synthetic simulates migrated seismic data. {A - Mannville (clastics); B - Wabamun (carbonate); C - Ireton (shale); D - Duvernay (shale); E - Cooking Lake (carbonate); F - Beaverhill Lake (shale); G - Leduc (reef); $v_E > v_B > v_G > v_D > v_F > v_C > v_A$}.*

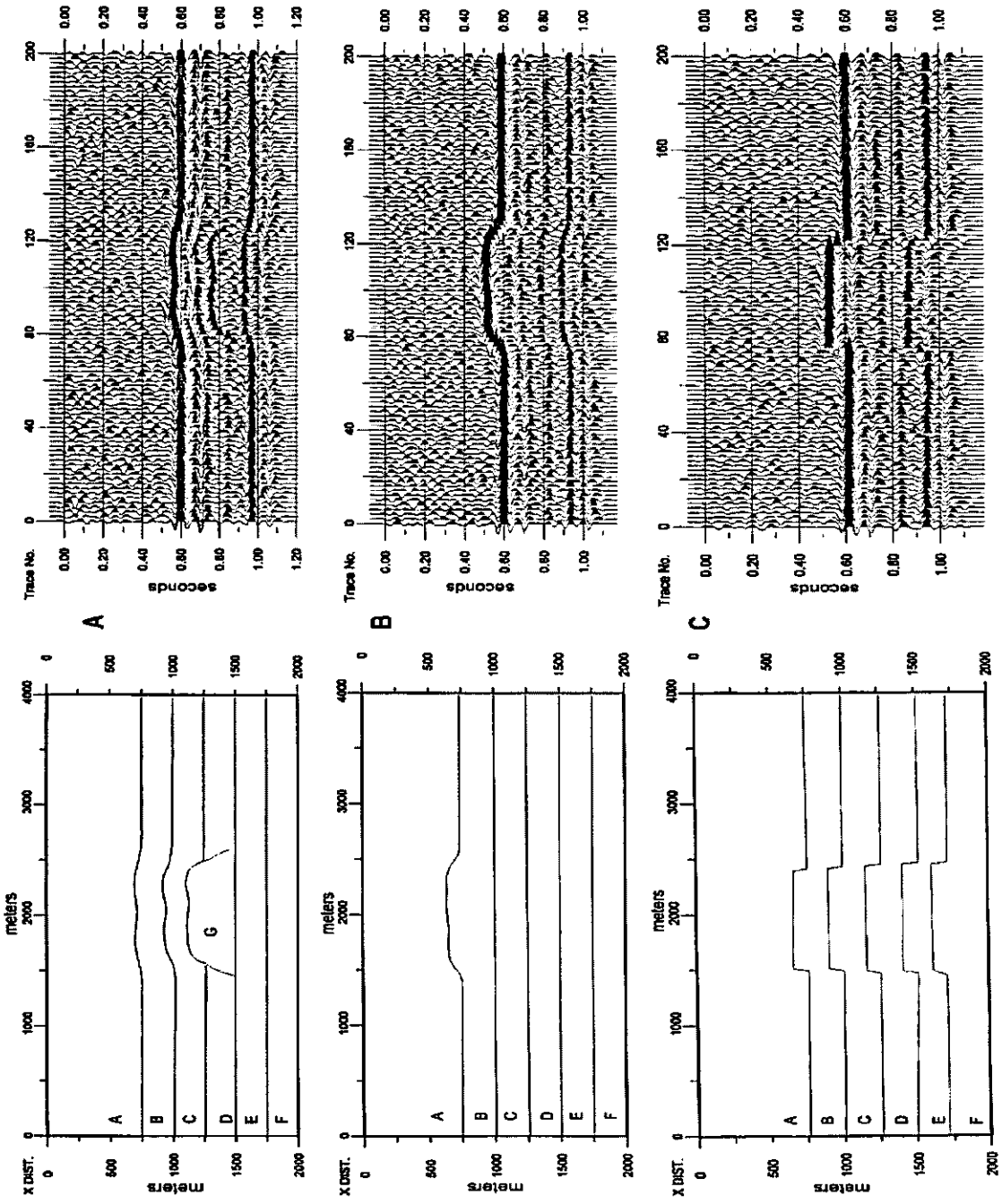

Figure 28: *Geologic models and corresponding vertical incidence, 2-D synthetic profiles. (A - reef model; B - fault model; C - unconformity model.)*

The experienced interpreter, examining excellent quality seismic data, would recognize (almost immediately) that the anomaly of Figure 27 is characteristic of Leduc reefs. More typically however, seismic data are contaminated by noise and interpretations are not so straightforward. The seismic signature of Figure 28A, for example, is very similar to those of Figures 28B and 28C. The interpreter working with the data of Figure 28A, would want to consider whether the anomaly could be attributed to either post-Devonian faulting or erosional relief at the top of the Devonian. It is important to remember that the interpretation of seismic data is not unique!

SUMMARY

The shallow seismic reflection technique is relatively straightforward from a conceptual perspective. In practice, however it is complex - mostly because the reflected events of interest are contaminated by coherent and random noise. To compensate, intricate methodologies have been developed to acquire and process reflection seismic data. Many of these methodologies are site and objective dependent, to the extent that many conventional seismic exploration techniques are not suitable for shallow reflection seismic work. The interpretation of reflection seismic data is also a complex process, and as much an art as a science. Travel time to depth conversions can be unreliable because of either inaccurate velocity control or incorrect event identification. Similarly, seismic amplitudes can be misinterpreted because of gain distortions. Forward seismic modelling and the inclusion of external geologic and geophysical constraints are often the key to successful interpretations, and the development of a reasonable subsurface geologic image.

REFERENCES

Anderson, N. L., Cardimona, S., and Roark, M. S., 1998, Forward modelling of reflection seismic and ground-penetrating radar signals to aid in field survey design and data interpretation: this volume.

Anderson, N. L., and Hedke, D., Editors, 1995, Geophysical Atlas for Kansas: Kansas Geological Survey Bulletin 237.

Brown, A. R., 1996, Interpretation of three-dimensional seismic data: American Association of Petroleum Geologists Memoir 42, 424 p.

Evans, B. J., 1997, A handbook for seismic data acquisition in exploration: Society of Exploration Geophysicists, 305 p.

Hinds, R., Anderson, N.L., and Kuzmiski, R., 1996, VSP Interpretative Processing: Theory and Practice: Society of Exploration Geophysicists, 205 p.

Keary, P., and Brooks, M., 1991, An Introduction to Geophysical Exploration: Blackwell Scientific Publications, 254 p.

McAnn, D. M., Eddleston, M., Fenning, P. J., and Reeves, G. M., editors, 1997, Modern geophysics in engineering geology: The Geological Society, 441 p.

Sheriff, R. E., 1991, Encyclopedic Dictionary of Exploration Geophysics, Third Edition: Society of Exploration Geophysicists, 376 p.

Sheriff, R. E., and Geldart, L. P., 1995, Exploration Seismology: Press Syndicate of the University of Cambridge, 592 p.

Steeples, D.W. and Miller, R.D., 1990, Seismic reflection methods applied to engineering, environmental and groundwater problems, *in* Ward , S.H., Editor, Geotechnical and engineering geophysics, volume 1: Society of Exploration Geophysicists, 389 p.

Weimer, P., and Davis, T.L., editors, 1996, Applications of 3-D seismic data to exploration and production: American Association of Petroleum Geologists and Society of Exploration Geophysicists, 270 p.

Yilmaz, O., 1987, Seismic data processing: Society of Exploration Geophysicists, 526 p.

APPENDIX F

GROUND-PENETRATING RADAR (GPR) AND REFLECTION SEISMIC STUDY OF KARSTIC DAMAGE TO HIGHWAY EMBANKMENTS, HANNIBAL, RALLS COUNTY, MISSOURI

Neil L. Anderson*, Steve Cardimona*,
Dennis Lambert^ and Tim Newton^

*Department of Geology and Geophysics, University of Missouri-Rolla, Rolla, Missouri
^Missouri Department of Transportation, Jefferson City, Missouri

ABSTRACT

In June 1998, the Department of Geology and Geophysics at University of Missouri-Rolla (UMR) conducted two geophysical surveys (designated herein as surveys A and B) for the Missouri Department of Transportation (MoDOT) in Ralls County, Missouri. In August, 1998, the UMR geophysics crew returned to the survey A site to acquire additional ground-truth in areas that had been interpreted as anomalous on the original (June, 1998) geophysical data set. Surveys A and B were conducted under the supervision of MoDOT District Geologist Dennis Lambert.

Survey A site was a 245m segment of Highway 79 in Hannibal, Missouri. The integrity of this two-lane section of roadway was suspect because small sinkholes had developed within and immediately adjacent to the Highway 79 drainage ditches, in places causing the partial collapse of the asphalt-covered roadway shoulder. In total, a suite of 24 parallel, equally spaced ground penetrating radar (GPR) profiles were acquired along the paved roadway and asphalt-covered shoulder. The objective was to determine whether the surveyed segment of Highway 79 was underlain by any substantive voids. All of the features identified as anomalous on the GPR profiles were investigated during the follow-up site visit. Our conclusion, based on the interpreted GPR profiles and follow-up site inspection, is that the surveyed segment of Highway 79 does not overlie any substantive, previously undetected, sub-pavement or sub-asphalt voids.

Survey B site included the right of way (ROW) and immediately adjacent area along a section of divided, four lane Highway 61, near the Salt River crossing immediately south of Hannibal. The objectives were to determine the probable cause of several small sinkholes (characterized by open depressions within the soil) that developed immediately adjacent to Highway 61, and to determine if substantive voids underlie the access road that parallels the highway. In total, three shallow seismic profiles and eight GPR profiles were acquired. Field observations and the interpretation of the survey B reflection seismic data suggests that natural spring waters and surface run-off (from the south bound lanes of Highway 61 and the access road) are channeled northward down the drainage ditch that separates the highway from the access road. These waters seep into the subsurface in the immediate proximity of the open sinkholes. These sinkholes are believed to be caused by the associated piping of fine-grained soil into underlying karstic cavities. The interpretation of GPR data acquired during survey B suggests that the access road does not overlie any substantive voids.

GENERAL SCOPE OF WORK

In June 1998, the UMR Department of Geology and Geophysics conducted two geophysical surveys (surveys A and B) in Ralls County, Missouri under the supervision of MoDOT District Geologist Dennis Lambert. In August 1998, the survey A site was revisited and the origins of anomalous features on the interpreted GPR profiles were conclusively established.

In survey A, a suite of 24 GPR profiles were acquired across the paved roadway and asphalt-covered shoulder of a 245m segment of two-lane Highway 79, in Hannibal, Missouri (Figures 1, 2, 3, 4 and 5). The objective was to identify and locate any sub-roadway voids of possible karst origin. The integrity of this section of roadway was suspect because small sinkholes (<1m diameter throats at 1m depth) had developed within and immediately adjacent to Highway 79 drainage ditches, in places causing the partial collapse of the asphalt-covered roadway shoulder. In August 1998, the UMR crew returned to

the Highway 79 (survey A) site, and investigated those features interpreted as anomalous on the original GPR data set.

In survey B, both shallow reflection seismic and GPR data were acquired (Figure 6). Three reflection seismic profiles were placed parallel and immediately adjacent to divided four-lane Highway Route 61 (immediately south of the Salt River bridge). These reflection seismic data were acquired with the goal of mapping the shallow subsurface (particularly bedrock) and determining the cause of isolated sinkholes that had developed along the service road immediately to the west of Route 61. Eight GPR profiles were acquired along length of the service roadway the to determine if this roadway was underlain by large sub-asphalt voids.

GPR SURVEY A, HIGHWAY 79, HANNIBAL

A total of twenty-four (24) GPR profiles were acquired along sixteen parallel 245m (800ft) transects at the Highway 79, Hannibal survey A site (Figures 1, 2 and 3). A 400 MHz monostatic antenna was used to acquire GPR profiles 1-16 (along transects 1-16, respectively). A 200 MHz monostatic antenna was used to acquire GPR profiles 17-24 (along transects 2, 4, 6, 8, 10, 12, 14, and 16, respectively). The 400 MHz antenna profiles provided superior horizontal and vertical resolution in the upper two meters of roadway material. The 200 MHz antenna data provided better resolution at greater depths. The 400 MHz and 200 MHz data were consistent in terms of their interpretations and the spatial locations of identified anomalies.

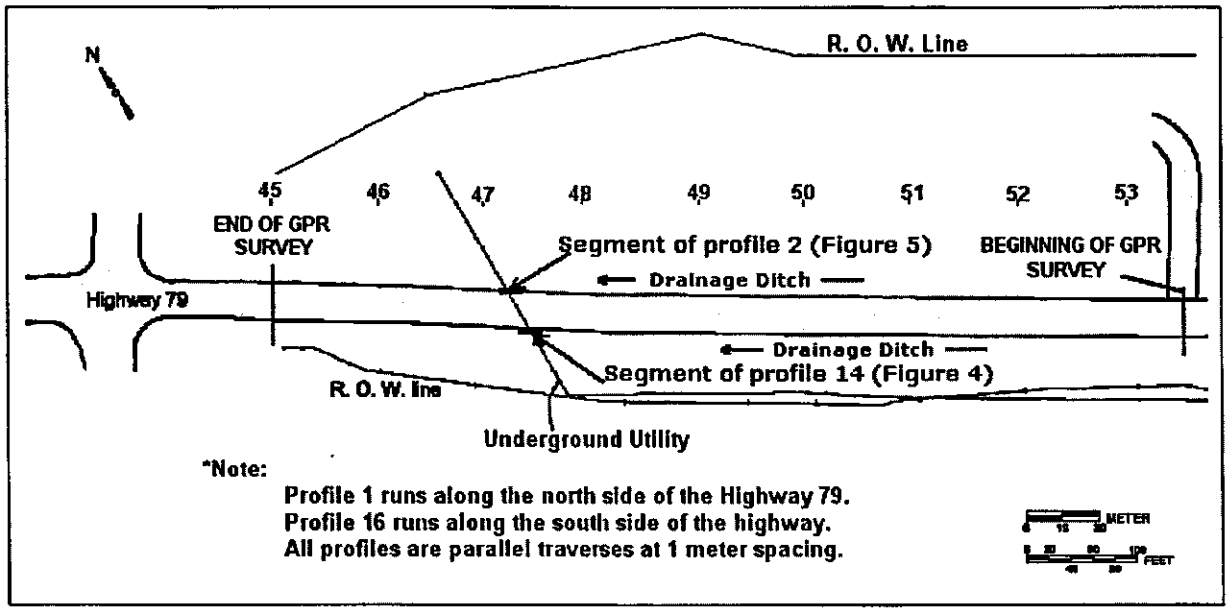

Figure 1: Map of the survey A site (Highway 79, Hannibal). A total of twenty-four GPR profiles were acquired. Profiles 1 -16 (400 MHz data) were acquired along transects 1-16, respectively. Profiles 17 -24 (200 MHz data) were acquired along transects 2, 4, 6, 8, 10, 12, 14, and 16, respectively. Transects are parallel, 245m (800 ft) long, and spaced at 0.9m (3ft). Detailed anomaly maps are shown as Figures 2 and 3. Segments from representative GPR profiles 14 and 1 are shown as Figures 4 and 5, respectively.

A number of prominent, high amplitude reflection/diffraction patterns (anomalies) were identified on the suite of GPR profiles. Most of these visually anomalous features were caused by the metal joints between adjacent 9m (30ft) long concrete roadway slabs, and could be correlated from profile to profile across the paved roadway. Most of the other anomalies identified were known to be caused by buried utilities or other sub-pavement construction features. GPR anomalies #2-#7 (Figures 2 and 3) were the only anomalous features identified on the interpreted survey A GPR data set that could not be attributed to either the contacts between adjacent slabs or buried utilities, and yet were of sufficient magnitude to justify further investigation. Example segments of GPR profiles 14 and 2 are presented as Figures 4 and 5, respectively.

Figure 2

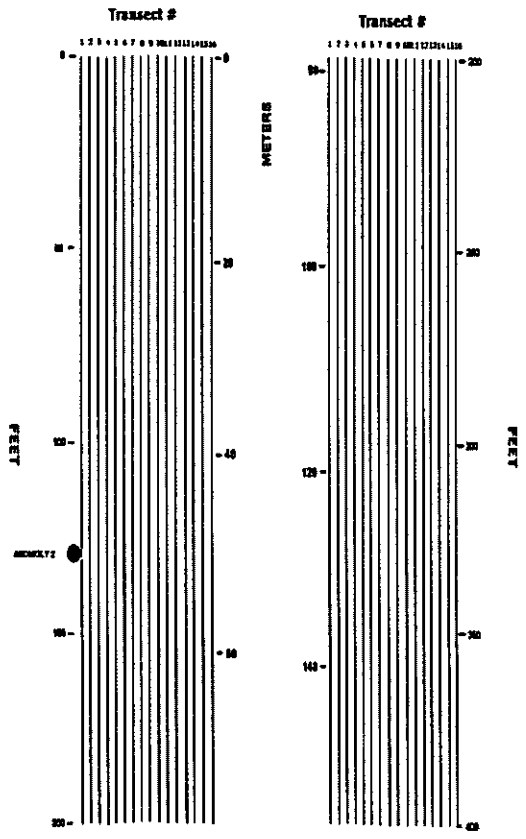

Figure 3

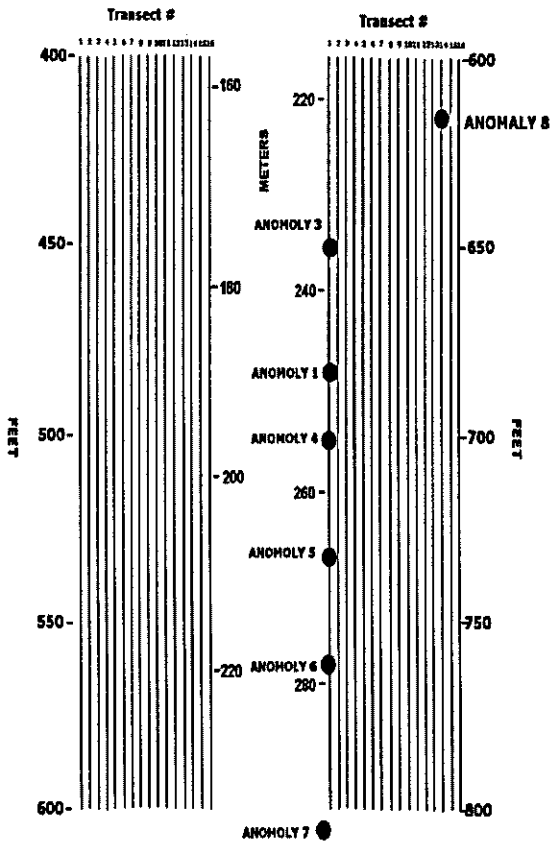

Figure 2: *Map of the southern half of survey A site (transects 1-16) depicting anomalies described herein. Segments from representative GPR profiles 14 and 2 are shown as Figures 4 and 5, respectively.*

Figure 3: *Map of the northern half of survey A site (transects 1-16) depicting anomalies described herein. Segments from representative GPR profiles 14 and 2 are shown as Figures 4 and 5, respectively.*

GPR Profile 14 (Figure 4) was acquired across paved roadway using a 400 MHz antenna. The vertical trace length is 40 nanoseconds, which translates into a depth of approximately 2.5m. The base of the pavement is not effectively imaged on this section. The contacts between adjacent slabs of pavement are characterized by high amplitude hyperbolic diffractions spaced at 9m (30ft) intervals. Anomaly #8 (Figures 3 and 4) is caused by underground utilities and can be correlated across a number of adjacent profiles. None of the prominent diffraction features on Profile 14 are attributed to the presence of sub-pavement voids.

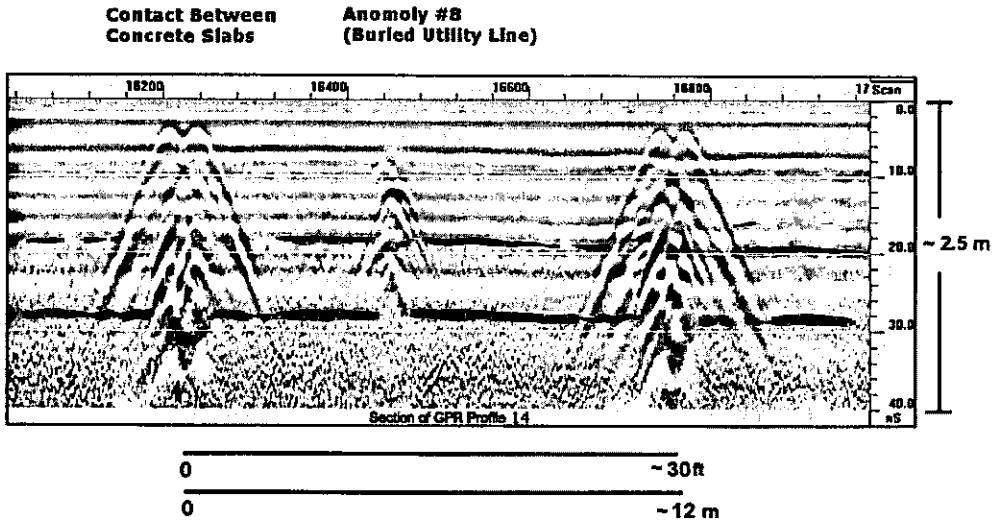

Figure 4: *Fifteen-meter segment of GPR profile 14 (400 MHz data; Figures 1, 2 and 3).*

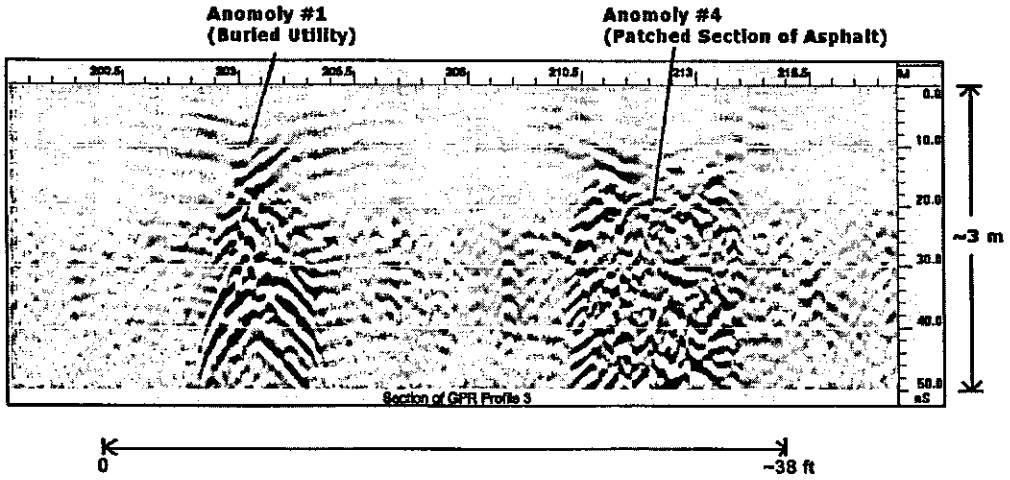

Figure 5: *Fifteen-meter segment GPR profile 2 (400 MHz data; Figures 1, 2 and 3).*

GPR Profile 2 (Figures 2, 3 and 5) was acquired across unpaved, asphalt-covered roadway. A 400 MHz antenna was employed. The vertical trace length is 50 nanoseconds, which translates into a maximum profile depth of about 3m. The base of the asphalt is not effectively imaged on this section, and the high amplitude hyperbolic diffractions that originate from the contacts between adjacent concrete slabs are not present (Figure 14). Seven prominent anomalies were identified on this profile (Figures 2 and 3); two of these are shown on Figure 5. Anomaly #1 is attributed to underground utilities. Anomaly #4 can be correlated across the GPR profiles 1, 2 and 3, but does not extend beneath the paved roadway.

Anomalies #2-#7 were investigated by MoDOT geologist Lambert and the UMR geophysics crew during the follow-up site visit in early August 1998. Anomaly #2 was known to be of shallow origin (based on its GPR signature) and could not be replicated in the follow-up GPR work, suggesting that anomaly #2 was probably caused by a temporary near-surface effect (e.g., piece of metal on the asphalt?). The site investigations also confirmed that anomalies #3 - #7 were associated with locations where previously detected voids had been in-filled and patched.

Based on our interpretation of the GPR profiles and our follow-up site investigations, we have determined that none of the anomalous features on the suite of GPR profiles acquired during survey A were caused by previously undetected sub-pavement or sub-asphalt voids. We conclude that there is no substantive geophysical evidence that the surveyed segment of Highway 79 overlies any large diameter sub-pavement or sub-asphalt voids.

SEISMIC AND GPR SURVEY B, ROUTE 61 SALT RIVER SITE

Three shallow reflection seismic profiles and eight GPR profiles were acquired at the Route 61 Salt River survey B site (Figure 6). The reflection seismic data were acquired using a Bison 24-channel reflection seismograph, a Bison EWG weight drop source, and 40 Hz geophones. Shot and geophone spacings of 1.5m (5ft) were employed. These seismic data were acquired with the objective of mapping bedrock and determining the cause of localized sinkholes (<1m throats at 1m depth) that had developed adjacent to the service road that lies immediately to the west of Highway 61 (figure 6).

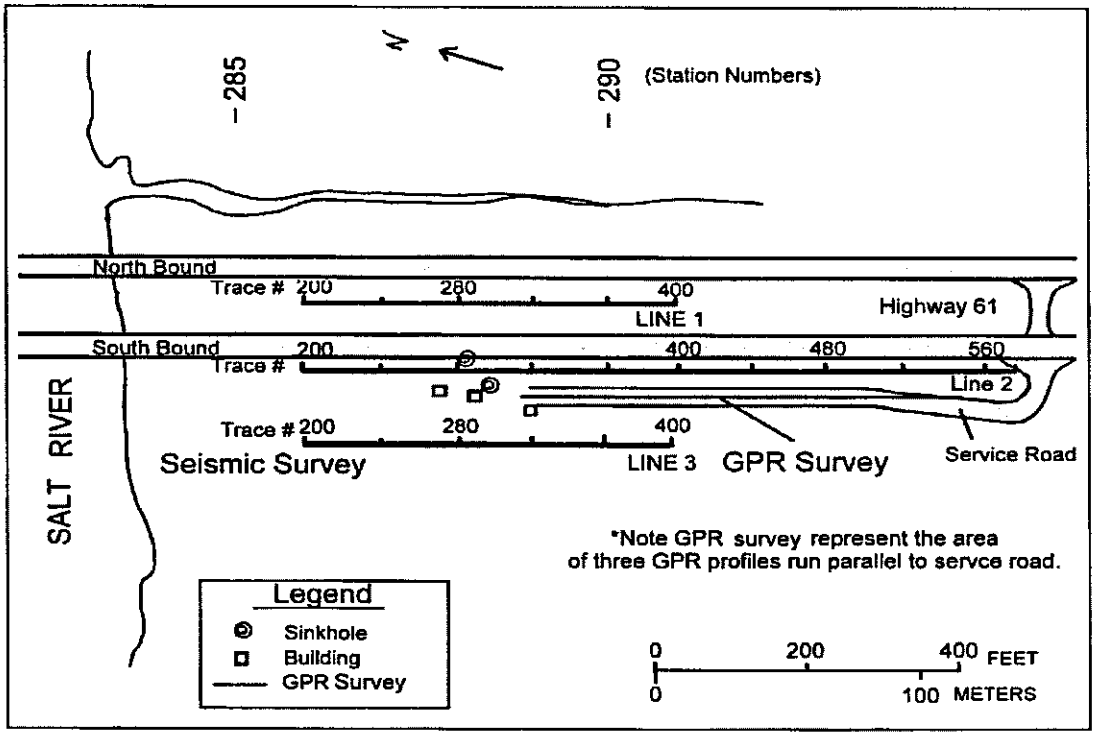

Figure 6: Map of survey B site (Route 61, Salt River). The locations of the reflection seismic profiles are superposed. The eight GPR profiles were acquired along the length of the service road. No prominent GPR anomalies were observed.

The eight GPR profiles were acquired as parallel transects along the length of the service road using a 400 MHz antenna. The objective was to determine if the section of roadway studied is underlain by large sub-pavement voids.

The locations of the reflection seismic profiles are shown in Figure 6. Two interpreted reflection seismic profiles are shown as Figures 7 and 8. The more significant interpretations have been superposed onto the study area base map of Figure 9.

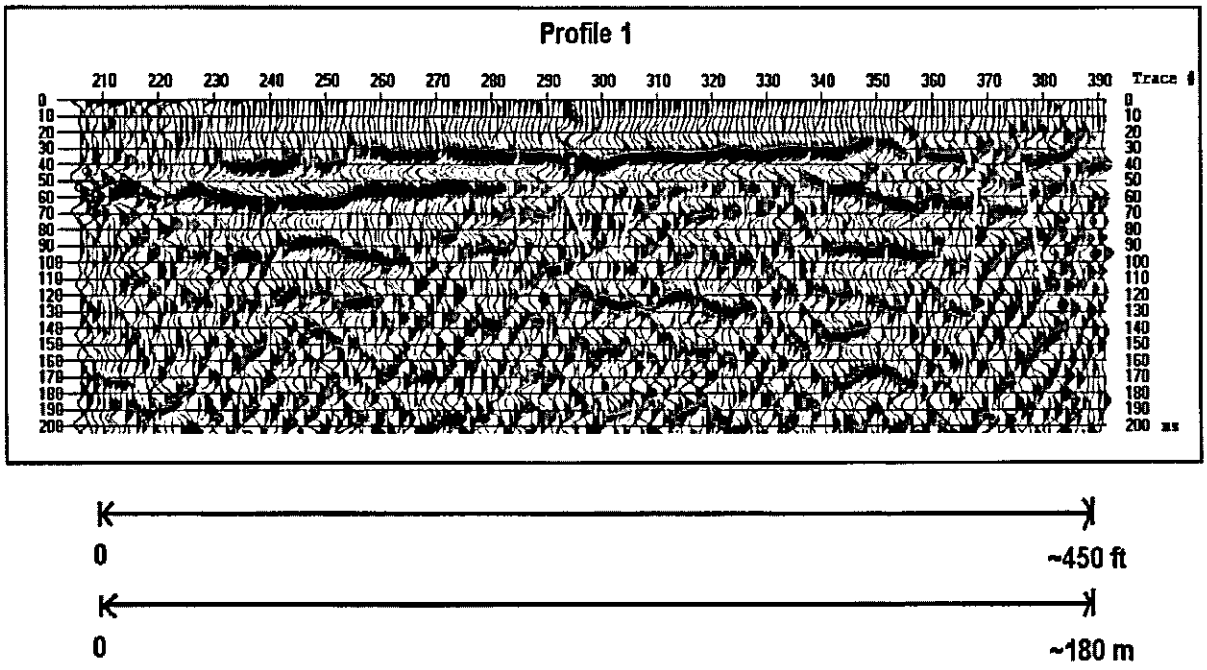

Figure 7: Survey B reflection profile 1 (Figures 6 and 9). Seismic bedrock is correlated across the profile.

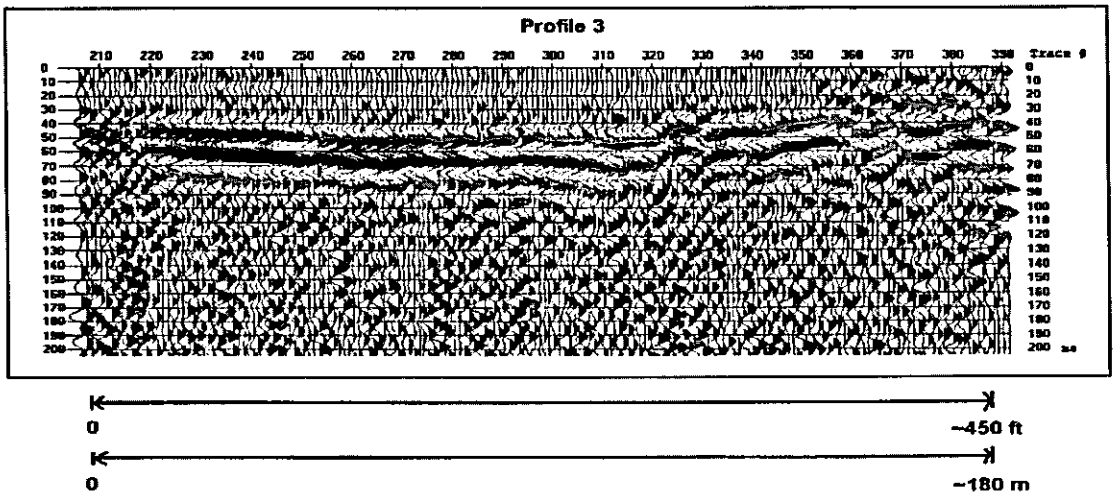

Figure 8: *Survey B reflection profile 3 (Figures 6 and 9). Seismic bedrock is correlated across the profile.*

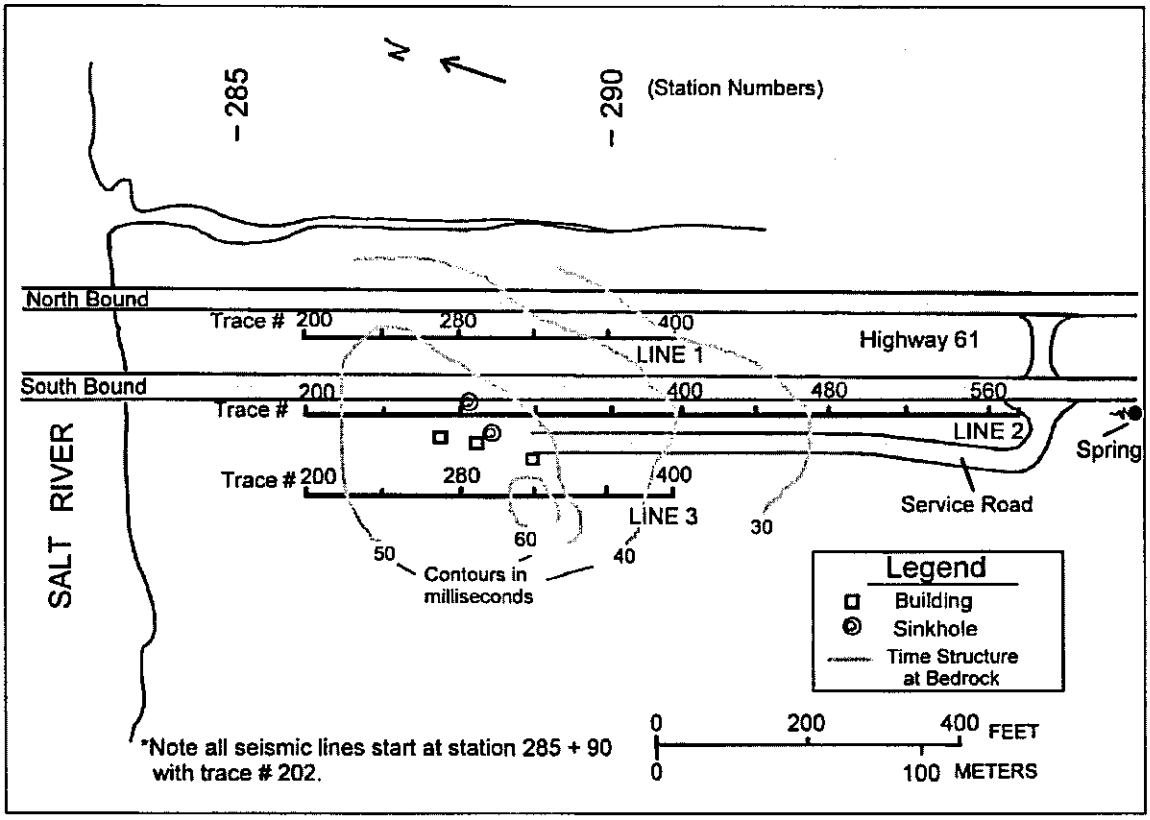

Figure 9: *Map of survey B, Route 61, Salt River site with superposed (interpreted) seismic depth-to-bedrock contours (in milliseconds).*

The conclusion is that natural spring water and surface run-off from both the south bound lanes of Highway 61 (a 245m [800ft] section in total) and the access road are channeled through the drainage ditch which separates the highway from the access road. In the immediate proximity of previously detected surface voids, there is a break in slope - both on the surface and at the bedrock level (Figures 7, 8 and 9). The interpretation of the seismic data suggests that this break in slope could be related to bedrock collapse. (The disrupted bedrock event and prominent diffractions on seismic profile #2 in the vicinity of trace 320 are probably indicative of karstic distress.)

As far as the development of the surface voids is concerned, our interpretation is that significant volumes of water within the drainage ditch (as well as other surficial waters) seep into the subsurface where the break in slope occurs. This process causes fine-grained sediment to be piped down the pre-existing permeable fault zone, and results in surface sinkholes.

Eight GPR profiles were acquired along the length of the service roadway (Figure 6). No significant GPR anomalies were observed on these data, suggesting that the service road is probably not underlain by any substantive air-filled voids.

CONCLUSIONS

The interpretation of the GPR profiles acquired during survey A supports the conclusion that substantive air-filled voids do not underlie the surveyed section of Highway 79, Hannibal Missouri. Our

recommendation is that MoDOT continue to monitor the northwestern segment of this roadway, due to the history of ongoing subsidence within and immediately adjacent to the roadway drainage ditch.

The interpretation of the reflection seismic data acquired during survey B at the Highway 61 Salt river site is consistent with the conclusion that channeled (via drainage ditch) natural spring water and surface roadway run-off have exacerbated pre-existing natural conditions, and contributed to the downward piping of fine-grained surficial sediment and the development of the small diameter surface sinkholes. Modifications to the existing drainage ditch may rectify this problem. As far as the service roadway at the Salt River site is concerned we find no substantive evidence, based on our interpretation of the acquired GPR profiles, that large voids have developed beneath this paved roadway.

APPENDIX G

GEOPHYSICAL SITE CHARACTERIZATION: GROUND-PENETRATING RADAR AND REFLECTION SEISMIC STUDY OF PREVIOUSLY MINED (LEAD/ZINC) GROUND, JOPLIN, MISSOURI

Neil L. Anderson*, Allen W. Hatheway+, Timothy E. Newton^,
Mike L. Shoemaker*, Steve Cardimona* and Jim Conley^

*Department of Geology and Geophysics, UMR, Rolla, Missouri
+Consultant, Rolla, Missouri
^Missouri Department of Transportation, Jefferson City, Missouri

ABSTRACT

The University of Missouri-Rolla (UMR) conducted a reflection seismic/ground-penetrating radar survey for the Missouri Department of Transportation (MoDOT) along segments of proposed interstate route 249, near Joplin, Missouri across ground previously mined for lead/zinc. A total of 14,600 lineal meters of shallow reflection seismic data, nine down-hole seismic calibration check-shots, and 15,000 lineal meters of ground penetrating radar (GPR) data were acquired. The seismic data were acquired to map Mississippian bedrock, locate and identify paleo-sinkholes and abandoned mine features, and determine structural geologic trends in the study area. The GPR data were acquired to identify and locate abandoned mine access and ventilation shafts in areas that were overlain by surficial milled ore rock (chat). Pre-construction knowledge of these anthropogenic and natural features will assist in route selection and geotechnical site mitigation, and minimize both the potential for contractor variable site condition claims and the potential for long-term subsidence-related problems.

The geophysical survey was successful in meeting MoDOT goals. The interpretation of the seismic data, and corroborative engineering geologic field mapping and drilling, established that the shallow reflection seismic technique can be used in the Joplin area to map bedrock structure (including probable fault lineaments and paleo-sinkholes), locate abandoned, in-filled and/or caved-in open pit mines; and define areas of probable shallow mining activity. The interpretation of the GPR data established that the GPR technique can be used in the Joplin area to locate abandoned mine access and ventilation shafts, even where such shafts are in-filled and overlain by a thin veneer of mill-waste products.

INTRODUCTION

During the winters of 1996/1997 and 1997/1998, the Department of Geology and Geophysics at the University of Missouri-Rolla conducted a geophysical survey for the Missouri Department of Transportation along proposed interstate route 249, Joplin, Missouri (Figure 1). The survey area had been extensively open-pit and subsurface mined for lead/zinc ore, and the integrity of the ground was suspect. In total, 14,600 lineal meters of shallow reflection seismic data, 15,000 lineal meters of ground-penetrating radar data, and nine down-hole seismic calibration check-shots were acquired.

These geophysical data were acquired to target specific objectives:

1. MoDOT wanted to determine whether reflection seismic data could provide a continuous image of the subsurface to a depth of 100m. The goal was to map Mississippian bedrock, locate and identify paleo-sinkholes and abandoned mine features, and determine structural geologic trends in the study area.

2. MoDOT wanted to determine whether GPR data could be used to detect and map abandoned mine access and ventilation shafts in areas where such shafts were in-filled and overlain by a thin veneer (<3 m) of surficial milled ore rock (chat).

Pre-construction knowledge of the location and nature of these anthropogenic and natural features will assist in route selection and geotechnical site mitigation, and minimize both the potential for contractor variable site condition claims and the potential for long-term subsidence-related problems.

GEOLOGICAL/MINING OVERVIEW OF STUDY AREA

Paleozoic bedrock in the Joplin area is extensively fractured Mississippian carbonate and chert (Figures 1, 2 and 3). These strata are typically overlain by up to 10 meters of alluvium, soil, and chat. In places, elongate paleo-sinkholes formed along predominantly north-northwest trending dissolution-widened joints (Figure 3). These paleo-sinkholes are typically in-filled as depositional inliers of Pennsylvanian shales, siltstones, sandstones, limestones and coals (some contain in excess of 50m of this secondary in-filling).

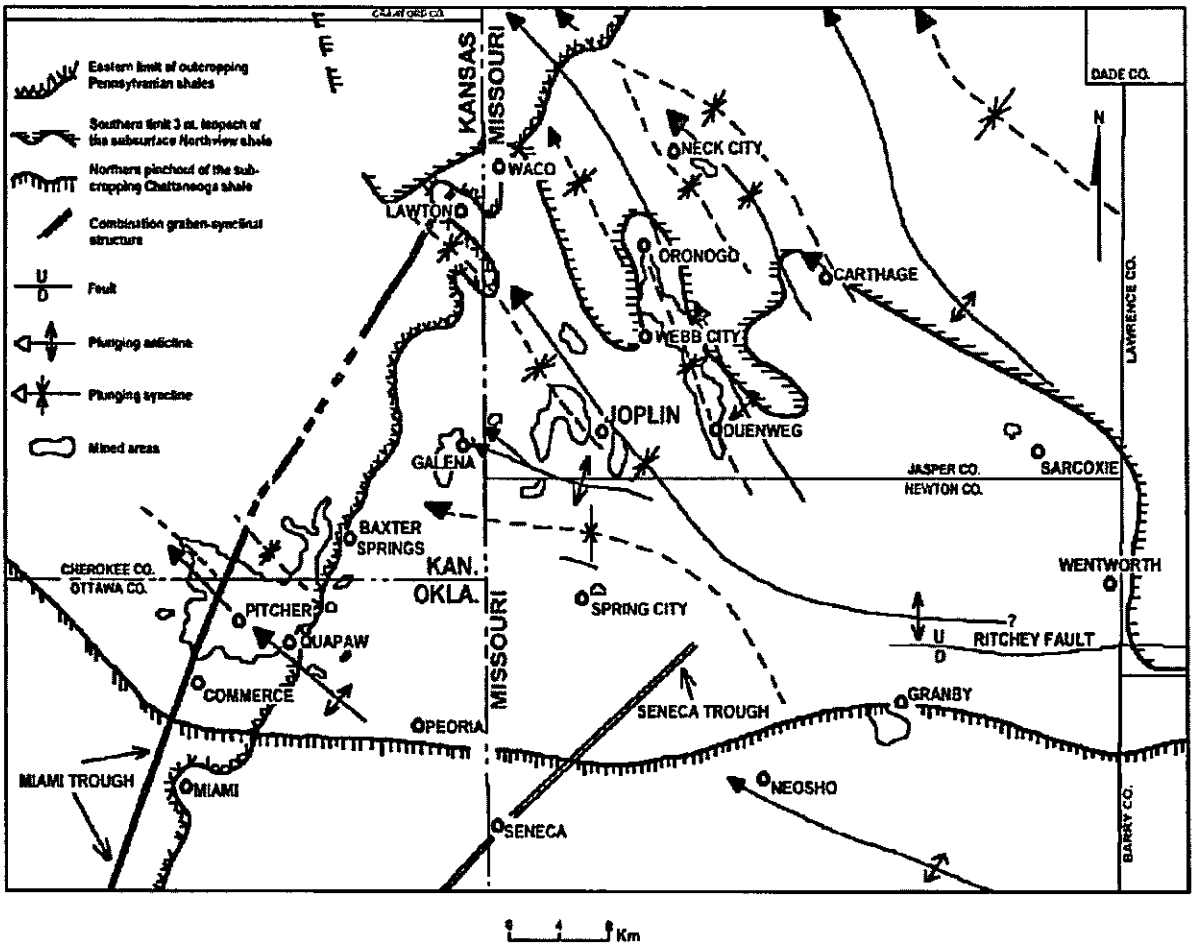

Figure 1: Map of the tri-State Lead-Zinc District. Significant geologic features and areas That have been extensively mined are highlighted. The interstate route 249 study area is located immediately to the southeast of the city of Joplin.

Lead/zinc ore in the Joplin area was preferentially deposited along pre-existing near-vertical joints or faults, along the margins of the Pennsylvanian sinkholes, and as sheet ground deposits within the Mississippian host rocks at depths on the order of 50m (Hatheway et al., 1998; Figure 3). The sinkhole and near-surface joint/fault zone ores are shallower and were recovered first (1850-1900) using either interconnected shafts or open-pit mining techniques. The sheet ground deposits are deeper and were mined later (1900-1950) using room-and-pillar methods. Typically, these mines were abandoned without mitigation and were often later robbed of ground support, thereby now constituting potential highway and/or construction hazards.

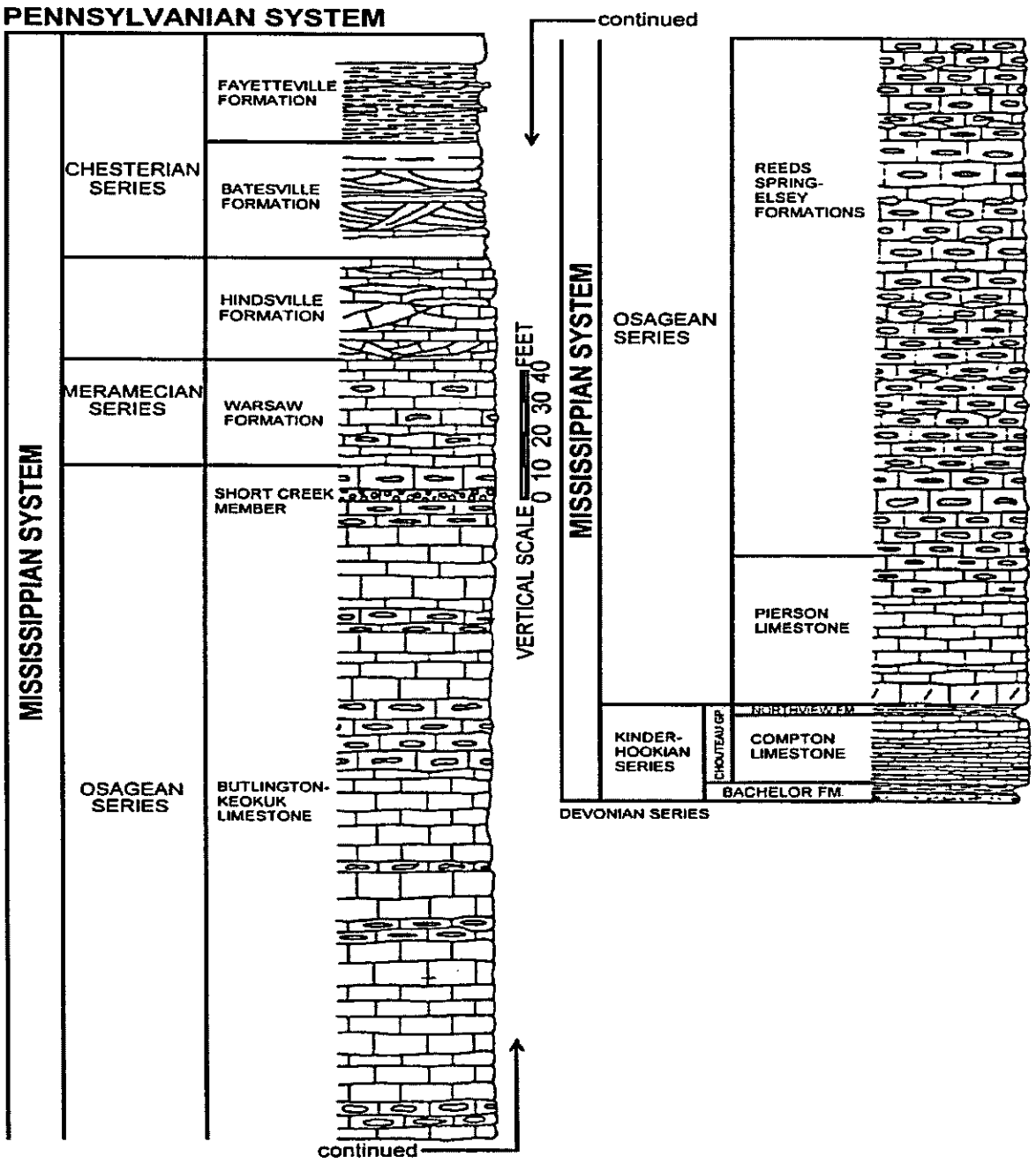

***Figure 2**: Stratigraphic table for the tri-State Lead-Zinc District. In the interstate route 249 study area, Mississippian Boone Formation bedrock is overlain by a veneer of soil and milled rock (chat), and localized pockets of residual Pennsylvanian-aged strata. Lead-zinc ore in the Joplin area was preferentially deposited along pre-existing near-vertical shear zones, around the margins of in-filled Pennsylvanian-aged karstic sinkholes, and as sheet-ground deposits within Mississippian carbonates and cherts at depths on the order of 50m below present topography.*

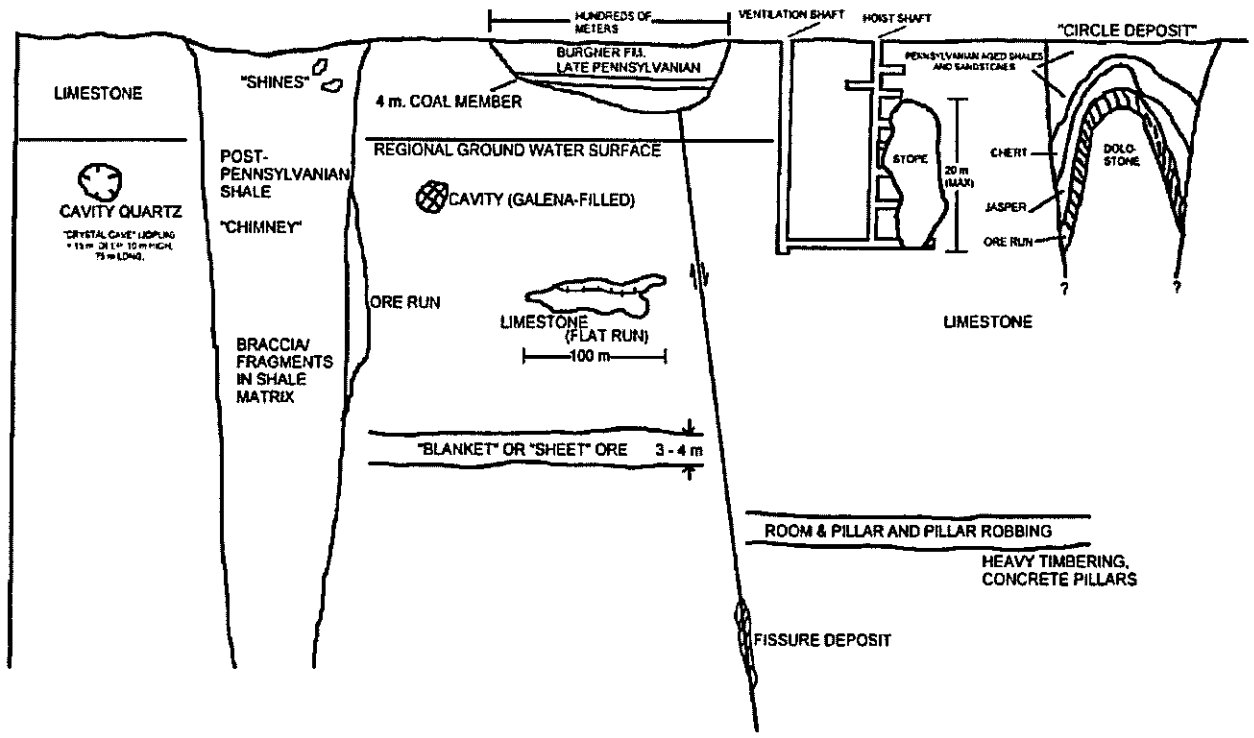

Figure 3. Schematic cross-section depicting the deposition of lead-zinc ore in the Joplin area. Lead-zinc ore in the Joplin area was preferentially deposited along pre-existing fractures, around the margins of in-filled Pennsylvanian sinkholes, and as sheet-ground deposits within Mississippian carbonates and cherts at depths on the order of 50 m.

From the perspective of a highway engineer, there are three principal types of abandoned-mine hazards in the study area. These are associated with the shallow mines that employed interconnected shafts, the shallow open-pit mines, and the deeper room-and-pillar mines that employed access and ventilation shafts.

1. Shallow mines that employed interconnected shafts that were not properly in-filled when abandoned, represent highway hazards for two reasons. First, open shafts could collapse under the new loads, resulting in incremental to catastrophic surface subsidence. Additionally, the open works of these abandoned shafts could provide vertical conduits for contaminant-bearing runoff and could also bring about the progressive "washout" of fine-grained sediment beneath the highway sub-base. (As noted previously, shallow mining activities were focused about the margins of Pennsylvanian sinkholes.

2. The abandoned and in-filled open pit mines represent sites of potential gradual to catastrophic subsidence for two reasons. First, their non-engineered in-filling material is under-compacted and could consolidate and settle when loaded. Second, improperly abandoned shafts may also extend outward from the open-pit mine into the adjacent strata, and cause additional gradual to catastrophic surface subsidence.

3. Improperly-abandoned access and ventilation shafts to the deeper room-and-pillar mines pose subsidence hazards because of the presence of void space and under compacted fill. They also could provide vertical conduits for surface runoff and facilitate the progressive "washout" of fine-grained sediment beneath the highway. The deeper room and pillar mines themselves are not considered to be a significant risk due to the likelihood that natural upward-failing back (roof) strata would choke-up by bulking and therefor would prevent significant collapse-related surface subsidence.

BOREHOLE AND CHECK-SHOT SURVEY CONTROL

MoDOT drilled 23 boreholes in the study area to provide subsurface lithologic/velocity control, and to confirm the interpretation of the reflection seismic data. Many of the boreholes were drilled into features that were interpreted on the seismic data as anomalous structural lows (in-filled Pennsylvanian sinkholes). Drilling was normally terminated when intact Mississippian bedrock was encountered. All of the acquired borehole control is consistent with seismic interpretations.

As an aid to the interpretation of the reflection seismic data, down-hole calibration check-shot survey data were acquired at nine borehole locations. The field procedure consisted of: 1) lowering a triaxial geophone to the bottom of the open borehole; 2) locking the geophones in place (coupling the geophone and the walls of the borehole); 3) generating an acoustic pulse at a surface immediately adjacent to the borehole; 4) recording direct arriving acoustic energy; 5) unlocking the geophone and raising it 1 m; and 6) repeating steps 2 through 5, as the geophone was raised to the surface.

The check-shot data were acquired to determine P-wave time-depth and velocity-depth relationships for the shallow subsurface (down to the base of the borehole). These data effectively tied the subsurface geology to the reflection seismic data. All of the check-shot data were consistent with the interpretation of the reflection seismic data and the applied stacking velocities used to correct normal moveout during seismic data processing.

REFLECTION SEISMIC PROFILING

The reflection seismic data were acquired using a 24-channel Bison engineering seismograph with roll-a-long capabilities, single channel 40 Hz geophones, and an Elastic Wave Generator weight drop source. A source, receiver and near-offset interval of 3m was generally employed. The weight drop source was impacted 6 to 14 times per shot record, dependent upon visual inspection of the incoming background noise on the shot gathers. Elevation control was acquired for each source and geophone location.

The reflection seismic data were processed on a pentium PC using WINSEIS (Kansas Geological Survey, 1996). A common processing sequence was applied to the data consisting of:

1. identification of reflection from bedrock,
2. muting of seismic energy arriving prior to bedrock event,
3. muting of first breaks and ground roll,
4. resorting the shot-gathered traces into common midpoint (CMP) gathers,
5. application elevation corrections,
6. performing velocity analysis for each line,
7. calculating and applying surface consistent statics,
8. application of normal moveout (NMO) corrections (muting to exclude excessively stretched data),
9. stacking the NMO corrected data,
10. application of residual statics and re-stacking statically corrected data, and
11. band-pass filtering.

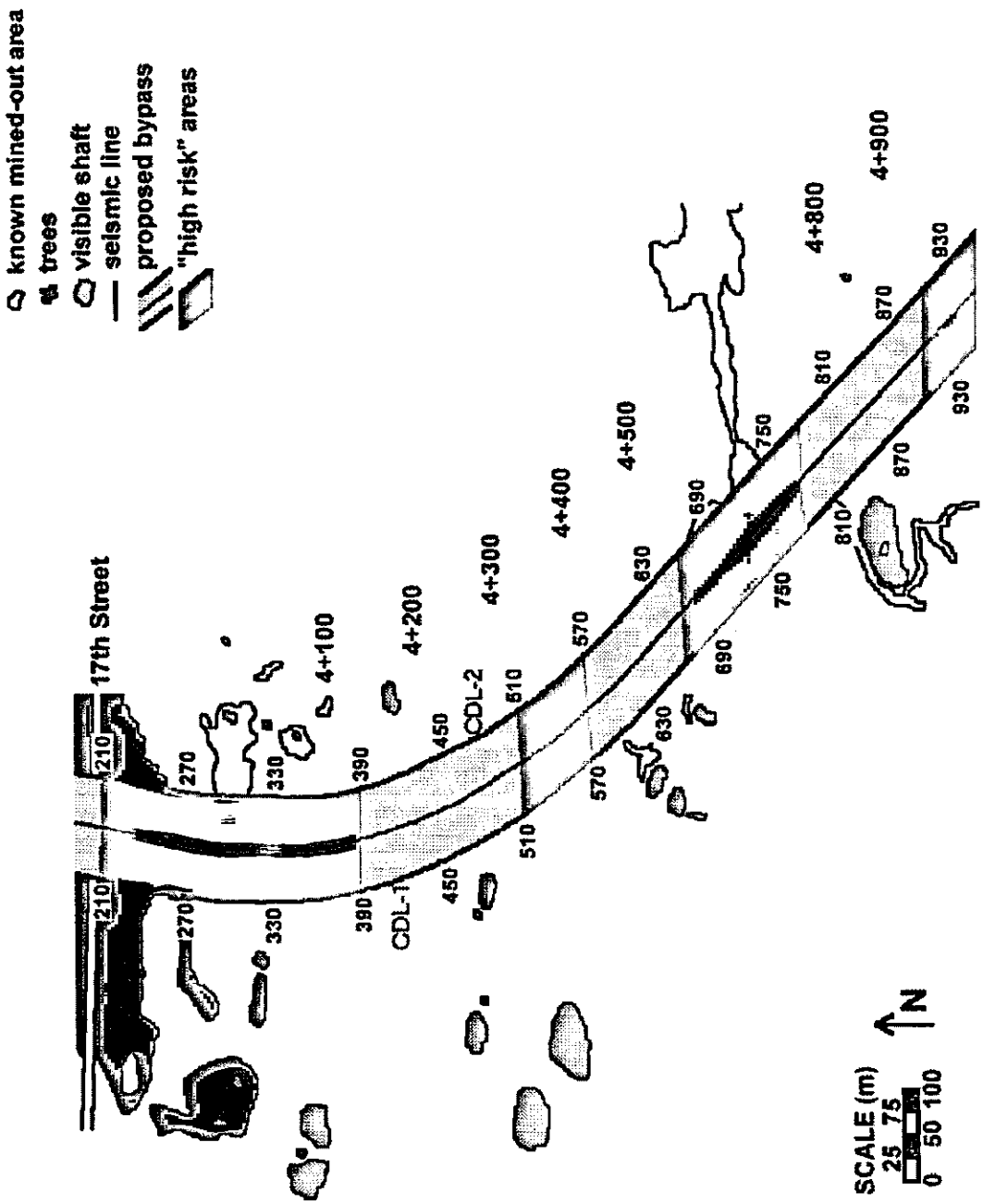

Figure 4: *Map of the CDL study area. Example profiles CDL-1 and CDL-2 (Figures 5 and 6) were acquired along the south-bound lane (edge of pavement) and the north-bound lane, respectively.*

INTERPRETATION

The shallow reflection seismic survey data were acquired to identify and spatially locate both natural and anthropogenic (abandoned mine) features that constitute potential construction or operational and maintenance problems or hazards. More specifically, MoDOT wanted to: 1) map Mississippian bedrock structure; 2) identify major bedrock fault and/or fracture zones; 3) locate paleo-sinkholes (generally Pennsylvanian); 4) locate abandoned and in-filled open-pit lead/zinc mines; and 5) identify areas of probable shallow historic mining activity (generally occurred around periphery of Pennsylvanian sinkholes). The intent was to transfer these geophysical interpretations and resulting hazards targets onto MoDOT compilations of archival mine location maps as an aid to MoDOT engineers involved in route planning, hazards assessment and site mitigation.

Two example reflection seismic profiles, CDL-1 and CDL-2, from the CDL study area (Figure 4) are shown as Figures 5 and 6, respectively. Three additional example reflection seismic profiles (A, B and C) from the Highway 71 interchange area (Figure 7) are presented as Figures 8, 9 and 10, respectively. These interpreted profiles are representative of the reflection seismic data acquired during the course of the study. Note that these reflection seismic data have not been deconvolved and are considered to be minimum-phase (at best). To facilitate the interpretation of these presented seismic profiles, the trough immediately following the onset of the interpreted bedrock reflection (initial peak, as identified on shot and CMP gathers) has been highlighted and correlated across each seismic section. This highlighted event is presented as the near-bedrock event. Seismic energy that arrived prior to the onset of the interpreted reflection from bedrock was muted during processing.

The reflected event (onset of the peak preceding the highlighted trough) from Mississippian carbonate bedrock, as correlated across each profile (Figures 5, 6, 8, 9 and 10), is consistent with both borehole and check-shot survey control. Limited borehole control in the area indicates depth to bedrock varies between 3m and 33m. (The depth to bedrock as calculated from two-way travel times along the seismic profiles indicates variations of between 5m and 35m.)

The more prominent structural features at Mississippian bedrock level in the Joplin study area trend NNW, and can be correlated across the suite of seismic profiles. For example, the structural low centered at trace 930 on profile CDL-2 (Figure 6) appears to correlate with the structural low centered at trace 720 on profile CDL-1 (Figure 5). Similarly, the structural low centered at trace 540 on profile CDL-2 appears to correlate with the structural low centered at trace 360 on profile CDL-1.

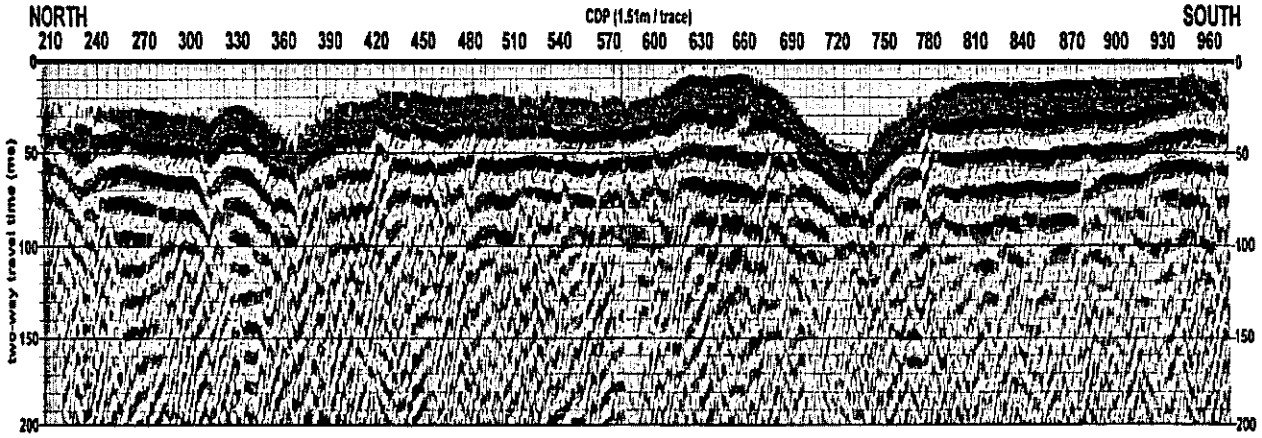

Figure 5: Seismic profile CDL-1 (Figure 4). The event corresponding to near-top of the Mississippian bedrock has been highlighted.

The prominent structural lows are elongate and often interpreted as bounded by fault scarps, suggesting they are Pennsylvanian karstic-collapse features (paleo-sinkholes) that developed along solution widened fractures. (The major fault/fracture system in the greater Joplin area trends NNW.) Such in-filled sinkholes were prospective/attractive sites for shallow mining activity, and as such have been denoted as high-risk areas with respect to the possible presence of abandoned in-filled open-pit mines and in-filled mine access and ventilation shafts (Figures 4 and 7). Areas where bedrock is structurally elevated are less likely to have been the site of extensive shallow mining and are denoted as relatively low risk.

These reflection seismic data are of utility to the Transportation Department for several reasons:

1) Depth to bedrock is highly variable at these sites (3-35 m). Knowledge of these variations and sometimes-associated structural geologic trends will affect the placement of foundation elements.

2) Pre-existing paleo-fracture zones, some of which are believed to have been widened by karstic dissolution, may provide vertical conduits for downward percolating water, leading to the progressive "wash out" (piping) of fine-grained sediment beneath roadways and resulting in gradual subsidence. Further dissolution widening of these fractures could result in catastrophic collapse, although this advanced scenario is far less likely as contemporary dissolution activity during the life of most roadways will be negligible in an engineering sense.

3) The Pennsylvanian-aged sinkholes are and were recognized after about 1910 as highly probable locations of ore, and should be considered to harbor improperly closed mine shafts. Improperly-filled shafts could collapse under the additional loads of new roadway structures, and therefor represent both short-term construction and long term highway hazards. Additionally, shafts could serve as conduits for downward percolating water, bearing the incidental contaminants from roadway traffic.

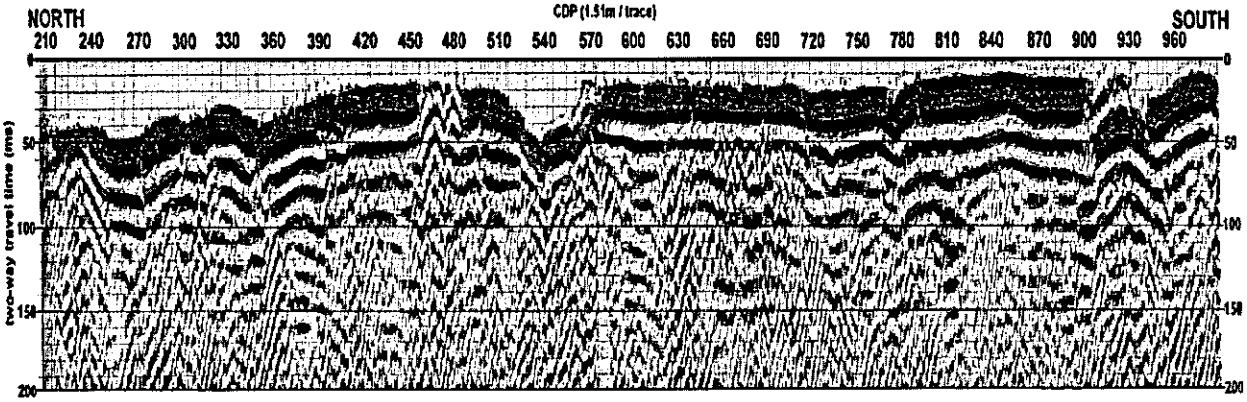

Figure 6: Seismic profile CDL-2 (Figure 4). The event corresponding to near-top of the Mississippian bedrock has been highlighted.

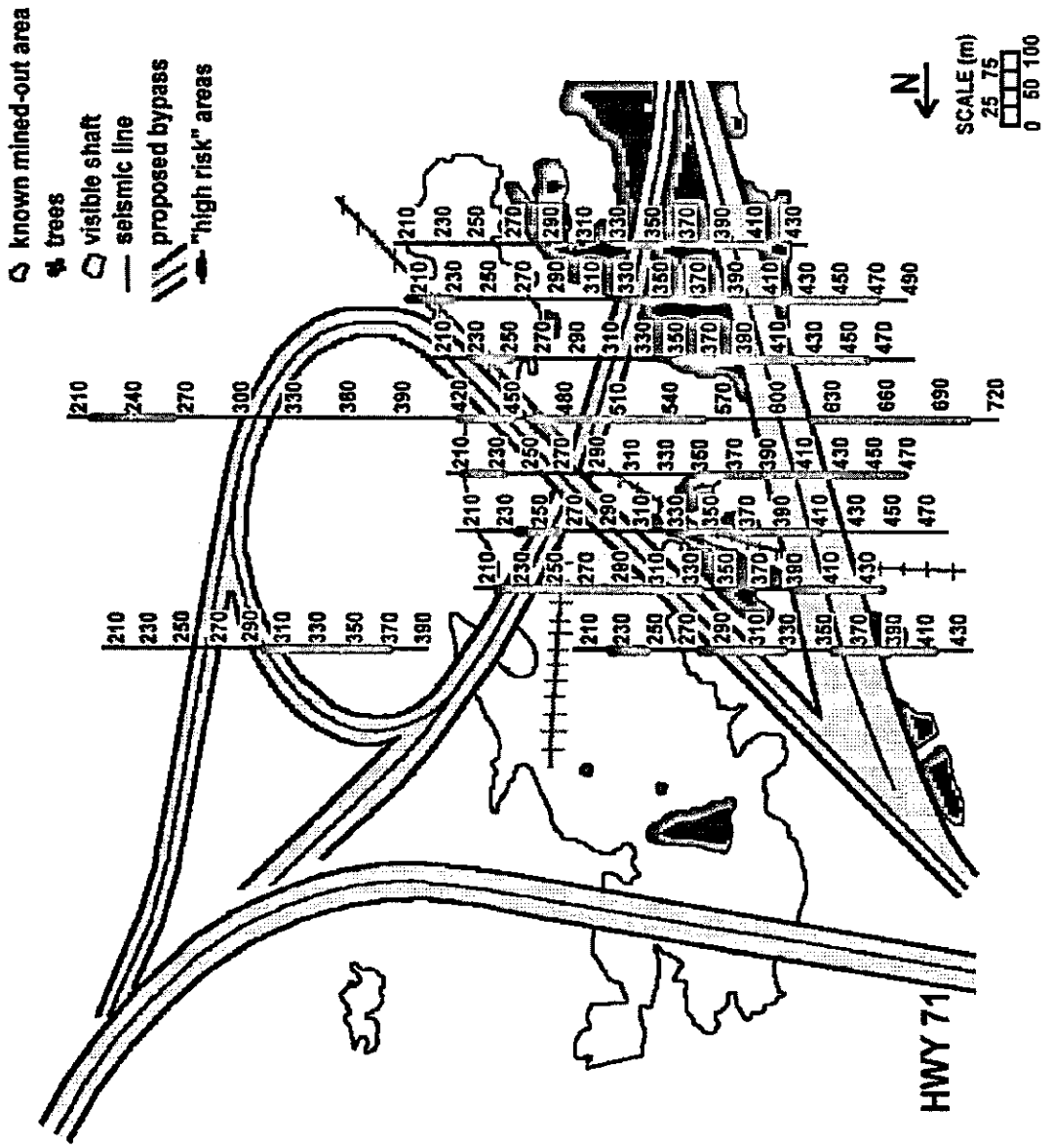

Figure 7: Map of the HWY 71 Interchange study area. Example seismic profiles A, B and C are shown as Figures 8, 9 and 10, respectively. (Parallel profiles A, B and C are the first three profiles on the extreme southern edge of the HWY 71 study area, respectively.)

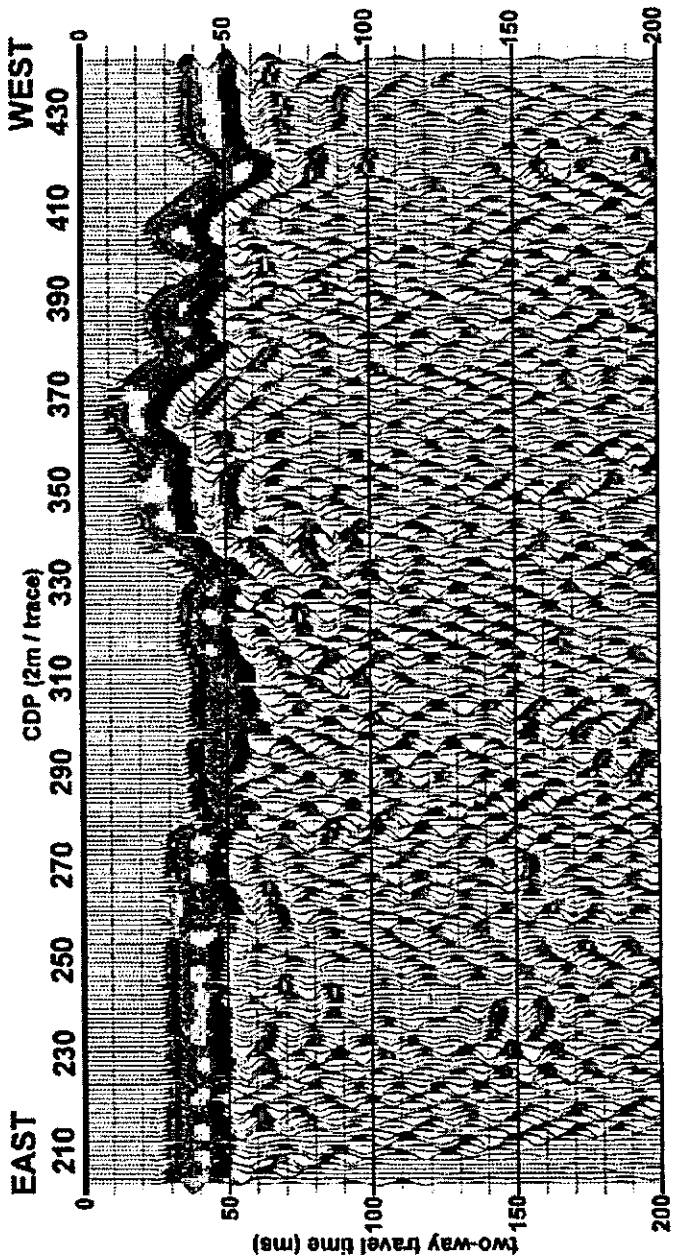

Figure 8: *Seismic profile A (Figure 7). The event corresponding to near-top of the Mississippian bedrock has been highlighted.*

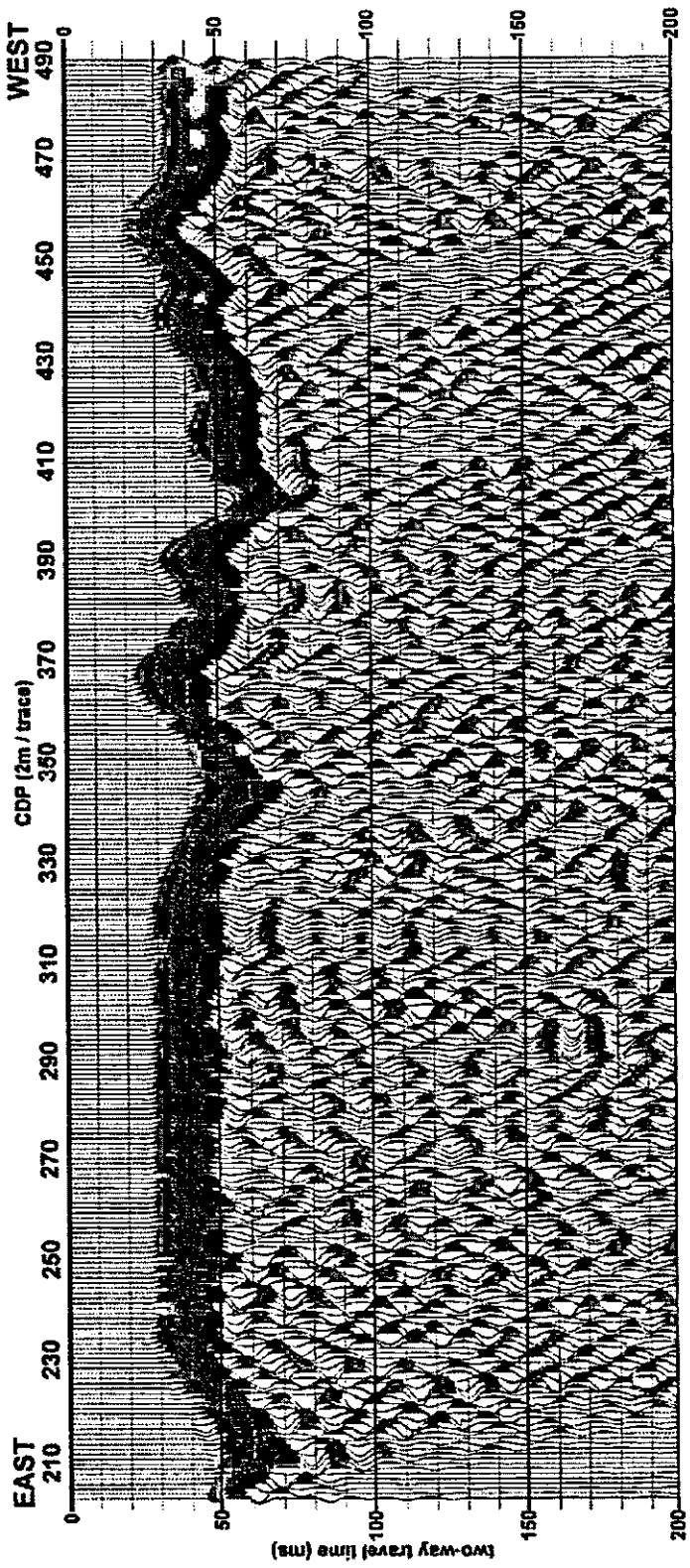

Figure 9: *Seismic profile B (Figure 7). The event corresponding to near-top of the Mississippian bedrock has been highlighted.*

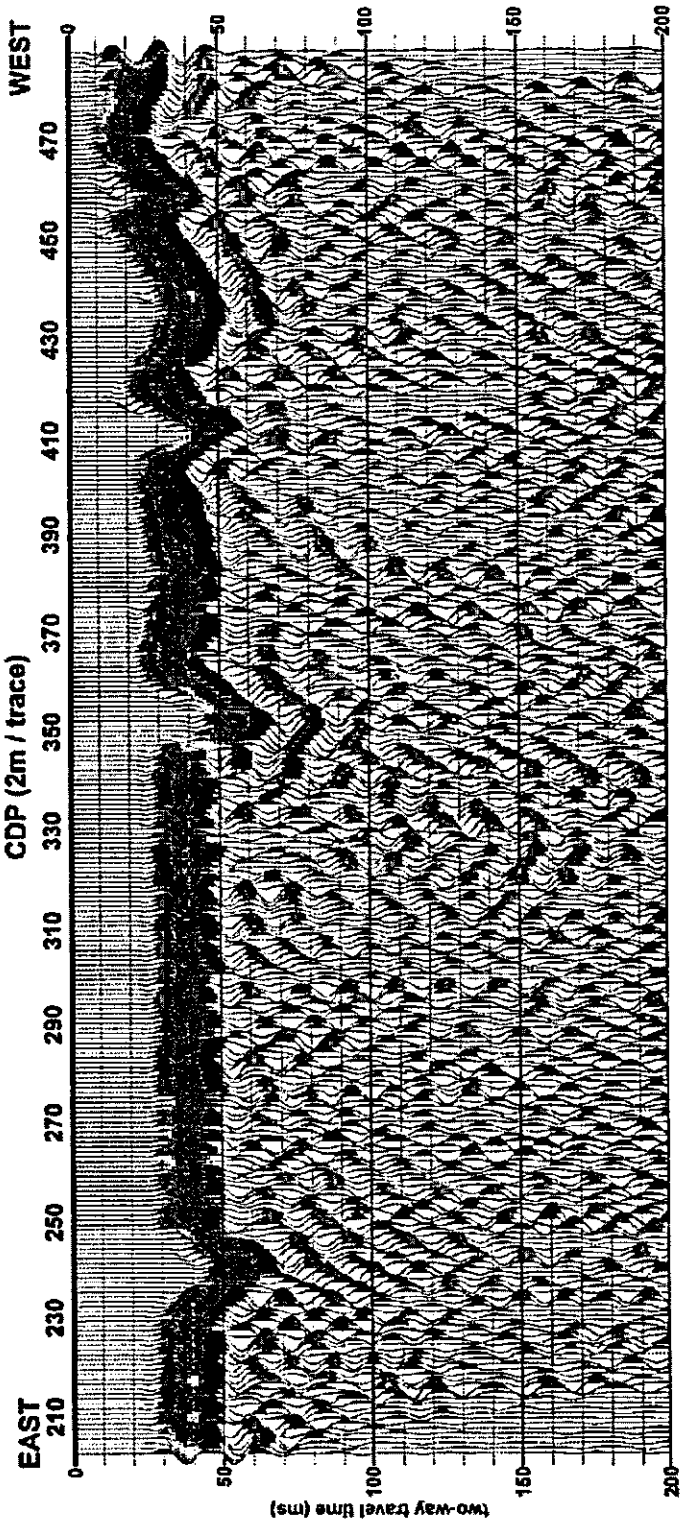

Figure 10: *Seismic profile C (Figure 7). The event corresponding to near-top of the Mississippian bedrock has been highlighted.*

GROUND-PENETRATING RADAR PROFILING

A Geophysical Survey Systems, Inc., Subsurface Interface Radar unit (SIR-8) equipped with a 500 MHz monostatic antenna was used to acquire a total of 15,000 lineal meters the ground-penetrating radar data (Baker et al., 1998). The data were acquired as suites of parallel GPR profiles (spaced at 1.5 m) in order to locate mine access and ventilation shafts. The sampling interval was 30 scans/foot. The trace length was 100 ns, providing for depth penetration on the order of 5 m. The GPR data was processed on a pentium PC using RADAN (Geophysical Services Systems, 1995). Our processing routine consisted of trace normalization, followed by application of vertical gain, horizontal filtering, and vertical filtering.

A segment of an example processed ground-penetrating radar profile from study area BW-15 Site 4 (Figure 7) is displayed as Figure 12. Area BW is located inside the circular highway "loop". A simple map showing the anomaly is displayed as Figure 11. These GPR profiles cross undisturbed clay-rich residual soil overlain by a thin veneer of chat. The chat/soil contact is easily identified and correlated across the GPR profile. The chat is comprised of small, flake-like fragments of crushed and milled carbonate rock. The GPR image of the chat is characterized by an internal pattern that is consistent with cross-bedding, which suggests that this material may have been moved about by a bulldozer, as much of the chat has been illegally gathered and removed for use as local fill and driveway/roadway surfacing. The latter has been a fact of considerable concern to the U.S. Environmental Protection Agency (Region VIII, Kansas City, KS) and the Hazardous Waste Program of the Missouri Department of Natural Resources. The subject highway project lies within the bounds of the SUPERFUND National Priority Site, designated for environmental remediation.

Segments of example ground-penetrating radar profiles from study area BW-8 Site 1 and BW-15 Site 2 are shown as Figures 13 and 14, respectively. These profiles image in-filled mine access shafts. The thin veneer of chat overlying the original ground surface is characterized by internal crossbedding. The chat/soil contact is identifiable and easily correlated across the GPR profile. This surface is regular in character and continuous except where the GPR profile crosses the throat of an abandoned mine access shaft. The mineshaft is characterized by an increased thickness of chat, which is consistent with area evidence that many abandoned shafts were in-filled with chat, during the illegal removal of that material.

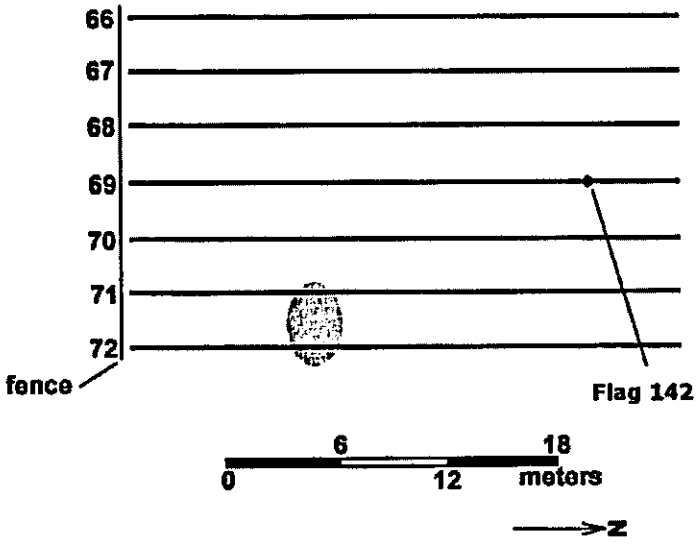

Figure 11: GPR study area BW-15 Site 4. GPR data were generally acquired as parallel profiles across chat-covered areas.

CONCLUSIONS

The interpretations of the reflection seismic data establish that this tool can be used, in the Joplin area, to map Mississippian bedrock and bedrock related features such as faults and paleo-sinkholes, and to delimit areas of probable historic mining activity. The recognition of these subsurface conditions is important because fault and shear zones, sinkholes, and improperly-abandoned mines constitute potential highway and/or construction hazards. Pre-construction knowledge of subsurface conditions will facilitate route planning and remediation efforts, and reduce short term construction and long term maintenance costs. Additionally, variations in subsurface conditions should be provided to the contractor as the basis for informed actions incidental to construction.

The interpretation of the GPR data establish that this technique can provide confirmatory evidence of abandoned mine access and ventilation shafts in areas that are overlain by chat. The chat is characterized by cross-bedding in the GPR profiles and can be readily differentiated from the underlying soil. The chat/soil interface is regular in character and continuous except where the GPR profile crosses the mine access or ventilation shafts. The mine shafts are characterized by an increased thickness of chat, which is consistent with the idea that many of the previously-open abandoned shafts were in-filled with chat. The act of in-filling is believed to have occurred entirely after the cessation of mining and was related to the illegal traffic in the lead/zinc-bearing mine waste. These improperly abandoned mine shafts constitute potential short-term construction and long-term highway hazards. Pre-construction knowledge of these features would assist in route selection and geotechnical site mitigation, and minimize both the potential for contractor variable site condition claims and the potential for long-term subsidence-related problems.

REFERENCES

Baker, J.A., Shoemaker, M.L., Anderson, N.L., Hatheway , A.W., Newton, T.E. and Conley, J.,1998, Ground-penetrating radar study of previously mined (lead/zinc) ground in Joplin, Missouri, *in* Anderson, N.L., Cardimona, S., and Newton, T., Editors, Highway Applications of Engineering Geophysics with an Emphasis on Previously Mined Ground: Missouri Department of Transportation Special Publication, 136-142.

Geophysical Services Systems, 1995, Radan For Windows Operating System: Geophysical Services Systems Inc. publication, NH, 194 p.

Hatheway, A.W., Newton, T.E., Anderson, N.L., and Shoemaker M.L., 1998, Characterization methodology for abandoned mined ground as a highway siting constraint, Joplin, Missouri, *in* Anderson, N.L., Cardimona, S., and Newton, T., Editors, Highway Applications of Engineering Geophysics with an Emphasis on Previously Mined Ground: Missouri Department of Transportation Special Publication, 105-123.

Kansas Geological Survey, 1996, Winseis User's Manual: Kansas Geological Survey publication: Kansas Geological Survey , KS, 133 p.

Shoemaker, M.L., Anderson, N.L., Shaw, A.E., Baker, J.A., Hatheway A.W., Newton, T.E. and Conley, J., 1998, Reflection seismic study of previously mined (lead/zinc) ground, Joplin, Missouri, *in* Anderson, N.L., Cardimona, S., and Newton, T., Editors, Highway Applications of Engineering Geophysics with an Emphasis on Previously Mined Ground: Missouri Department of Transportation Special Publication, 124-135.

Theil, J., 1942, Geological maps showing mining and mineralization areas of the Joplin area: Missouri Geological Survey and Water Resources, 4 p. text and 6 geologic maps.

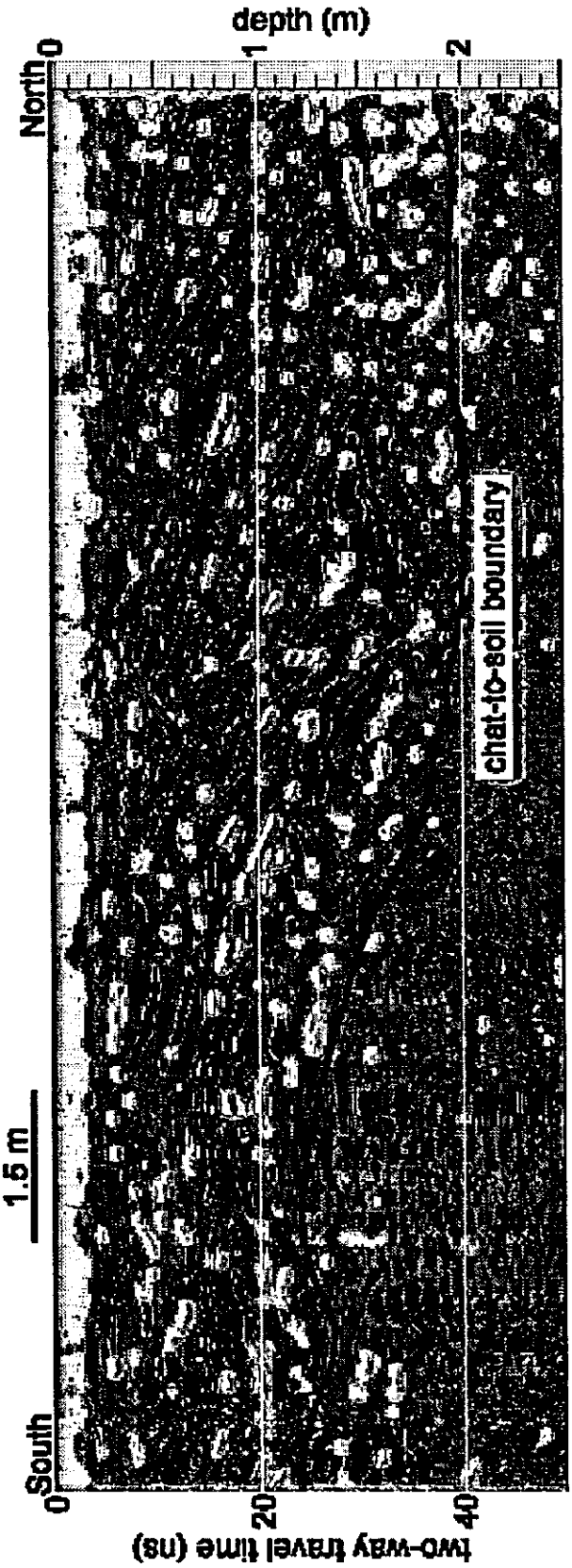

Figure 12. *Segment of GPR profile 66 (Study area BW-15 Site 4; Figure 11). The GPR profile crosses undisturbed clay-rich residual soil overlain by a thin veneer of chat. The chat/soil contact is readily correlated across the GPR profile. The internal pattern (GPR reflection character) of the chat suggests this material may have been moved by bulldozer during illegal chat removal activities in the post-mining era.*

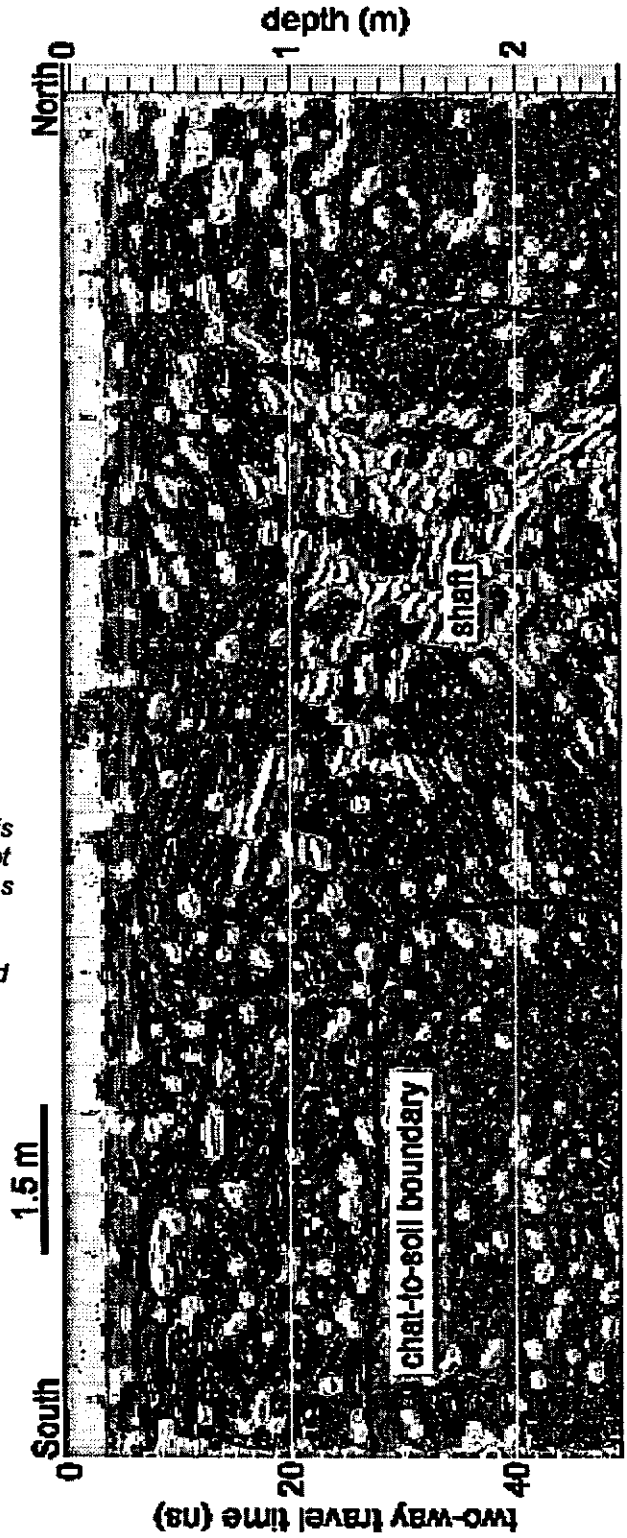

Figure 13: Segment of GPR profile 3 (Study area BW-8 Site 1). The chat/soil contact is regular and continuous except where the GPR profile crosses the abandoned mine access shaft. The shaft throat is characterized by an increased thickness of in-filled chat which suggests non-engineered in filling with this material.

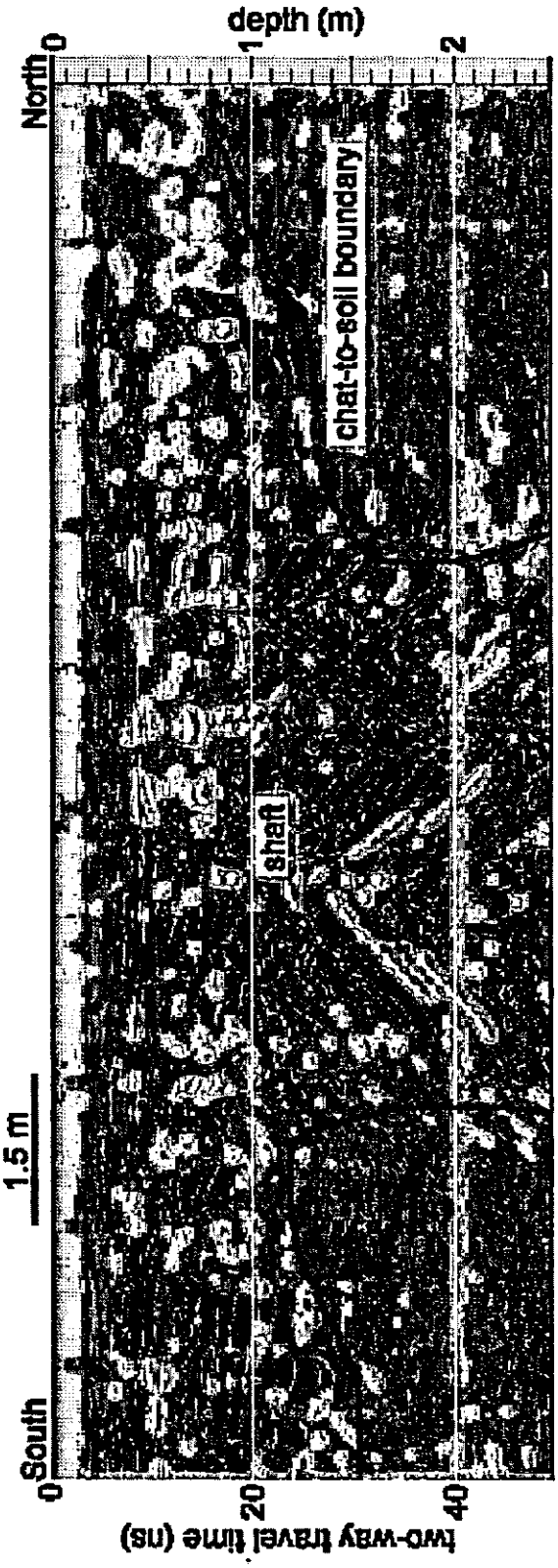

Figure 14: Segment of GPR profile 60 (Study area BW-15 Site 3). The chat/soil contact is regular and continuous except where the GPR profile crosses the abandoned mine access shaft. The shaft throat is characterized by an increased thickness of in-filled chat which suggests non-engineered in filling with this material.

APPENDIX H

NON-INVASIVE DETECTION AND DELINEATION OF UNDERGROUND STORAGE TANKS

Steve Cardimona*, Tim Newton^ and Neil Anderson*

*Department of Geology and Geophysics,
University of Missouri–Rolla,
Rolla, MO, 65401

^ The Missouri Department of Transportation,
1617 Missouri Blvd., P.O. Box 270, Jefferson City, MO 65102

ABSTRACT

The proposed expansion of selected highways in Missouri required several gas stations to be demolished. During demolition of a gas station property, damage can occur to the underground fuel storage tanks and associated utility lines. Non-invasive mapping of these features prior to excavation can greatly reduce problems associated with unexpected tank discovery.

In this study, geophysical methods were used to map the underground fuel storage tanks and associated utility lines. To accomplish the goals of the project, the electromagnetic induction and ground penetrating radar techniques were chosen. The complementary use of ground penetrating radar and electromagnetic methods increased the likelihood of detecting and delineating subsurface anomalies.

The locations of the existing tanks and associated utility lines can be interpreted in both ground penetrating radar profiles and contoured electromagnetic induction maps. Electromagnetic induction maps provided an excellent cost effective initial survey for the detection of the underground storage tanks. Ground penetrating radar proved important for the accurate delineation of these tanks. The integrated use of ground penetrating radar and electromagnetic induction methods allowed us to create a map of exact tank locations at each site in this study.

INTRODUCTION

The locations of underground fuel storage tanks on gas station properties are not always accurately known. This leads to problems during excavation or demolition of the gas station property. For example, if a tank is unexpectedly encountered and ruptured, hydrocarbon contamination of the ground and ground water can occur.

Recently, proposed highway expansion in Missouri has necessitated identifying the location of the underground fuel storage tanks to aid in the demolition of the gas station structures. In an effort to ensure that any abandoned tanks were not unexpectedly encountered, the geophysics group at the University of Missouri–Rolla was asked to acquire geophysical data at the sites with a view to mapping the location of the tanks. The primary objective of the project was to detect and delineate the underground fuel storage tanks and associated utility lines using cost effective geophysical techniques that were both nondestructive and noninvasive.

This paper summarizes the data acquisition and interpretation from two sites: The Fastop Gas Station in Lee's Summit, MO, and the Simpson Oil Service Station in Shelbina, MO. Two complementary geophysical methods were employed, ground penetrating radar (Daniels, 1996), and electromagnetic induction (Kearey and Brooks, 1991, Telford et al., 1976). The geophysical methods are especially needed where the existence of the tanks is unknown in order to avoid puncturing the tanks or piping which could cause contamination of the soils as well as to avoid delays associated with tank discovery during highway construction.

FASTOP SITE LOCATION AND SURVEY DESIGN

The Fastop Gas station is located at the intersection of Highways 291 and 150 in Lee's Summit, MO (Figure 1). The Fastop Gas Station has four areas where the nature of the underground fuel storage tanks is unknown. These four areas include an active tank farm, two suspect tank farms, and a former tank farm. The active tank farm includes three underground storage tanks. There are two locations where the existence of tanks is unknown, termed suspect tanks. The former tank farm location was investigated to make sure no tanks were buried in this region.

The geophysical survey for the Fastop area was separated into ten sections to facilitate data acquisition and processing (Figure 1). The most important areas include Area A (suspect tanks and utility lines), Area E (suspect tanks), Area F (former tank farm), and Area G (active tank farm).

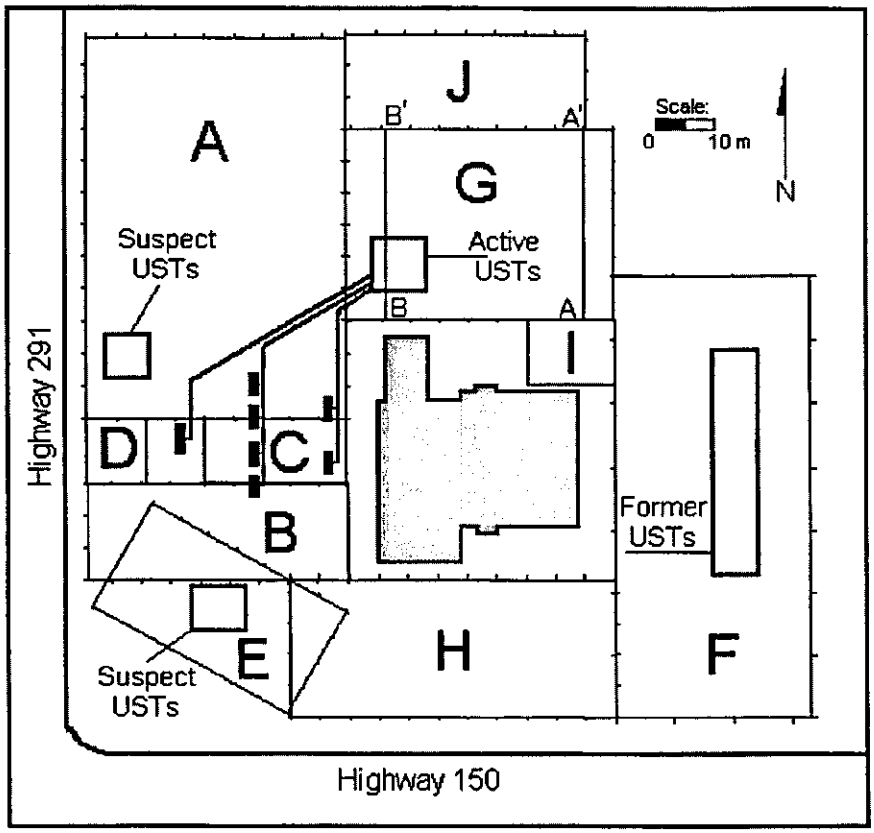

Figure 1: Fastop Gas Station property including active and suspect tank farms, and showing GPR line locations A-A' and B-B'. Letters A-J designate sub-sections of the complete survey.

FASTOP GAS STATION INTERPRETATION

Fastop Gas Station is separated into 10 Areas, A through I (Figure 1), which contained a variety of targets including active underground storage tanks (USTs), suspect USTs, former USTs, utility lines, and feeder lines. The complementary use of electromagnetic induction and ground penetrating radar methods increased the likelihood of detecting the underground storage tanks and associated utility lines.

Electromagnetic Induction Data

The electromagnetic induction method clearly distinguished the targets. The data were collected with frequencies from 330 through 19950 Hz. Figure 2 displays the USTs and utility lines interpreted with a priori information of the location of the active USTs. The magnitudes of the in–phase component of the secondary magnetic field, essentially the absolute values of the in–phase component, are plotted using a contouring program. By plotting the absolute value of the in–phase component, the anomalies were enhanced.

The Active USTs are located just north of the building in section G (Figure 1). The Active USTs produce a halo effect that is indicative of buried metal objects. The anomaly at the edge of the building next to the tanks was caused by a surface 50–gallon drum that was present during the initial day of data collection, but not present during the subsequent days of data collection. Therefore, the anomaly is not located on the neighboring section. This shows the importance of surface features in the survey area while using the electromagnetic induction equipment. The UST signature in Area G is used throughout the interpretation of the Fastop Gas Station site as a typical tank signature to compare with other anomalies. A sewer line is also evident that extends from the building to the septic tank in the northeast corner of Area G.

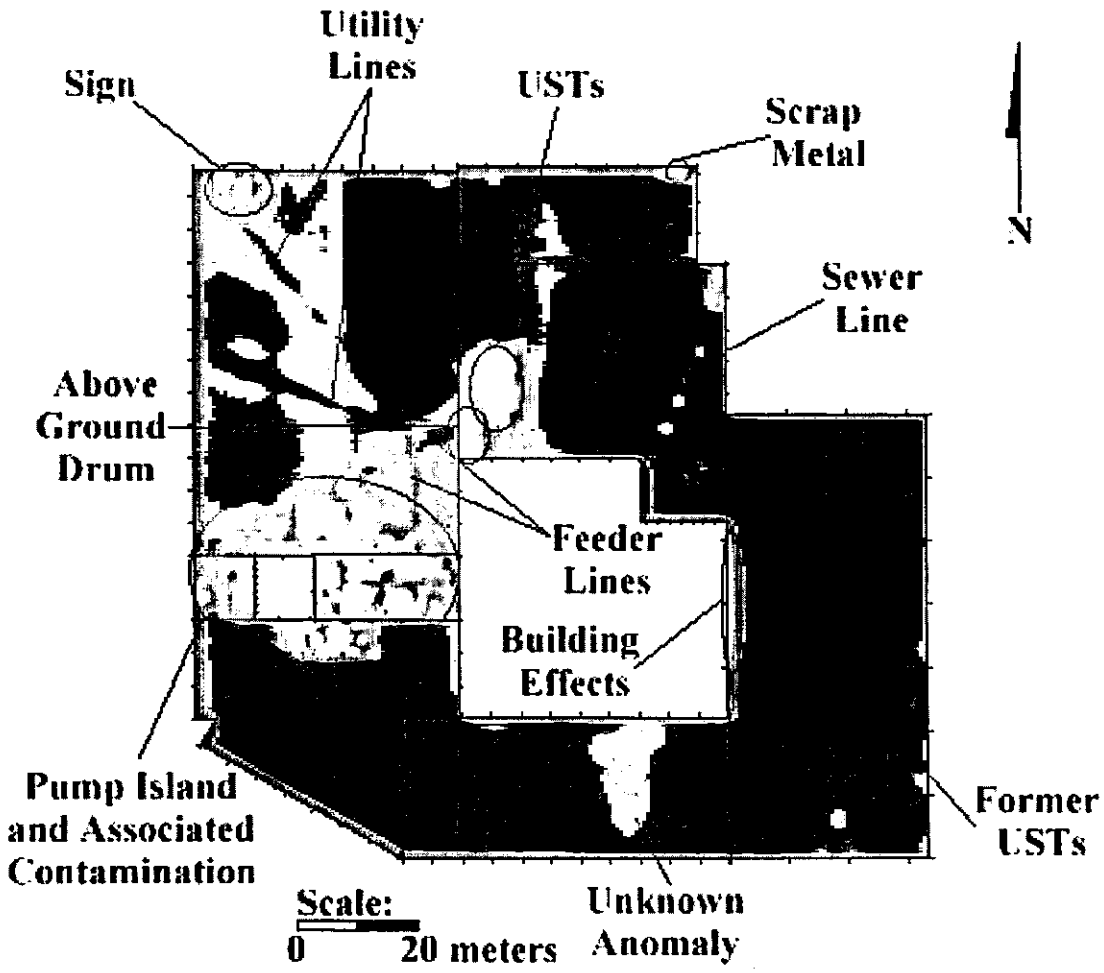

Figure 2: Fastop Gas Station using the 19950 Hz EM induction data – a relative color scale is used to show signal amplitude variation for qualitative anomaly detection

Area A (Figure 1) is denoted by the location of the utility lines, feeder lines and an above–ground sign. The utility lines are clearly distinguishable in the high frequency (e.g. 19950 Hz) contoured data as presented in Figure 2. The contoured electromagnetic induction map aids in the interpretation of the feeder lines and the associated hydrocarbon contamination. However, the utility lines and feeder line are not evident in the low frequency (e.g. 330 Hz) contoured electromagnetic induction data due to the size of the respective lines. One of the utility lines leads from the building to a sign in the northwest corner of Area A, illustrated as a conductivity high on the contoured electromagnetic induction map.

Area A contains one of the suspect tank locations. The nature of these tanks is unknown by the Missouri Department of Transportation. The owner of the Fastop Gas Station is not certain of the UST removal prior to the addition of the new active tank farm, but believes the USTs have been removed. The interpretation of the data confirms this belief that the tanks were previously removed.

Areas E and F (Figure 1) area relatively subdued compared with the other areas. Neither data from Area E nor Area F displays a large amplitude anomaly that would be characteristic of a buried tank. The interpretation of the electromagnetic induction data is that the USTs have been previously removed resulting in no tank signature in the EM induction maps.

Areas I and J (Figure 1) are relatively free of anomalies that are related to the goals of this project. In the north–east section of the Area J, an anomaly is present (Figure 2). The anomaly is caused by scrap metal located on the surface. The anomaly in the center of Area J is caused by standing water, which was on the surface during the collection of the data.

Area H (Figure 1), just north of Highway 150, contains an anomaly (Figure 2) that is evident only on the plot of the magnitude of the in–phase component and not obvious in the in–phase component data. The grape–shaped anomaly is similar to the anomaly in Area J, which was interpreted as standing water. The linear feature looks like a utility line; however, that has not been confirmed.

Ground Penetrating Radar Data

The ground penetrating radar method delineated most of the underground storage tanks successfully. The ground penetrating radar method clearly defined the USTs and septic tank located on site; however, GPR did not detect the utility lines or feeder lines effectively. The interpretation of the ground penetrating radar profiles provided additional information to improve the a priori knowledge of the lateral and vertical positioning of the tanks. In particular, the interpretation of the GPR data allowed for more accurate depth control and delineation of the sides of the tanks. The locations of the ground penetrating radar profiles are in Figure 1.

Area G (Figure 1) contains the underground fuel storage tanks and septic line. Figure 3 shows a disturbed area from 20 to 28 meters along the GPR profile interpreted as the underground septic tank for the Fastop building. The septic tank was not imaged on the electromagnetic induction data because the concrete structure did not provide a conductive anomaly. Another anomaly is evident in Figure 3, located at 7 meters along the profile. This anomaly is interpreted as the septic line running from the building to the septic tank as interpreted in the contoured electromagnetic induction map.

Area G is the location of the active underground fuel storage tank farm. Three tanks are located in close proximity to one another. Figure 4 shows the USTs between 7 and 12 meters along the profile. The radar data is nonmigrated; therefore, the USTs will appear as a disturbed area rather than horizontal bright spots. The close proximity of the USTs creates interference in the GPR profile. Therefore, without the use of the electromagnetic induction technique, the USTs would be difficult to detect because the GPR signature looks similar to disturbed ground, or an area where the USTs have been replaced by infill. The infilled soil usually does not completely subside for more than five years. The electromagnetic induction technique confirmed a conductive body at the same location as the anomaly in the GPR profile; therefore, the anomaly interpretation based on the integrated electromagnetic induction and ground penetrating radar data is the active tank farm. The majority of the northern section of the Fastop Gas Station property has been excavated since the geophysical survey was conducted. Area G (Figure 1) contained the active tank farm, sewer line, and septic tanks. All of these anomalies were found in the locations determined by the integrated electromagnetic induction and ground penetrating radar data. No tanks were found during the excavation of Area A (Figure 1), confirming the electromagnetic induction and ground penetrating radar data interpretation.

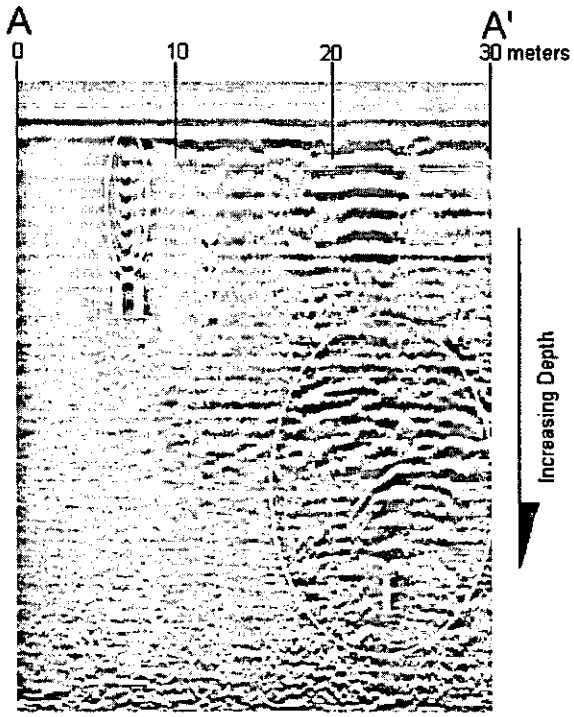

Figure 3: GPR data from Area G using a 400 MHz antenna (Profile A-A' on Figure 1) – buried concrete septic tank between 20-28 meters along the profile (I) and a sewer line at 7 meters along the profile (II)

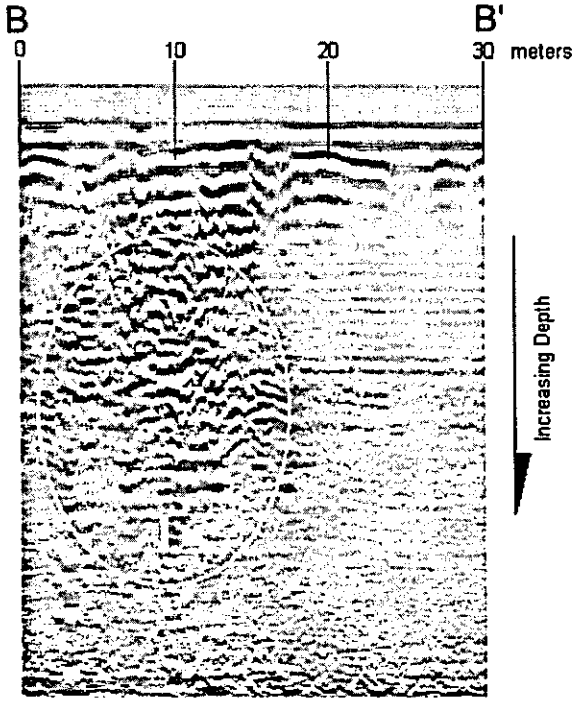

Figure 4: GPR data from Area G using a 400 MHz antenna (Profile B-B' on Figure 1) – buried USTs between 7 and 12 meters along the profile (I)

SIMPSON OIL STATION SITE LOCATION AND SURVEY DESIGN

The Simpson Oil Company, located at the intersection of Highway 15 and Elm St. in Shelbina, MO, is an abandoned petroleum service station. It has four tanks registered with the Missouri Department of Natural Resources (MDNR) – two 2,000-gallon tanks, one 10,000-gallon tank, and one 5,000-gallon tank (Figure 5). The exact locations and orientations of the underground storage tanks are unknown. The only surface evidence are the fill caps and monitoring wells located above and around the tanks, respectfully. The lateral extension and orientation of the underground storage tanks can be assumed by using the fill caps and a priori information provided by MDNR (Figure 5). The location of the associated feeder lines is unknown. The Simpson survey was separated into two overlapping sections which covered the four possible underground storage tank locations (Figure 5). Area A covered the area between the building and the pump island. Area B probed the section with boundaries of Highway 15 and Elm St. and the two pump islands.

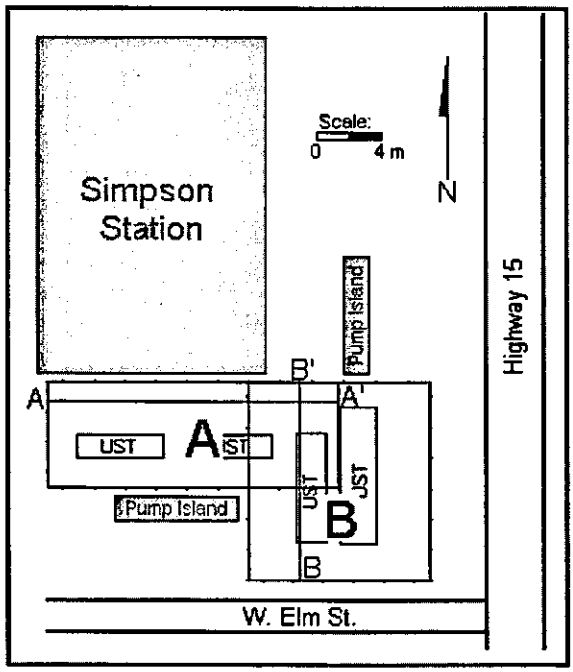

Figure 5: Survey design for Simpson Oil Co. property, with survey subsections A and B, and GPR lines A-A' and B-B' marked.

SIMPSON OIL COMPANY INTERPRETATION

Simpson Oil Company, located in Shelbina, Missouri, has four suspect underground fuel storage tank locations (Figure 5). Two grids covered the area of the suspect tanks. The electromagnetic induction and ground penetrating radar data discovered that all four underground fuel storage tanks existed; however, the USTs were not situated in their expected spatial location.

Electromagnetic Induction Data

The electromagnetic induction data was plotted as the absolute value of the in–phase and quadrature components of the secondary magnetic field using the low frequency (e.g. 330 Hz) data. The two underground fuel storage tanks just north of the pump island are interpreted in Figure 6. The surface features, including the fill caps, confirm the placement of the two tanks as found in the contoured

electromagnetic induction maps. Because of the close proximity of the USTs, only two anomalies are evident. The conductivities recorded by the electromagnetic induction equipment blend the USTs together creating one large anomaly from two tanks. This makes it difficult to distinguish between the tanks using only the EMI technique. However, when the ground penetrating radar technique is implemented along with the electromagnetic induction technique, the individual tanks can be delineated.

The high frequency (e.g. 19950 Hz) data is considerably noisier than the low frequency data caused by surface features and surrounding conductive artifacts. The feeder line was not imaged due to large amount of electromagnetic noise. The anomaly in the eastern section of Figure 6 is interpreted as a water line running along Highway 15. The water line was marked on the pavement by the water; however, the water line was incorrectly marked. The water line was marked half a meter outside the survey area to the east. As shown in Figure 6, the water line is located within the survey area.

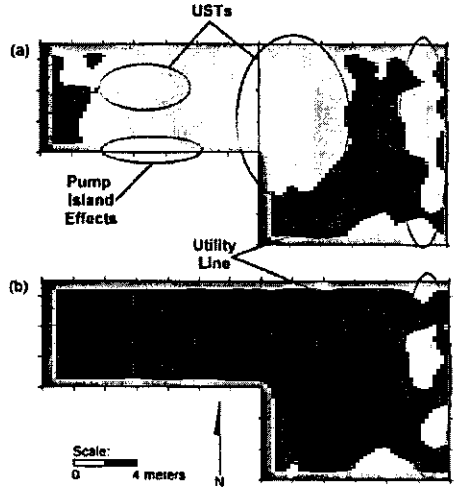

Figure 6: Simpson Oil Company, electromagnetic induction data (a) 330 Hz, in–phase – USTs and water line are evident; (b) 330 Hz, quadrature – only the water line is evident

Ground Penetrating Radar Data

The ground penetrating radar data provided the ability to delineate the USTs with much greater accuracy than the electromagnetic induction method. In contrast to the electromagnetic induction equipment, the interpreted GPR data yields accurate depth approximations. Area A contains 4 USTs and Area B, which overlaps Area A, contains 2 USTs (Figure 5). The ground penetrating radar data for the Simpson Oil Co. property was not migrated; therefore, the tanks are imaged as a diffraction and will not have sharp delineation of the tank edges.

Area A (Figure 5) contains 4 USTs and associated feeder lines that required delineation to aid in the removal of the USTs and demolition of the site. Figure 7 shows three UST locations. One of the tanks, oriented parallel with the survey line (A–A'), is positioned from 2 to 9 meters along the profile (I in Figure 7) and the second and third tanks, oriented perpendicular to the survey line, are centered at 13 and 17 meters (II and III in Figure 7) along the profile, respectively. The USTs oriented perpendicular to the survey lines are more easily detected because they form a narrow diffraction rather than the oblong diffraction created by the tanks oriented parallel with the survey line.

The depths to Tanks 3 and 4 were calculated using a hyperbolic spreading function to estimate ground dielectric constant. The depth to Tank 3 is approximately 1.4 meters and the depth to Tank 4 is approximately 1.2 meters. Tank 1 and 2 are aligned parallel with the survey line unlike Tanks 3 and 4, which are orientated perpendicular to the survey line. The depth to Tanks 1 and 2 are approximately 1.5 meters deep. These depths were determined by using the dielectric constant determined in the depth calculations for Tanks 3 and 4.

Area B overlaps Area A and contains two USTs including Tanks 3 and 4 (Figure 5), both of which are also located in Area A. The interpreted GPR profiles (Figure 8) from Area B are used to delineate the underground storage tanks with further precision. In contrast to Area A where the USTs are perpendicular to the survey direction, Tanks 3 and 4 are parallel with the survey direction in Area B. The

USTs are more difficult to detect when the tanks are parallel with the survey line; however, the edges of the tanks can be more accurately mapped (Figure 9).

The feeder line is located in both Area A and Area B, connecting the two pump islands with the USTs. The feeder line is evident in most of the ground penetrating radar profiles, but is absent from several lines. The feeder line is mapped from the GPR profiles along the lines indicated in Figure 9. The dashed lines of Figure 9 indicate the estimated location of the feeder line in areas where it was not evident in the GPR data.

The complementary use of the electromagnetic induction and ground penetrating radar methods enabled the a priori information to be corrected and the location of the USTs to be plotted in their correct spatial location. Figure 9 shows the proper location of the USTs as taken from the interpreted contoured electromagnetic induction map and ground penetrating radar profiles (cf. Figure 5). The USTs in Area A were found to be located in different positions and orientations than expected. The tanks are numbered 1 through 4 from west to east, respectfully. Tank 1 was interpreted to be closer to the pump islands than what the a priori information suggested. Tank 2, parallel with Tank 1, is located approximately two meters north of Tank 1. Tanks 3 and 4, oriented perpendicular to Tanks 1 and 2, are repositioned to the west.

CONCLUSIONS

The Missouri Department of Transportation was required to excavate several gas station sites to make room for the expansion of the adjacent highways. There was a necessity to locate underground fuel storage tanks and associated utility lines at these gas station properties to aid in the excavation of the site and to eliminate costs created by the problems associated with destruction or damage of unknown USTs.

The electromagnetic induction and ground penetrating radar techniques were chosen from a variety of geophysical methods because of the ability of the methods to detect and delineate the underground storage tanks and associated utility lines. The integrated use of the ground penetrating radar and electromagnetic induction techniques increased the accuracy of anomaly identification. Where surface noise created anomalies in the electromagnetic induction data, the ground penetrating radar data proved that those anomalies were not underground fuel storage tanks. Where ground penetrating radar showed some anomalies that were difficult to interpret, the electromagnetic induction data did not show confirmation of underground storage tanks or associated utility lines.

The complementary use of the electromagnetic induction and ground penetrating radar techniques was successful in the detection and delineation of the underground fuel storage tanks and associated utility lines. The electromagnetic induction technique provided an excellent initial detection of the USTs using a cost effective system. The ground penetrating radar delineated the tanks more clearly and provided depth approximations.

REFERENCES

Daniels, D.J., 1996, Surface-Penetrating Radar. The Institution of Electrical Engineers.

Kearey, P. and Brooks, M., 1991, An Introduction to Geophysical Exploration. Blackwell Scientific Publications.

Telford, W.M., Geldart, L.P., Sheriff, R.E., and Keys, D.A., 1976, Applied Geophysics. Cambridge University Press.

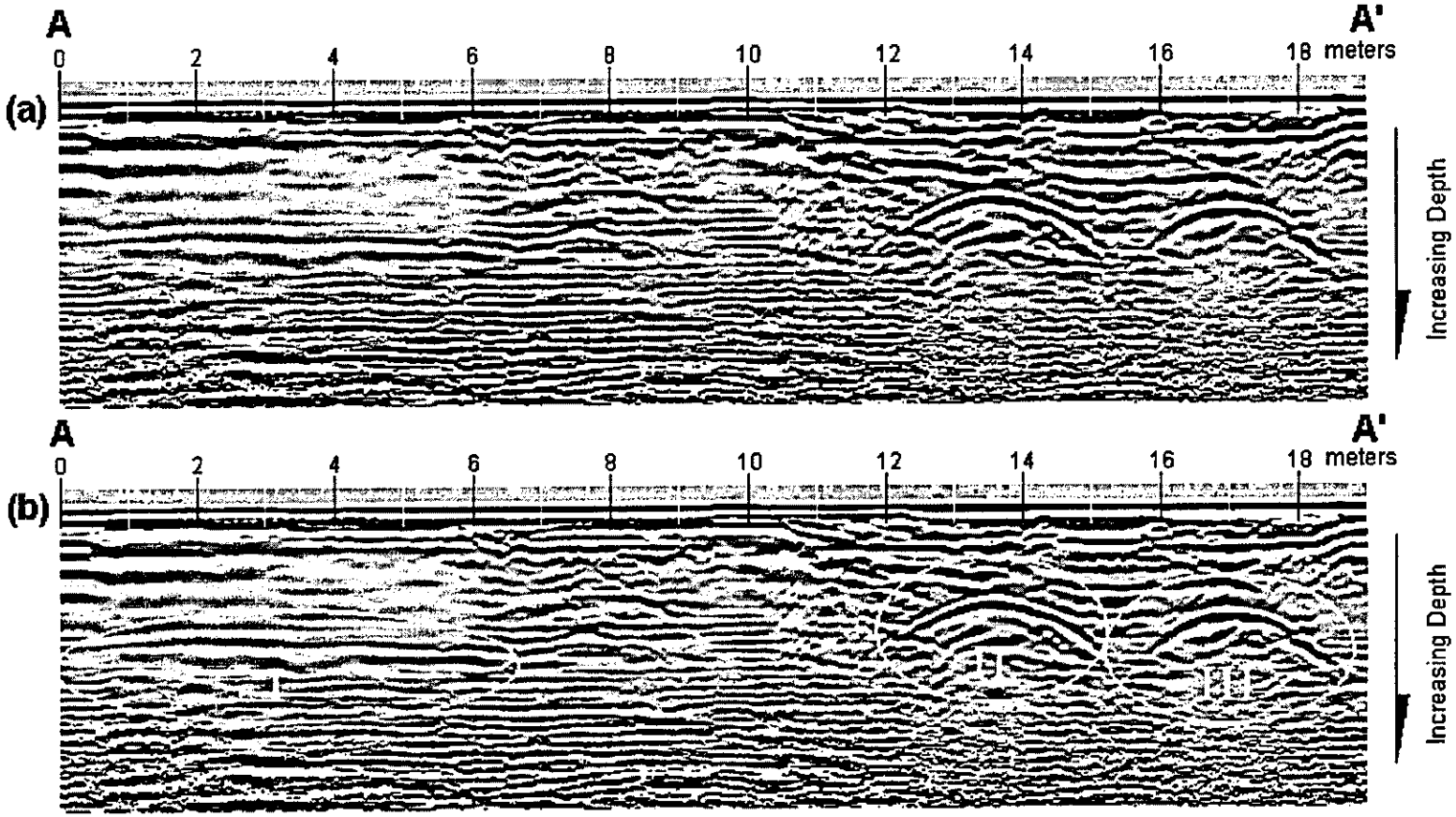

Figure 7: GPR profile from Simpson Oil Company Area A along line A-A' (Figure 2) using the 400 MHz antenna – (a) uninterpreted and (b) interpreted sections with the tanks 2, 3, and 4 identified as anomalies I, II, and III respectfully

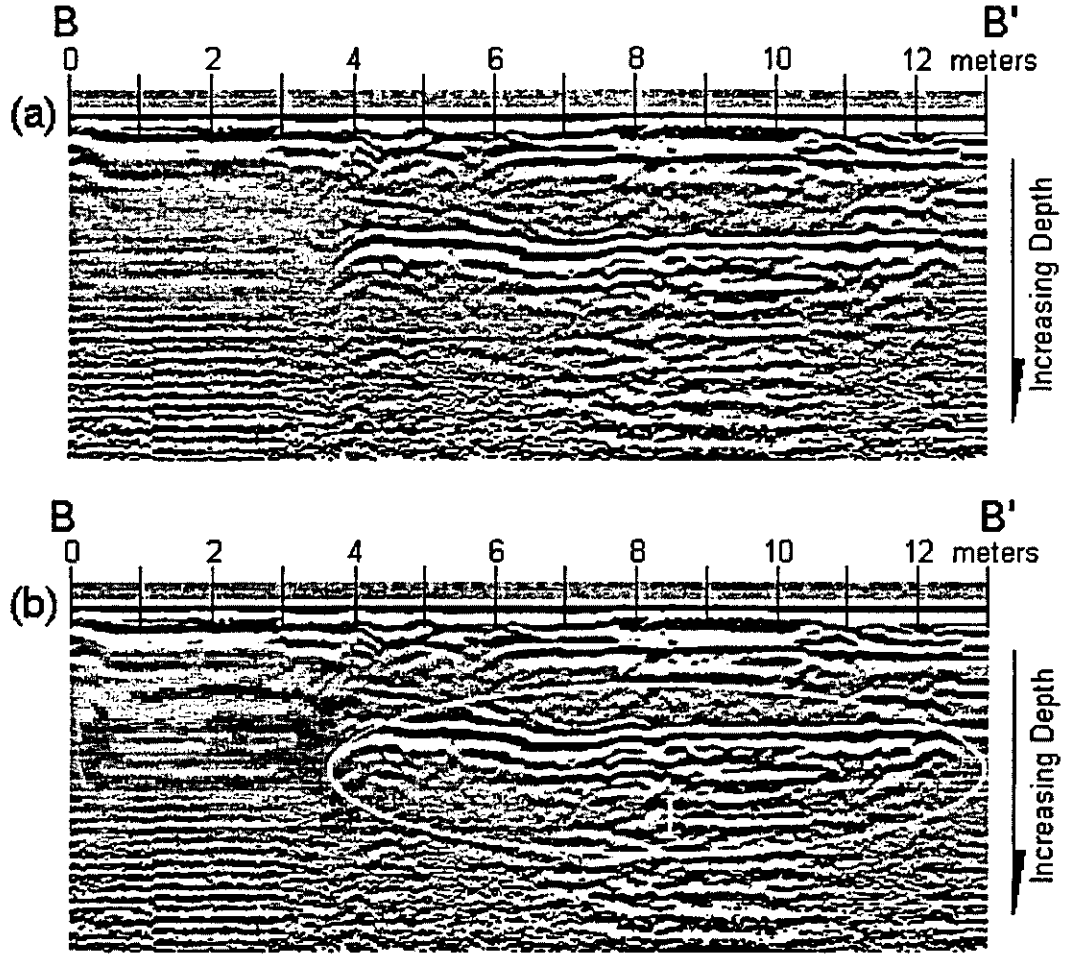

Figure 8: GPR profile of Area B from Simpson Oil Company along line B-B' (Figure 2) using the 400 MHz antenna – (a) uninterpreted and (b) interpreted sections with the UST (I)

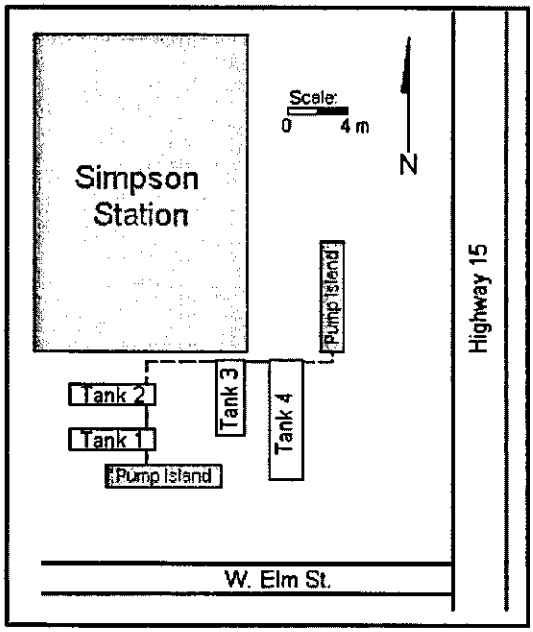

Figure 9: Simpson Oil Co. (cf. Figure 5) – the USTs in their proper spatial locations and the location of the feeder line (dashed line is the assumed position of the feeder line)

APPENDIX I

SUBSURFACE INVESTIGATION WITH ELECTRICAL RESISTIVITY

Steve Cardimona*

*Department of Geology and Geophysics, University of Missouri-Rolla, Rolla, MO

ABSTRACT

Geophysical resistivity techniques are based on the response of the earth to the flow of electrical current. With an electrical current passed through the ground and two potential electrodes to record the resultant potential difference between them, we can obtain a direct measure of the electrical impedance of the subsurface material. The resistivity of the subsurface, a material constant, is then a function of the magnitude of the current, the recorded potential difference, and the geometry of the electrode array. Depending upon the survey geometry, the data are plotted as 1-D sounding or profiling curves, or in 2-D cross-section in order to look for anomalous regions. In the shallow subsurface, the presence of water controls much of the conductivity variation. Measurement of resistivity is, in general, a measure of water saturation and connectivity of pore space. Resistivity measurements are associated with varying depths relative to the distance between the current and potential electrodes in the survey, and can be interpreted qualitatively and quantitatively in terms of a lithologic and/or geohydrologic model of the subsurface.

INTRODUCTION

Geophysical resistivity techniques are based on the response of the earth to the flow of electrical current. In these methods, an electrical current is passed through the ground and two potential electrodes allow us to record the resultant potential difference between them, giving us a way to measure the electrical impedance of the subsurface material. The apparent resistivity is then a function of the measured impedance (ratio of potential to current) and the geometry of the electrode array. Depending upon the survey geometry, the apparent resistivity data are plotted as 1-D soundings, 1-D profiles, or in 2-D cross-sections in order to look for anomalous regions.

In the shallow subsurface, the presence of water controls much of the conductivity variation. Measurement of resistivity (inverse of conductivity) is, in general, a measure of water saturation and connectivity of pore space. This is because water has a low resistivity and electric current will follow the path of least resistance. Increasing saturation, increasing salinity of the underground water, increasing porosity of rock (water-filled voids) and increasing number of fractures (water-filled) all tend to *decrease* measured resistivity. Increasing compaction of soils or rock units will expel water and effectively increase resistivity. Air, with naturally high resistivity, results in the opposite response compared to water when filling voids. Whereas the presence of water will reduce resistivity, the presence of air in voids should increase subsurface resistivity.

Resistivity measurements are associated with varying depths depending on the separation of the current and potential electrodes in the survey, and can be interpreted in terms of a lithologic and/or geohydrologic model of the subsurface. Data are termed *apparent* resistivity because the resistivity values measured are actually averages over the total current path length but are plotted at one depth point for each potential electrode pair. Two dimensional images of the subsurface apparent resistivity variation are called *pseudo*-sections. Data plotted in cross-section is a simplistic representation of actual, complex current flow paths. Computer modeling can help interpret geoelectric data in terms of more accurate earth models.

This paper reviews the working ideas behind basic geoelectric methods. In the following sections we present some of the basic resistivity theory, followed by discussions on resistivity field methods and survey geometry associated with the three main surveying techniques: vertical electric sounding (VES),

constant separation traversing (CST), and combined sounding and traversing methods. Comprehensive overviews of resistivity methods are presented in Telford (1976), Ward (1990), Kearey and Brooks (1991), and Burger (1992).

BACKGROUND

Ohm's Law

Ohm's Law describes the electrical properties of any medium. Ohm's Law, $V = I R$, relates the voltage of a circuit to the product of the current and the resistance. This relationship holds for earth materials as well as simple circuits. Resistance, however, is not a material constant. Instead, resistivity is an intrinsic property of the medium describing the resistance of the medium to the flow of electric current. Resistivity ($\rho = \delta A\, \delta R / \delta L$) is defined as a unit change in resistance scaled by the ratio of a unit cross-sectional area and a unit length of the material through which the current is passing (Figure 1). Resistivity is measured in ohm-m or ohm-ft, and is the reciprocal of the conductivity of the material. Table 1 displays some typical resistivities. Earth resistivities can range over nine orders of magnitude, from .1-10^8 ohm-m.

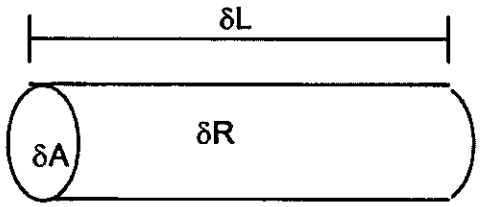

Figure 1. Resistivity is defined based on the change in resistance δR for a given change in length δL and cross-sectional area δA of material.

Table 1

Common Resistivities (ohm-m)

Material	Resistivity range	Typical Value
Igneous & Metamporphic rocks	10^2 - 10^8	10^4 10^3
Sedimentary rocks	10 - 10^8	10^3
Unconsolidated	10^{-1} - 10^4	10^3
Groundwater	1 - 10	5
Pure water		10^3

Note that, in Table 1, the resistivity ranges of different earth materials overlap. Thus, resistivity measurements cannot be directly related to the type of soil or rock in the subsurface without direct sampling or some other geophysical or geotechnical information. Porosity is the major controlling factor for changing resistivity because electricity flows in the near surface by the passage of ions through pore

space in the subsurface materials. The porosity (amount of pore space), the permeability (connectivity of pores), the water (or other fluid) content of the pores, and the presence of salts all become contributing factors to changing resistivity. Because most minerals are insulators and rock composition tends to increase resistivity, it is easier to measure conductive anomalies than resistive ones in the subsurface. However, air, with a theoretical infinite resistivity, will produce large resistive anomalies when filling subsurface voids.

Poisson's Equation

The recordings we make in resistivity methods are surface measurements of the potential field distribution due to the current passing through the ground. This potential is a solution to Poisson's equation, $\nabla^2 P = 0$, where ∇^2 is a second derivative operator and P is the potential. For the potential P at a distance r from the current source I on the surface of the earth (an infinite half space below), the solution is given by $P = I\rho/2\pi r$. In reality, a single electrode cannot pass current through a half-space because two electrodes are required to complete the electrical circuit. Also, we do not measure potential, but measure the potential difference between two electrodes. The solution to Poisson's equation for each pair of current and pair of potential electrodes would give a general form for a measured potential difference with electrodes placed anywhere on the surface. In practice, however, the current and potential electrodes are arranged most often in a collinear pattern (Figure 2).

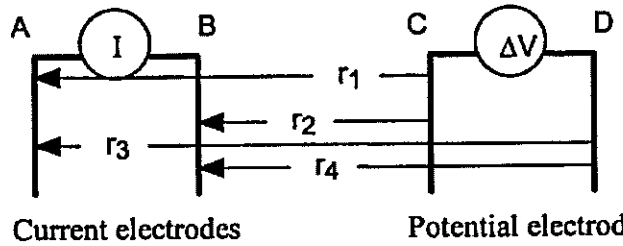

Figure 2. Geoelectric survey with current and potential electrodes collinear.

The resulting equation for the measured potential (voltage) difference is

$$\Delta V = \frac{I\rho}{2\pi}\left[\left(\frac{1}{r_1} - \frac{1}{r_2}\right) - \left(\frac{1}{r_3} - \frac{1}{r_4}\right)\right]$$

By solving the above equation for ρ, we can determine the resistivity of the subsurface region. We derive the above equation assuming a homogeneous and isotropic half-space. Because the earth is neither homogeneous nor isotropic, a measured voltage difference yields a resistivity value that is an average over the path length the current follows. Thus, we can determine only apparent resistivity, given by

$$\rho_a = \frac{2\pi V}{I}\left[\frac{1}{\left(\frac{1}{r_1} - \frac{1}{r_2}\right) - \left(\frac{1}{r_3} - \frac{1}{r_4}\right)}\right] = \frac{\Delta V}{I} G(r).$$

G(r) is a geometric factor and is dependent upon the spatial arrangement of electrodes for specific arrays.

DC Resistivity

The preceding discussion implies D.C., or zero-frequency current (no reactance). Electrode polarization can occur whenever the mode of current conduction changes from ionic (subsurface) to metallic (electrode). Because energy is required to cause the current to flow across the subsurface/electrode interface, a barrier is established which causes an electrical impedance (Ward, 1990). This barrier is generally composed of mobile ions and acts as an insulator. By alternating the polarity of the induced current, mobile ions do not build up excessively around the electrode and the electrode polarization is

minimized. Thus the use of an alternating current source decreases the effect of natural earth potentials that can affect the voltage measurements. So, alternating currents are used in most surveys in order to alleviate noise and measurement problems associated with direct current.

SURVEY DESIGN

Three categories of field techniques exist for conventional resistivity analysis of the subsurface. These techniques are vertical electric sounding (VES), constant separation traversing (CST), and combined procedures which utilize characteristics of both VES and CST.

Vertical electric sounding

Vertical electric sounding (VES) employs collinear arrays designed to output a 1-D vertical apparent resistivity versus depth model of the subsurface at a specific observation point. In this method a series of potential differences are acquired at successively greater electrode spacings while maintaining a fixed central reference point. The induced current passes through progressively deeper layers at greater electrode spacing. The potential difference measurements are directly proportional to the changes in the deeper subsurface. Apparent resistivity values calculated from measured potential differences can be interpreted in terms of overburden thickness, water table depth, and the depths and thicknesses of subsurface strata. The two most common arrays used for VES are the Wenner array and the Schlumberger array.

In the Wenner array configuration, potential electrodes are nested within the current electrodes with a common lateral distance between adjacent electrodes called the electrode *a*-spacing (Figure 3). For sounding measurements, the electrodes in a Wenner array are expanded about a center point by equally incrementing the *a*-spacing. The current therefore progressively passes into deeper layers, with the nominal depth of investigation being equal to the a-spacing. This procedure provides apparent resistivity values that are dependent upon vertical conductivity variations of the subsurface. The geometric factor for the Wenner array is $G(r) = 2\ a$, and this simplicity of algebraic form as well as in-field set-up is part of this array's appeal. The Wenner array generally provides for high signal-to-noise ratios, good resolution of horizontal layers, and good depth sensitivity. Conversely, the Wenner array is not good at determining the lateral location of deep inhomogeneities (Ward, 1990) because the large *a*-spacing degrades lateral resolution, and the potential electrodes are located within the spread of the current electrodes. It is possible to perform limited profiling with the Wenner array by keeping the *a*-spacing constant and moving the entire array laterally between resistivity readings. However, investigation depth and resolution are limited for the profiling Wenner array if the *a*-spacing is held constant throughout the entire survey.

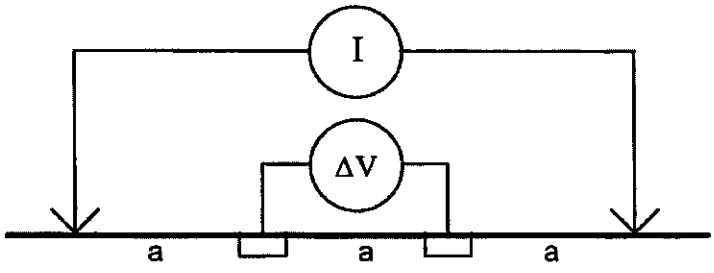

Figure 3. Wenner array. depth of sounding controlled by distance a, or a-spacing.

The Schlumberger array is similar to the Wenner array with respect to having a nested electrode configuration except the potential electrodes have an internal spacing of *a* and the current electrodes are spaced an increased distance of *na* from the potential electrodes, where the integer value *n* varies dependent upon target size and depth. The geometric factor is $G(r) = \pi n(n+1)a$, which can be shown to

be just a modification of the Wenner array result. The Schlumberger array of electrodes provides for high signal-to-noise ratios, good resolution of horizontal layers, and good depth sensitivity (Ward, 1990). The Schlumberger technique is somewhat easier to use than the Wenner technique because only two of the four electrodes are moved between successive readings. As an example, we can conduct a Schlumberger VES survey by keeping the potential electrodes fixed at one location while the current electrodes are expanded about a center point. Only when the current electrodes become relatively distant does the potential electrode spacing need to be expanded in order to have measurable potentials.

Constant separation traversing

Electrical profiling, known as constant separation traversing (CST), uses collinear arrays to determine lateral resistivity variations in the shallow subsurface at a more or less fixed depth of investigation. The current and potential electrodes are moved along a profile with constant spacing between electrodes. The two most common array types used for CST are the dipole-dipole and pole-dipole arrays, where a dipole is a pair of current or potential electrodes.

The dipole-dipole resistivity technique consists of a collinear array with current dipole separation of length *a*, potential dipole separation of length *a*, with a total distance between the dipoles of length *na* (Figure 4). Figure 4 also shows where the apparent resistivity value calculated from the measured potential difference is plotted to aid later interpretation. The apparent resistivity value is plotted along intersecting 45 degree lines centered on the dipoles (Hallof, 1957). The geometric factor for the dipole-dipole array is $G(r) = n(n+1)(n+2)a$. The dipole-dipole technique records the largest anomalies in comparison to other arrays, but its low signal-to-noise ratio limits its applications. Finding small changes in resistivity at great depth would be difficult (Ward, 1990).

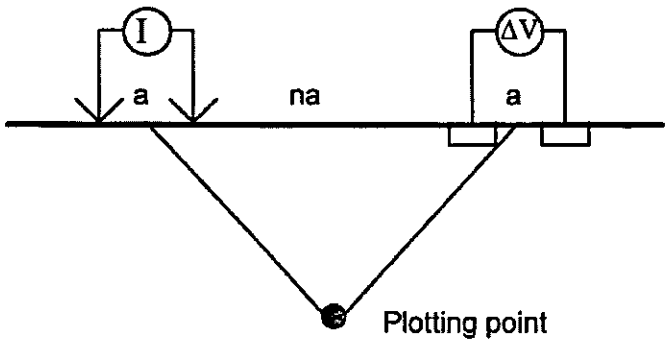

Figure 4. Dipole-Dipole array yields a depth of investigation relative to the value of the integer n which determines the offset between current and potential electrode pairs.

The pole-dipole array has potential electrodes offset from a "single" current source. The single current source actually is a two electrode dipole system with the second electrode (the current sink) placed very far away. The collinear potential electrodes are kept at a constant spacing of *a* and are moved incrementally over intervals of length *a* for distances equal to 10*a* on either side of the local current electrode. By utilizing multiple source locations it is possible to determine depth and size of subsurface anomalies. The geometric factor is derived as $G(r) = 2\ n(n+1)a$. The main strengths of the pole-dipole method are its sensitivity to subsurface inhomogeneities and depth of penetration. Weaknesses of the method include low signal-to-noise ratios, insensitivity to dipping structures, and the problems encountered with extensive array lengths (Ward, 1990). The pole-dipole array produces apparent resistivity data similar to dipole-dipole configurations, but associated asymmetry (introduced by the "single" current electrode) decreases lateral resolution. For this reason, the dipole-dipole method of data acquisition has been favored over the pole-dipole method in more recent resistivity studies. Regarding subsurface cavity detection, Spiegel et al. (1980) demonstrated, with the help of modeling software, that the pole-dipole method with 2 meter spacing could detect positive anomalies from 2 x 2 meter air-filled

tunnels at depths of 19 meters and 30 meters even over uneven terrain. It is also possible to detect water-filled voids found below the water table by applying the same technique focusing on negative, or low, resistivity anomalies (Smith, 1986). Fountain (1977) demonstrated that the pole-dipole method successfully imaged subsurface cavities, both air- and clay-filled, below roads in Birmingham, Alabama, above mines in Idaho Springs, Colorado, and over complex cave environments at the Southwest Research Institute's Medford Cave Test Site.

Combination of VES and CST

The clear delineation of subsurface anomalies often requires a technique for determining both lateral and vertical features. Three of the previously discussed resistivity arrays (Wenner, Schlumberger, pole-dipole) are capable of performing either lateral measurements (CST) or vertical measurements (VES), but it is generally inefficient for the individual arrays to simultaneously accomplish both sounding and profiling. A combination VES and CST array, such as a multi-level dipole-dipole array, can overcome the limitations associated with purely profiling or sounding techniques.

The dipole-dipole method has sounding capability as well as profiling applications. By increasing *na* while retaining fixed current electrode locations, multiple potentials may be taken representing greater depth of penetration and increased lateral coverage (Figure 5). In the past, combined sounding-profiling surveys performed with the dipole-dipole method increased *n* from *n*=1,2,3,4 for adequate depth of penetration without introducing spurious noise (Bodmer and Ward, 1968). Now, with the technological advances in resistivity equipment and filtering, multiple levels (up to n=12) can be obtained with reproducible results. The multi-level dipole-dipole technique allows for the efficient acquisition of resistivity values at multiple lateral and vertical locations. For these combined VES/CST surveys, the data are plotted in pseudo-section as apparent resistivity in order to look for anomalous regions. Data are plotted midway between current and potential electrode pairs, associated with varying depths relative to the varying distance between the two active pairs of electrodes (Figure 5).

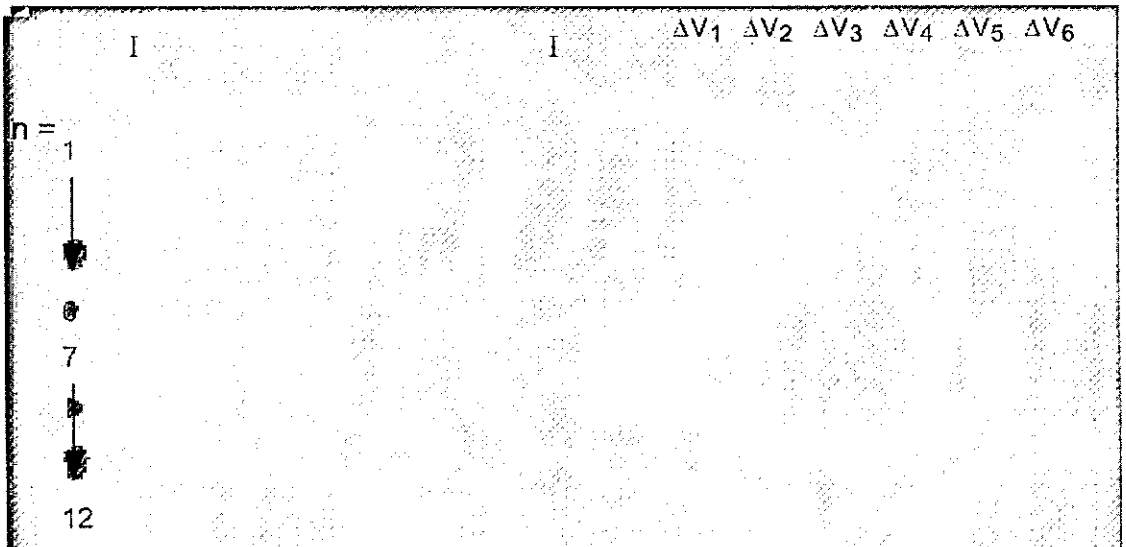

Figure 5. Multichannel dipole-dipole survey utilizing more than one current electrode pair and multiple potential electrodes in order to conduct a simultaneous VES and CST survey. Data are plotted at intersection of lines from surface dipoles (e.g., along dashed lines as survey continues one step to right).

Azimuthal resistivity

When conducting electrical resistivity surveys with a collinear set of electrodes as described above, most of the current path samples the subsurface below the survey line. We can take advantage of this

specific subsurface sampling by varying the azimuth of resistivity surveys in an effort to measure directional variations of electrical properties. This technique can be sensitive to variations in a subsurface that has preferentially aligned fractures. Line azimuths that are perpendicular to water-filled fractures should exhibit higher resistivities, allowing us to map the direction of subsurface fracturing.

3-D and cross-borehole resistivity

Current research is directed toward expanding the applications of resistivity surveying to cross-borehole resistivity tomography and 3-D geometries. The basic concepts for these advanced techniques are the same as for the 1-D and 2-D surveying discussed above; however the details of the survey procedures and analysis techniques can be much more involved. These advanced procedures are not in common practice; however they may become more routine in the near future as recent advances in instrumentation, computer power, and sophistication of computer algorithms allow us to attack these more difficult problems.

ANALYSIS

Interpretation

Because the earth's subsurface is not homogeneous, the electrical properties of the ground (resistivity/conductivity) alter the current density. The equipotential surfaces, perpendicular to the current flow, are modified by the deflection of the electrical current near inhomogeneities. The resistivity method measures the resulting variation in potential differences yielding information about the subsurface inhomogeneity. The measured variations are primarily due to the subsurface material directly below the survey line (in the survey plane), although this is not completely true because the earth is not isotropic. Data are termed *apparent* resistivity because they are averages over a complex current path but are associated with a single depth point in the survey plane. The wide resistivity ranges of earth materials (Table 1) suggest that resistivity data may look noisy. Often data are plotted as the logarithm of the apparent resistivity.

Interpretation of vertical electric sounding data can be as simple as plotting the measurements with respect to some parameter describing the expanding spread (e.g., the increasing *a*-spacing for the Wenner array), and then comparing sounding curves from different areas or different azimuths (Figure 6). We can perform a more detailed analysis through computer simulation of the data, and comparing the resulting calculations with the measured data (curve matching). This latter technique assumes horizontal layering, which is not too limiting an assumption since VES surveys are not sensitive to lateral variation.

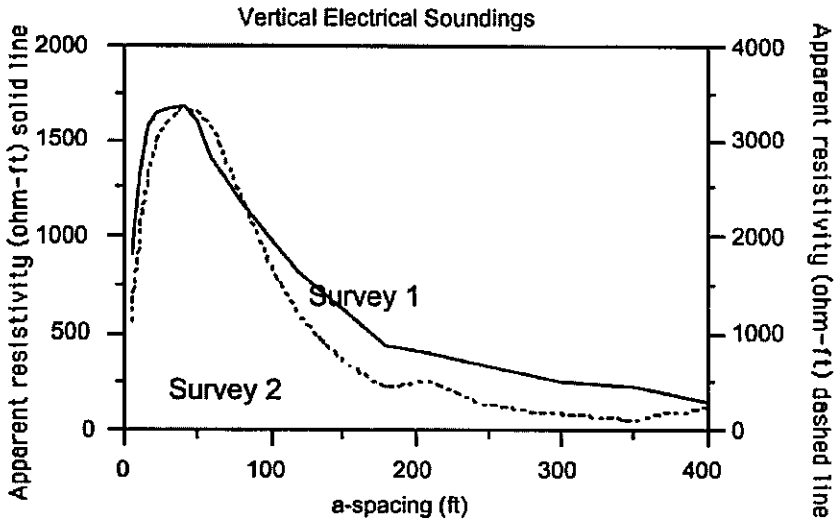

Figure 6. Two VES Wenner array data sets collected with an increasing a-spacing between current and potential electrodes. Note different scale for Survey 1 (left scale) and Survey 2 (right scale). Lower resistivity values are evident for Survey 1, indicating higher conductivity below that survey than nearby at location of Survey 2.

Constant separation traversing is an ideal survey mode for detecting anomalies (Figure 7). Multiple CST surveys can be run along parallel lines, and an anomaly map can be contoured showing the horizontal extent of subsurface features. Resolution of the causative feature is poor, however. Some sort of ground truth, or measurements from another geophysical technique, would be needed to obtain a more quantitative interpretation of the data.

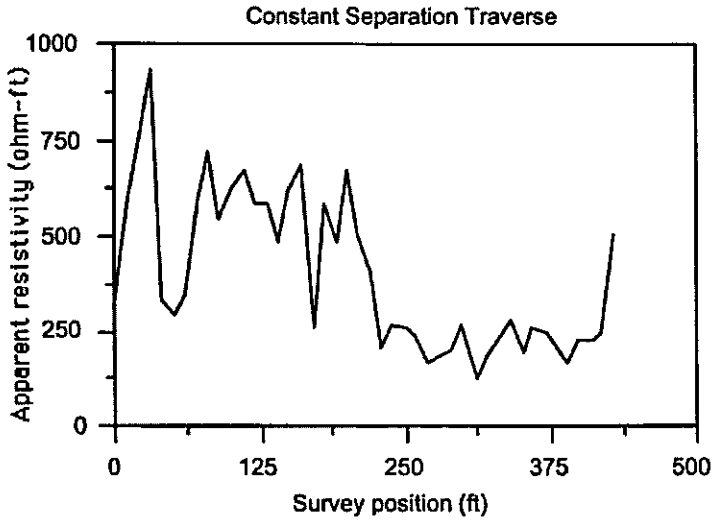

Figure 7. CST dipole-dipole data collected with a constant separation of 10 ft between current and potential dipoles, and a survey step interval of 10 ft. Zone of low resistivity (higher conductivity) is evident on right side of plot.

Combined VES/CST surveys offer the most information (Figure 8). As with CST alone, multiple VES/CST surveys can be planned in order to characterize (image) the vertical as well as horizontal extent of subsurface variations. Images of the subsurface are called *pseudo*-sections because data measurements with respect to depth are only simply represented (Figure 5). Also, caution must be employed when interpreting the pseudo-sections at the sides of the image. The edges (at the ends of the survey) have less data control and are smoothed (extrapolated) estimates of apparent resistivity.

Inversion

Forward modeling can be used to create resistivity models of the subsurface that would simulate apparent resistivities that correlate with the measured data. This procedure is iterative. A starting resistivity model is chosen based on a priori information (from ground truth or averaged geophysical measurements), and apparent resistivity data are modeled for the type of field survey geometry used. These calculated data are compared with the actual data and the resistivity model is updated based on the difference between observed and calculated data. This procedure is continued until the calculated data match the actual measurements to within an interpreter-defined level of error. One of the most important results of inversion is better estimates of depth for cross-section plots, turning pseudo-sections into better approximations of the subsurface variation.

Limitations

The limitations of the resistivity technique include the more difficult interpretation in the presence of complex geology and the existence of natural currents and potentials. The advantages of the resistivity method are the simple theory and methodology. The ability to obtain both sounding data (variations with respect to depth) and profiling data (variations with respect to a horizontal coordinate) is a distinct plus. Data can be obtained and qualitatively interpreted reasonably rapidly, although combined VES/CST surveys will necessarily require more effort than VES or CST alone. Without inversion of the geoelectric data, depths as plotted in pseudo-section are normally an overestimation of the true investigation depth.

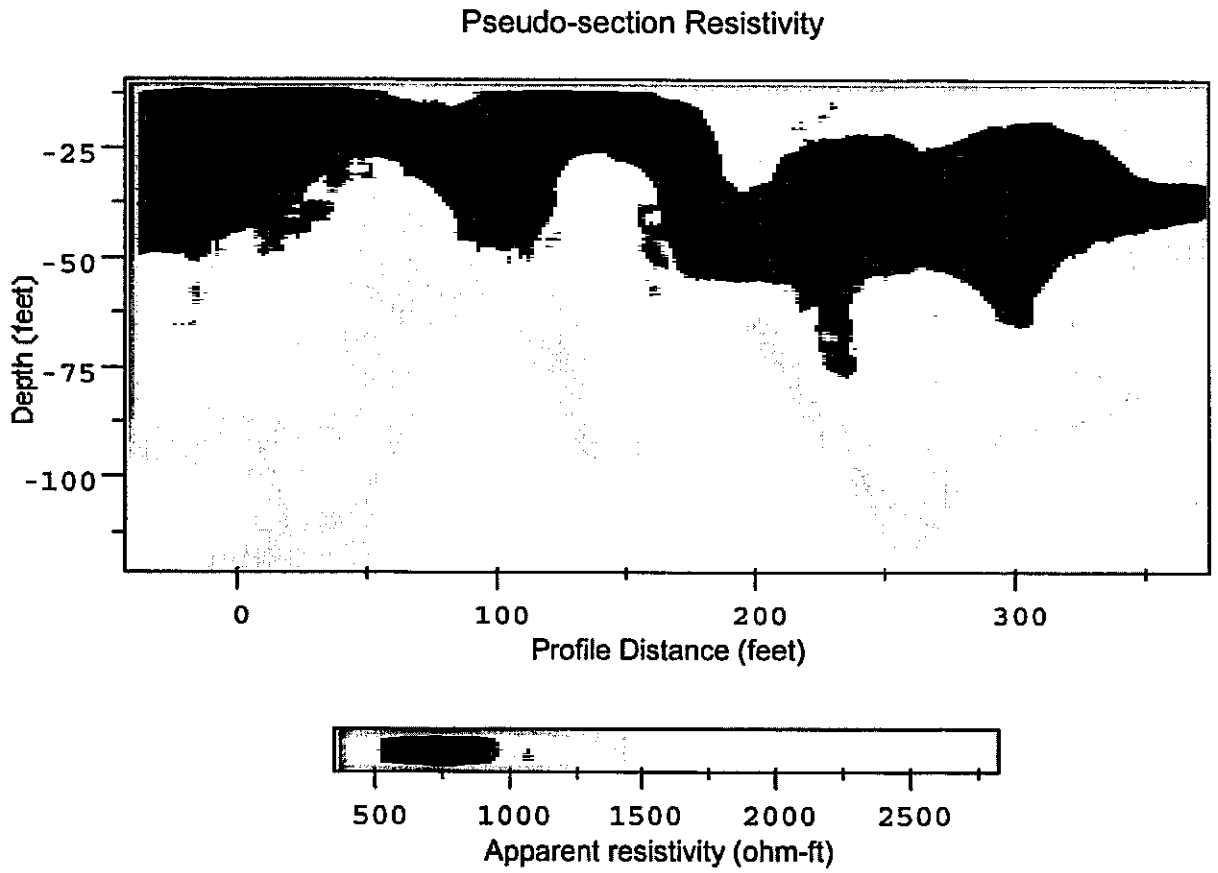

Figure 8. Combined VES and CST resistivity data plotted in pseudo-section. Data were collected with a dipole-dipole multichannel array, with a constant separation of 20 ft between poles in each dipole.

CONCLUSION

Geophysical resistivity techniques are based on the response of the earth to the flow of electrical current. In this method, an electrical current is passed through the ground and two potential electrodes allow us to record the resultant potential difference between them, giving a direct measure of the electrical impedance of the subsurface material. The resistivity, a material constant, is then a function of the measured impedance and the geometry of the electrode array.

In the shallow subsurface, the presence of water controls much of the conductivity variation. Measurement of the resistivity is, in general, a measure of the amount of water saturation and connectivity of pore space. Increasing water content and increasing salinity of the underground water will decrease the measured resistivity. So, increasing porosity of rock and increasing number of fractures will tend to decrease measured resistivity if the voids are water filled. Increasing compaction of soils or rocks will counteract the water-filled porous nature and effectively increase resistivity. Air, with naturally high resistivity, will work opposite to water when filling voids. Whereas the presence of water will reduce resistivity, the presence of air in voids should increase resistivity.

Resistivity measurements at the surface of the earth are associated with varying depths relative to the geometry of the current and potential electrodes in the survey. The apparent resistivity data are routinely plotted as 1-D sounding curves, 1-D profiles, or in 2-D cross-section in order to look for anomalous regions. Computer modeling can be used to help interpret geoelectric data in terms of correct physical

earth models. The data can be interpreted qualitatively and quantitatively in terms of a lithologic and/or geohydrologic model of the subsurface.

REFERENCES

Bodmer, R., and Ward, S. H., 1968, Continuous sounding-profiling with a dipole-dipole resistivity array: Geophysics, **33**, 838-842.

Burger, H. R., 1992, Exploration Geophysics of the Shallow Subsurface: Prentice Hall, Inc.

Fountain, L. S., 1977, Detection of subsurface cavities by surface remote sensing techniques: *in* Symposium on Detection of Subsurface Cavities, 12-15 July 1977, Office, Chief of Engineers, U. S. Army, Washington, D. C., and U. S. Army Engineer Waterways Experiment Station Soils and Pavements Laboratory, P. O. Box 631, Vicksburg, MS 39180.

Hallof, P. G., 1957, On the interpretation of resistivity and induced polarization measurements: Cambridge, MIT, Ph.D. thesis.

Kearey, P. and Brooks, M., 1991, An Introduction to Geophysical Exploration: Blackwell Scientific Publications.

Smith, D. L., 1986, Application of the pole-dipole resistivity technique to the detection of solution cavities beneath highways: Geophysics, **51**, 833-837.

Spiegel, R. J., Sturdivant, V. R., and Owen, T. E., 1980, Modeling resistivity anomalies from localized voids under irregular terrain: Geophysics, **45**, 1164-1183.

Telford, W. M., Geldart, L. P., Sheriff, R. E., and Keys, D. A., 1976, Applied geophysics: Cambridge University Press.

Ward, S. H., 1990, Resistivity and induced polarization methods: *in* Geotechnical and Environmental Geophysics, Vol. 1, Ward, S. H., ed: Society of Exploration Geophysicists.

APPENDIX J

INTEGRATED GEOPHYSICAL SITE CHARACTERIZATION

*Steve Cardimona, *Neil Anderson, and †Tim Newton

*The University of Missouri-Rolla
Department of Geology and Geophysics
125 McNutt Hall, 1870 Miner Circle
Rolla, MO 65409-0410

†The Missouri Department of Transportation
1617 Missouri Blvd., P.O. Box 270
Jefferson City, MO 65102

ABSTRACT

We performed an integrated survey using ground penetrating radar (GPR), shallow high-resolution reflection seismic and dipole-dipole electrical resistivity methods in order to characterize a site slated for roadway development. The intent of this project was to investigate the subsurface and determine the structure of the dolomite bedrock along a proposed expansion area for Highway 63, near Cabool, Missouri. We acquired a total of 68 GPR profiles to cover the area of highest interest, including a sinkhole visible at the time of the survey. Five high-resolution seismic reflection profiles and four multi-channel resistivity lines were positioned along key GPR survey lines. The soil to weathered bedrock interface appears as high amplitude disturbed reflections and diffractions on the GPR profiles. The seismic images contain anomalous sections of bedrock represented by diffractions and missing or offset reflections. Pseudo-section resistivity data indicates highly resistive regions within the subsurface that correlate with areas of concern on both the seismic and GPR data. We ranked areas based on whether one, two, or all three of the methods indicated anomalies. Five of these areas were drilled and it was found that two of the holes encountered void space, while the other three encountered heavily fractured bedrock. The results of this survey and the resulting core data will help to determine what, if any precautions must be taken for using this area to expand the highway.

SCOPE OF WORK AND SUMMARY OF RESULTS

Utilizing ground-penetrating radar (GPR), high-resolution shallow reflection seismic, and electrical resistivity methods, the Department of Geology and Geophysics of the University of Missouri-Rolla (UMR) acquired geophysical data for the Missouri Department of Transportation (MoDOT). The intent was to

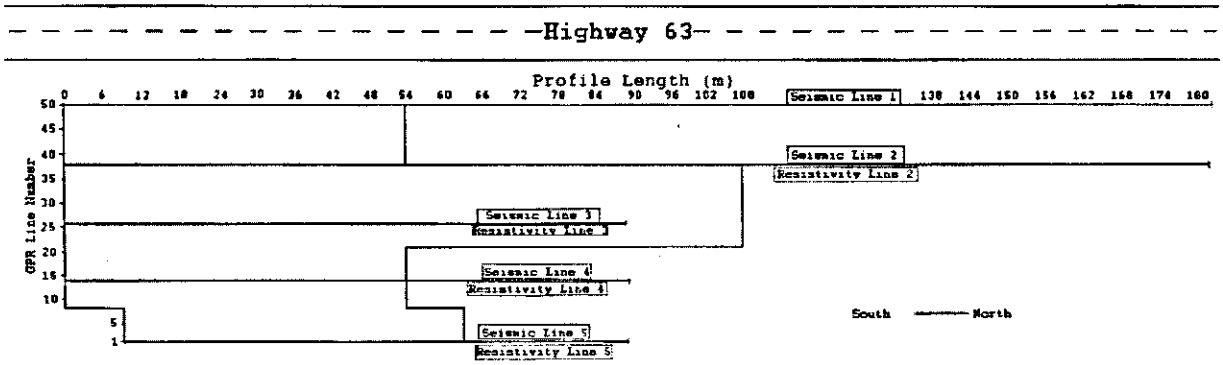

Figure 1. *Sixty-eight GPR, five seismic, and four resistivity lines were acquired at the site as shown. The locations seismic lines 2,3,4, and 5 correspond with locations of resistivity lines 2,3,4, and 5.*

investigate the subsurface and determine the structure of the dolomite bedrock with particular interest in finding possible voids along the proposed expansion area for Highway 63 north of Cabool, Missouri. UMR acquired 50 GPR profiles across the study area covering the area of highest interest, including a sinkhole visible at the time of the survey. The profiles were spaced one meter apart and were either 54 or 108 meters in length as shown in figure 1. Five seismic lines were located along GPR lines 50, 38, 26, 14, and 2 and four resistivity lines along GPR lines 38, 26, 14, and 2. These lines began on the south end of the site and were acquired parallel to Highway 63. GPS was used to determine the position of the lines at the site.

Both ground-penetrating radar and the shallow seismic method proved to be useful in defining the shallow bedrock structure. The soil to weathered bedrock interface appears as high amplitude disturbed reflections and diffractions on the GPR profiles. The seismic method appears to have imaged the deeper weathered bedrock to solid bedrock interface. This interface contains anomalous sections represented by diffractions and missing or offset reflections. Resistivity data displays highly resistive regions within the subsurface that correlate with areas of concern on both the seismic and GPR data. We have recommended that the Missouri Department of Transportation acquire ground truth in these locations to both validate the interpretations and provide additional information with which revised depth interpretations can be made.

OVERVIEW OF GROUND PENETRATING RADAR

Utilizing a GSSI Subsurface Interface Radar (SIR) System 10B and a 200 MHz antenna, we acquired 50 GPR profiles along a grid set up at the southern end of the site. Each profile, spaced at one-meter intervals, had a length of either 54 or 108 meters as shown in figure 1. A ground speed of about 1 m/s was used with data acquisition set at 25 scans/sec allowing horizontal resolution on the order of several centimeters. Profile spacing of one-meter allowed anomalies to be correlated from line to line. A two-way time range of 120 nanoseconds (ns) with the 200 MHz antenna allowed nominal depth of penetration to be calculated at 6m below the surface assuming a dielectric constant of 9. The amount of water in the soil affects the conductivity of the ground and thus the actual penetration of the SIR pulse. More water will increase the conductivity and decrease the depth of penetration (Daniels, 1996; Cardimona et al., 1998a).

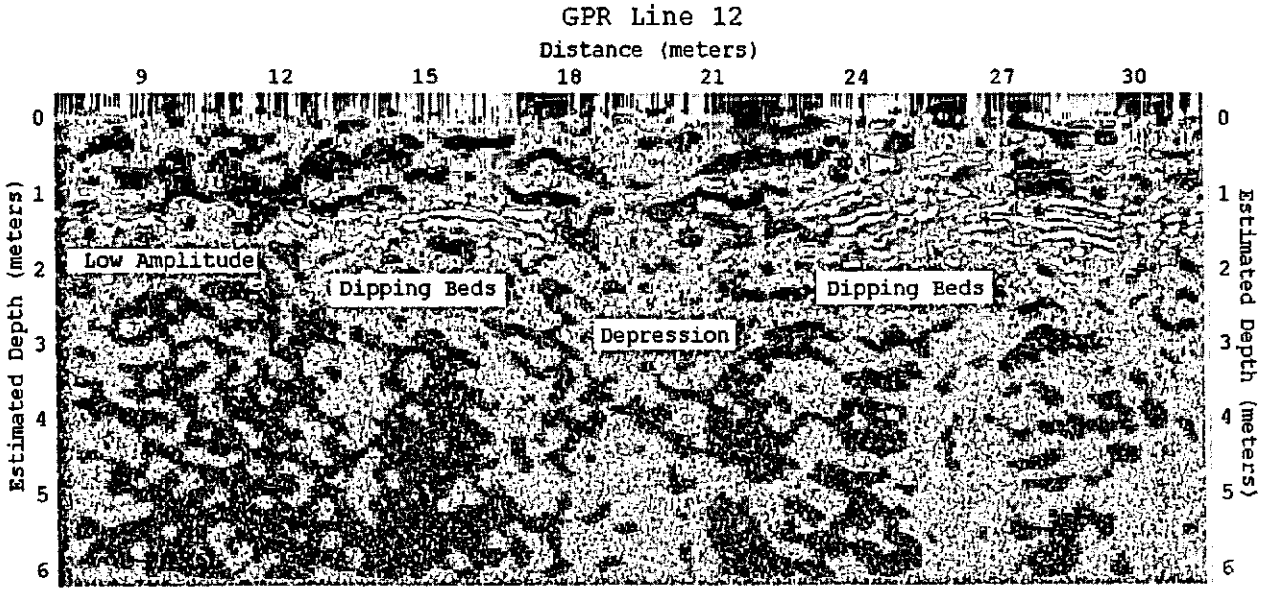

Figure 2. *GPR data was acquired to image a nominal depth of 6m. However, noise in the subsurface limited interpretation to the upper 2.5m. Several regions of depressions or channels were observed across much of the data. Often these features were associated with dipping beds. Two large regions of the site exhibited low amplitude reflections.*

Other acquisition parameters include a four-point automatic gain applied to boost signal arriving at later times. Vertical and horizontal infinite impulse response (IIR) filters, applied at the time of acquisition, helped remove some of the constant background noise. After being downloaded from the field computer, the data underwent several processing steps including horizontal normalization, predictive deconvolution, and horizontal and vertical filters. Figure 2 shows an example GPR data profile after processing.

OVERVIEW OF HIGH-RESOLUTION SHALLOW SEISMIC

The conventional seismic reflection technique uses acoustic wave energy to image the subsurface. A constant reflection is associated with strong interfaces such as a soil to bedrock interface (Telford et al., 1976; Anderson, et al, 1998). Where this interface is disturbed due to dissolution, voids, fractures, or faults, the reflection is replaced by a weaker reflection or by diffractions.

Acquisition was performed with a 24-channel, Bison 9000 series seismograph. Forty-Hertz geophones measured the acoustic energy produced from a sledgehammer source. Five-foot geophone and source spacing allowed high-resolution data in the shallow subsurface to be acquired. A 20ft near offset

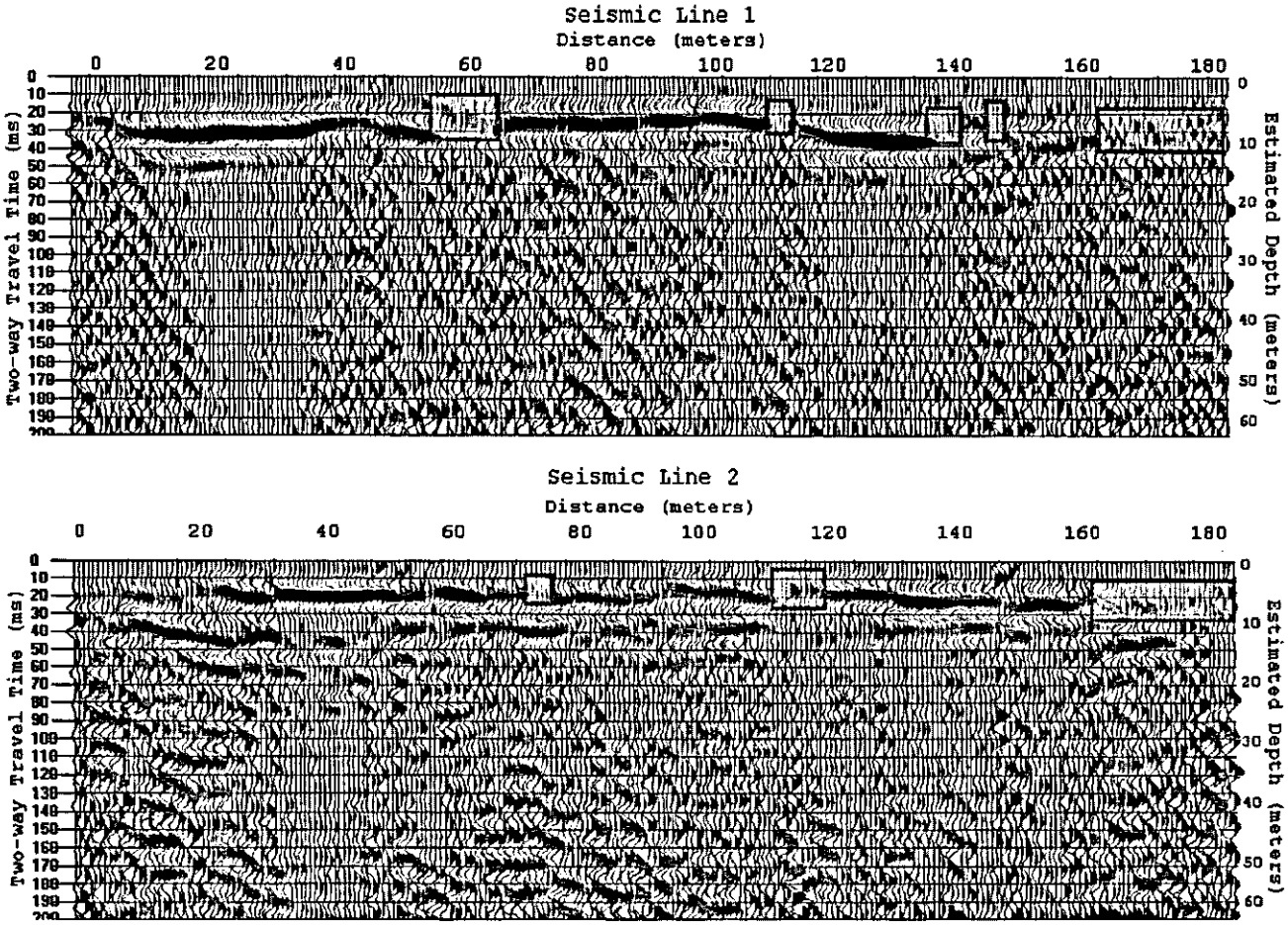

Figure 3. *Seismic data imaged the solid bedrock interface. This interface contains anomalous sections represented by diffractions and missing or offset reflections. Many of these anomalies directly correlate with GPR anomalies and highly resistive regions.*

recorded energy with a minimum amount of groundroll and refraction energy. Data quality limited depth of interpretation to approximately 30m, which was sufficient for mapping the shallow bedrock.

Data processing included muting to remove first arrival and refraction data that can mask the true reflection data; and time-domain and frequency/wavenumber domain filters to remove both cultural and natural noise. Enhancements were made with an automatic gain control and residual static corrections. Figure 3 displays the final processed seismic lines.

OVERVIEW OF THE DIPOLE-DIPOLE RESISTIVITY METHOD

The resistivity method is based on the earth's response to the flow of electrical current. Compact soils or rock units will lack water content and have a resistive nature. Regions where the soil or rock is weathered and filled with water will tend to decrease the measured resistivity. However, if the weathered soil or rock contains pockets of air-filled voids, the resistivity will increase due to the resistive nature of air (Telford, 1976; Kearey and Brooks, 1991; Cardimona et al., 1998b).

Four Resistivity lines were acquired at the site beginning on GPR lines 38, 26, 14, and 2 and extending north of the GPR grid. These four lines correlate with seismic lines 2, 3, 4, and 5 (Figure 1). No resistivity data were acquired over seismic line location 1.

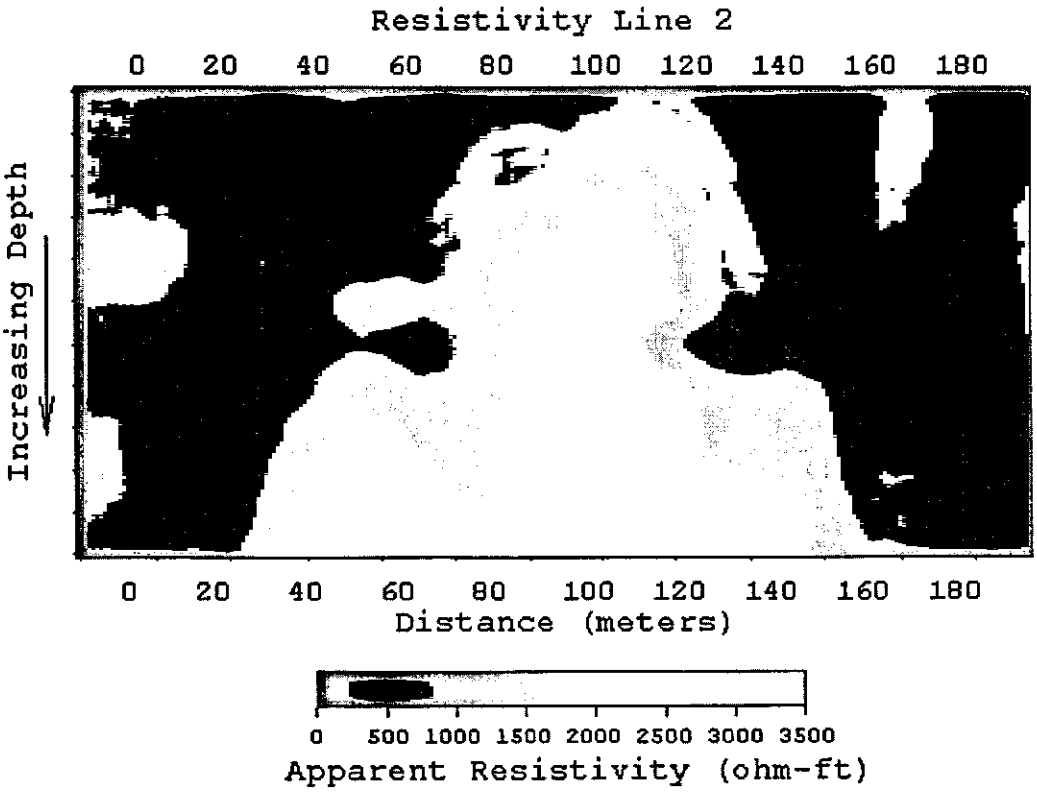

Figure 4. *Anomalous regions of high resistivity occur in all four profiles and often directly correlate with GPR and seismic anomalies. Distances are given in meters however exact depths are not determined in pseudo-section. The location of resistivity line 2 corresponds with the location of seismic line 2.*

A Zonge Engineering XMT-16 Transmitter Controller delivered the alternating current source through current electrodes spaced 10 meters apart (15 meters for line 2). A Zonge Engineering GDP-16 Data

Processing unit measured the potential differences across seven potential electrode pairs spaced 10 meters apart (15 meters for line 2).

The potential difference data are plotted as apparent resistivities in pseudo-section (Figure 4). These resistivity values are averages over the total current path length and are plotted at one depth point for each source-receiver combination.

RESULTS OF THE GEOPHYSICAL INVESTIGATION

Ground-Penetrating Radar

All 68 GPR profiles imaged an interface at approximately 1 to 2 meters in depth based on an estimated dielectric constant of 9. This interface is interpreted to be that of the soil to weathered bedrock (dolomite) contact. An interface such as this should produce a non-continuous region of reflectors and diffractions caused by loose rock and intermixed soil. Concern lies in those areas where the signature of this weathered interface changes or disappears. These areas have been plotted in Figure 5. At some locations the interface appears to be replaced by localized channel features or depressions. Many of these features appear to correlate from line to line. The location of the known sinkhole lies in the vicinity of one such feature. Surrounding these depressions are dipping beds possibly indicating dissolution in or below the features. Weak or missing reflections from the interface occur across parts of the site and may indicate where the interface between soil and weathered bedrock becomes suddenly deeper or is missing. Although our time window was set to record to a depth of approximately 6m, no reflections were visible deeper than 2.5m due to signal attenuation and a decreasing signal to noise ratio.

Shallow Reflection Seismic

Five seismic lines were acquired, each imaging a reflection across the site at depths between 3 and 9 meters. This is based on an estimated near-surface velocity of 610m/s (2000ft/s). The reflection is interpreted to be that of the interface between weathered and solid bedrock (Figure 3). Line 1 shows this bedrock reflection to vary between an estimated depth of 3 and 7 meters. The interface here is relatively

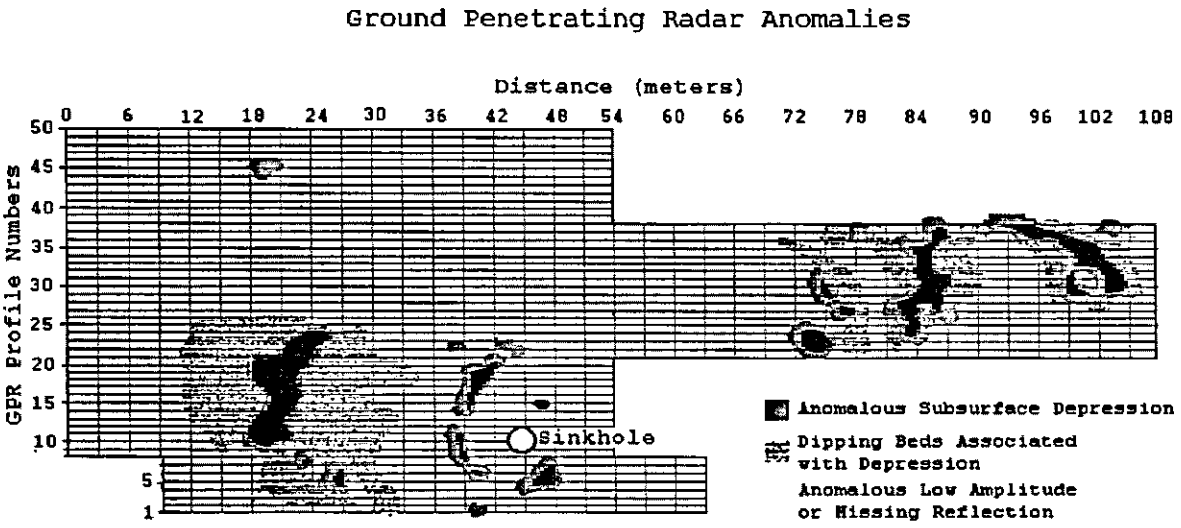

Figure 5. *GPR data anomalies are plotted with solid black indicating those sections where a channel or depression was interpreted. Dipping beds were often associated with those depressions (black/gray texture). Two large regions of low amplitude reflections are plotted in gray. Both the depression features and low amplitude regions correlate well with seismic and resistivity.*

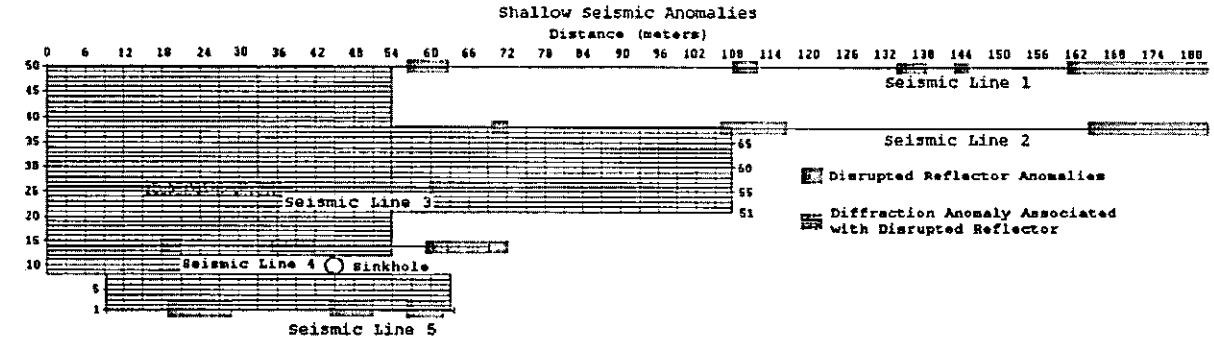

Figure 6. *Seismic anomalies are plotted and indicate sections where the interpreted bedrock reflector is broken up, missing, or shifted. These anomalies correlated well to both GPR and resistivity anomalies. The known sinkhole lies in the vicinity of such anomalies. A large pair of diffractions was observed as shown on line 3 and directly correlates with large anomalies observed on GPR and resistivity profiles.*

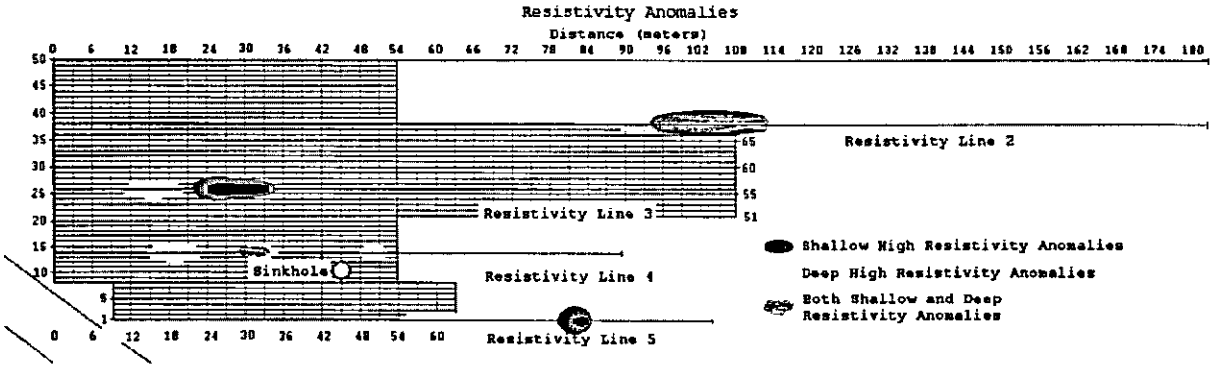

Figure 7. *The locations of high apparent resistivities (low conductivity) are shown. Black indicates those areas of high apparent resistivity located in the shallow subsurface. Gray ovals represent the locations of anomalously high apparent resistivities located deeper in the subsurface. At some locations both shallow and deep high apparent resistivities were observed as shown. Many of these anomalies correlate with seismic and GPR anomalies.*

undisturbed but displays some anomalous sections delineated in Figure 6. Line 2 images a reflection more irregular than line 1. Notable anomalies similar to those in line 1 are observed. In addition, some of the reflections seem to be shifted in time indicating possible breakup along the bedrock interface (fracturing). Without further depth control and more accurate velocity information, the depth values must be viewed as only estimates.

Dipole-Dipole Resistivity

Resistivity data can be evaluated for spatial variations in resistivity and qualitative assessment of depth relationships, but no depth estimates are based on this data (Figure 4). High resistivity values indicating the presence of possible air filled voids are plotted in Figure 7.

Many of the anomalies from all three methods directly correlate with one another. These are the areas of highest concern. Anomalies from all methods were apparent within three meters of the known sinkhole.

RESULTS OF CORE DRILLING

After joint interpretation of the data was concluded, we recommended several areas for exploratory drilling. The areas were given a ranking based on how many methods indicated anomalies, the strength of those anomalies, and the confidence in the interpretations of the anomalies. Five locations were chosen for coring and they were all drilled in areas that demonstrated anomalous signatures in the geophysical data. The cores showed that the subsurface consisted of a layer of loose soil that was underlain by a thin gravel layer. Under the gravel layer, clayey soil was found and then dolomite bedrock at around 3 m. Two of the cores encountered void space, while the other three encountered heavily fractured bedrock. Four of the drill holes accepted all water during drilling, which suggests that the features encountered are part of a larger system. The cores also contained samples with smooth surfaces suggesting water flow through the area over an extended period of time. The geophysical data indicated problems at all five drill locations and all five cores indicated problems that should be mitigated prior to expansion of the highway in this area.

CONCLUSIONS

Although all three methods used at the site can provide valuable information regarding the subsurface, it is the combination of the three techniques, which provides the most useful interpretations. Each method provided valuable information by which a model of the subsurface can be drawn. The ground-penetrating radar method was successful in evaluating the near-surface soil and weathered bedrock interface that was too shallow for the seismic method to resolve. In contrast, the seismic data imaged the solid bedrock at depths deeper than apparent on the GPR profiles. Resistivity information was unable to resolve a definite boundary between soil and bedrock further indicating that the change was gradational with a weathered zone above solid rock. Thus, the combination of these methods was very successful at complementing one another to provide a complete look at the shallow subsurface. Coring information from near the site provided by MoDOT indicates a point of auger refusal at approximately three to five meters. This refusal depth is within the weathered zone above solid dolomite. Depth estimation of both GPR and seismic methods is limited by a lack of velocity information. However, the lateral correlation of anomalous areas across the three methods was successful and provides spatial information for further investigation. Each method provides a different view of the subsurface properties. Locations where two or three of the methods indicate anomalies should be examined thoroughly. For this reason, we recommended exploratory drilling at several locations across the site. These recommendations were rated based on size of anomalies, number of methods indicating anomalies, and confidence in data. Five cores were drilled and two of them encountered void space while the other three were heavily fractured. The core control supports our interpretations and will allow the geophysical data to be used more confidently for planning the construction of the highway expansion.

REFERENCES

Anderson, N., Shoemaker, M., and Hatheway, A., 1998, *Overview of the Shallow Seismic Reflection Technique*: in Highway Applications of Engineering Geophysics with an Emphasis on Previously Mined Ground. Missouri Department of Transportation, publishers., Jefferson City, Missouri.

Cardimona, S., Roarke, M., Webb, D.J., and Lippincott, T., 1998a, *Ground Penetrating Radar*: in Highway Applications of Engineering Geophysics with an Emphasis on Previously Mined Ground. Missouri Department of Transportation, publishers., Jefferson City, Missouri.

Cardimona, S., Williams, S., Brady, T., Hickman, S., 1998b, *Geoelectric Methods for Subsurface Investigation*: in Highway Applications of Engineering Geophysics with an Emphasis on Previously Mined Ground. Missouri Department of Transportation, publishers., Jefferson City, Missouri.

Daniels, D.J., 1996, Surface-Penetrating Radar. The Institution of Electrical Engineers.
Geophysical Survey Systems, Inc., 1995 GSSI Manual #MN43-116, Radan for Windows. Geophysical Survey Systems, Inc., New Hampshire.
Kearey, P. and Brooks, M., 1991, An Introduction to Geophysical Exploration. Blackwell Scientific Publications.
Telford, W.M., Geldart, L.P., Sheriff, R.E., and Keys, D.A., 1976, Applied Geophysics. Cambridge University Press.
Williams, R.S., 1996, Application of the Dipole-Dipole Resistivity Technique for Detection and Delineation of Subsurface Air-filled Cavities. Thesis, University of Missouri, Rolla.